UNCLASSIFIED

AD NUMBER
AD336461
CLASSIFICATION CHANGES
TO: unclassified
FROM: confidential
LIMITATION CHANGES
TO: Approved for public release, distribution unlimited
FROM: Distribution authorized to U.S. Gov't. agencies and their contractors; Apr 1963. Other requests shall be referred to Ballistic Research Labs., Aberdeen Proving Ground, MD.
AUTHORITY
SECDEF Memo, 2 Aug 1960; USAARDC ltr, 24 Jan 1979

THIS PAGE IS UNCLASSIFIED

REPORT No. 51
COPY No. 42

BALLISTIC ANALYSIS LABORATORY

PROJECT THOR
TECHNICAL REPORT No. 51
APRIL 1963

THE RESISTANCE OF VARIOUS NON-METALLIC MATERIALS TO PERFORATION BY STEEL FRAGMENTS; EMPIRICAL RELATIONSHIPS FOR FRAGMENT RESIDUAL VELOCITY AND RESIDUAL WEIGHT (U)

Contract DA-36-034-ORD-29RD
Philadelphia Procurement District

ARMY MATERIEL COMMAND, M.S. Code No. 5025.11.57500

Ballistic Research Laboratories
Aberdeen Proving Ground, Maryland

THE RESISTANCE OF VARIOUS NON-METALLIC MATERIALS

TO PERFORATION BY STEEL FRAGMENTS;

EMPIRICAL RELATIONSHIPS FOR FRAGMENT RESIDUAL

VELOCITY AND RESIDUAL WEIGHT (U)

PROJECT THOR TECHNICAL REPORT NO. 51

APRIL 1963

Ballistic Analysis Laboratory
Institute for Cooperative Research
The Johns Hopkins University
3506 Greenway
Baltimore 18, Maryland

Contract DA-36-034-ORD-29RD
Philadelphia Procurement District

AMC MS No. 5025.11.37500

Ballistic Research Laboratories
Aberdeen Proving Ground, Maryland

CONFIDENTIAL

THE RESISTANCE OF VARIOUS NON-METALLIC MATERIALS TO PERFORATION BY STEEL FRAGMENTS; EMPIRICAL RELATIONSHIPS FOR FRAGMENT RESIDUAL VELOCITY AND RESIDUAL WEIGHT (U)

PROJECT THOR TECHNICAL REPORT NO. 51

APRIL 1963

Ballistic Analysis Laboratory
Institute for Cooperative Research
The Johns Hopkins University
3506 Greenway
Baltimore 18, Maryland

Contract DA-36-034-ORD-29RD
Philadelphia Procurement District

AMC MS No. 5025.11.57300

Ballistic Research Laboratories
Aberdeen Proving Ground, Maryland

CONFIDENTIAL

CONFIDENTIAL

ABSTRACT

Perforation data for steel fragments impacting on each of seven non-metallic materials have been collected and analyzed. The experimental data are characterized by compact fragments weighing five to 825 grains, striking velocities as high as 12,000 feet per second, and obliquities of strike as high as 70 degrees. Empirical formulas of a given type have been fitted to the data for each target material, thereby relating fragment residual velocity and residual weight, in separate equations, to important impact parameters.

The two sets of formulas, used jointly, serve as a basis for several extensions or applications such as 1) a comparison, for equal weight of target per unit area, of the resistance of target materials to perforation, 2) a calibration of the resistance of a target material to perforation in terms of the maximum thickness of a standard medium that the residual fragment can perforate, and 3) a determination of the effect of an intermediate barrier on the potential of a fragment to damage a primary target beyond the barrier.

TABLE OF CONTENTS

CONFIDENTIAL

LIST OF APPENDICES

CONFIDENTIAL

LIST OF TABLES

LIST OF TABLES (continued)

LIST OF FIGURES

LIST OF FIGURES (continued)

INTRODUCTION

For several years, this laboratory has been participating in programs sponsored by the Weapon Systems Laboratory, Ballistic Research Laboratories (BRL), to supply information for vulnerability analysts and weapon designers on the resistance of various materials to perforation by steel fragments and projectiles. All of these materials have military significance but do not necessarily constitute primary targets. These materials are representative of those used for body-armoring, transparencies, and special functions. Their use may be justified because they have some property or properties necessary or desirable for a given function or structural purpose. For example, bullet-resistant glass is a standard windshield material in aircraft; aircraft canopies are often made of Plexiglas, as cast or stretched; a packaged parachute contains a large number of folds of nylon cloth. These materials might offer considerable resistance to an impacting fragment. A vulnerability analyst must contend with the problem of determining the extent of protection afforded by these materials in situ even though the primary function of these materials may not be one of armoring.

A substantial amount of investigation is being made to devise light-weight armoring materials which offer more protection, - to personnel, for example. Several composites (combinations of two or more materials) as well as entirely new materials are being examined. For comparing the resistance of light-weight materials to perforation by fragments, it becomes necessary to establish a firm measure of the resistance of certain basic materials to perforation. This report should help to meet this need while suggesting a rational method for a comparison of materials in this particular

respect.

Several reports have been published by this laboratory dealing with the resistance of materials to perforation by fragments and projectiles. The designations and titles of these reports are outlined in Table I. A recent report, Technical Report No. 47, is similar in scope and format to the present one, but deals with a sample of ten metallic materials while the present report evaluates the resistance to perforation of seven non-metallic materials.

The bulk of the experimental data required to furnish information on the resistance of these materials to perforation has been provided by BRL. Data from other sources such as a) Army Chemical Center, Edgewood, Md., b) Watertown Arsenal Laboratories, Watertown, Mass., c) Development and Proof Services, Aberdeen Proving Ground, Md., and d) Midwest Research Institute, Kansas City, Missouri have supplemented the basic sample; together, these data make this study possible.

A listing of the experimental data is given in Appendix I. Whereas more than one set of homologous steel fragments was used in the experimental work, all of these fragments can properly be classified as compact and reasonably alike in shape. The shapes of these fragments can be described simply as cylinders, cube-on-cylinders, or near-cylinders.

Studies in the realm of fragment and projectile impact are continuing at this laboratory. The resistance to perforation of composite materials, spaced materials, and new materials is being examined. The relationship of hole size in the target to impact parameters is receiving some attenti n as well as the weight, velocity, and spatial distributions and the number of particles formed from an impact. The influence of certain projectile

TABLE I

Other Ballistic Analysis Laboratory Reports on Studies of the Perforation of Target Materials by Fragments and Projectiles

Report No.	Date	Title	Classification
14*	Sept. 1954	A Suggested Technique for Predicting the Performance of Armor-Piercing Projectiles Acting on Rolled Homogeneous Armor (U)	C
25*	July 1956	A Comparison of Various Materials in Their Resistance to Perforation by Steel Fragments; Empirical Relationships (U)	C
36*	April 1958	A Study of Residual Velocity Data for Steel Fragments Impacting on Four Materials; Empirical Relationships (U)	C
41	May 1959	A Comparison of the Performance of Fragments of Four Materials Impacting on Various Plates (U)	C
44	Jan. 1960	The Resistance of Two Nose-Cone Materials to Perforation by Steel Fragments; Empirical Relationships for Fragment Residual Velocity and Residual Weight (U)	S
47	April 1961	The Resistance of Various Metallic Materials to Perforation by Steel Fragments; Empirical Relationships for Fragment Residual Velocity and Residual Weight (U)	C
50	July 1962	The Calibration of a Collection Medium for the Determination of Particle Velocity (U)	U

* Out of Print

parameters on the performance of the projectile is being investigated. Impact data for bullets, flechettes, and other projectiles are being collected for study. In this respect, reference is made to a current Ballistic Research Laboratories Memorandum Report entitled "An Empirical Method for Predicting Target Penetration and Residual Velocity for Small Bullets (U)". An important conclusion from this memorandum suggests that whenever the projectile remains essentially intact after impact, its performance seems to be directly related to the weight and the presented area of the entire projectile.

The objectives of this report are: 1) the consolidation, revision, and extension of information pertaining to perforation of seven non-metallic materials by steel fragments, 2) the development of empirical equations permitting estimates of the residual weight and velocity associated with the largest portion of steel fragment that perforates the target material, 3) the extension of these empirical equations to provide estimates of minimum velocities for which perforation is possible, 4) a comparison of the resistance of non-metallic materials to perforation by steel fragments, and 5) the determination of a measure of the maximum capacity of the residual fragment for additional perforation assuming, initially, the perforation of a non-metallic barrier target with known impact parameters.

The main technique of the work for this report is outlined as follows:

a. Obtain for each target material a small sample of approximately fifty data points spanning the impact conditions of interest. These data points should include a careful recording of all the important parameters describing the impact condition as well as measurements describing the result.

b. Fit independent equations of a given type to the raw data to permit initial estimates of residual weight and residual velocity for the largest portion of fragment perforating the target.

c. By comparing actual with calculated values for residual weight and actual with calculated values for residual velocity, determine impact conditions for which the variation between actual and calculated values is unduly large.

d. Repeat steps b and c, after the results of new impact conditions are included for testing, to provide a firmer basis for reporting.

e. Provide graphical information which renders the equations more useful. Combine the information from empirical equations for several materials onto a single set of graphs for the sake of comparison of target materials, while appropriately absorbing inequities in comparison due to differences in densities of the target materials.

This technique finally provides a practical set of formulas for each material for the prediction of a) minimum velocity for which perforation is possible with given fragment weight and shape, b) residual velocity and weight when perforation occurs, and c) impact conditions for which the fragment will shatter completely. These formulas are especially useful whenever good predictions are needed over broad ranges of impact parameters rather than when pin-point accuracy is needed for a few specialized sets of impact conditions. The formulas include the important impact parameters and are established with relatively modest experimental effort and expense.

The target materials selected for inclusion in this report are listed in Table II which follows. Table III summarizes the characteristics of the experimental data for each target material. Table IV provides the dimensions and weights of the fragments used in the experimental program.

Table II

Description of Target Materials

Designation	Military Specification	Composition	Manufacturer	Tensile Strength (psi)	Compressive Strength (psi)	Shear Strength (psi)	Rockwell Hardness	Density lb/ft^3
Unbonded Nylon*	MIL-C-12369A,C (QMC)	Nylon 66	Dupont	------	------	------	------	43-50
Bonded Nylon	MIL-C-12369A,C (QMC)	Nylon 66 Phenolic Butyral Resin (10-13% by wt.)	Victory Plastics Co., etc.	------	------	------	------	56-60
Lexan	------	Polycarbonate Resin	------	8000-9000	11000	------	M70-R118	74.9
Cast Plexiglas II UVA or Plexiglas 55	MIL-P5425 Finish A	Cast Thermoplastic Acrylic Resin	Rohm & Haas, Bristol, Pa.	10500-11000 (rupture)	18000-19000	9000-9500	M93	75
Stretched Plexiglas	MIL-P-25690A	Methylmethacrylate Sheet Material	Goodyear Aircraft Co.	9000	------	3000	------	76
Doron II, etc.	MIL-A-17855 Amr	Glass fabric base with polyester resin	1) Continental Diamond Fibre Corp., Newark, Del. 2) Moulded Plastics, Bristol, Va. 3) Swedlow Corp., Calif.	44000-51000	60000	17100-17500	M74	125
Bullet-Resistant Glass	------	Inorganic product of fusion, cooled to a rigid condition without crystallizing	Various	10000	50000	very low	------	154

* Breaking strength: 1000 lb ; Ultimate elongation: 25%

b. Fit independent equations of a given type to the raw data to permit initial estimates of residual weight and residual velocity for the largest portion of fragment perforating the target.

c. By comparing actual with calculated values for residual weight and actual with calculated values for residual velocity, determine impact conditions for which the variation between actual and calculated values is unduly large.

d. Repeat steps b and c, after the results of new impact conditions are included for testing, to provide a firmer basis for reporting.

e. Provide graphical information which renders the equations more useful. Combine the information from empirical equations for several materials onto a single set of graphs for the sake of comparison of target materials, while appropriately absorbing inequities in comparison due to differences in densities of the target materials.

This technique finally provides a practical set of formulas for each material for the prediction of a) minimum velocity for which perforation is possible with given fragment weight and shape, b) residual velocity and weight when perforation occurs, and c) impact conditions for which the fragment will shatter completely. These formulas are especially useful whenever good predictions are needed over broad ranges of impact parameters rather than when pin-point accuracy is needed for a few specialized sets of impact conditions. The formulas include the important impact parameters and are established with relatively modest experimental effort and expense.

The target materials selected for inclusion in this report are listed in Table II which follows. Table III summarizes the characteristics of the experimental data for each target material. Table IV provides the dimensions and weights of the fragments used in the experimental program.

Table III

Summary of Characteristics of Experimental Data

Target Material	Target Thickness Range e (inches)	Areal Density Range E (lb/ft^2)	Obliquity Range θ (degrees)	Striking Velocity Range V_s (fps)	Fragment Size Range m_s (grains)
Unbonded Nylon	0.02 - 3.0	0.1 - 12.5	0 - 70	300 - 10000	5 - 207
Bonded Nylon	0.43 - 2.0	2.1 - 9.7	0 - 70	1000 - 12000	5 - 825
Lexan	.125 - 1.0	0.8 - 6.2	0 - 70	1000 - 11500	5 - 240
Plexiglas as Cast	.20 - 1.1	1.2 - 6.7	0 - 70	200 - 9500	5 - 475
Stretched Plexiglas	.05 - 1.0	0.3 - 6.4	0 - 70	500 - 11000	5 - 475
Doron	.05 - 1.5	0.5 - 15.6	0 - 70	500 - 11000	2.5 - 630
Bullet-Resistant Glass	.20 - 1.65	2.6 - 21.2	0 - 70	200 - 10000	15 - 475

Note: Graphs in the appendices contain contours which, for the most part, are limited by the intervals of the experimental data, as shown above.

CONFIDENTIAL

Table IV

Fragment Sizes and Dimensions

Type I

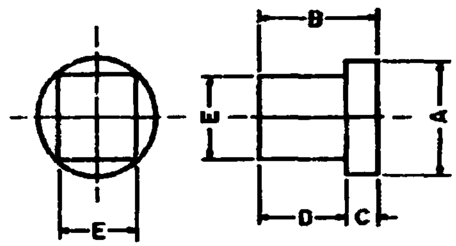

Type II

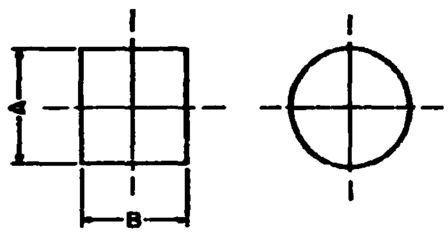

Type	A	B	C	D	E	m_s (grains)
I	.587	.579	.225	.354	.414	240
I	.499	.389	.170	.219	.353	120
I	.399	.303	.131	.172	.282	60
I	.299	.282	.115	.167	.211	30
I	.233	.230	.093	.137	.167	15
II	.687	.654				475
II	.587	.450				240
II	.499	.313				120
II	.399	.243				60
II	.299	.213				30
II	.233	.180				15

(All dimensions in inches)

EMPIRICAL RELATIONSHIPS

The resistance of a material to perforation by steel fragments has been measured in many ways. Here, the assumption is made that this resistance can be related to the losses in weight and velocity sustained by the fragment during perforation. Accordingly, experimental data have been collected for steel fragments impacting on each material of a variety of non-metallic target materials. Those data cases where perforation was achieved were singled out for the analysis. Measurements of both the residual velocity and the residual weight were recorded. These measurements refer to the largest piece of the original fragment which perforates the target material.

In Technical Report . . . (see Table I), a method is described for obtaining empirical equations from residual velocity data to relate residual velocity to important impact parameters. The type of equation proposed is:

$$V_r = V_s - 10^c (eA)^\alpha m_s{}^\beta (\sec\theta)^\gamma V_s{}^\lambda ,$$

where V_r is the fragment residual velocity in fps,

V_s is the fragment striking velocity in fps,

e is the target thickness in inches,

A is the average presented area of the fragment in square inches,

m_s is the weight of the original fragment in grains,

θ is the angle between the trajectory of the fragment and the normal to the target material, and

c, α, β, γ, λ are constants determined separately for each material.

The derived values of the constants specifying the estimating

equation for fragment residual velocity for each material are tabulated in Tables V and VI of the Results Section.

The exponential form of this equation is simple, yet it includes the important impact parameters. The form has the additional merit of being convertible into a corresponding logarithmic form which is useful because of its linearity.

For a comparison of the resistances of target materials to perforation by fragments, it has been found useful to replace e, the thickness parameter, by another variable, E, in the estimating equation. The new variable refers to the areal density of the target material and is measured in pounds per square foot (see Figure 1). It is obtained by multiplying the target thickness in feet by the density of the target material in pounds per cubic foot. By altering the formulas so that the thickness parameter is replaced by the areal density parameter, it becomes possible to compare the resistances of target materials to perforation on the basis of equal weight of target per unit area. For such a comparison, refer to the section entitled "Measuring the Maximum Capacity of the Residual Fragment for Perforation".

The criterion for goodness of fit of the estimating equation is the magnitude of σ defined below. If $|\Delta V_r|_i$ is the magnitude of the error made in estimating the fragment residual velocity in the i-th set of N sets of experimental conditions, then

$$\sigma^2 = \frac{\sum_{i=1}^{N} |\Delta V_r|_i^2}{N} .$$

Thickness of Target Materials vs Areal Density of Target

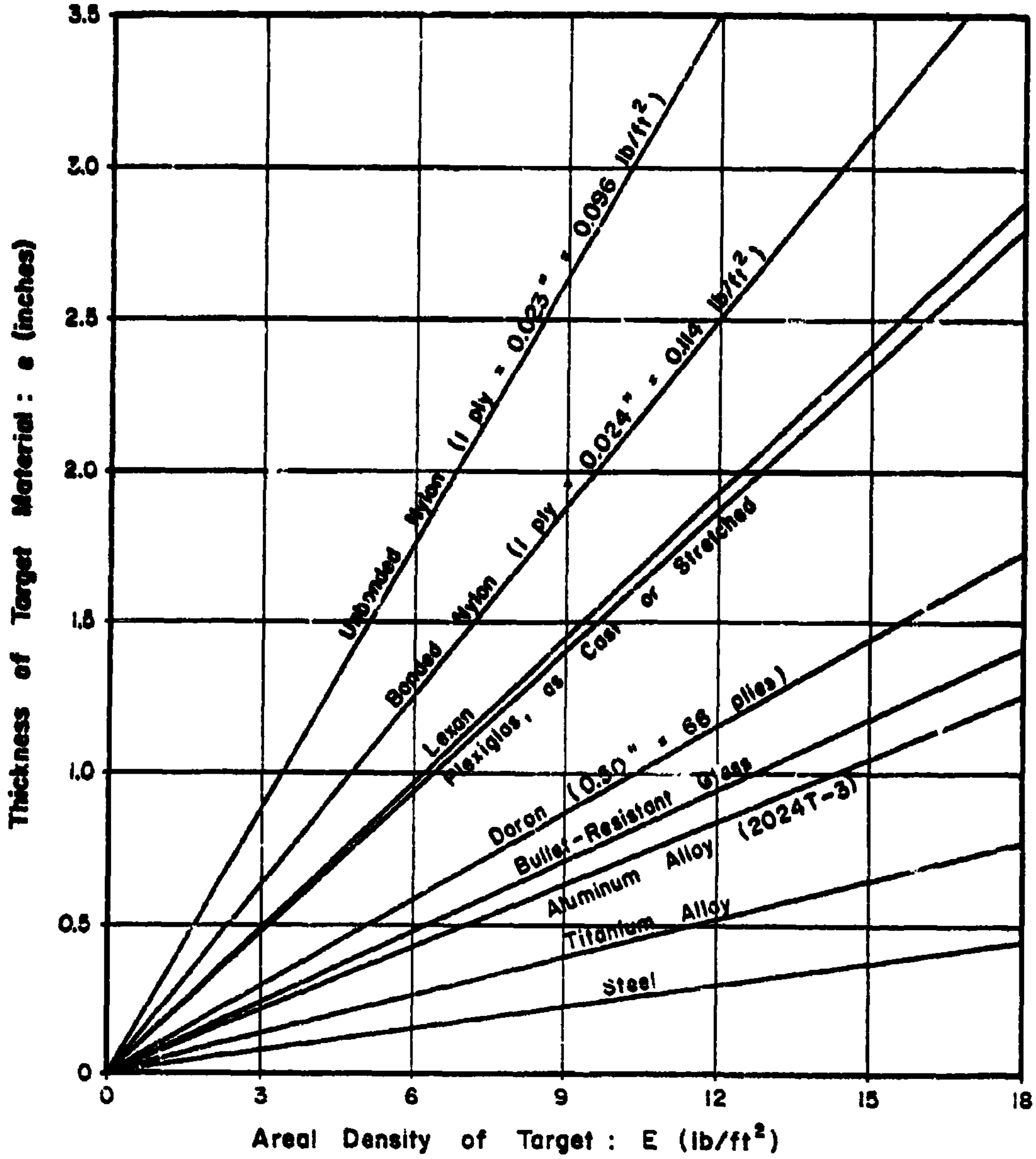

Fig. 1

It is understood that the selection of fit for each target material is made to correspond with the lowest obtainable value of σ. The value of σ for each residual velocity estimating equation is given in Table V of the Results Section.

In order to obtain an empirical formula for estimating residual velocity for steel fragments impacting on each target material, the basic formula is converted into the associated common logarithmic form:

$$\log(V_s - V_r) = c + \alpha \log(sA) + \beta \log m_s + \gamma \log \sec \theta + \lambda \log V_s .$$

With this linear form, the method of least squares is employed to determine a satisfactory set of values for c, α, β, γ, λ. Admittedly, this procedure minimizes S, defined below, rather than σ, where

$$S^2 = \frac{\sum_{i=1}^{N} \left[\log(\Delta V)_i - \log(\overline{\Delta V})_i \right]^2}{N} ,$$

and $(\Delta V)_i$ is the fragment loss in velocity as determined from the estimating equation and $(\overline{\Delta V})_i$ is the actual fragment loss in velocity, both numbers referring to the i-th experimental set of impact conditions. This method of calculating the constants has proved to be entirely satisfactory. It is often possible, by slight alterations of the constants, to improve the fit of the estimating equation. Experience has shown, however, that the minor improvements obtainable do not justify the effort.

For the type of equation assumed, it is possible to solve for V_s when V_r is zero. This striking velocity shall be designated V_o. The constants which define the V_o equation for each target material are specified in Tables VII and VIII of the Results Section. The significance of V_o has been established in previous reports by this laboratory where V_o has been found

to be a good analytical approximation to the protection velocity; the latter is defined to be the highest striking velocity below the ballistic limit for which the probability of perforation is zero. In other words, the V_o values are estimates of the limiting striking velocities for which the target always prevents perforation by the fragment. A set of graphs featuring V_o values for each target material is included in Appendix A.

In an analogous manner, an empirical equation is developed for each target material for estimating fragment residual weight. The form of the equation fitted to the data for each target material is

$$m_s - m_r = 10^c \; (eA)^{\alpha} \; m_s^{\beta} \; (\sec \theta)^{\gamma} \; V_s^{\lambda} \; ,$$

where the only new symbol is m_r, the weight in grains of the largest portion of steel fragment perforating the target. To accommodate a similar least squares treatment on the associated logarithmic equation, the assumption is made that the minimum loss in fragment weight is one-tenth of a grain rather than zero grains. The criterion of goodness of fit is σ^* defined below. If $|\Delta m_r|_i$ is the magnitude of the error in estimating the fragment residual weight in the i-th set of N sets of experimental conditions, then

$$(\sigma^*)^2 = \frac{\sum_{i=1}^{N} |\Delta m_r|_i^2}{N} \; .$$

The values of the constants specifying the equation for estimating fragment residual weight for each target material are given in Tables IX and X of the Results Section.

With low striking velocities, the loss in weight of a fragment during perforation is small and is usually ignored. In such cases, the residual velocity, alone, serves as a good measure of the resistance of the

target to perforation and the capacity of the residual fragment for perforating another target. As the striking velocity increases, the break-up of the fragment becomes more and more pronounced until, finally, this aspect of the impact has to be taken into account. The residual weight of the fragment must be determined as well as the residual velocity before a proper estimate of the capacity of the fragment for perforating another target is possible.

Fragment recovery after impact is accomplished by the use of a bank of fiberboard (Maftex) sheets. The residual fragment is located within this bank and weighed; the depth of penetration of the particle into the Maftex is recorded. More refined techniques and other recovery materials are in use, but recovery in Maftex was adopted as the most practical method for this study. The weight of the residual fragment together with the depth of penetration into Maftex suggest a striking velocity on the Maftex which serves as a rough check on the residual velocity recorded for the fragment. Even this simple recovery technique is tedious and time-consuming, but for the objectives of this report, the derived information was deemed important enough to outweigh these disadvantages.

In many experimental cases, the weight of the largest piece of residual fragment approximates the total weight of fragment perforating the barrier target. At any rate, the capacity of a fragment to perforate a primary target beyond an initial barrier can be conservatively estimated by considering only the largest piece of fragment which perforates the barrier. This approach is justified whenever the hypothetical primary target is one for which damage from the impact of small, slow-moving particles is not anticipated, i.e., damage to such a target will essentially be that caused by the largest, fastest particle that impacts on it. Examples of such tough

primary targets are the internal components of guided missiles and aircraft. These components are often large and difficult to protect, so they contribute heavily to the vulnerability of the target complex.

On the other hand, when a large, hypothetical, primary target is extremely vulnerable to impact, even from a small, slow fragment, then a solution based on the largest, fastest fragment is helpful but incomplete. A typical high-speed impact may result in one main fragment particle, several smaller fragment particles, and, possibly, hundreds of spall particles of variable size issuing from the rear surface of the target. If any one of many of these particles can kill the primary target, then it becomes necessary to account for the total number, sizes, and velocities of these particles before a proper measure of the damage resulting from the impact of the original fragment can be made.

In the laboratory, it is more practical to keep track of the largest portion of residual fragment than to recover every portion of residual fragment regardless of size. Ideal information would provide the weight, speed, and direction of each particle of the original fragment that successfully perforates the target material as well as the weight, speed, and direction of every spall particle.

* * * * *

Sets of graphs for estimating both fragment residual velocity and residual weight are presented in Appendix B. The use of double ordinates in these graphs requires some explanation. Two sets of thickness contours are to be found on each graph of this type. The thickness contours drawn with solid lines refer to the left-hand ordinate; the dashed contours refer to the right-hand ordinate. Thus, for a given graph and a given striking

velocity, two ratios are found. The contours are shown only where both ratios are non-negative. The dotted lines on these graphs suggest th the associated residual velocities apply to a particle of insignificant weight (no more than one or two grains).

No commitment is made on the spall particles which are formed from the plate material. Limited observations of spall patterns reveal wide experimental fluctuations in the number, size, and velocity of the spall particles from one round to the next where the same impact conditions are employed.

The previous remarks emphasize the need for using the empirical equations for residual weight and residual velocity jointly. In this way, it becomes apparent where the results are valid. The double-ordinate graphs clearly display the regions of validity, i.e., where both m_r and V_r are non-negative.

An alternate form of the estimating equation for predicting fragment residual weight is:

$$(1) \quad m_s - m_r = 10^k e^{\alpha} m_s^{\beta} (\sec \theta)^{\gamma} V_s^{\lambda} \; .$$

The omission of the parameter A, the average presented area of the fragment, implies that fragments of a fixed shape are under consideration.

In a manner similar to that used in developing a V_o equation from the estimating equation for predicting residual velocity, an auxiliary equation is developed for predicting conditions for which the fragment shatters completely upon impact.

Let $m_r = 0$ in equation (1). Let the value of m_s corresponding to this condition be called m_o. Then

$$(2)\quad m_o = k^{1/(1-\beta)}\, e^{\alpha/(1-\beta)}\, (\sec\theta)^{\gamma/(1-\beta)}\, V_s^{\lambda/(1-\beta)}.$$

Equation (2) produces estimates of impact conditions for which the fragment shatters on impact. For discrete sets of values of e, θ, and V_s, values of m_o are generated. Each set of values of m_o, e, θ, and V_s satisfying equation (2) defines an impact condition for which the fragment is expected to disintegrate during the perforation of the target. Before this result can be accepted, it must be ascertained that $V_s \geq V_o$ corresponding to the remaining values of the parameters e, m_s, and θ.

To illustrate, a graph is provided corresponding to the impact condition of e=0.5", $\theta = 60^o$, with Bullet-Resistant Glass as the target. In Figure 2, the V_o contour for this condition is shown as well as the "shatter contour". These contours divide the m_s, V_s plane into three regions: 1) no perforation, 2) perforation with $m_r \geq 0$, and 3) perforation where $m_r = 0$. This figure emphasizes the fact that the predictions of impact conditions for which the fragment will shatter are valid only when target perforation is anticipated.

Values of the constants defining the m_o equation for each of several target materials are given in Table XI. With two of the seven target materials, these constants are not given since the fragment break-up data for these two target materials were inadequate to establish such equations. For such materials, the higher striking velocities necessary to establish the values for these constants could not be achieved with available experimental facilities.

RESULTS

The empirical formulas developed from the experimental data on each of the non-metallic targets for the purpose of estimating residual velocity are of the form:

$$V_r = V_s - 10^c (eA)^\alpha m_s^\beta (\sec \theta)^\gamma V_s^\lambda .$$

The values of c, α, β, γ, and λ are tabulated in Table V for each of the non-metallic targets. In addition, the sample size N of experimental data and the value of σ are displayed.

For fragments of a given shape, these formulas can be simplified by removal of the impact parameter A to the form:

$$V_r = V_s - 10^{c^*} e^\alpha m_s^{\beta^*} (\sec \theta)^\gamma V_s^\lambda ,$$

since for any fragment shape approximating that of a regular convex polyhedron, the average presented area is nearly directly proportional to the two-thirds power of the mass.

Note that whenever a form of the estimating equation is desired which omits the impact parameter A, then some assumption has to be made about the shape of the fragments under consideration. When the fragments under consideration are similar in configuration to those used in the experimental work for this report, it can be assumed that the simplified equations, graphs, and conclusions based on the master estimating equations are valid. In fact, extrapolated predictions from these equations for bullets with lead, steel, and tungsten carbide cores show good agreement with experimental results. If the fragments under consideration have large length-to-diameter ratios,

like some flechettes, then these estimating equations may not apply. The experimental data which have been used to fix the estimating equations involve compact fragments, i.e., fragments with length-to-diameter ratios close to unity. The simplified equations for non-compact fragments would be different from those used here since some new relationship between average impact area and fragment weight would be appropriate.

The values of c^*, α, β^*, γ, and λ for the equations associated with compact fragments are tabulated in Table VI.

The V_o formulas derived from the empirical residual velocity formulas are of the form:

$$V_o = 10^{c_1} (eA)^{\alpha_1} m_s^{\beta_1} (\sec\theta)^{\gamma_1} .$$

The values for c_1, α_1, β_1, and γ_1 for each target material are tabulated in Table VII.

For fragments of a given shape, these formulas can be simplified, as before, to the form:

$$V_o = 10^{c_1^*} e^{\alpha_1} m_s^{\beta_1^*} (\sec\theta)^{\gamma_1} .$$

The values of c_1^*, α_1, β_1^*, and γ_1 for the equations associated with compact fragments are tabulated in Table VIII.

The empirical formulas developed from the experimental data for the purpose of estimating fragment residual weight are of the form:

$$m_r = m_s - 10^{c} (eA)^{\alpha} m_s^{\beta} (\sec\theta)^{\gamma} V_s^{\lambda} .$$

The values of c, α, β, γ, and λ are tabulated in Table IX for each

target material. In addition, the sample size N^* of experimental data used to obtain the residual weight equation and the associated value of σ^* are noted.

For fragments of a given shape, these formulas can be simplified by removal of the impact parameter A, as before, to the form:

$$m_r = m_s - 10^{c^*} e^{\alpha} m_s^{\beta^*} (\sec \theta)^{\gamma} V_s^{\lambda} .$$

The resulting values of c^*, α, β^*, γ, and λ for the equations associated with compact fragments are tabulated in Table X.

The Interaction of V_0 Estimates with Estimates of Impact Conditions for Fragment Shatter

Target Material: Bullet-Resistant Glass
Target Thickness: e = 0.50"
Obliquity: θ = 60°

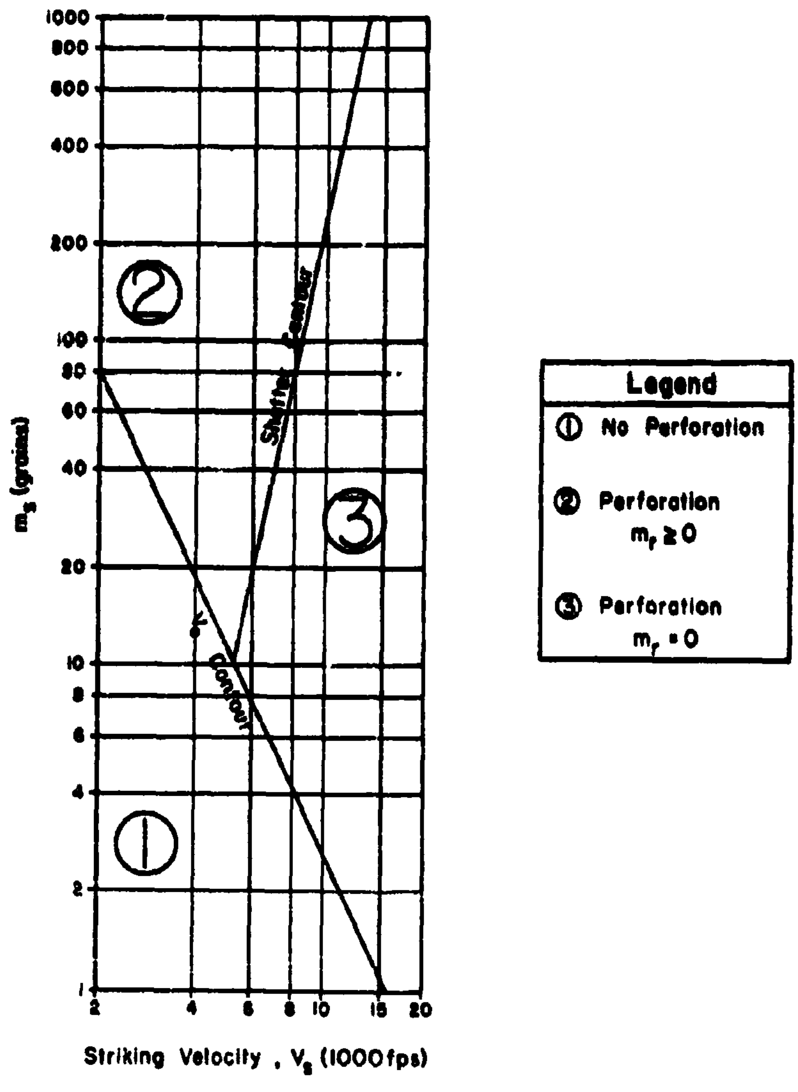

Fig. 2

CONFIDENTIAL

Table V

Constants for the Estimating Equations for Residual Velocity

(No Particular Fragment Shape Assumed)

Form of Equation: $V_r = V_s - 10^c (eA)^{\alpha} m_s^{\beta} (\sec\theta)^{\gamma} V_s^{\lambda}$

Target Material	c	α	β	γ	λ	N	σ
Unbonded Nylon	5.816	0.835	-0.654	0.990	-0.162	339	658
Bonded Nylon	4.672	1.144	-0.968	0.743	0.392	96	700
Lexan	2.908	0.720	-0.657	0.773	0.603	72	608
Plexiglas as Cast	5.243	1.044	-1.035	1.073	0.242	97	589
Stretched Plexiglas	3.605	1.112	-0.903	0.715	0.686	76	700
Doron	7.600	1.021	-1.014	0.917	-0.362	230	640
Bullet-Resistant Glass	3.743	0.705	-0.723	0.690	0.465	68	695

CONFIDENTIAL

Table VI

Constants for the Estimating Equations for Residual Velocity

(Compact Fragment Shape Assumed)

Form of Equation: $V_r = V_s - 10^{c^*} e^{\alpha} m_s^{\beta^*} (\sec \theta)^{\gamma} V_s^{\lambda}$

Target Material	c^*	α	β^*	γ	λ
Unbonded Nylon	4.051	0.835	-0.097	0.990	-0.162
Bonded Nylon	4.672	1.144	-0.968	0.743	0.392
Lexan	1.387	0.720	-0.177	0.773	0.603
Plexiglas as Cast	3.035	1.044	-0.338	1.073	0.242
Stretched Plexiglas	1.255	1.112	-0.161	0.715	0.686
Doron	5.443	1.021	-0.334	0.917	-0.362
Bullet-Resistant Glass	2.254	0.705	-0.253	0.690	0.465

Table VII

Constants for the Estimating Equations for V_o

(No Particular Fragment Shape Assumed)

Form of Equation: $V_o = 10^{c_1} (mA)^{\alpha_1} m_s^{\beta_1} (\sec \theta)^{\gamma_1}$

Target Material	c_1	α_1	β_1	γ_1
Unbonded Nylon	5.006	0.719	-0.563	0.852
Bonded Nylon	7.689	1.883	-1.593	1.222
Lexan	7.329	1.814	-1.652	1.948
Plexiglas as Cast	6.913	1.377	-1.364	1.415
Stretched Plexiglas	11.468	3.537	-2.871	2.274
Doron	5.581	0.750	-0.745	0.673
Bullet-Resistant Glass	5.991	1.316	-1.351	1.289

Table VIII

Constants for the Estimating Equations for V_o

(Compact Fragment Shape Assumed)

Form of Equation: $V_o = 10^{c_1^*} e^{\alpha_1} m_s^{\beta_1^*} (\sec\theta)^{\gamma_1}$

Target Material	c_1^*	α_1	β_1^*	γ_1
Unbonded Nylon	3.486	0.719	-0.084	0.852
Bonded Nylon	3.709	1.883	-0.338	1.222
Lexan	3.495	1.814	-0.445	1.948
Plexiglas as Cast	4.002	1.377	-1.364	1.415
Stretched Plexiglas	3.992	3.537	-0.513	2.274
Doron	3.997	0.750	-0.245	0.673
Bullet-Resistant Glass	4.209	1.316	-0.473	1.289

Table IX

Constants for the Estimating Equations for m_r

(No Particular Fragment Shape Assumed)

Form of Equation: $m_r = m_s - 10^c (eA)^{\alpha} m_s^{\beta} (\sec \theta)^{\gamma} V_s^{\lambda}$

Target Material	c	α	β	γ	λ	N^*	σ^*
Unbonded Nylon*	-7.538	-0.067	0.903	-0.351	1.717	64	5
Bonded Nylon*	-13.601	0.035	0.775	0.045	3.451	65	18
Lexan	-6.275	0.480	0.465	1.171	1.765	104	27
Plexiglas as Cast	-2.342	1.402	-0.137	0.674	1.324	110	53
Stretched Plexiglas	-5.344	0.437	0.169	0.620	1.683	75	13
Doron	-10.404	0.215	0.363	0.706	2.906	96	19
Bullet-Resistant Glass	-5.926	0.305	0.429	0.747	1.819	85	33

* Within the limitations of the experimental data, this material did not cause the steel fragments to break up considerably upon impact. Higher striking velocities than those now obtainable in the laboratory would be required to produce the necessary information to establish a satisfactory set of constants for the m_r equations for this material.

CONFIDENTIAL

Table X

Constants for the Estimating Equations for m_r

(Compact Fragment Shape Assumed)

Form of Equation: $m_r = m_s - 10^{c^*} e^{\alpha} m_s^{\beta^*} (\sec\theta)^{\gamma} V_s^{\lambda}$

Target Material	c^*	α	β^*	γ	λ
Unbonded Nylon*	-7.396	-0.067	0.859	-0.351	1.717
Bonded Nylon*	-13.676	0.035	0.799	0.045	3.451
Lexan	-7.288	0.480	0.785	1.171	1.765
Plexiglas as Cast	-5.305	1.402	0.797	0.674	1.324
Stretched Plexiglas	-6.267	0.437	0.460	0.620	1.683
Doron	-10.858	0.215	0.485	0.706	2.905
Bullet-Resistant Glass	-6.571	0.305	0.632	0.747	1.819

* Within the limitations of the experimental data, this material did not cause the steel fragments to break up considerably upon impact. Higher striking velocities than those now obtainable in the laboratory would be required to produce the necessary information to establish a satisfactory set of constants of the m_r equations for this material.

Table XI

Constants for the Estimating Equations for m_o

(Compact Fragment Shape Assumed)

Form of Equation: $m_o = 10^k e^{\alpha'} (\sec\theta)^{\gamma'} v_s^{\lambda'}$

Target Material	k	α'	γ'	λ
Unbonded Nylon*	-	-	-	-
Bonded Nylon*	-	-	-	-
Lexan	-33.881	2.230	5.441	8.205
Plexiglas as Cast	-26.163	6.914	3.324	6.529
Stretched Plexiglas	-11.904	0.809	1.148	3.116
Doron	-21.143	0.418	1.375	5.658
Bullet-Resistant Glass	-17.875	0.829	2.031	4.949

* Within the limitations of the experimental data, this material did not cause the steel fragments to break up considerably upon impact. Higher striking velocities than those now obtainable in the laboratory would be required to produce the necessary information to establish a satisfactory set of constants for the m_o equations for this material.

CONFIDENTIAL

ADAPTATIONS TO VULNERABILITY ANALYSES

The vulnerability analyst, calculating the effects of a hypothetical fragmenting weapon as used against some primary target, usually relies on experimental evidence from fragments fired singly against facsimile or mock-up targets. The target is considered as an assembly of sets of vital components shielded by structural "shell" members or other components. Firings are conducted to determine the level and extent of damage required to "defeat" or "kill" each vital component under various kill criteria. These firings provide the basis for an empirical formula relating the conditional probability of killing each vital component, given a hit, to some appropriate function of the weight and velocity of the impacting fragment.

Assuming that such a relationship is established, one can proceed with the analysis when the impact weight and velocity of the fragment are known. If the fragment impinges first on some barrier target, then it is important to be able to estimate the losses sustained by the fragment in both weight and velocity during the perforation of this barrier.

The advent of guided missiles and other space targets has forced vulnerability analysts to consider higher and higher impact velocities. With these higher striking velocities, the fragment tends to break up more and more while is is perforating the target. While the significance of fragment break-up for various specific conditions of impact has been acknowledged for some time, there has hitherto been little quantitative evidence to account for this aspect of impact on non-metallic targets.

The present study makes it possible to account more fully for the effect of barrier targets, as represented by any one of the seven non-metallic

materials, on the original fragment. The appropriate estimating equations can be used to provide estimates of the effective fragment residual weight and velocity for a hypothetical impact situation. The analyst can then evaluate any suitable function of fragment weight and velocity to determine the probability of killing a particular component. It is, of course, the responsibility of the analyst to determine the function of fragment weight and velocity to be used with each component type. The function that is chosen will depend on the type of component and the criterion for damage. Finally, the corresponding probability of killing or incapacitating the primary target is obtained.

In graph Set III of Appendix C, for a fixed combination of m_s, θ, and V_s, four different functions of m_r and V_r are plotted against target areal density. These graphs serve to show that the ordering of the contours for the target materials varies with the function of m_r and V_r being used. Therefore, any comparison of the resistance of target materials to perforation, using as a basis some selected function of m_r and V_r, is weakened by this arbitrary selection. Nevertheless, some particular function of m_r and V_r may be entirely appropriate as a measure of the probability of killing a given component.

MEASURING THE MAXIMUM CAPACITY OF THE RESIDUAL FRAGMENT FOR PERFORATION

Establishing minimum requirements for perforation of these non-metallic materials is needed, but this knowledge is hardly useful in estimating the capacity for additional perforation when these minimum requirements are exceeded. A technique for measuring this capacity for additional perforation will be discussed in this section. This technique was first described in Technical Report No. 47.

Usually, the non-metallic materials are not themselves primary targets, so their perforation by fragments is of interest mainly in the sense of the resulting changes in the characteristics of the fragment during perforation. The two outstanding characteristics which determine the capacity of a fragment for perforation are the weight and velocity of the fragment. Thus, it is important to be able to estimate the losses in both fragment weight and velocity during perforation. When these factors are properly estimated, it becomes possible to make a first-order approximation of the maximum capacity of the residual fragment for perforation. With the advent of fragment break-up, it becomes necessary to compromise in this matter by assuming that this capacity can be estimated by considering only the largest piece of fragment which perforates the target material along with the associated residual velocity. This compromise still provides a useful measure of the capacity of the residual fragment for perforation, since the largest portion of the residual fragment is the only portion that matters for the tough primary target. These tough primary targets exist and are of major concern to vulnerability analysts and designers of weapons.

By means of the empirical formulas developed for relating fragment residual velocity and residual weight to the main impact parameters, one can

make satisfactory estimates of the values for these two parameters. Admittedly, spall (particles of target material) and particles of residual fragment other than the largest particle issuing from the target material at time of impact are not considered. Usually, the most lethal element resulting from an impact for which there is a perforation is the largest particle of residual fragment. This is the particle which most regularly penetrates deepest into the recovery target behind the target material in the experimental work.

The empirical formulas feature a single exponent for the product of target thickness and average presented area of the fragment. This, in effect, suggests that if certain results are anticipated for a given impact condition, than the same results should be expected for, say, an impact situation where the target thickness is halved and the fragment shape is altered so that the average presented area is doubled. As long as the product of target thickness and fragment presented area remains constant, the same results are expected. This assumption has been found tenable at least for those fragment shapes which are not distantly removed from compact shapes.

Initial efforts to compare the resistance of target materials to perforation used either fragment residual velocity or residual weight as the basis for the comparison. Neither basis is entirely satisfactory. For example, how does one compare the relative capacity for perforation of 1) a small residual fragment with high velocity and 2) a large residual fragment with low velocity?

For the condition that the original target materials are perforated, a more useful comparison of the resistance of these materials to perforation can be obtained by examining the capacity of the residual fragment to

perforate a calibrating material. The latter may be arbitrarily selected.

For purposes of calibration, the simplest aspect (normal impact) is assumed for the impact of the residual fragment on the calibrating material regardless of the angle of impact of the fragment on the barrier target.

The impact parameters which determine the capacity of a steel fragment for perforation of a given medium include the fragment weight, velocity, shape, and the angle of obliquity. Estimates of values for the first two parameters are provided by the empirical formulas. The shape of the largest portion of a residual fragment is usually similar to the shape of the original fragment whenever the residual fragment is of appreciable size. There is a tendency for the fragment to be squashed and thereby rendered less compact.

When there is considerable break-up of the fragment during the perforation of the initial target material, the residual fragment may have a shape other than that which could reasonably be called compact. In such cases, the residual fragment may have an average presented area (assuming random orientation) several times that of a compact fragment of the same weight. It is also of importance to recognize that, for a non-compact fragment, there is a greater interval between the minimum and the maximum presented areas than for a compact fragment of the same weight. This implies a greater possible variation in performance for the non-compact, residual fragment against a given primary target.

Furthermore, recovered portions of fragments after impact reveal, in many cases, a shredded appearance suggesting much less unity than the original fragment possesses. Such a particle appears more susceptible to further break-up on impact with a second target than a fresh, unfired particle of the same weight. This increased susceptibility to break-up no doubt

results in a lower capacity for additional perforation.

The importance of each particle formed from an impact of a fragment upon some barrier target depends on the vulnerability of the primary target to particle impact. If the primary target is extremely sensitive to such impact, it is important to know how many particles are formed, and the weight and velocity of each particle. If the primary target is one which is not likely to be damaged by the impact of small, slow particles, then these particles can be ignored.

The present report deals primarily with the characteristics of the largest particle of fragment origin resulting from impact on a barrier target. From the point of view of protecting the primary target, if the primary target can withstand the impact of the largest, fastest-moving particle of fragment origin, then it is reasonable to assume that the primary target can withstand the impact of all particles formed from the initial impact.

A basis is now offered for measuring the maximum capacity of the largest particle of residual fragment for perforation of a second medium. The maximum thickness of this medium which can possibly be perforated by the largest portion of residual fragment striking the calibrating medium at normal impact will be used as the measure. To arrive at this measure, estimates of the fragment residual weight and velocity are required. To favor the performance of this residual fragment, it will be assumed that this particle has the same capacity for perforation as a fresh, unfired fragment of the same weight.

Sets of graphs, relating maximum thickness of calibrating material that can possibly be perforated to areal density of the non-metallic target materials for each of twenty-seven combinations of fragment weight, velocity,

and angle of obliquity are displayed in Appendix D. An aluminum alloy, 2024T-3, has been selected as a calibrating material since much experimental work in ballistic impact has been performed on this well-known structural material.

In Appendix E, a similar set of graphs is presented using Maftex as the calibrating material. Technical Report No. 50 (see Table 1) provides a comprehensive treatment of the resistance of Maftex to penetration by fragments of any one of several materials.

Under the assumptions which have been clearly stated, it is a simple matter to use these graphs to compare the resistance of the non-metallic materials to perforation by steel fragments. For a given value of areal density, the "best" target material is that one for which the least thickness of calibrating medium is needed to stop the residual fragment.

If the change in shape of the residual fragment and the weakened condition are taken into account, lower estimates of maximum thicknesses of the calibrating medium will result. For purposes of comparison of the resistance of the initial target materials to perforation, this would not be necessary. The proposed technique does tend to over-estimate this maximum thickness. Certainly if the distortion, change in shape, and weakened condition of the residual fragment are taken into account, some lesser thickness of calibrating material will be found to be equally adequate in stopping the residual fragment.

On each graph in Appendices D and E, each of the non-metallic target materials is represented by a separate contour. One might ask, how do these non-metallic target materials compare with metallic materials in this matter? In anticipation of this question, an appropriate contour for 2024T-3 Aluminum

Alloy has been properly inserted on each of these graphs.

Taken together, Technical Report No. 47 and the present report provide the basis for a broad comparison of the resistance of various materials to perforation by steel fragments. The separation of materials into two categories, metallic and non-metallic, represents an arbitrary method of classifying materials. Insofar as resistance to perforation is concerned, it appears that some non-metallic materials show to advantage, for certain impact situations, over metallic materials normally considered as armor. There are, understandably, many other factors to consider in the selection of a material for some particular function.

CONCLUSIONS

1. Fragment shatter (complete disintegration) upon impact on non-metallic targets is not likely unless the impact condition is an extreme one, e.g., thick target, high obliquity, small fragment, and striking velocity in excess of 8000 fps.

2. Fragment break-up is not as critical a consideration for intermediate striking velocities with non-metallic targets as with metallic targets. This being the case, the fragment residual velocity, alone, can serve adequately as a criterion in the comparison of the resistance of such target materials to ballistic impact.

3. With Bonded and Unbonded Nylon, used in moderate thicknesses corresponding to their military functions, it is virtually impossible to locate impact conditions which produce serious fragment break-up during the perforation.

4. For remarks concerning the comparative resistance of the seven non-metallic target materials, two different sets of graphs apply.

4'. The first set of graphs estimates the thickness of calibrating medium needed to stop the fragment which has impacted on a known target material with given areal density. With such graphs, the "best" target material is that one for which the least thickness of calibrating medium is required to stop the residual fragment. Whether the calibrating material is 2024T-3 or Maftex, the following observations have been made from such graphs:

a) At low velocities (~ 3000 fps), Unbonded Nylon offers the greatest protection of the non-metallic target materials, surpassing even the resistance

offered by 2024T-3, a typical armoring material.

b) At intermediate velocities (~ 6000 fps), a surprising feature is that all the materials considered offer essentially the same resistance to perforation.

c) At high velocities (~ 9000 fps) and for small fragments, Doron and Bullet-Resistant Glass seem to show some superiority over the other non-metallic target materials. As the fragment size increases, this superiority tends to vanish.

d) At low velocity the resistance of Stretched Plexiglas is similar to that of Plexiglas as cast; however, with increasing fragment velocity, Stretched Plexiglas shows to increasing advantage over Plexiglas, as cast.

e) Whereas Unbonded Nylon offers more resistance to perforation than Bonded Nylon at low velocities, the reverse is true at high velocities.

f) Among the transparencies, Bullet-Resistant Glass appears to offer the most resistance, in general.

g) For certain impact conditions, 2024T-3 Aluminum Alloy, a typical metallic target material, appears to offer less resistance than one or another of the non-metallic materials. In fact, only at high velocity and low obliquity, is it demonstrated that the aluminum alloy shows a clear advantage over the non-metallic target materials.

4". The second set of graphs relates V_o to areal density of target. Again, a contour for 2024T-3 Aluminum Alloy has been inserted on each such graph to compare the non-metallic target materials with a representative metal. On the basis of the positions of the contours on these graphs, the following conclusions may be drawn:

a) For impact conditions with low areal density of target (< 5 lb/ft^2), Unbonded Nylon and Doron offer generally the most resistance to perforation; their resistance is comparable to that of 2024T-3 Aluminum Alloy for such conditions.

b) For impact conditions with high areal density of target (8-15 lb/ft^2), there is little evidence to guide the selection of an outstanding target material. This would suggest, that for such a range of areal density, the target material selected for a given function would be selected on the basis of other considerations, rather than resistance to perforation.

c) Plexiglas, as cast, exhibits somewhat more resistance than Stretched Plexiglas for impact conditions with low areal density of target; as the areal density increases, this slight superiority disappears.

d) Bonded Nylon offers a slight advantage in resistance over Unbonded Nylon at impact conditions of high areal density; otherwise, the Unbonded Nylon is definitely superior.

e) Generally, Lexan offers the least resistance to perforation of all the materials tested.

Appendix A

Graph Set I: V_o vs m_s for Selected Values of e

Figs. 3-23

Note: V_o is the value of striking velocity, V_s, obtained from the empirical formulas by setting the residual velocity, V_r, equal to zero. The significance of the V_o values has been established in previous reports by this laboratory where V_o has been found to be a good analytical approximation to the protection velocity; the latter is defined to be the highest striking velocity below the ballistic limit for which the probability of perforation is zero. In other words, the V_o values are estimates of the limiting striking velocities for which the target always prevents perforation by the fragment.

Dashed contours in this set represent thicknesses of target material exceeding those used in the BRL experimental work for that target material.

V_o vs Fragment Weight for Selected Target Thicknesses

Obliquity: 0°

Target Material: Unbonded Nylon

Fragment:

Shape: Compact

Material: Steel

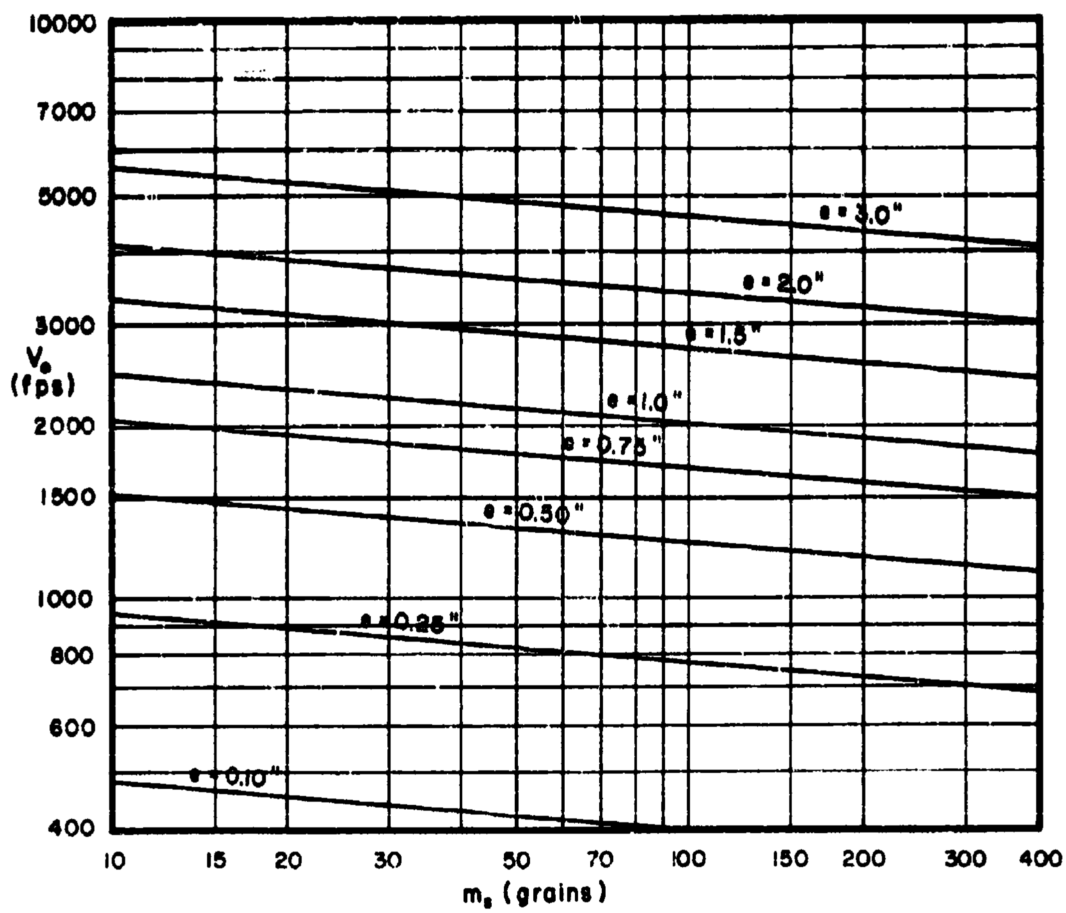

Fig. 3

V_e vs Fragment Weight for Selected Target Thicknesses

Obliquity: 60°

Target Material: Unbonded Nylon

Fragment:

Shape: Compact

Material: Steel

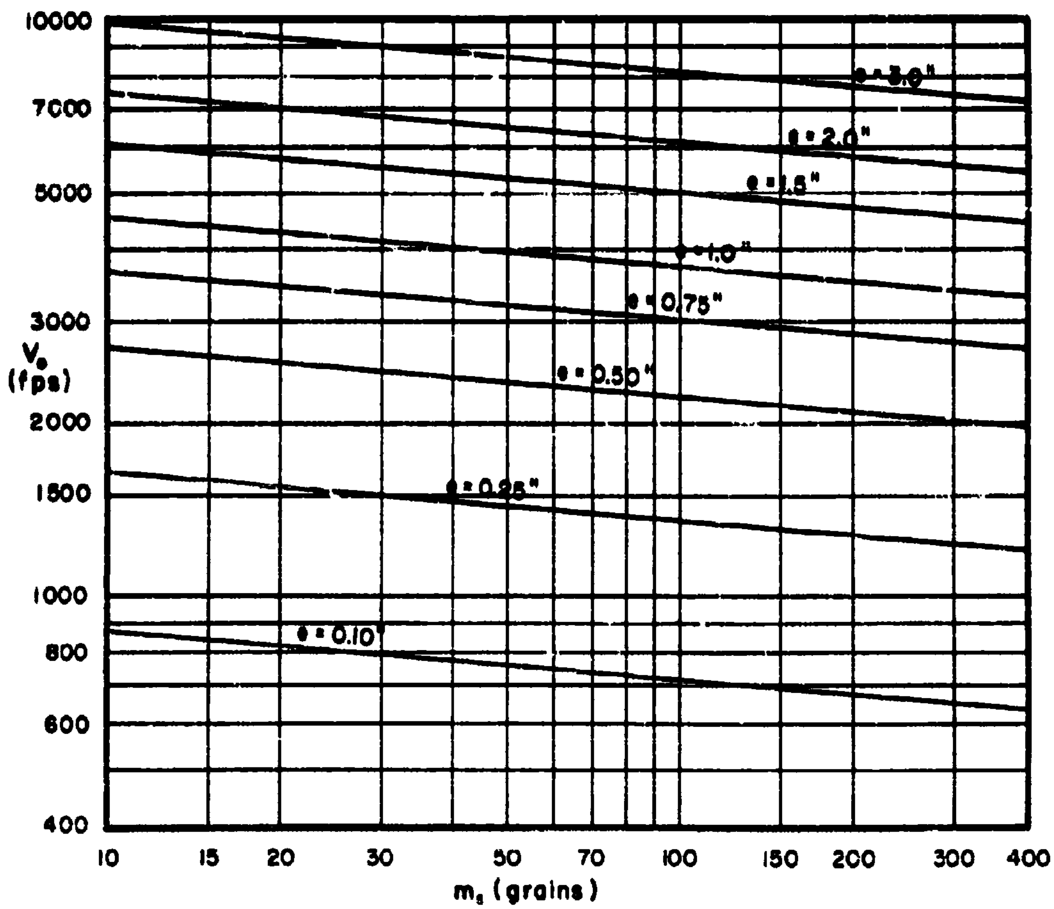

Fig. 4

V_o vs Fragment Weight for Selected Target Thicknesses

Obliquity: 70°

Target Material: Unbonded Nylon

Fragment:

Shape: Compact

Material: Steel

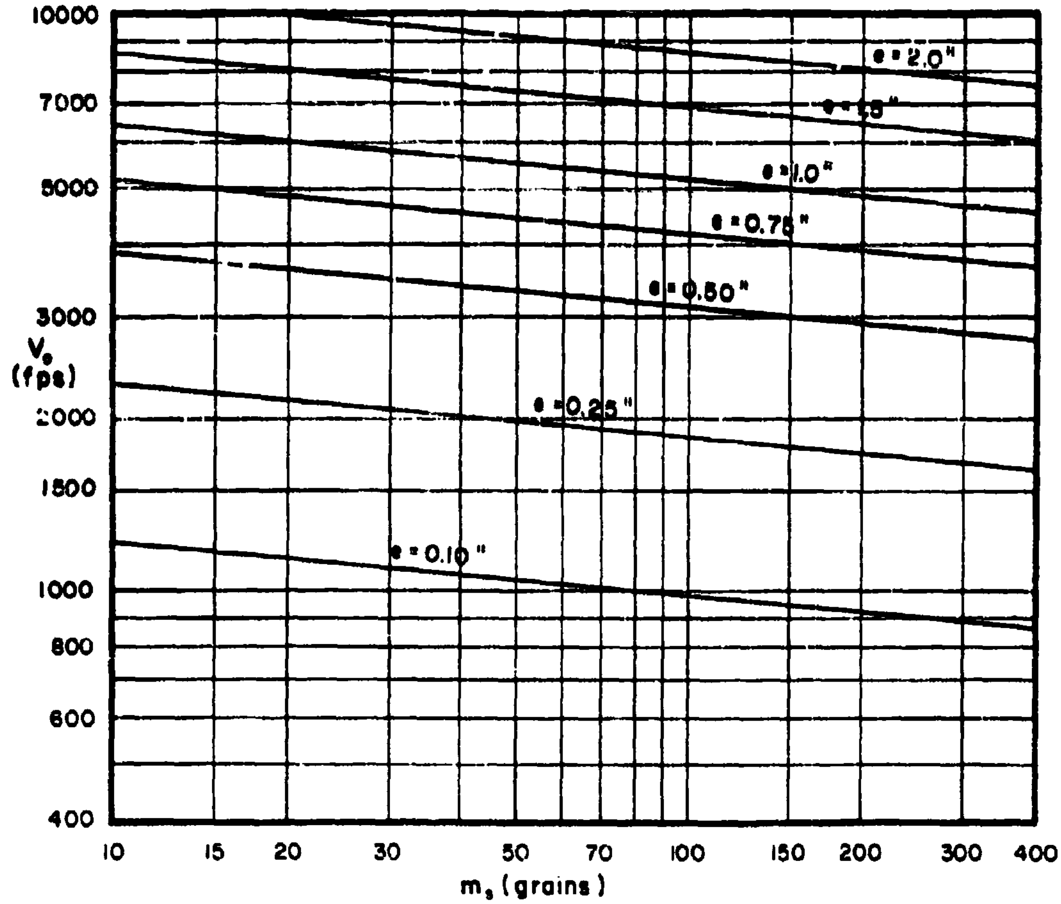

Fig. 5

V_o vs Fragment Weight for Selected Target Thicknesses

Obliquity: 0°

Target Material: Bonded Nylon

Fragment:

Shape: Compact

Material: Steel

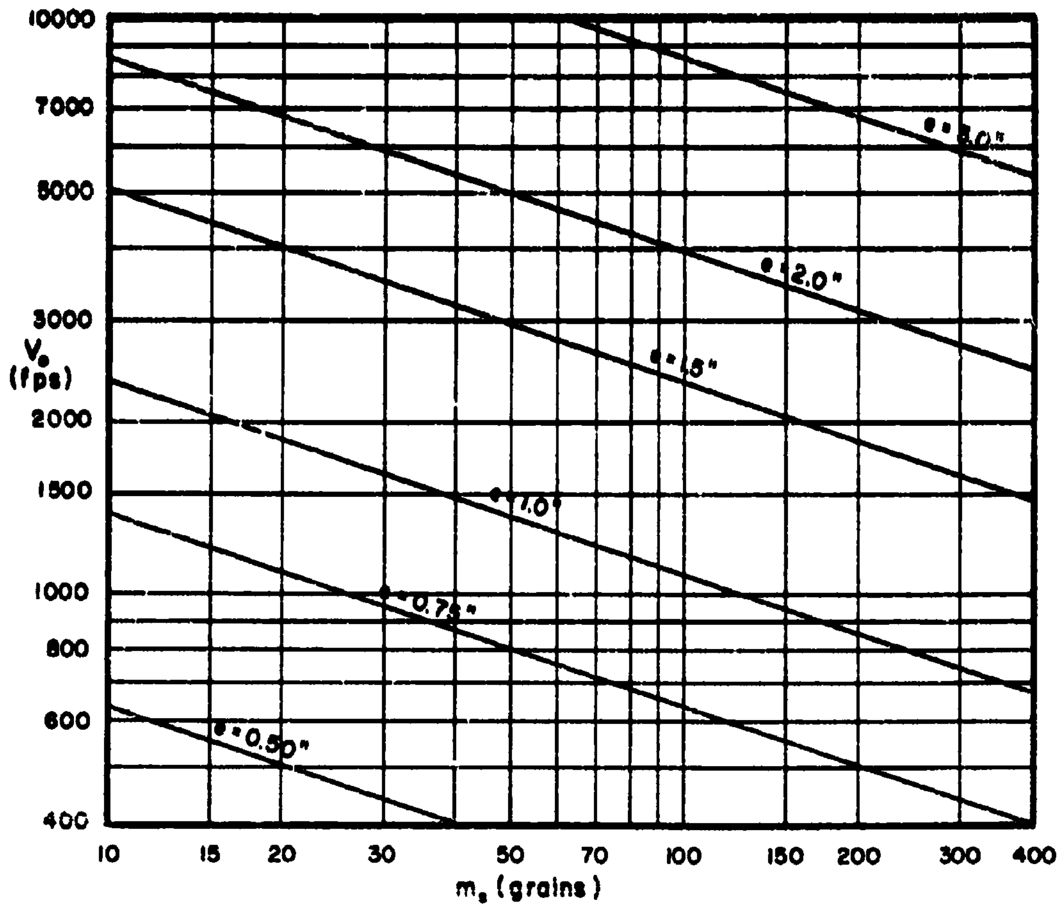

Fig. 6

V_e vs Fragment Weight for Selected Target Thicknesses

Obliquity: 60°

Target Material: Bonded Nylon

Fragment:

Shape: Compact

Material: Steel

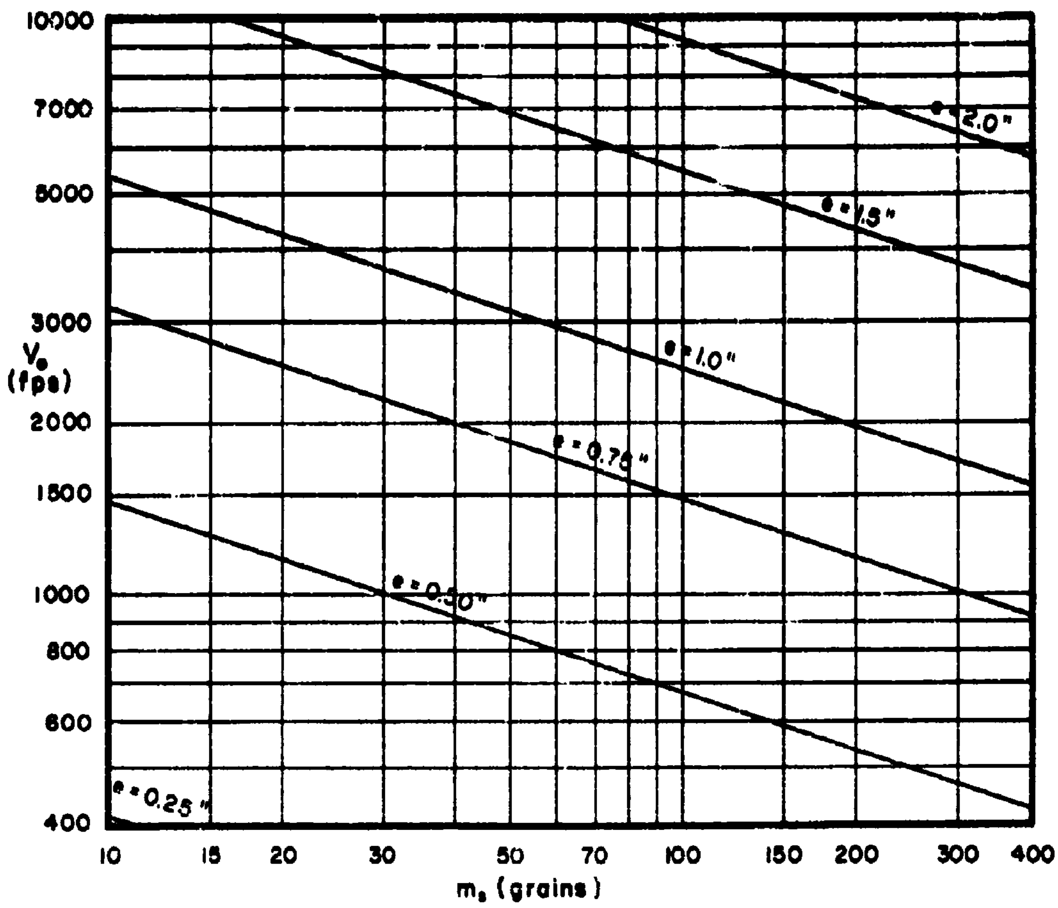

Fig. 7

V_o vs Fragment Weight for Selected Target Thicknesses

Obliquity: 70°

Target Material: Bonded Nylon

Fragment:

Shape: Compact

Material: Steel

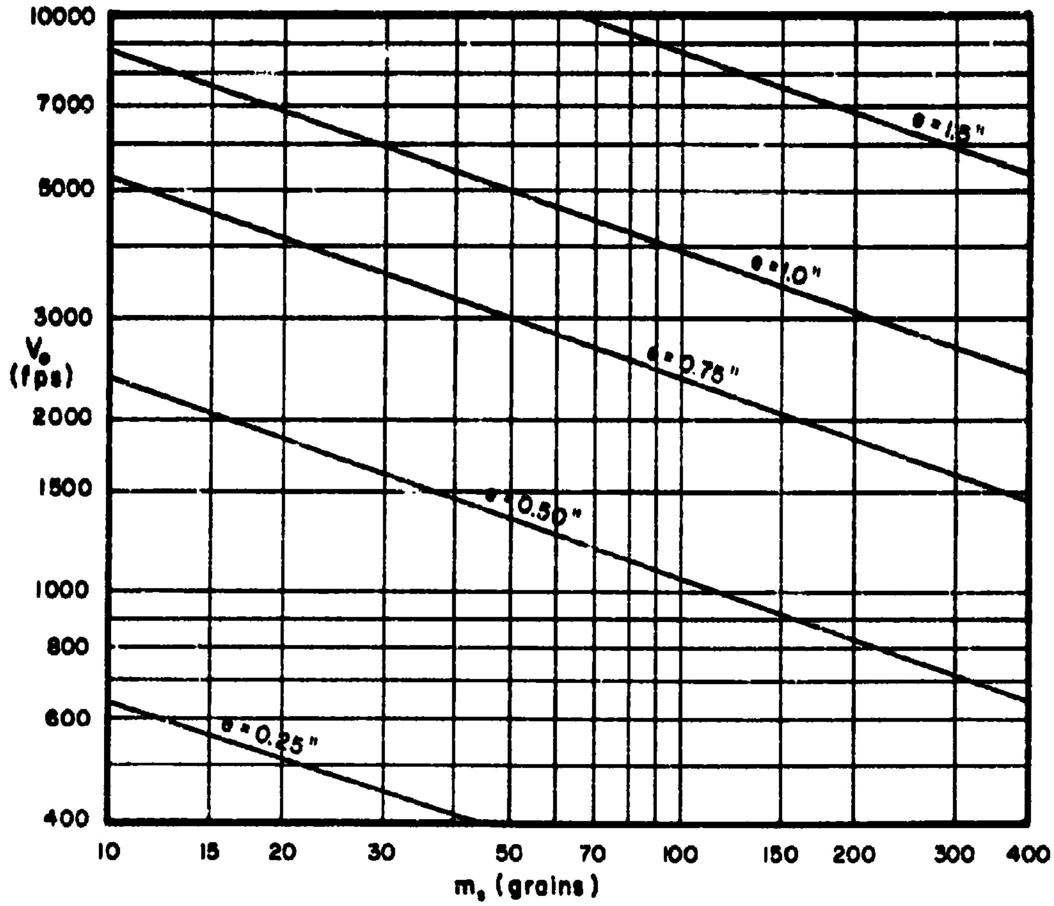

Fig. 8

V_o vs Fragment Weight for Selected Target Thicknesses

Obliquity: 0°

Target Material: Lexan

Fragment:

Shape: Compact

Material: Steel

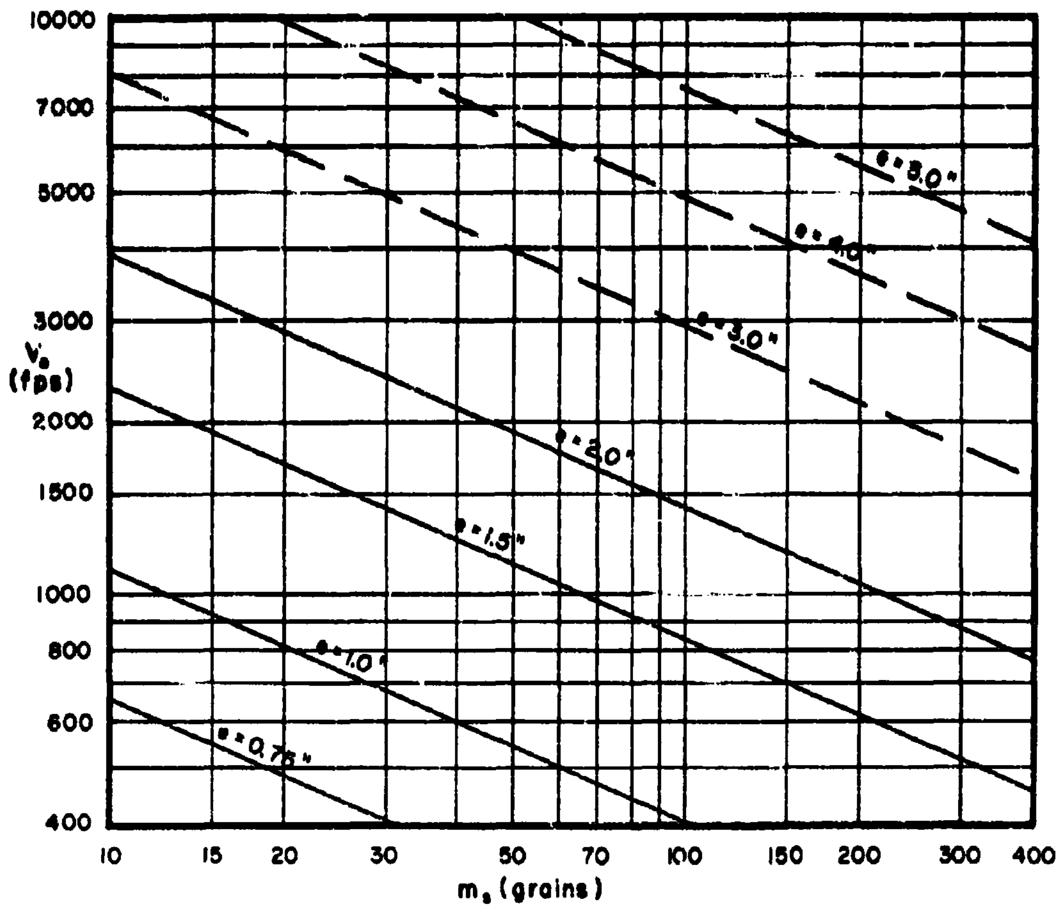

Fig. 9

V_e vs Fragment Weight for Selected Target Thicknesses

Obliquity: 60°

Target Material: Lexan

Fragment:

Shape: Compact

Material: Steel

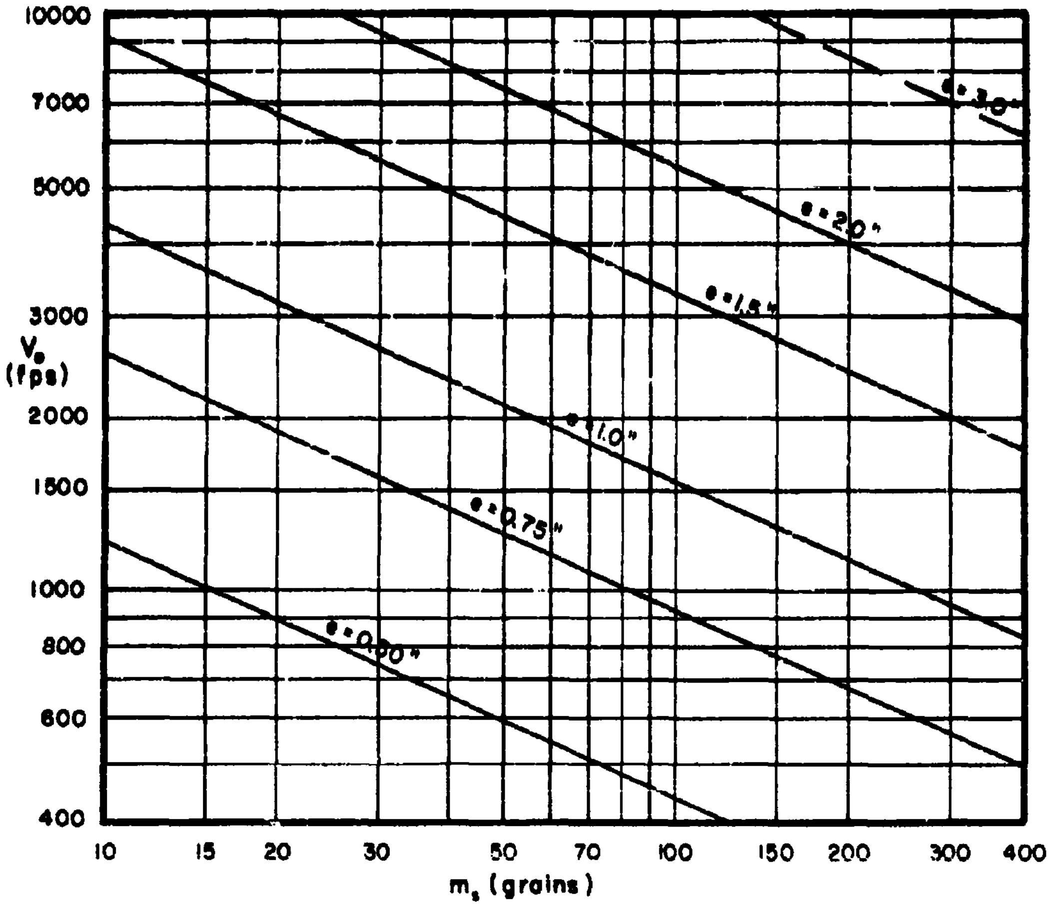

Fig. 10

V_o vs Fragment Weight for Selected Target Thicknesses

Obliquity: 70°

Target Material: Lexan

Fragment:

Shape: Compact

Material: Steel

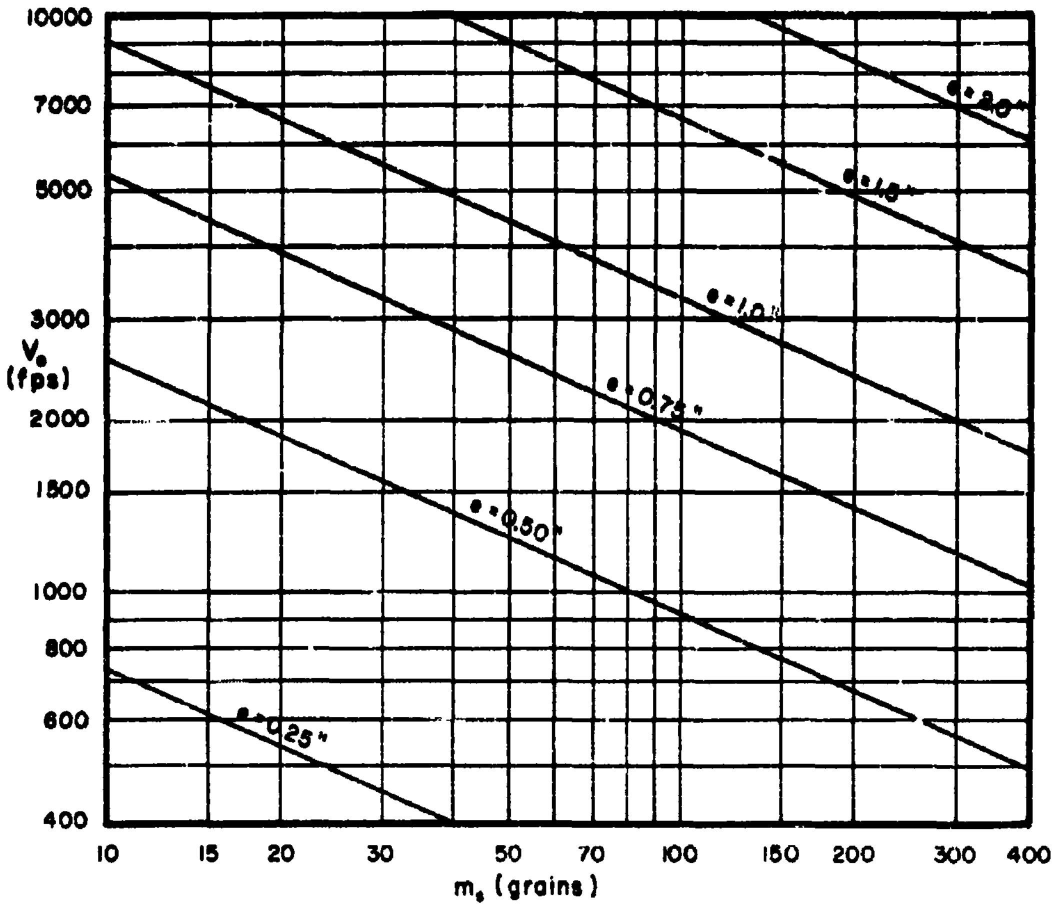

Fig. 11

V_e vs Fragment Weight for Selected Target Thicknesses

Obliquity: 0°

Target Material: Plexiglas, as Cast

Fragment:

Shape: Compact

Material: Steel

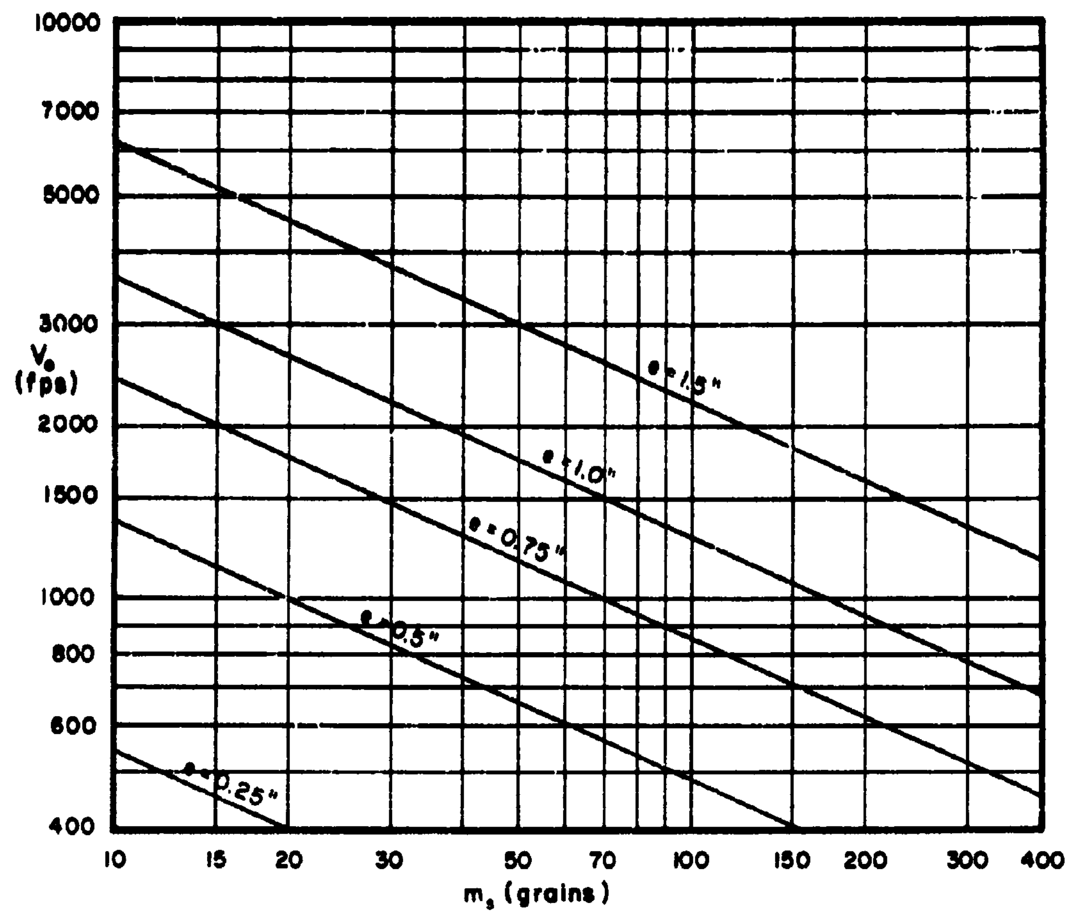

Fig. 12

V_e vs Fragment Weight for Selected Target Thicknesses

Obliquity: 60°

Target Material: Plexiglas, as Cast

Fragment:

Shape: Compact

Material: Steel

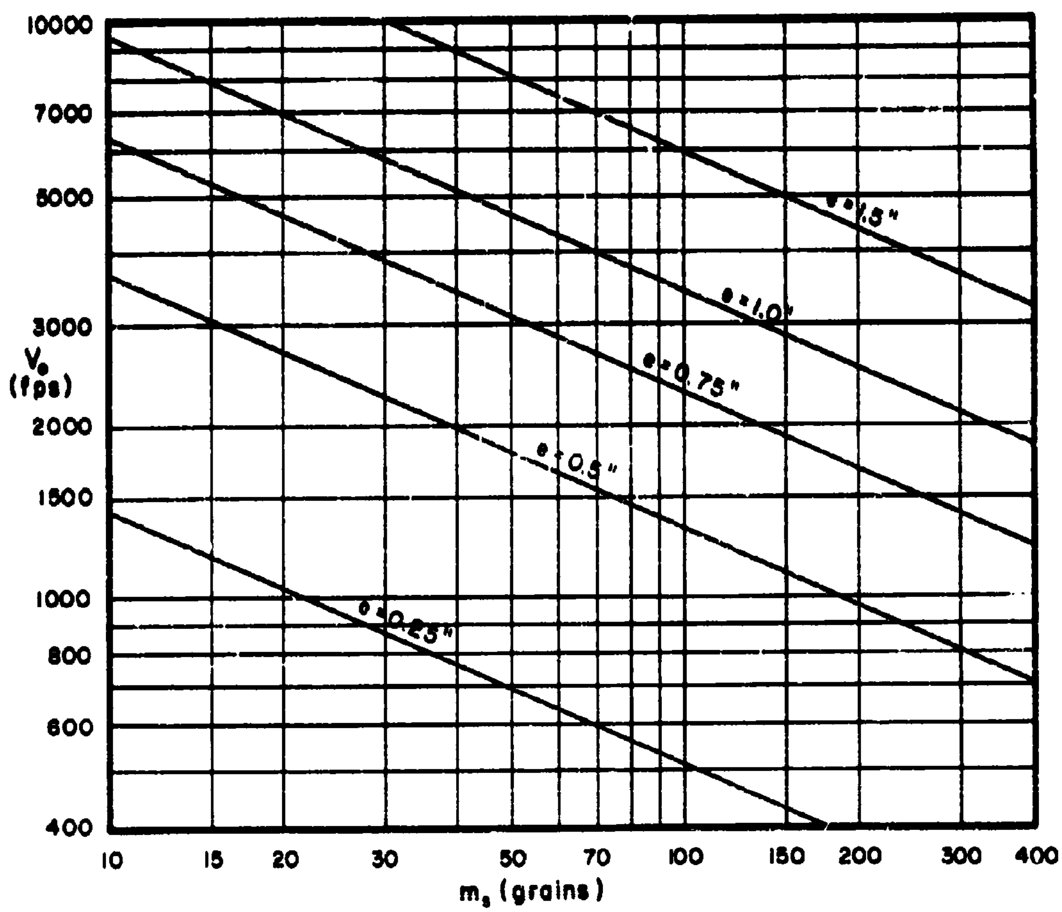

Fig. 13

V_o vs Fragment Weight for
Selected Target Thicknesses

Obliquity: 70°
Target Material: Plexiglas, as Cast

Fragment:
Shape: Compact
Material: Steel

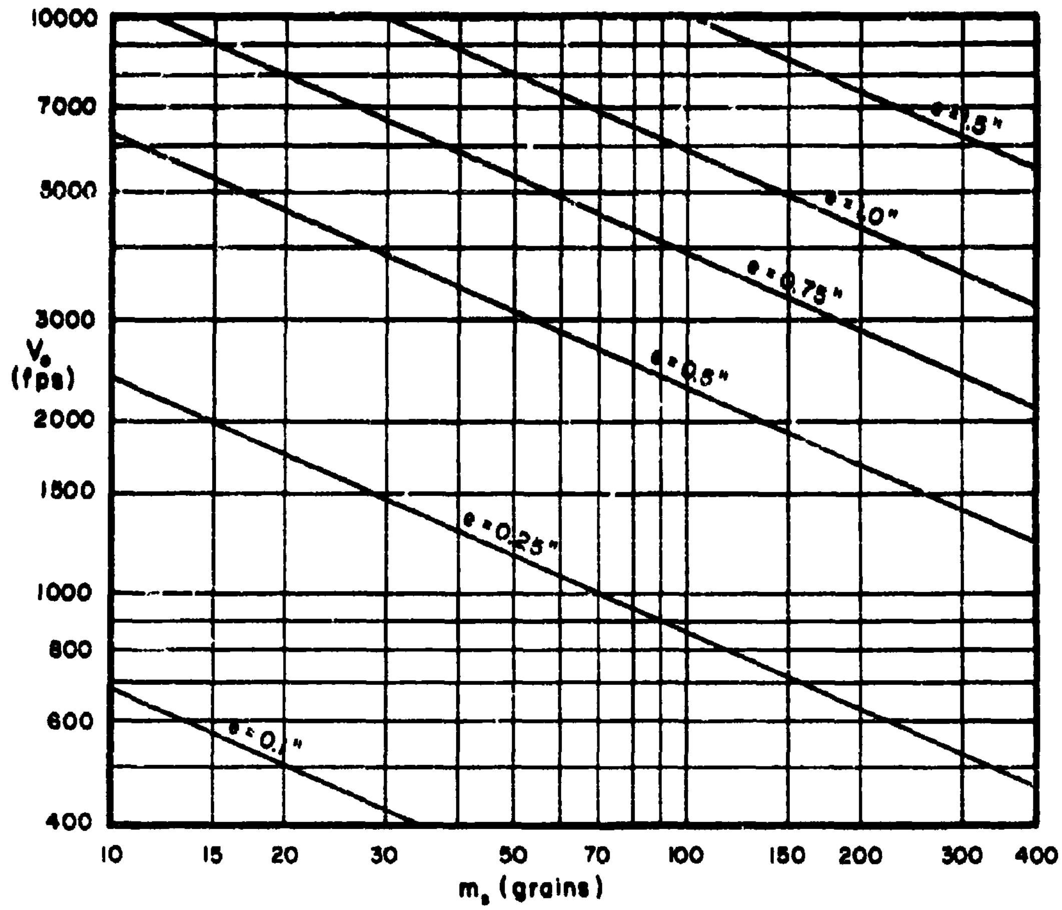

Fig. 14

V_e vs Fragment Weight for Selected Target Thicknesses

Obliquity: 0°

Target Material: Stretched Plexiglas

Fragment:

Shape: Compact

Material: Steel

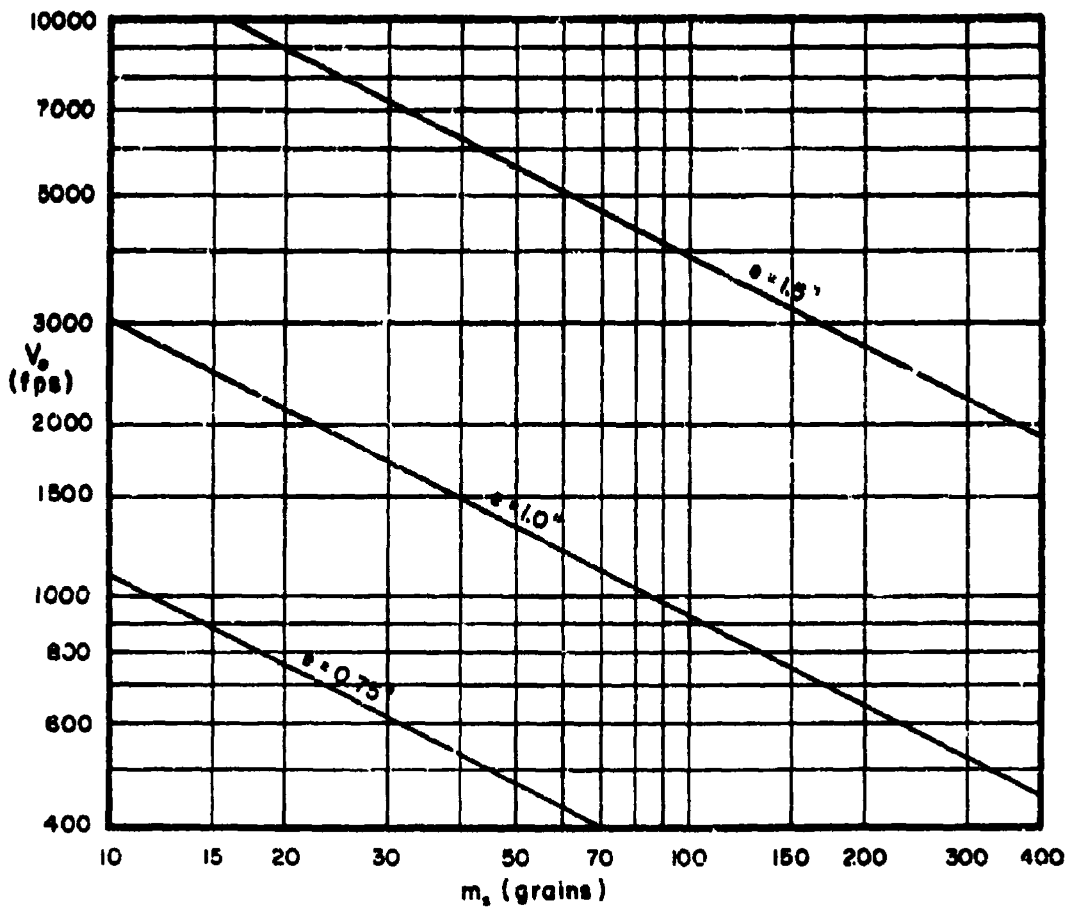

Fig. 15

V_o vs Fragment Weight for Selected Target Thicknesses

Obliquity: 60°

Target Material: Stretched Plexiglas

Fragment:

Shape: Compact

Material: Steel

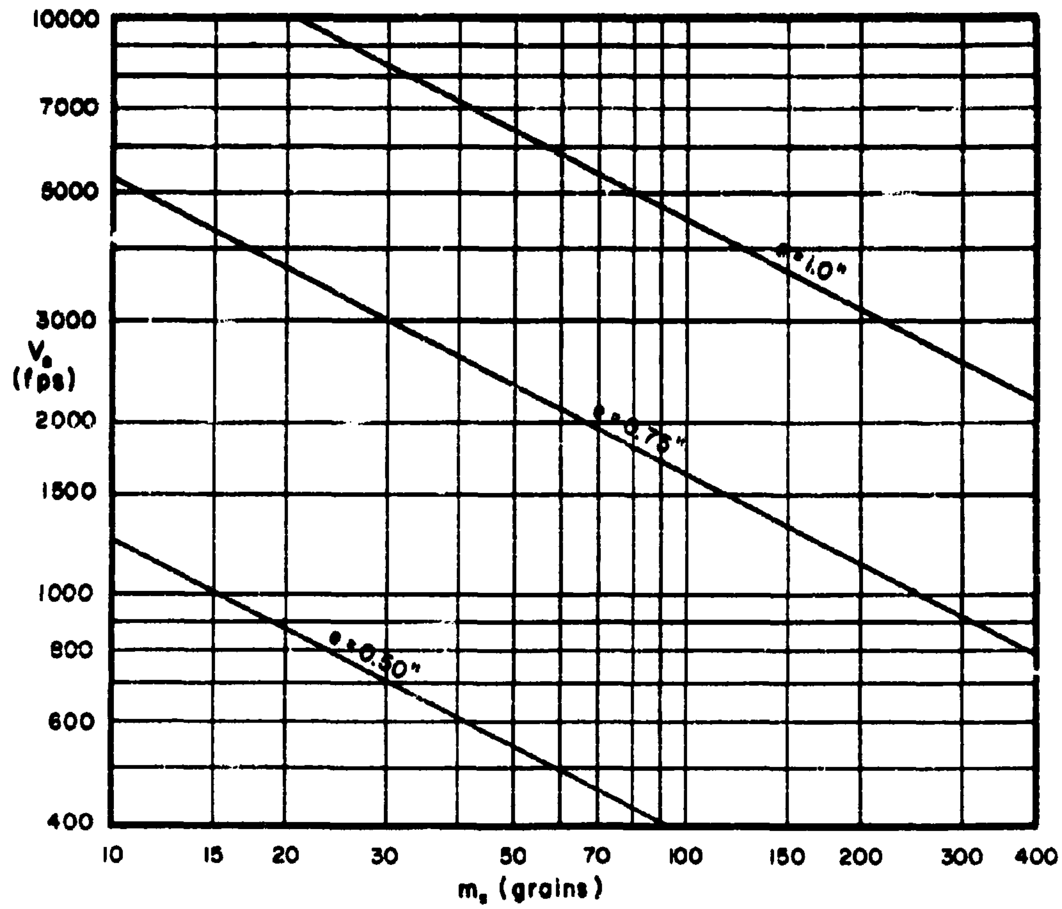

Fig. 16

V_o vs Fragment Weight for Selected Target Thicknesses

Obliquity: 70°

Target Material: Stretched Plexiglas

Fragment:

Shape: Compact

Material: Steel

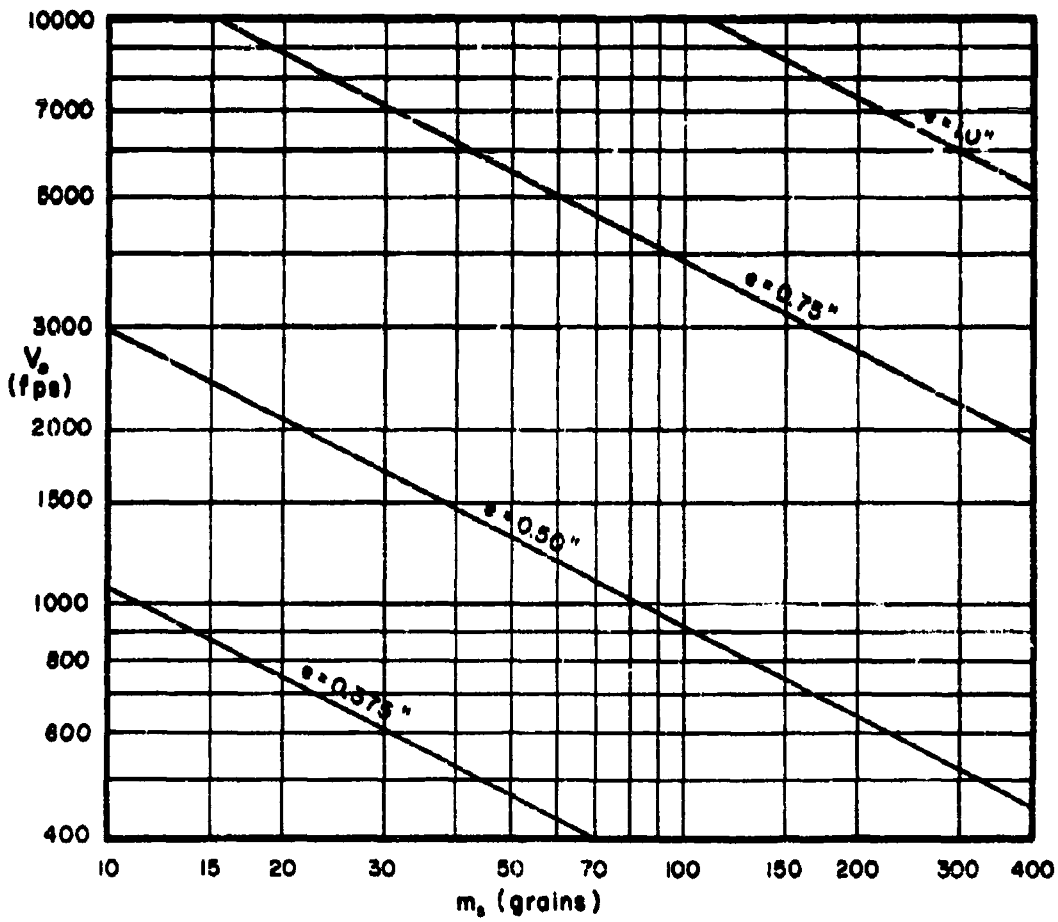

Fig. 17

V_o vs Fragment Weight for Selected Target Thicknesses

Obliquity: 0°

Target Material: Doron

Fragment:

Shape: Compact

Material: Steel

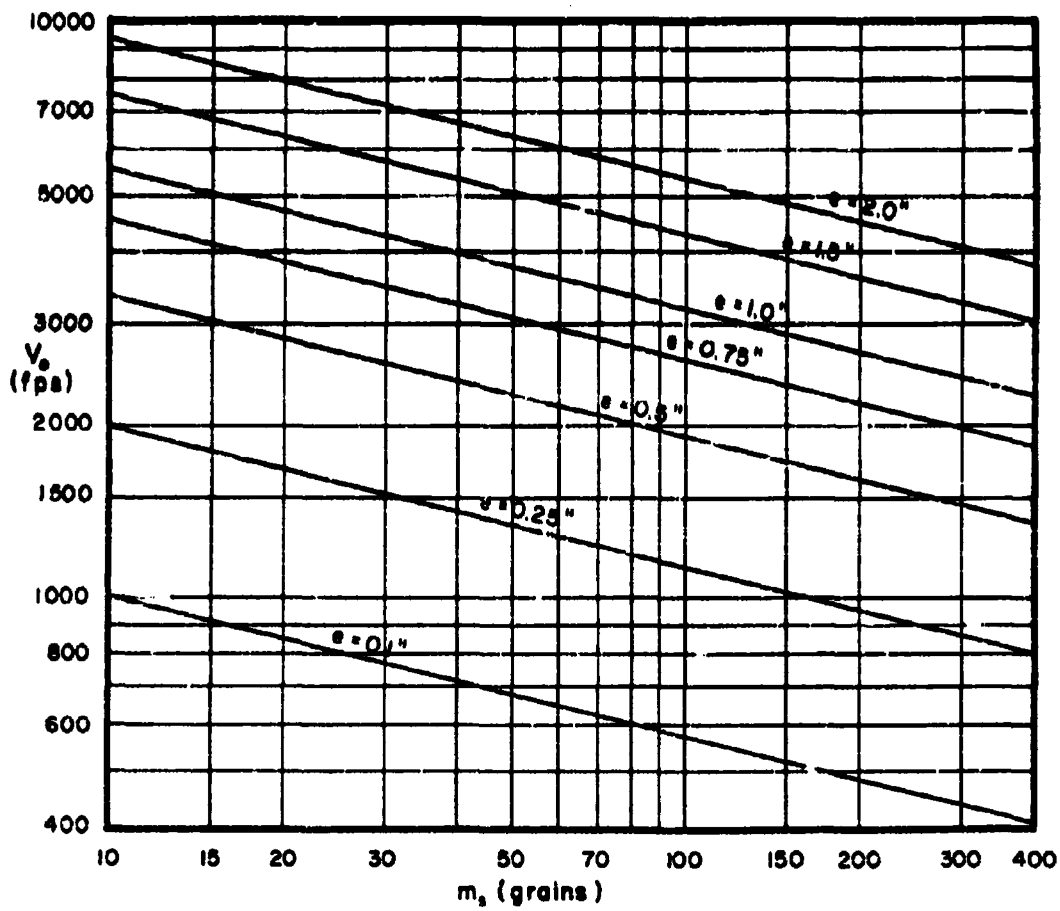

Fig. 18

V_o vs Fragment Weight for Selected Target Thicknesses

Obliquity: 60°

Target Material: Doron

Fragment:

Shape: Compact

Material: Steel

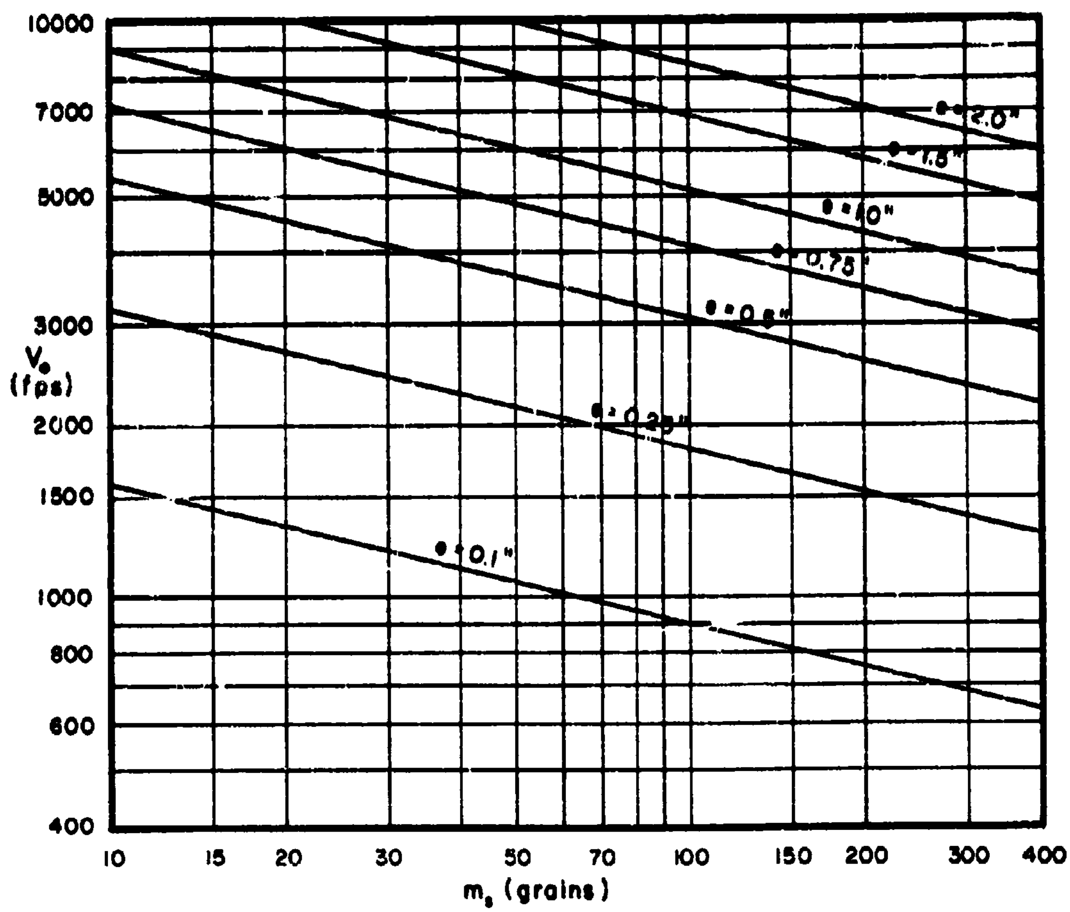

Fig. 19

V_o vs Fragment Weight for Selected Target Thicknesses

Obliquity: 70°

Target Material: Doron

Fragment:

Shape: Compact

Material: Steel

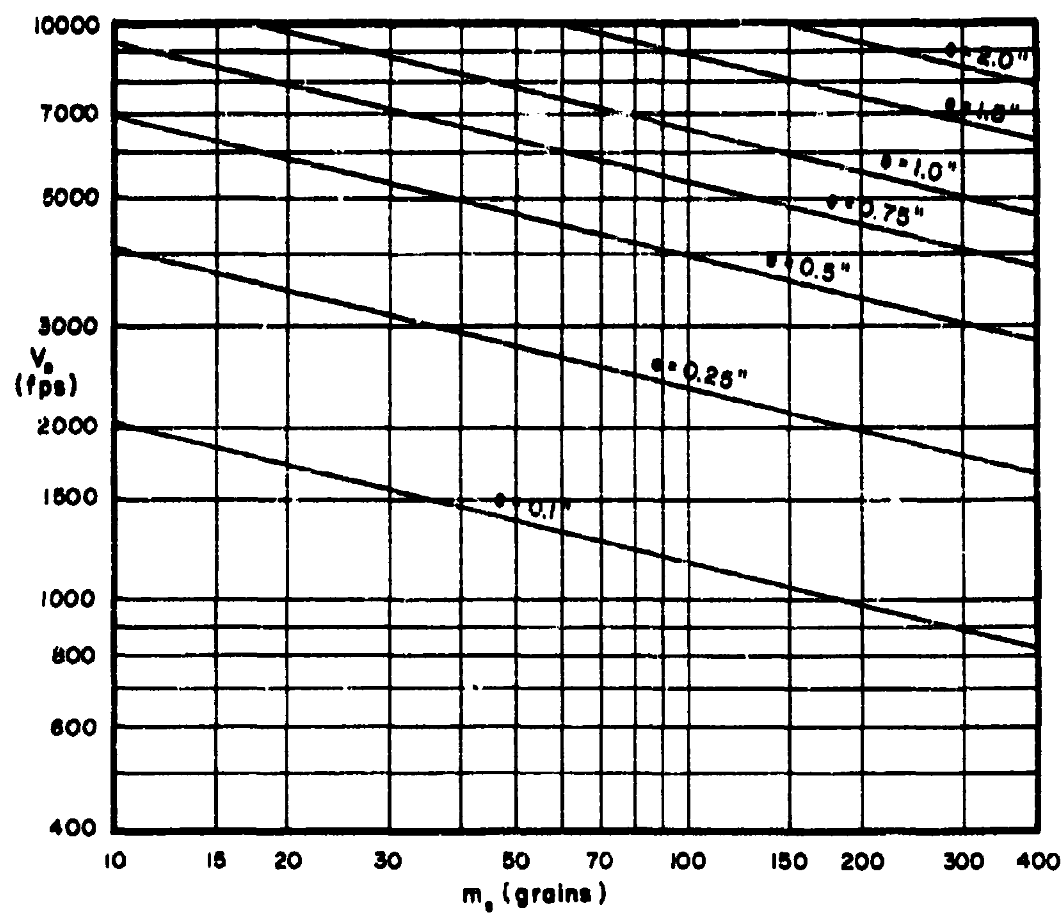

Fig. 20

V_e vs Fragment Weight for Selected Target Thicknesses

Obliquity: 0°

Target Material: Bullet-Resistant Glass

Fragment:

Shape: Compact

Material: Steel

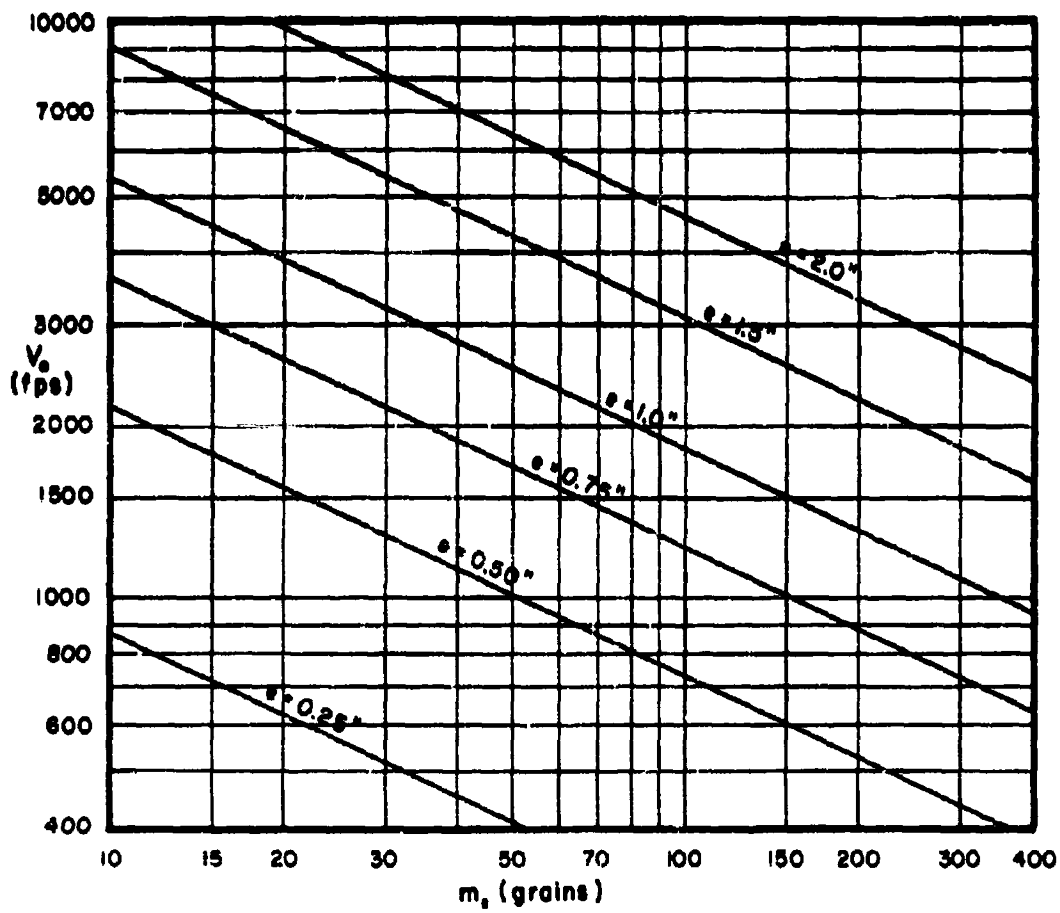

Fig. 21

V_e vs Fragment Weight for Selected Target Thicknesses

Obliquity: 60°

Target Material: Bullet-Resistant Glass

Fragment:

Shape: Compact

Material: Steel

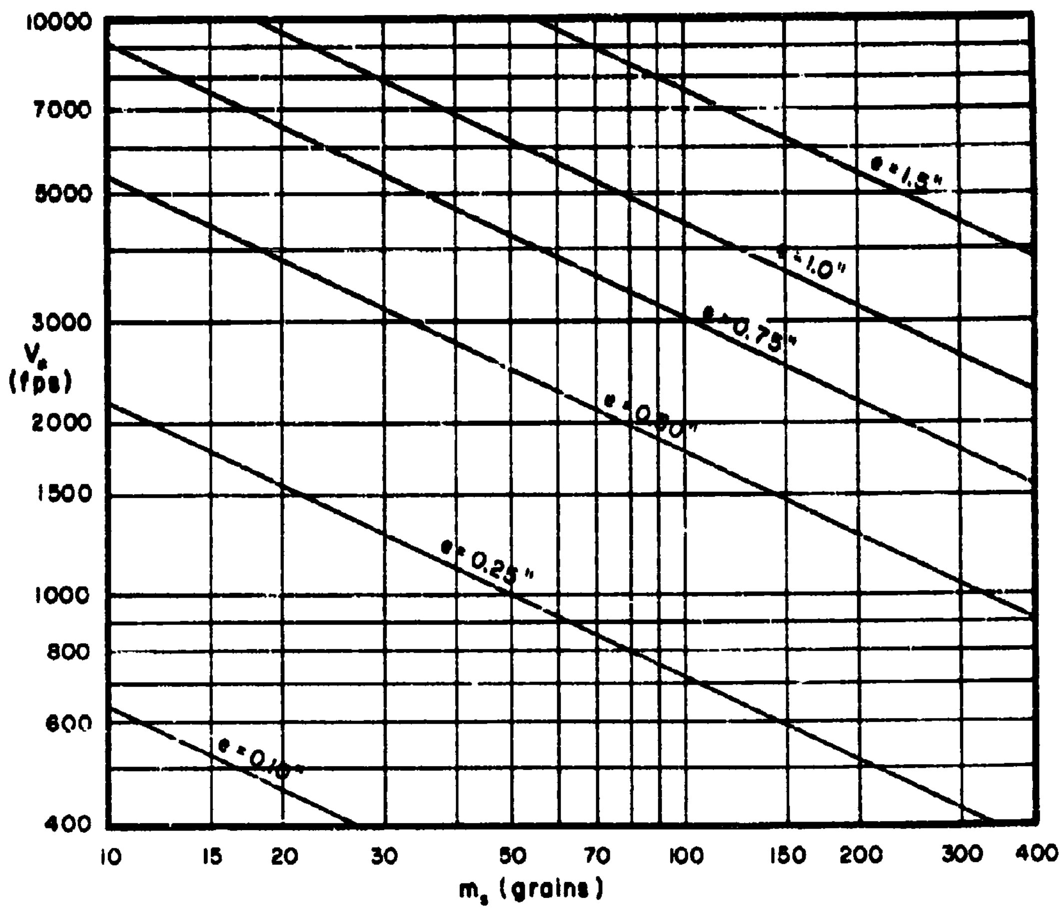

Fig. 22

V_e vs Fragment Weight for Selected Target Thicknesses

Obliquity: 70°

Target Material: Bullet-Resistant Glass

Fragment:

Shape: Compact

Material: Steel

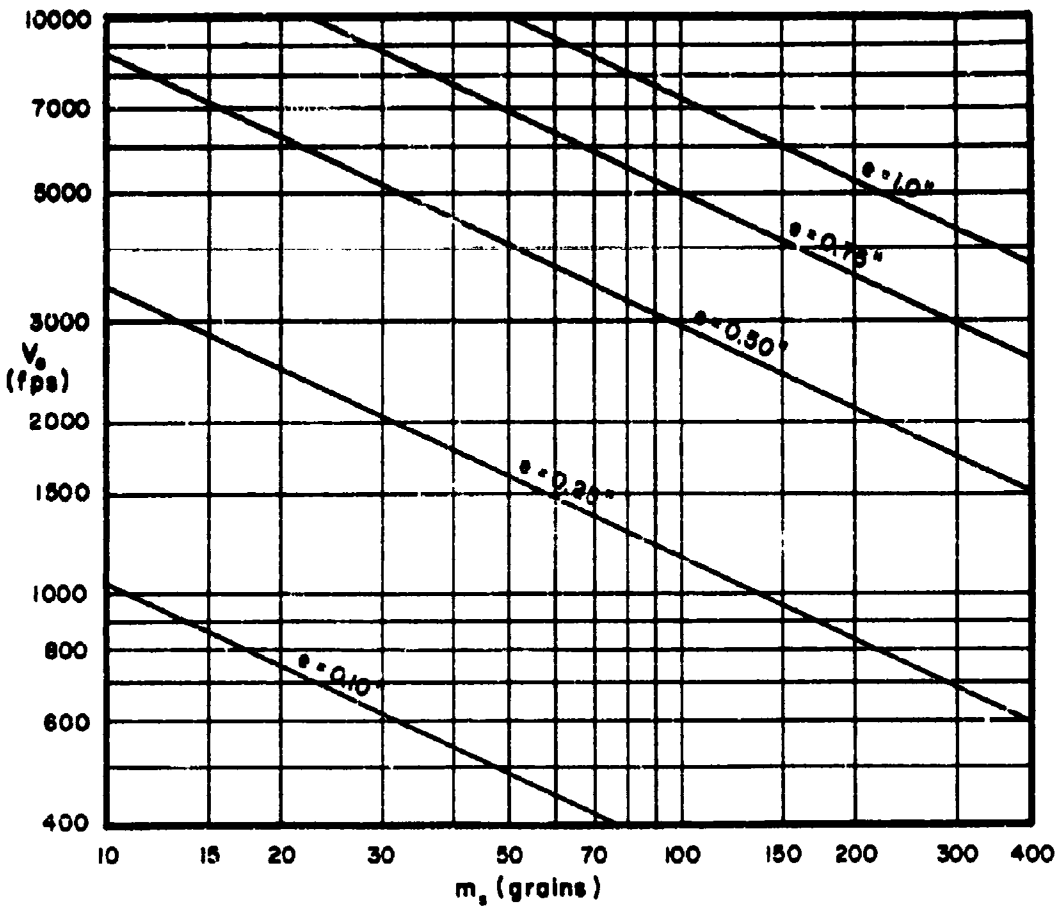

Fig. 23

V_e vs Fragment Weight for Selected Target Thicknesses

Obliquity: 60°

Target Material: Bullet-Resistant Glass

Fragment:

Shape: Compact

Material: Steel

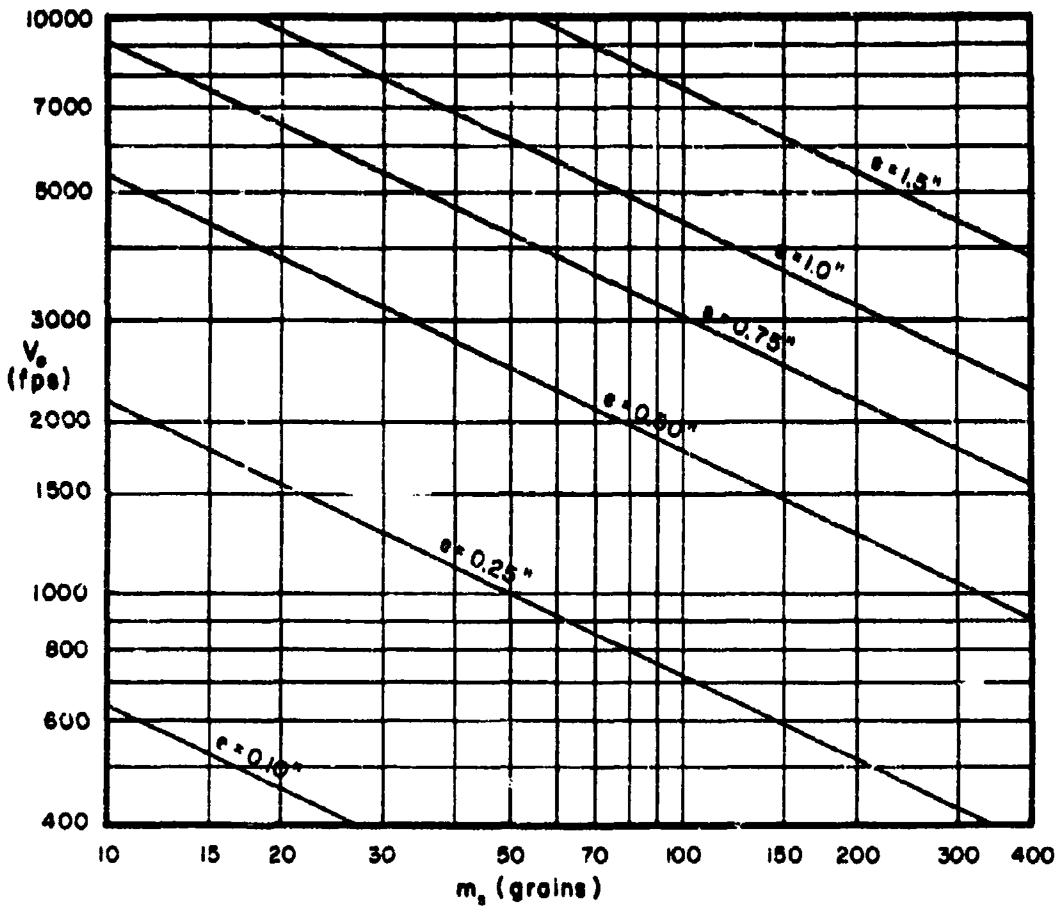

Fig. 22

Appendix B

Graph Set II: $\frac{V_r}{V_s}$ and $\frac{m_r}{m_s}$ vs V_s for Selected Values of m_s and θ

Figs. 24-86

Note: The use of double ordinates in these graphs requires some explanation. Two sets of thickness contours are to be found on each graph of this type. The thickness contours drawn with solid lines refer to the left-hand ordinate; the dashed contours refer to the right-hand ordinate. Thus, for a given graph and a given striking velocity, two ratios are found. The contours are shown only where both ratios are positive. The dotted lines on these graphs suggest that the associated residual velocities apply to a particle of insignificant weight. These remarks emphasize the need for using the empirical equations for residual velocity and residual weight jointly. In this way it becomes apparent where the estimates are valid, i.e., where both estimates are positive.

CONFIDENTIAL

$\frac{V_r}{V_s}$ and $\frac{m_r}{m_s}$ vs V_s for Selected Target Thicknesses

Target: Unbonded Nylon

Obliquity: 0°

Fragment Size: 30 grains

Dashed Thickness Contours Refer to $\frac{m_r}{m_s}$ Ordinate

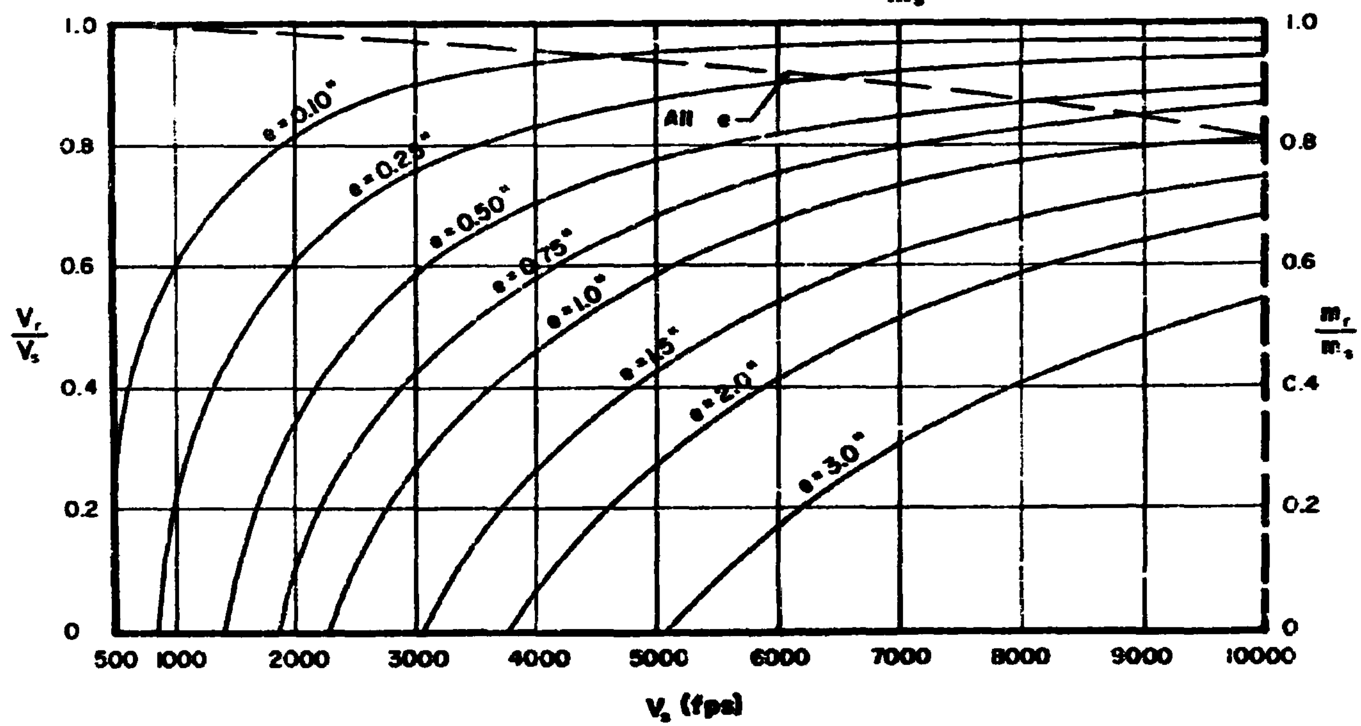

Fig. 24

CONFIDENTIAL

$\frac{V_r}{V_s}$ and $\frac{m_r}{m_s}$ vs V_s for Selected Target Thicknesses

Target: Unbonded Nylon

Obliquity: 60°

Fragment Size: 30 grains

Dashed Thickness Contours Refer to $\frac{m_r}{m_s}$ Ordinate

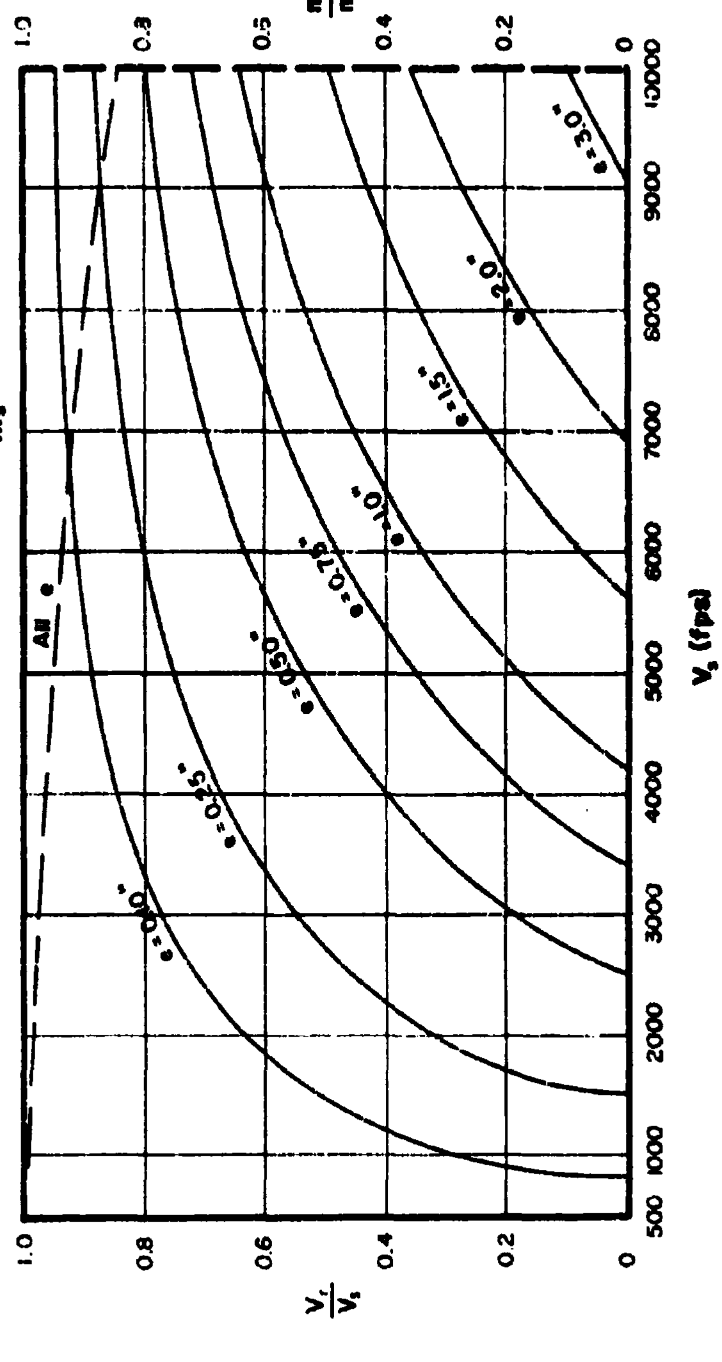

Fig. 25

$\frac{V_r}{V_s}$ and $\frac{m_r}{m_s}$ vs V_s for Selected Target Thicknesses

Target: Unbonded Nylon

Obliquity: 70°

Fragment Size: 30 grains

Dashed Thickness Contours Refer to $\frac{m_r}{m_s}$ Ordinate

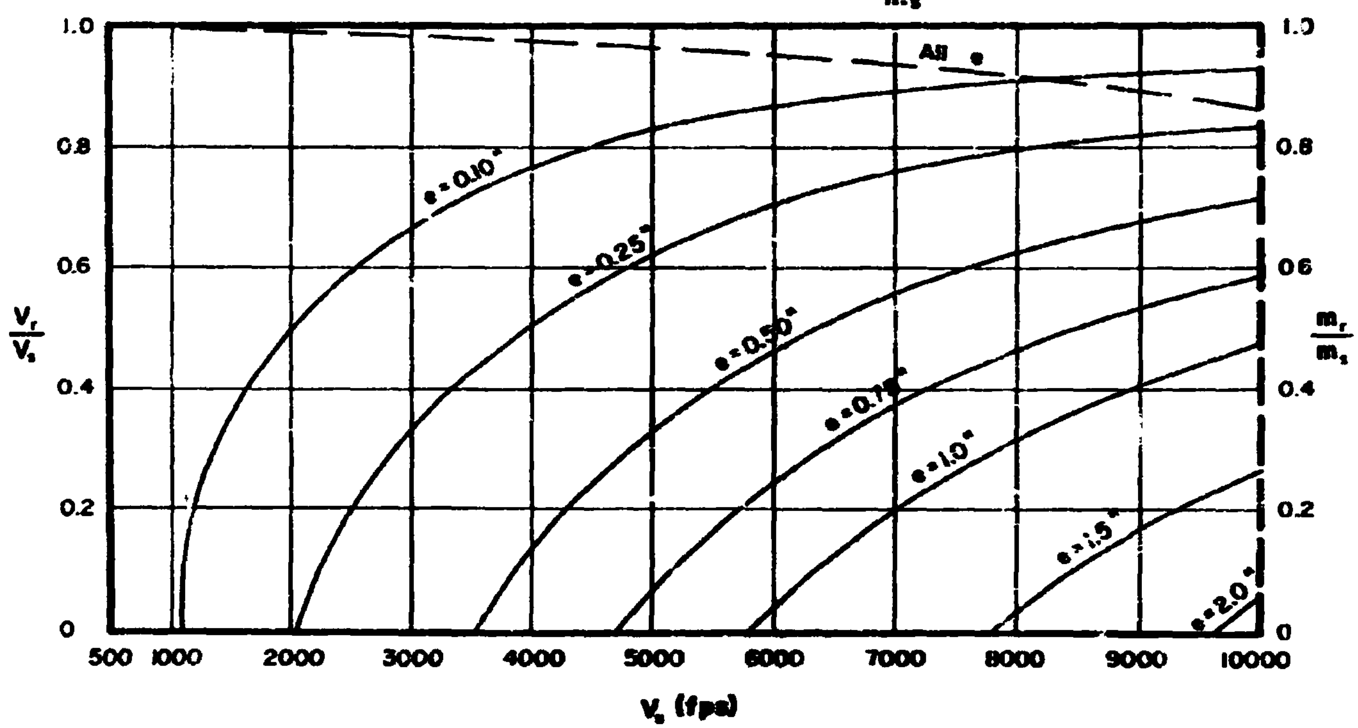

Fig. 26

$\frac{V_r}{V_s}$ and $\frac{m_r}{m_s}$ vs V_s for Selected Target Thicknesses

Target: Unbonded Nylon

Obliquity: 0°

Fragment Size: 100 grains

Dashed Thickness Contours Refer to $\frac{m_r}{m_s}$ Ordinate

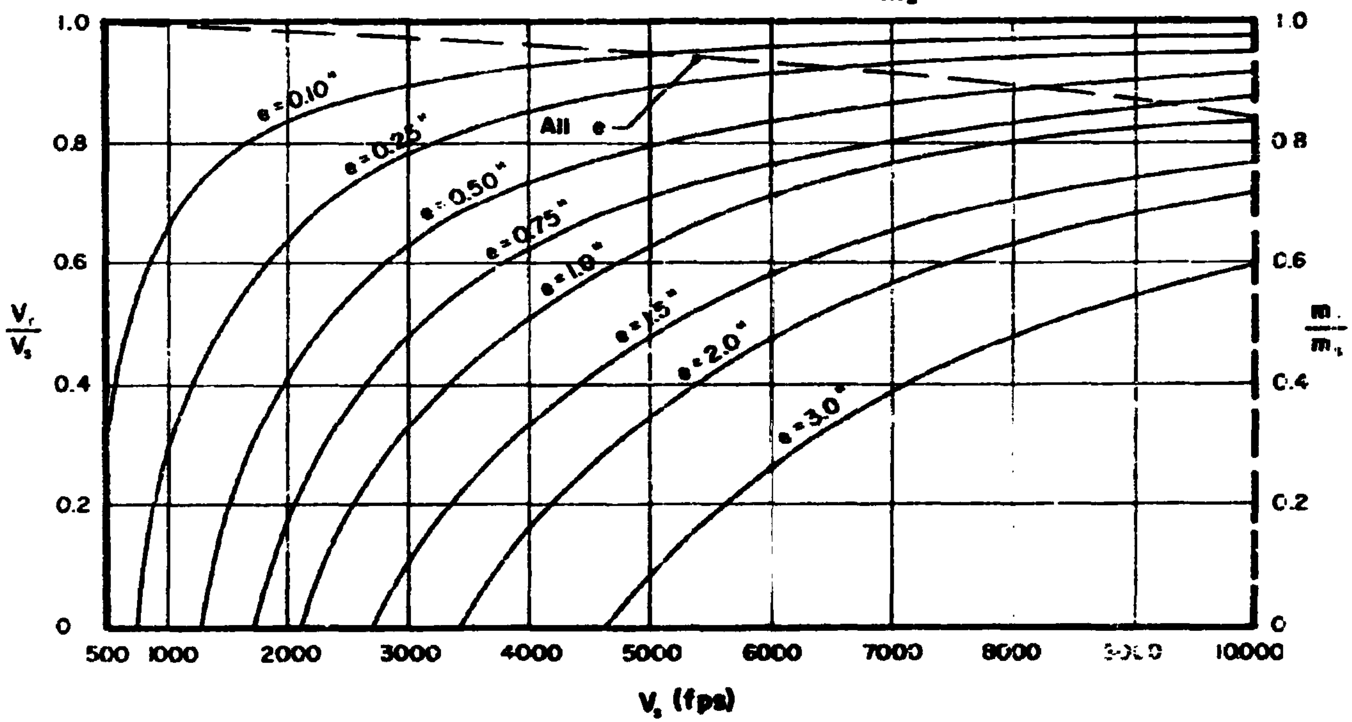

Fig. 27

$\frac{V_r}{V_s}$ and $\frac{m_r}{m_s}$ vs V_s for Selected Target Thicknesses

Target: Unbonded Nylon

Obliquity: 60°

Fragment Size: 100 grains

Dashed Thickness Contours Refer to $\frac{m_r}{m_s}$ Ordinate

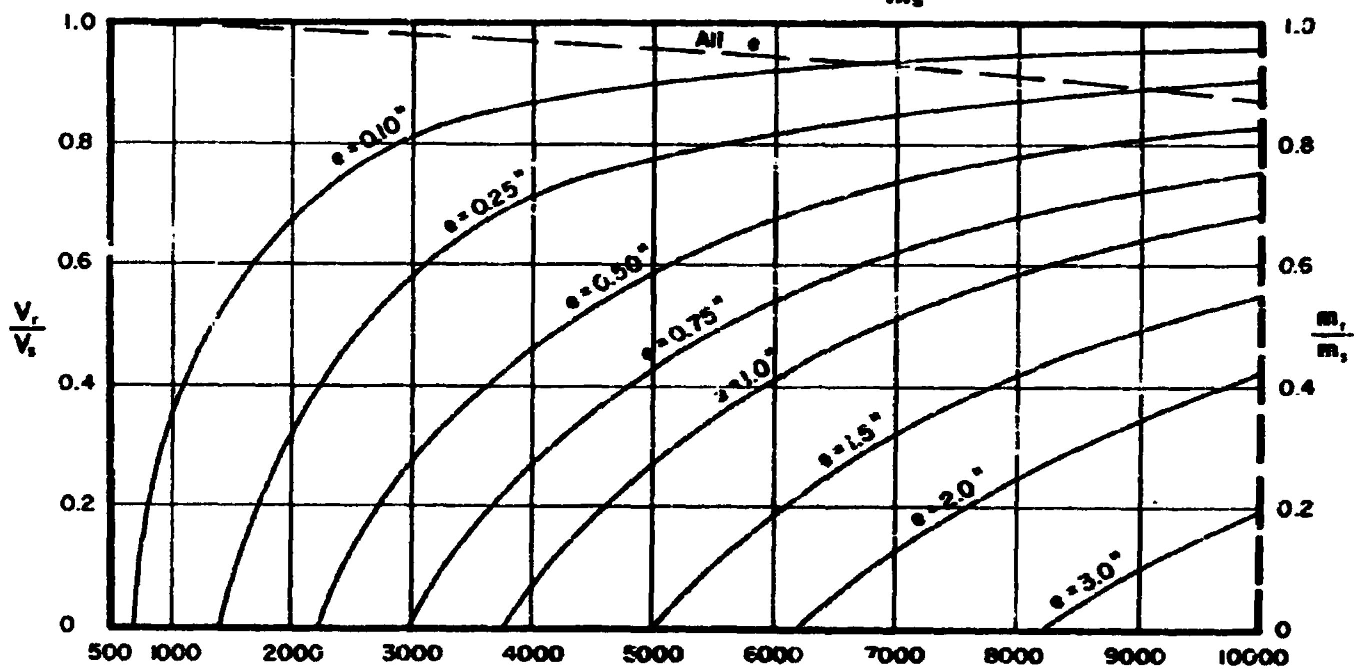

Fig. 28

$\frac{V_r}{V_s}$ and $\frac{m_r}{m_s}$ vs V_s for Selected Target Thicknesses

Target: Unbonded Nylon

Obliquity: 70°

Fragment Size: 100 grains

Dashed Thickness Contours Refer to $\frac{m_r}{m_s}$ Ordinate

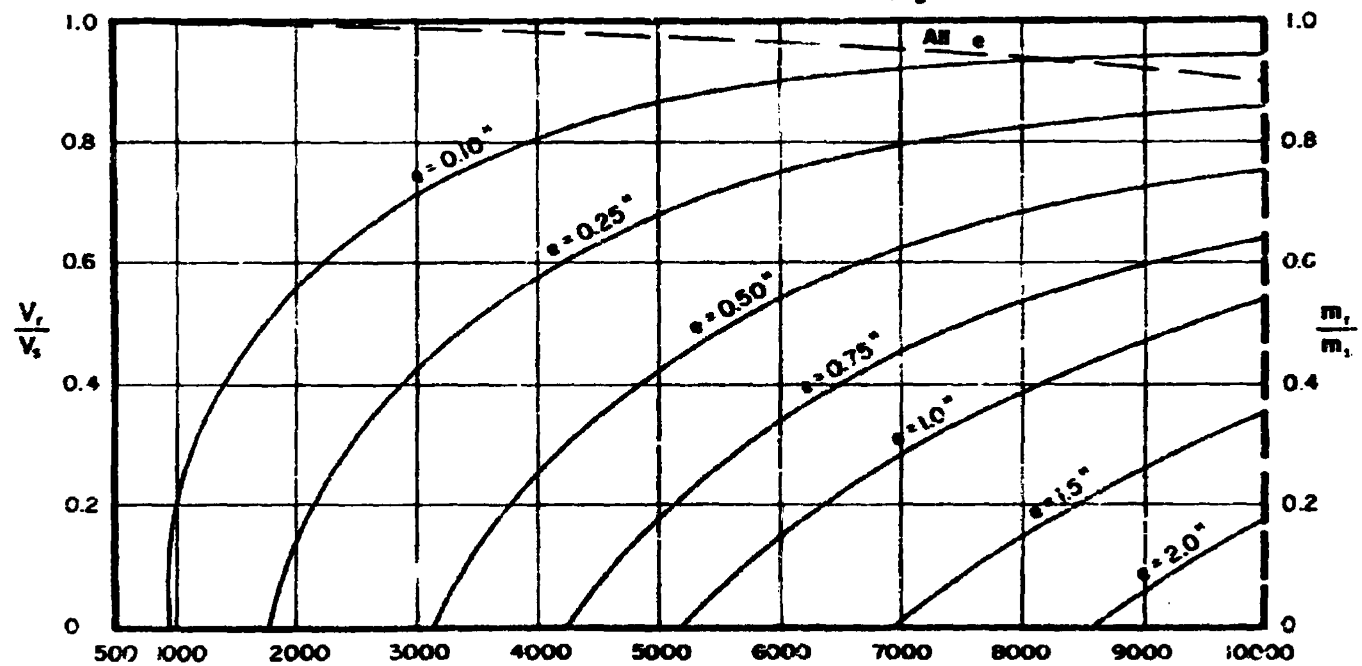

Fig. 29

$\frac{V_r}{V_s}$ and $\frac{m_r}{m_s}$ vs V_s for Selected Target Thicknesses

Target: Unbonded Nylon

Obliquity: 0°

Fragment Size: 300 grains

Dashed Thickness Contours Refer to $\frac{m_r}{m_s}$ Ordinate

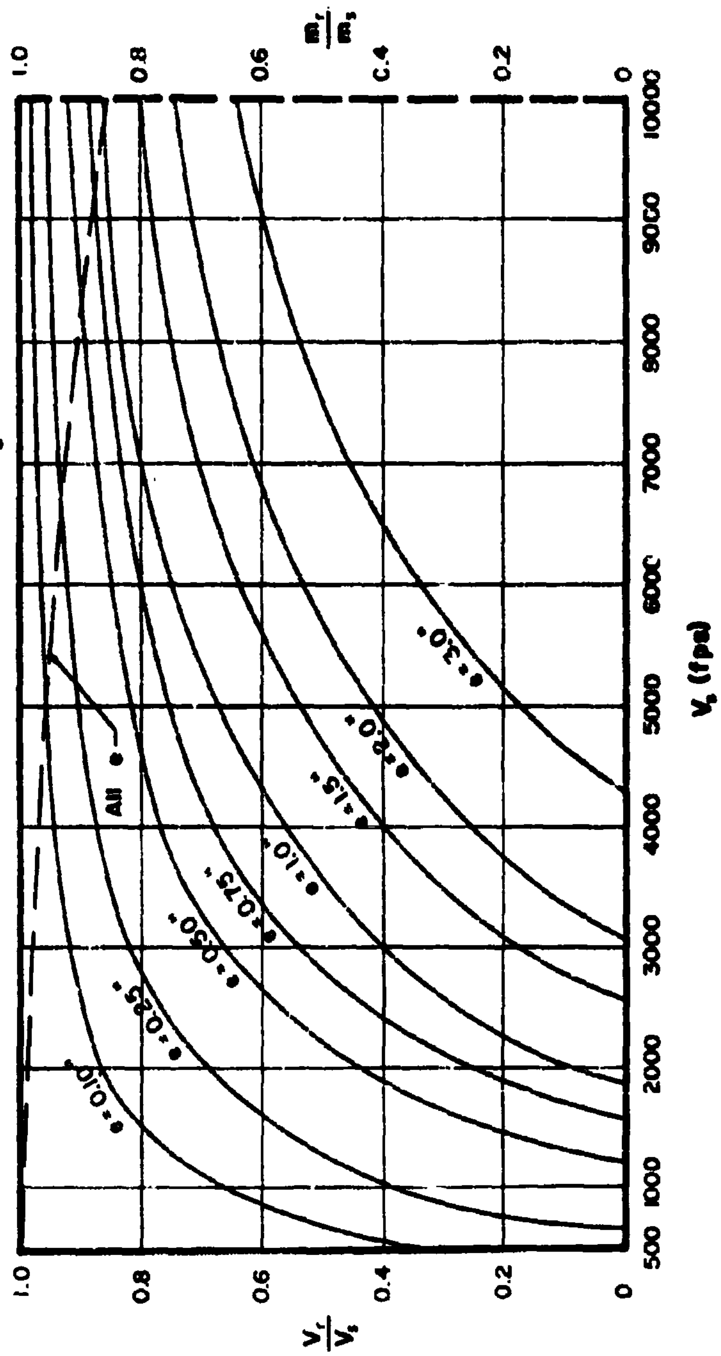

Fig. 30

$\frac{V_r}{V_s}$ and $\frac{m_r}{m_s}$ vs V_s for Selected Target Thicknesses

Target: Unbonded Nylon

Obliquity: 60°

Fragment Size: 300 grains

Dashed Thickness Contours Refer to $\frac{m_r}{m_s}$ Ordinate

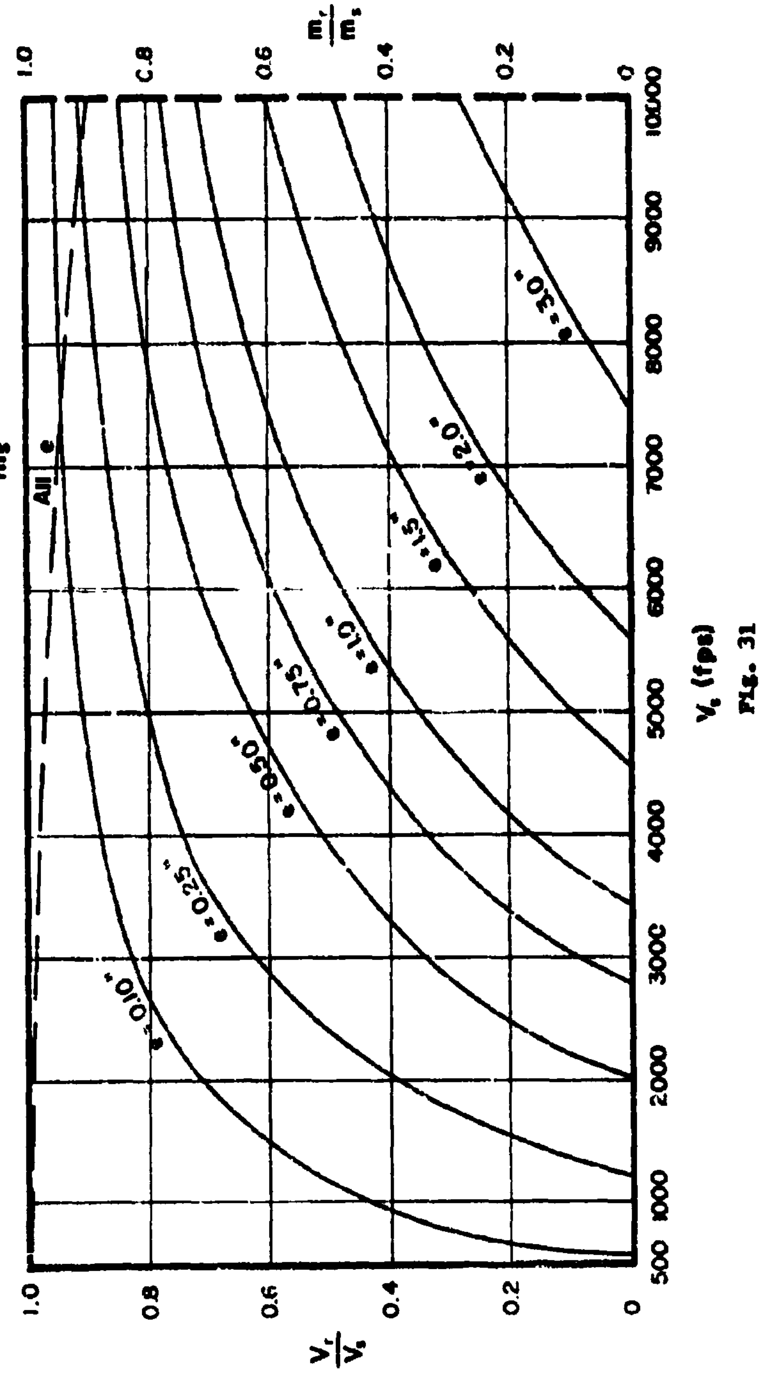

Fig. 31

$\frac{V_r}{V_s}$ and $\frac{m_r}{m_s}$ vs V_s for Selected Target Thicknesses

Target: Unbonded Nylon

Obliquity: 70°

Fragment Size: 300 grains

Dashed Thickness Contours Refer to $\frac{m_r}{m_s}$ Ordinate

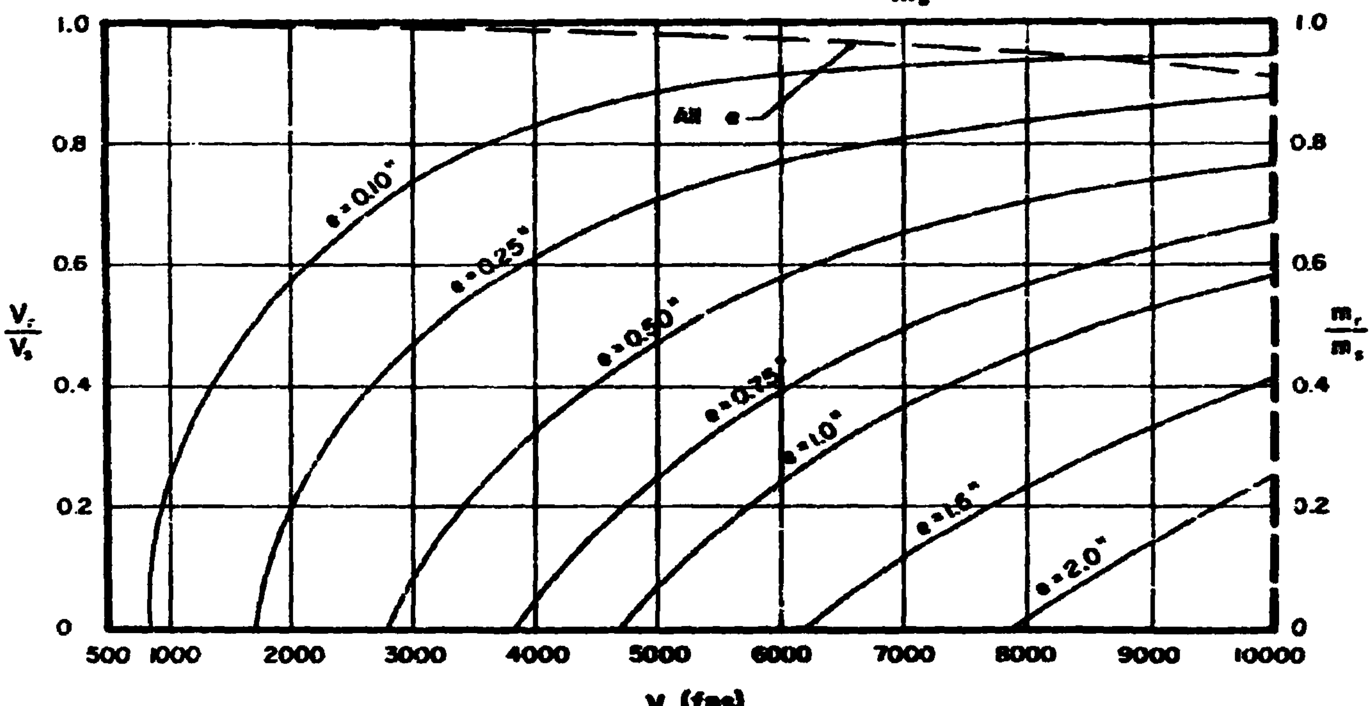

Fig. 32

$\frac{V_r}{V_s}$ and $\frac{m_r}{m_s}$ vs V_s for Selected Target Thicknesses

Target: Bonded Nylon

Obliquity: 0°

Fragment Size: 30 grains

Dashed Thickness Contours Refer to $\frac{m_r}{m_s}$ Ordinate

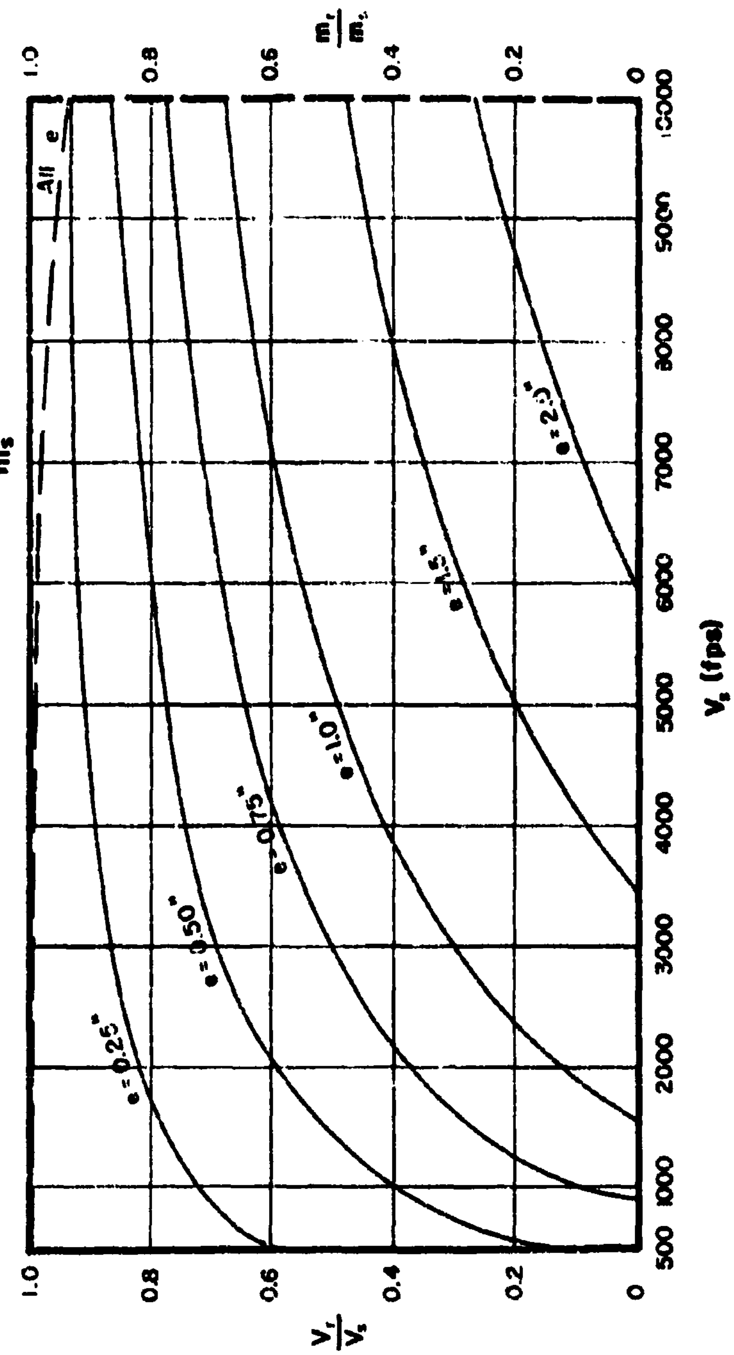

Fig. 33

$\frac{V_r}{V_s}$ and $\frac{m_r}{m_s}$ vs V_s for Selected Target Thicknesses

Target: Bonded Nylon

Obliquity: 60°

Fragment Size: 30 grains

Dashed Thickness Contours Refer to $\frac{m_r}{m_s}$ Ordinate

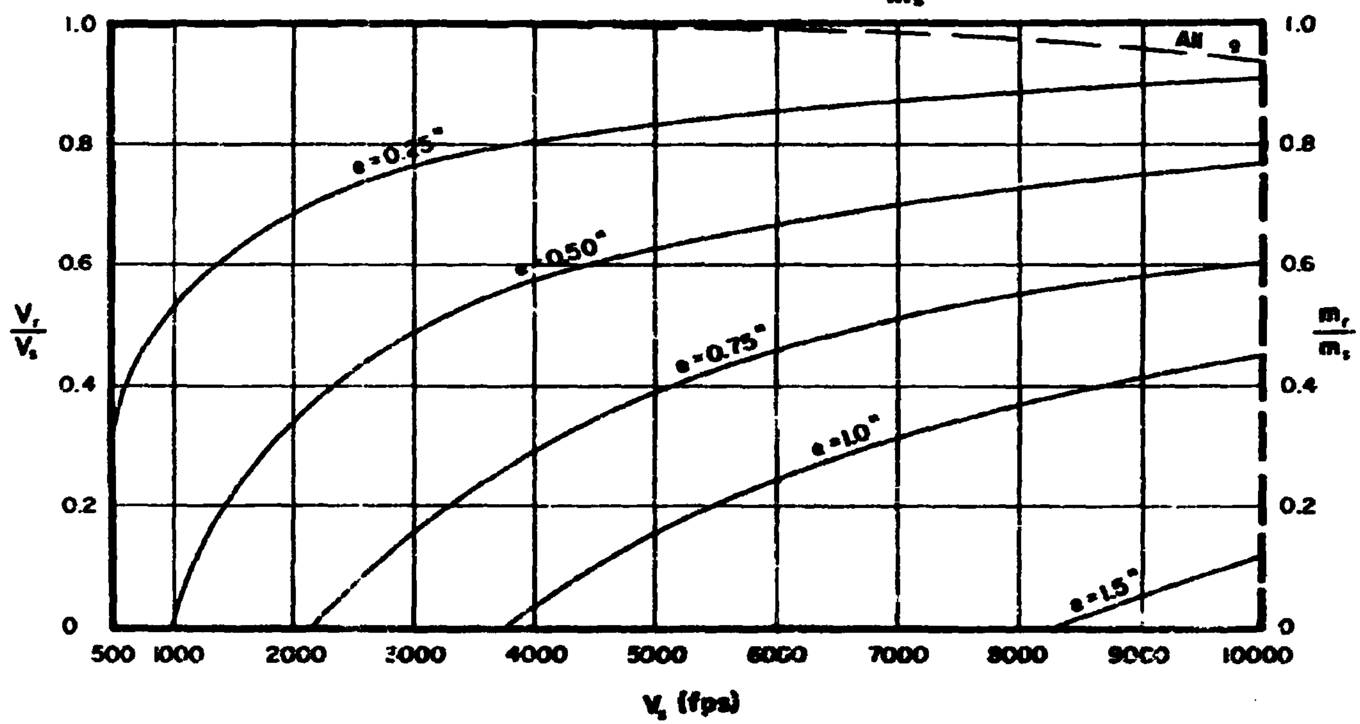

Fig. 36

$\frac{V_r}{V_s}$ and $\frac{m_r}{m_s}$ vs V_s for Selected Target Thicknesses

Target: Bonded Nylon

Obliquity: 70°

Fragment Size: 30 grains

Dashed Thickness Contours Refer to $\frac{m_r}{m_s}$ Ordinate

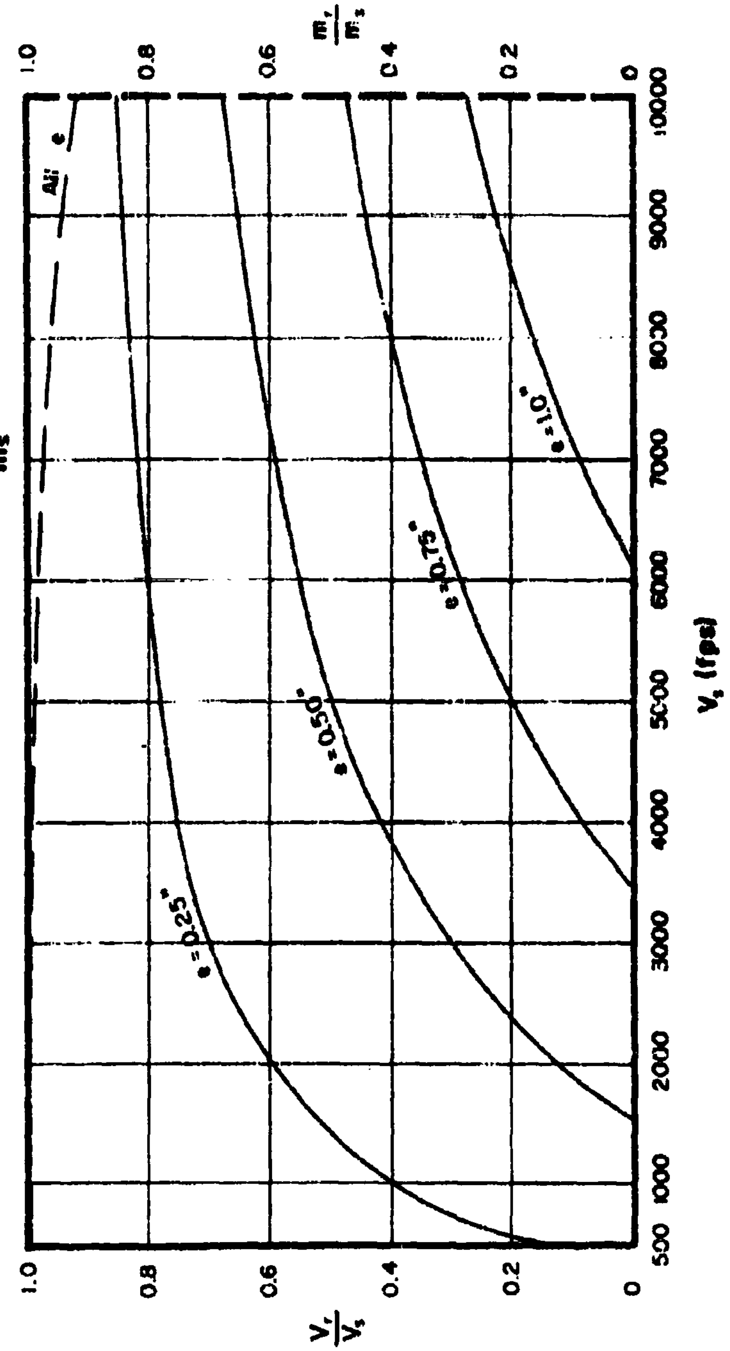

Fig. 35

$\frac{V_r}{V_s}$ and $\frac{m_r}{m_s}$ vs V_s for Selected Target Thicknesses

Target: Bonded Nylon

Obliquity: 0°

Fragment Size: 100 grains

Dashed Thickness Contours Refer to $\frac{m_r}{m_s}$ Ordinate

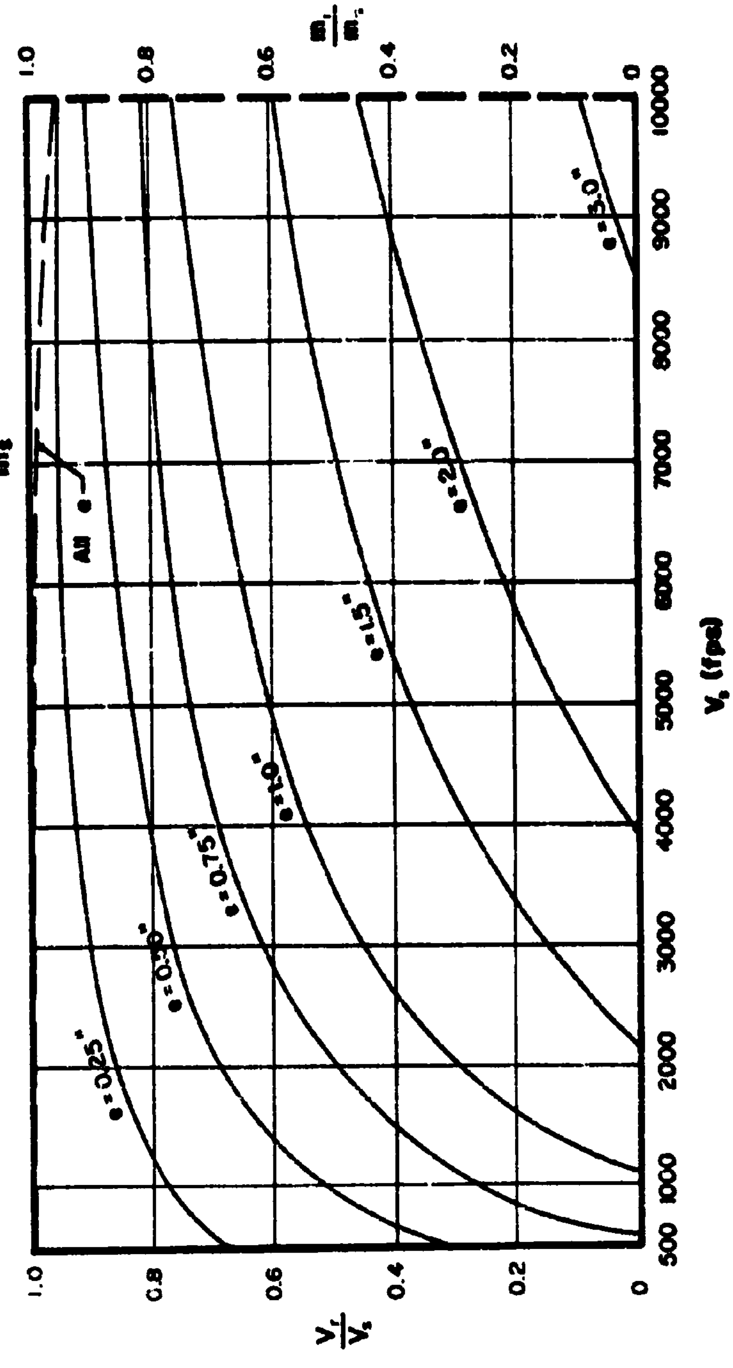

Fig. 36

$\frac{V_r}{V_s}$ and $\frac{m_r}{m_s}$ vs V_s for Selected Target Thicknesses

Target: Bonded Nylon

Obliquity: 60°

Fragment Size: 100 grains

Dashed Thickness Contours Refer to $\frac{m_r}{m_s}$ Ordinate

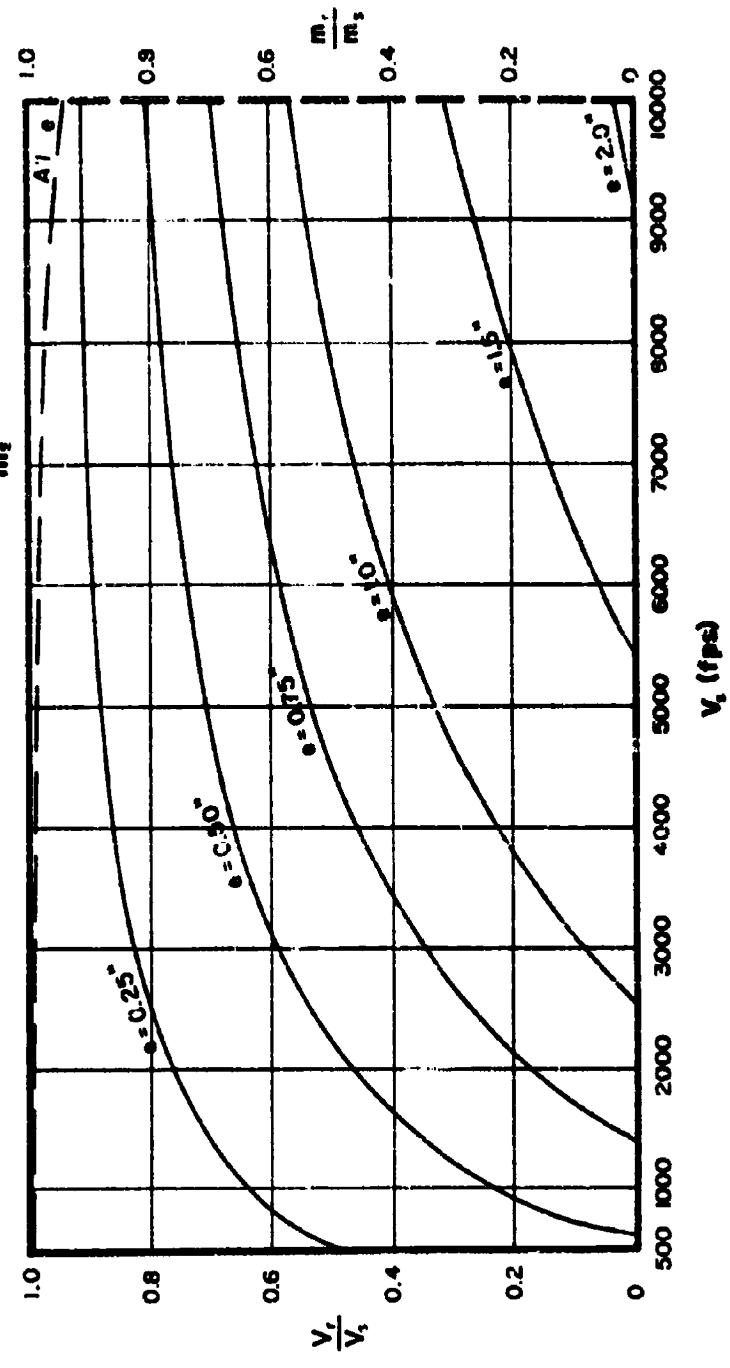

Fig. 37

$\frac{V_r}{V_s}$ and $\frac{m_r}{m_s}$ vs V_s for Selected Target Thicknesses

Target: Bonded Nylon

Obliquity: 70°

Fragment Size: 100 grains

Dashed Thickness Contours Refer to $\frac{m_r}{m_s}$ Ordinate

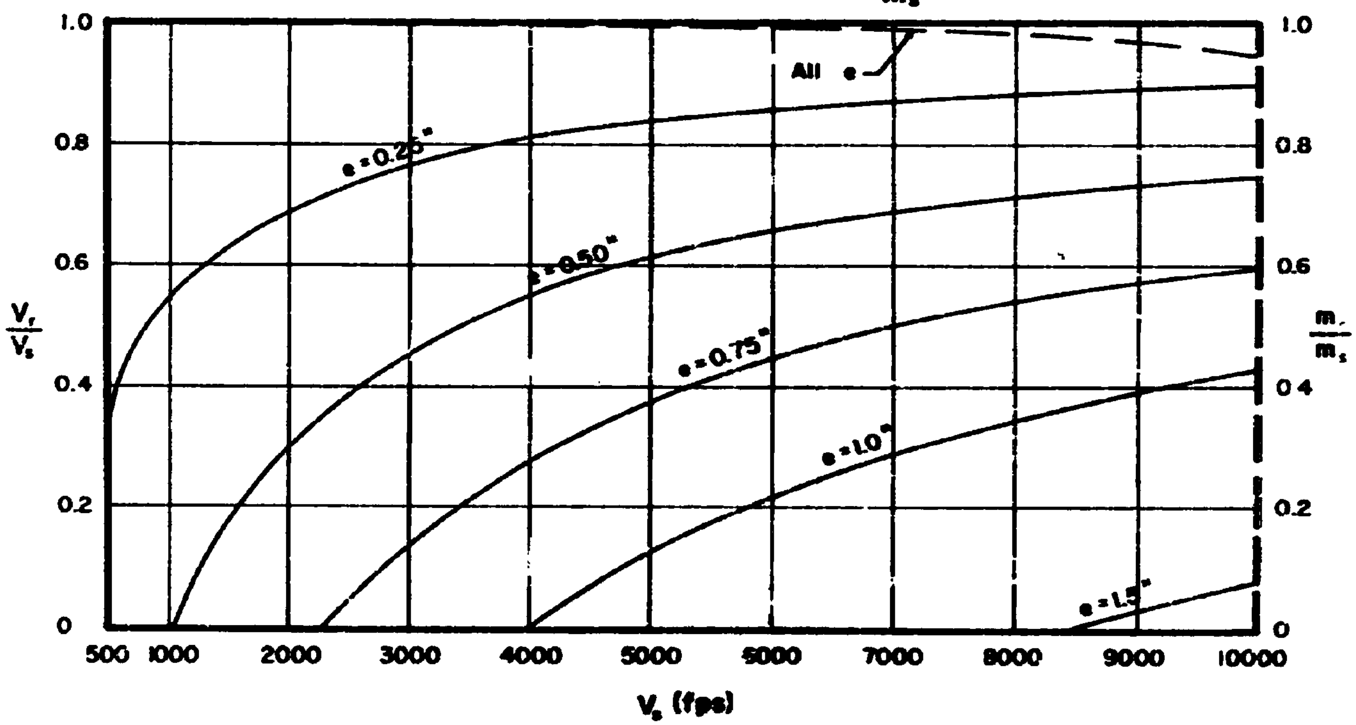

Fig. 38

$\frac{V_r}{V_s}$ and $\frac{m_r}{m_s}$ vs V_s for Selected Target Thicknesses

Target: Bonded Nylon

Obliquity: 0°

Fragment Size: 300 grains

Dashed Thickness Contours Refer to $\frac{m_r}{m_s}$ Ordinate

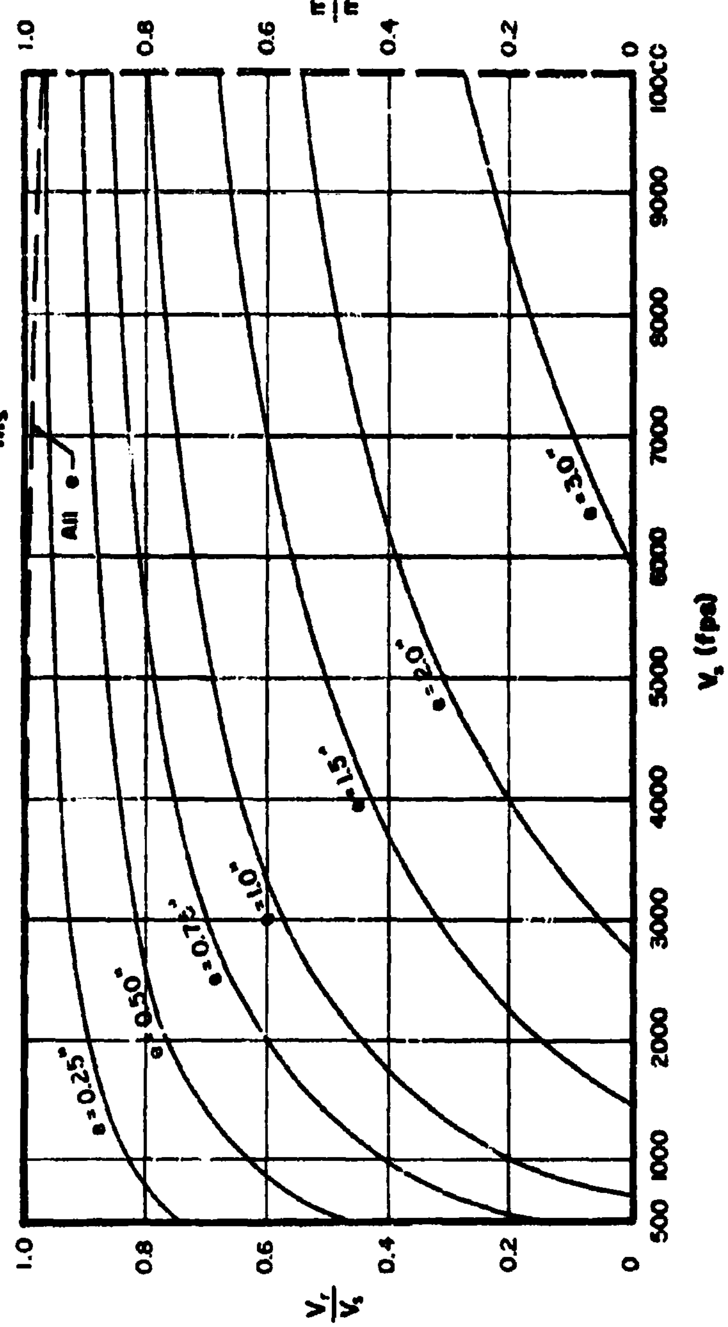

Fig. 39

$\frac{V_r}{V_s}$ and $\frac{m_r}{m_s}$ vs V_s for Selected Target Thicknesses

Target: Bonded Nylon

Obliquity: 60°

Fragment Size: 300 grains

Dashed Thickness Contours Refer to $\frac{m_r}{m_s}$ Ordinate

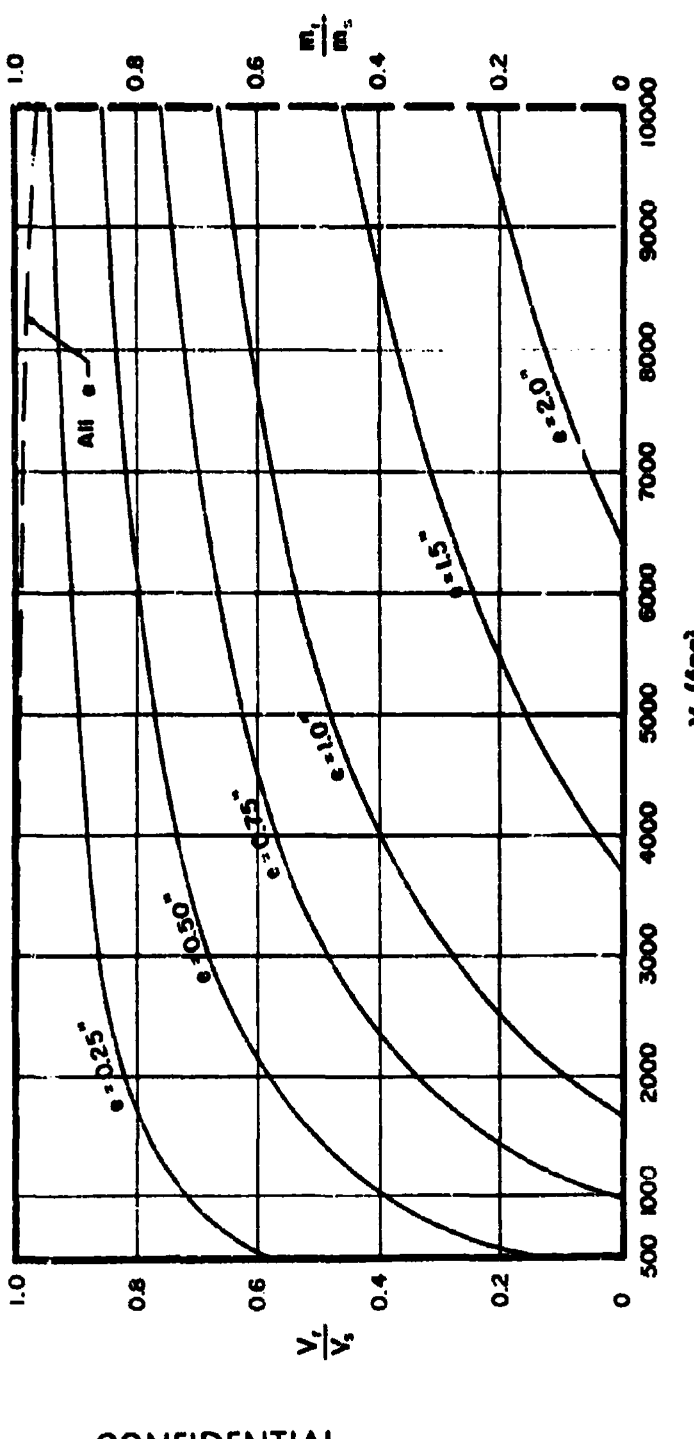

Fig. 40

$\frac{V_r}{V_s}$ and $\frac{m_r}{m_s}$ vs V_s for Selected Target Thicknesses

Target: Bonded Nylon

Obliquity: 70°

Fragment Size: 300 grains

Dashed Thickness Contours Refer to $\frac{m_r}{m_s}$ Ordinate

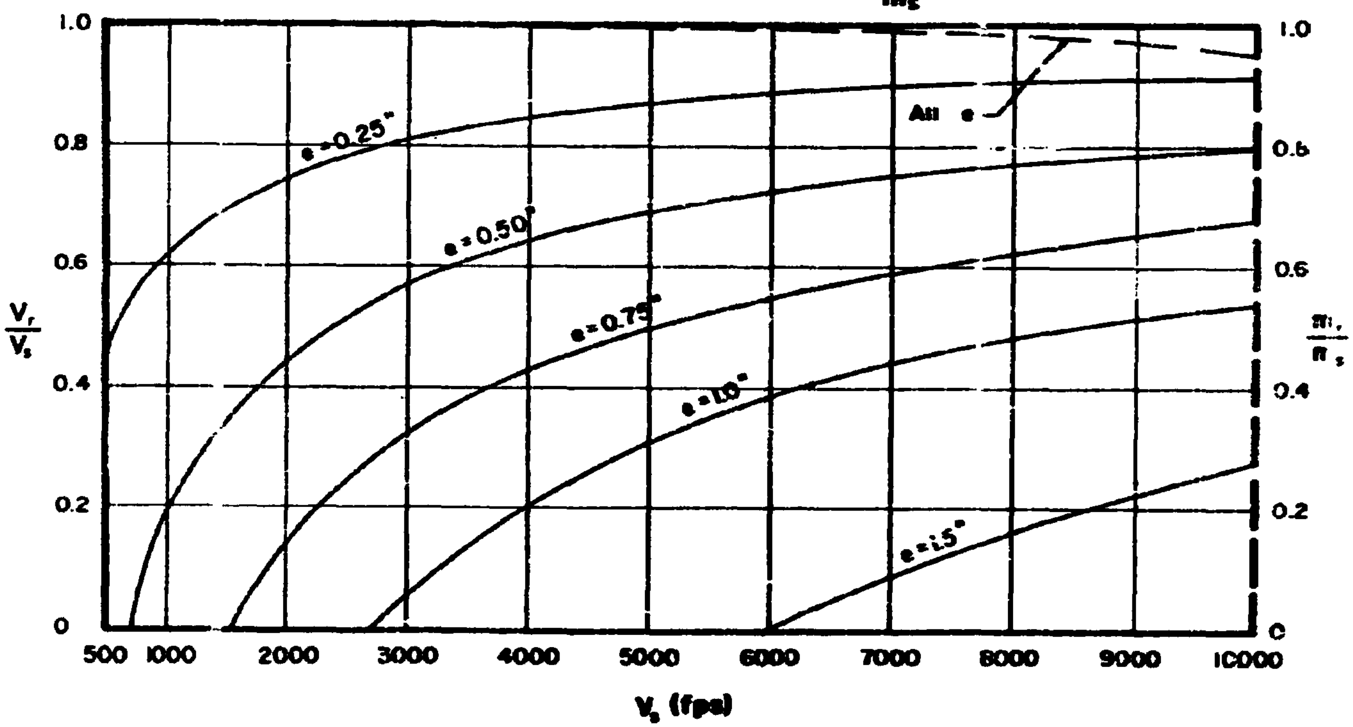

Fig. 41

$\frac{V_r}{V_s}$ and $\frac{m_r}{m_s}$ vs V_s for Selected Target Thicknesses

Target: Lexan

Obliquity: 0°

Fragment Size: 30 grains

Dashed Thickness Contours Refer to $\frac{m_r}{m_s}$ Ordinate

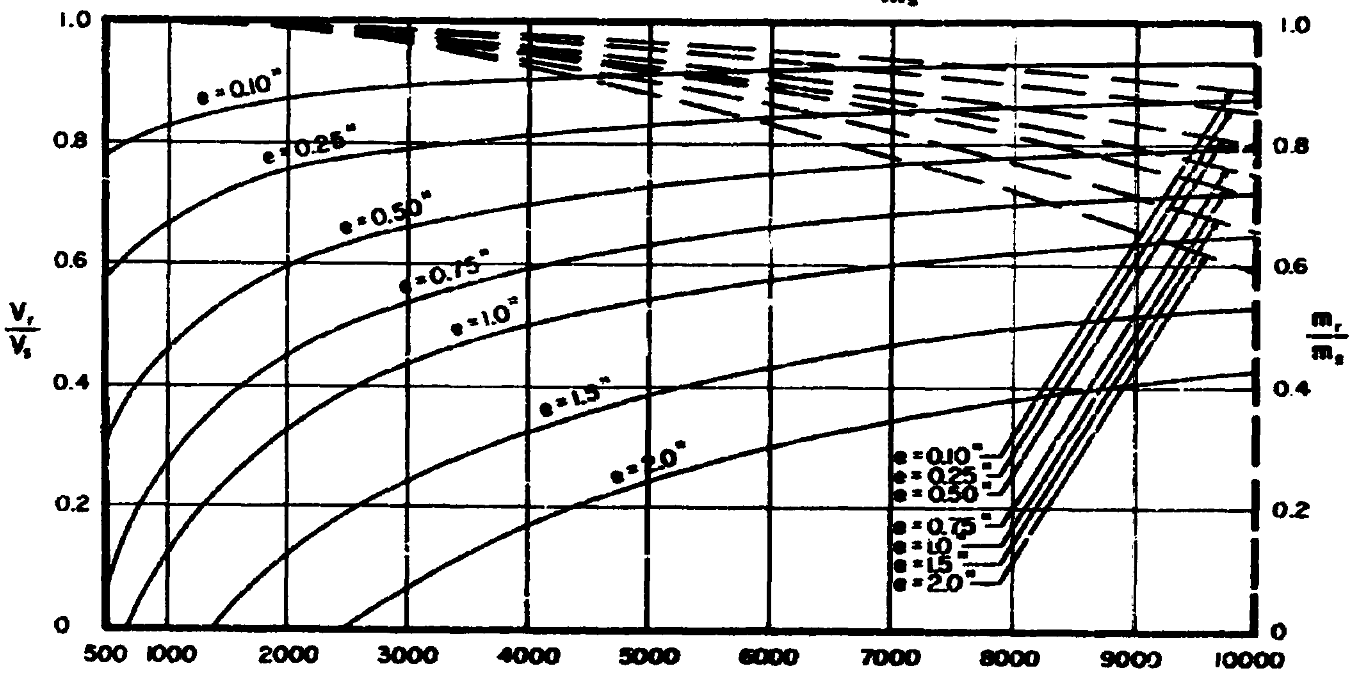

Fig. 42

CONFIDENTIAL

$\frac{V_r}{V_s}$ and $\frac{m_r}{m_s}$ vs V_s for Selected Target Thicknesses

Target: Lexan

Obliquity: 60°

Fragment Size: 30 grains

Dashed Thickness Contours Refer to $\frac{m_r}{m_s}$ Ordinate

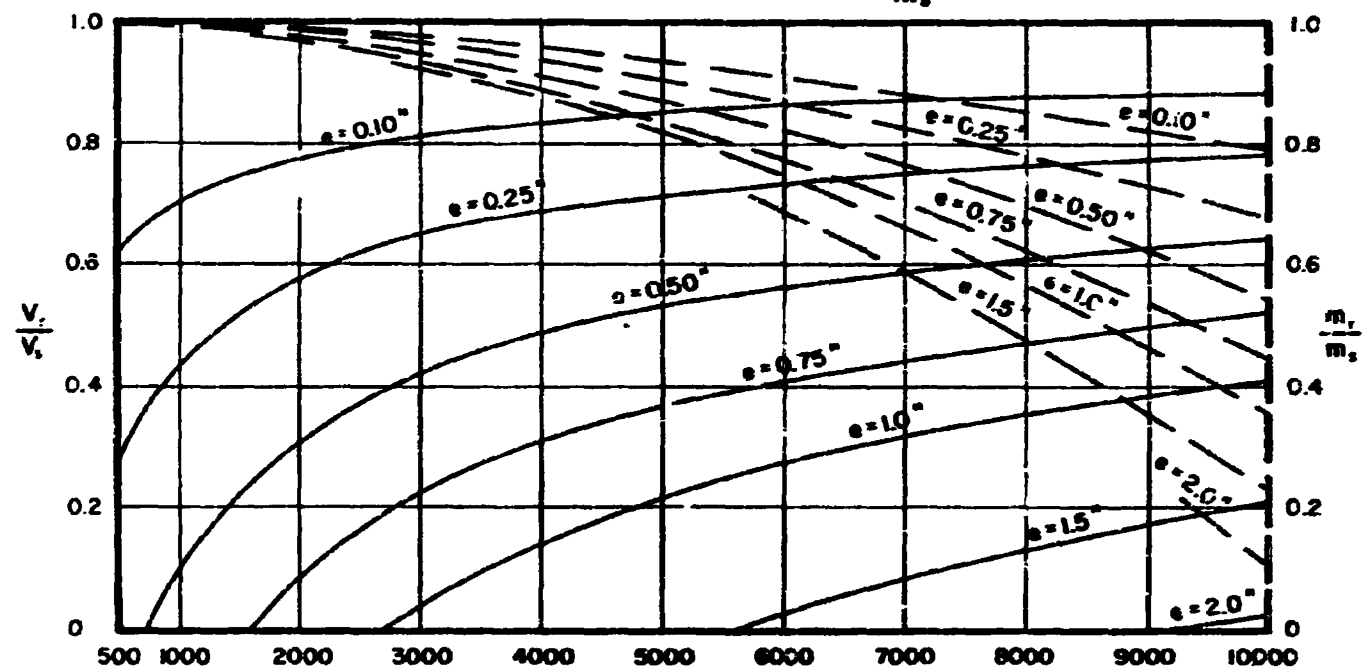

V_s (fps)

Fig. 43

$\frac{V_r}{V_s}$ and $\frac{m_r}{m_s}$ vs V_s for Selected Target Thicknesses

Target: Lexan

Obliquity: 70°

Fragment Size: 30 grains

Dashed Thickness Contours Refer to $\frac{m_r}{m_s}$ Ordinate

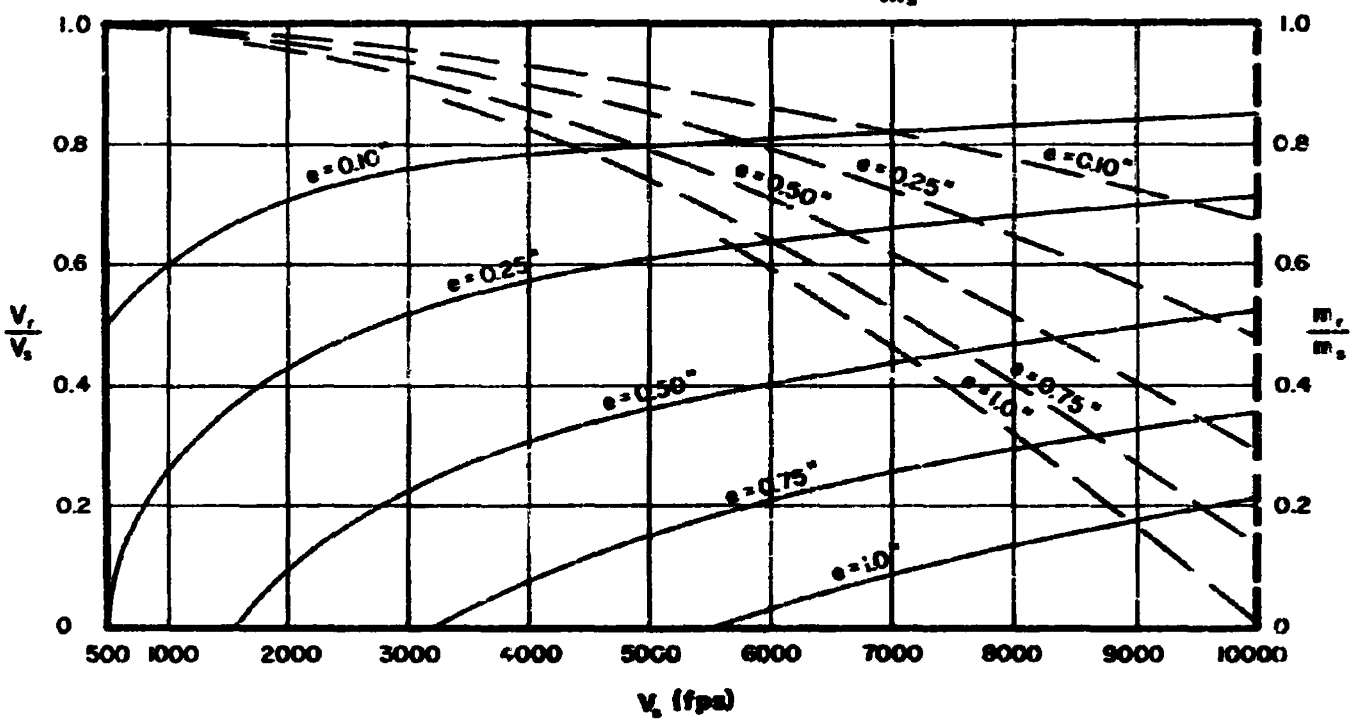

Fig. 44

$\frac{V_r}{V_s}$ and $\frac{m_r}{m_s}$ vs V_s for Selected Target Thicknesses

Target: Lexan

Obliquity: 0°

Fragment Size: 100 grains

Dashed Thickness Contours Refer to $\frac{m_r}{m_s}$ Ordinate

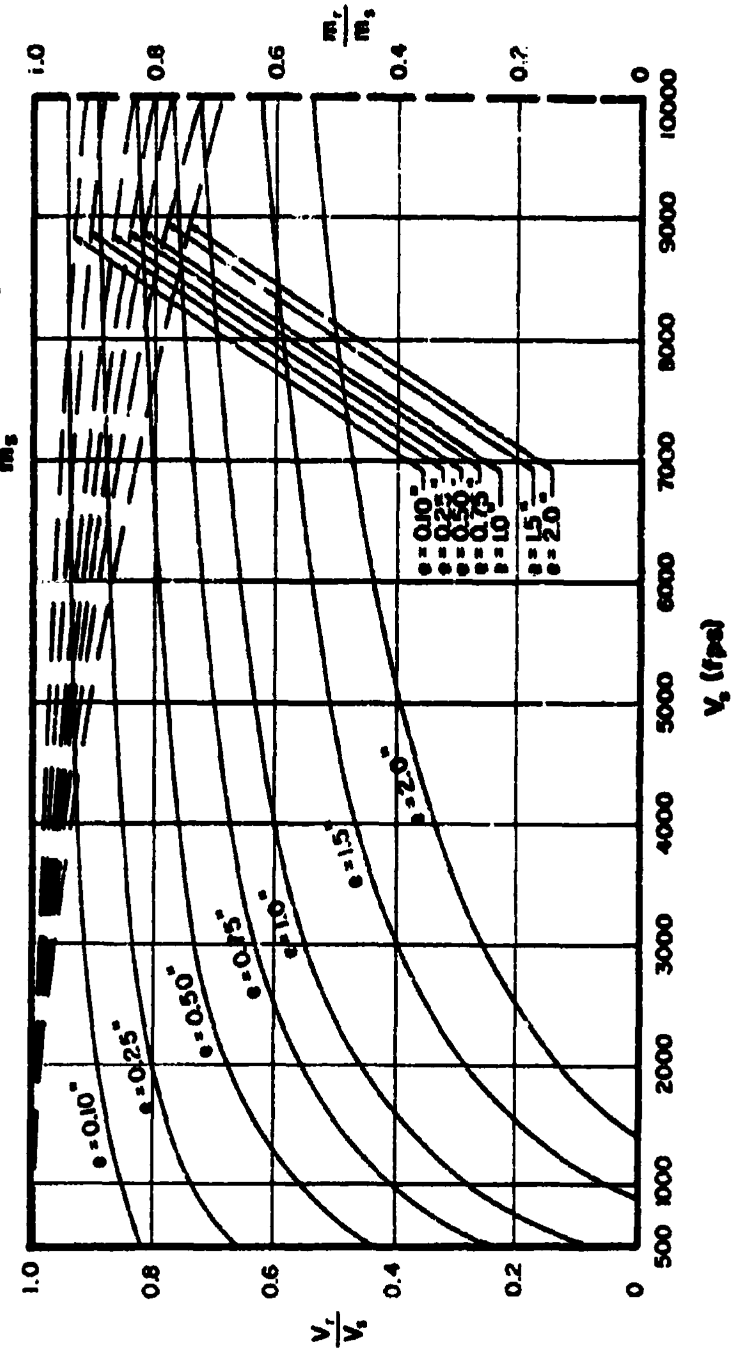

Fig. 45

$\frac{V_r}{V_s}$ and $\frac{m_r}{m_s}$ vs V_s for Selected Target Thicknesses

Target: Lexan

Obliquity: 60°

Fragment Size: 100 grains

Dashed Thickness Contours Refer to $\frac{m_r}{m_s}$ Ordinate

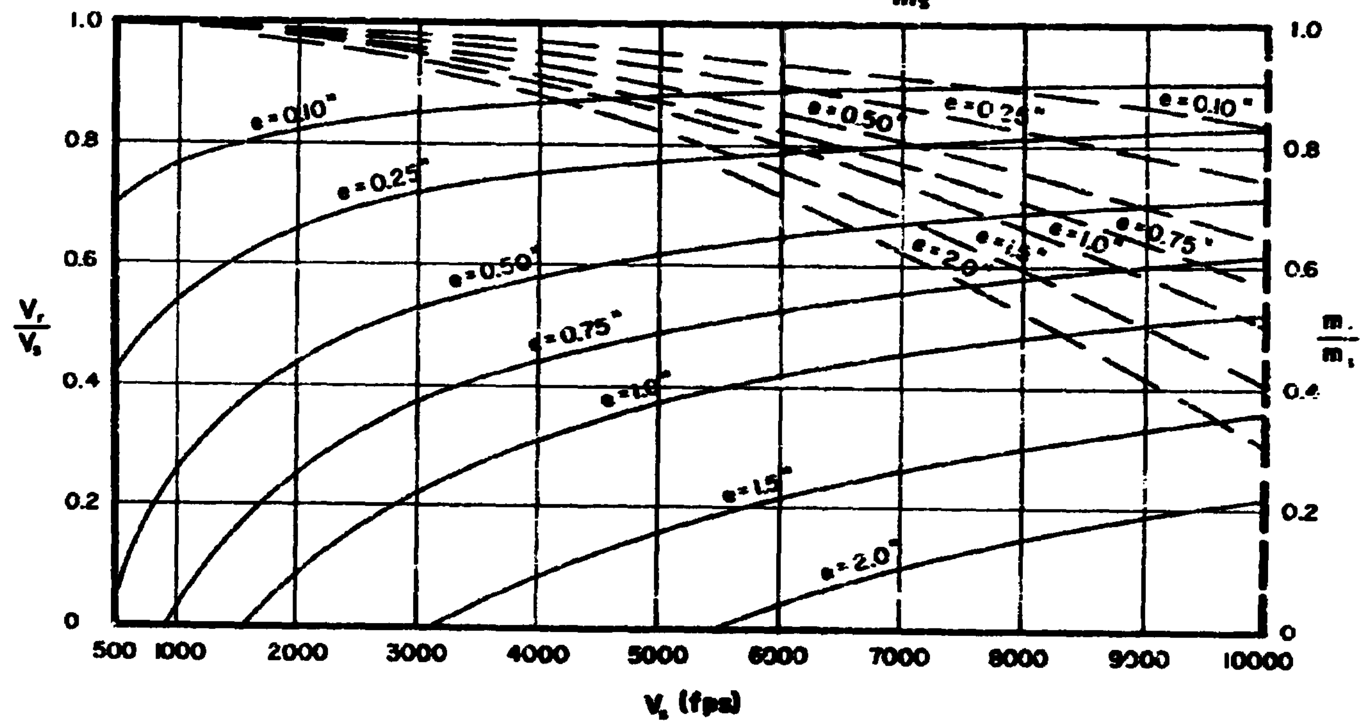

Fig. 46

$\frac{V_r}{V_s}$ and $\frac{m_r}{m_s}$ vs V_s for Selected Target Thicknesses

Target: Lexan

Obliquity: 70°

Fragment Size: 100 grains

Dashed Thickness Contours Refer to $\frac{m_r}{m_s}$ Ordinate

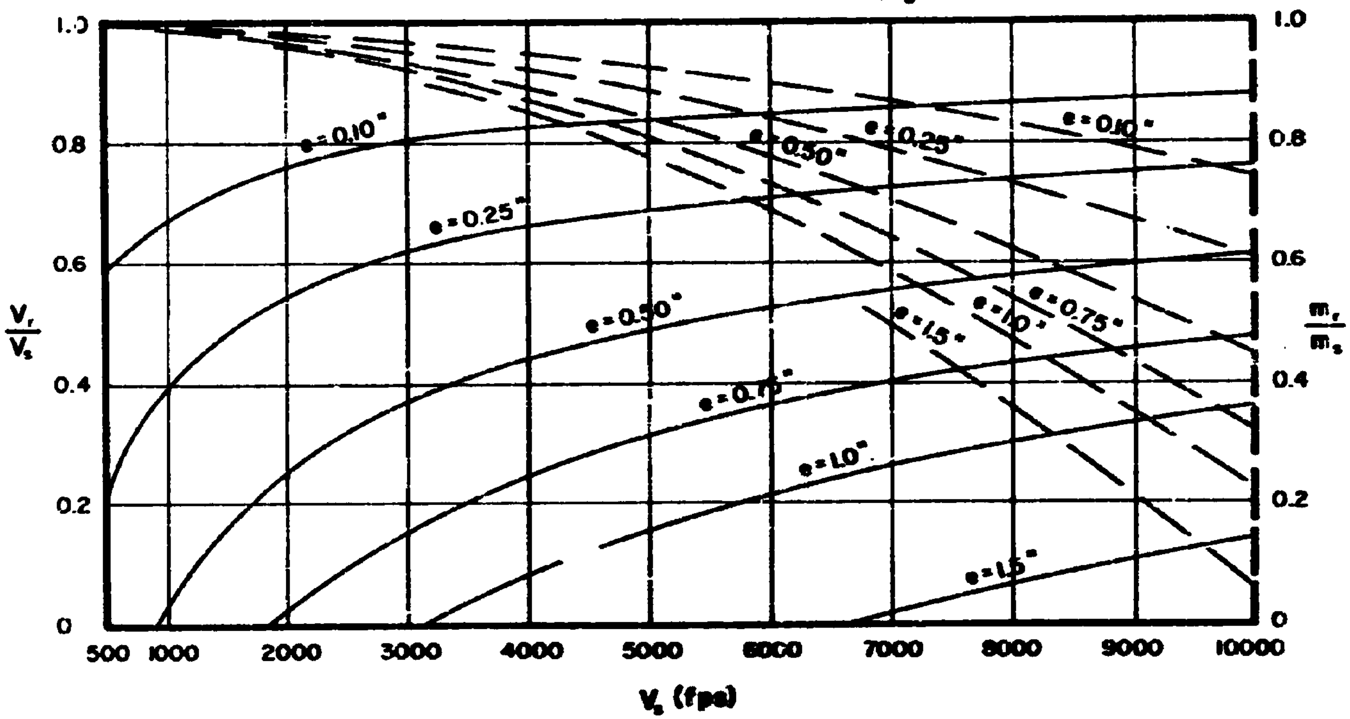

Fig. 47

CONFIDENTIAL

$\frac{V_r}{V_s}$ and $\frac{m_r}{m_s}$ vs V_s for Selected Target Thicknesses

Target: Lexan

Obliquity: 0°

Fragment Size: 300 grains

Dashed Thickness Contours Refer to $\frac{m_r}{m_s}$ Ordinate

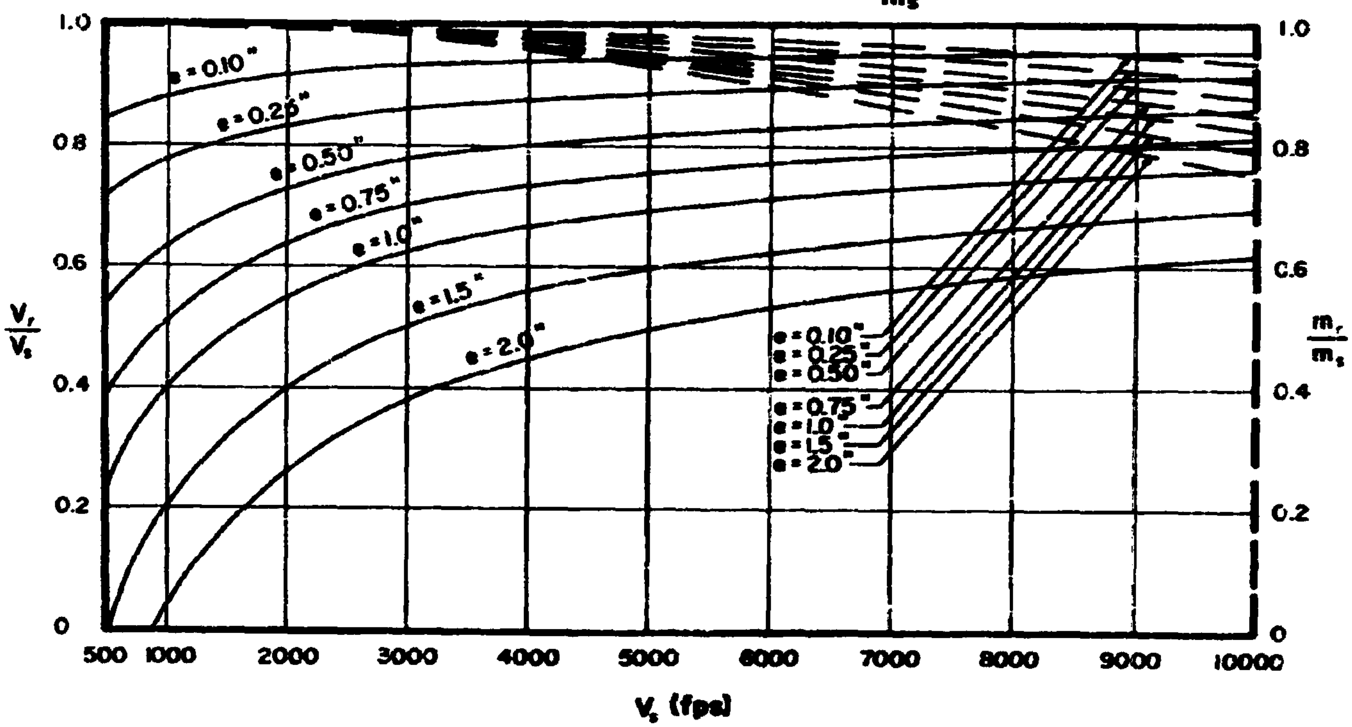

Fig. 48

CONFIDENTIAL

$\frac{V_r}{V_s}$ and $\frac{m_r}{m_s}$ vs V_s for Selected Target Thicknesses

Target: Lexan

Obliquity: 60°

Fragment Size: 300 grains

Dashed Thickness Contours Refer to $\frac{m_r}{m_s}$ Ordinate

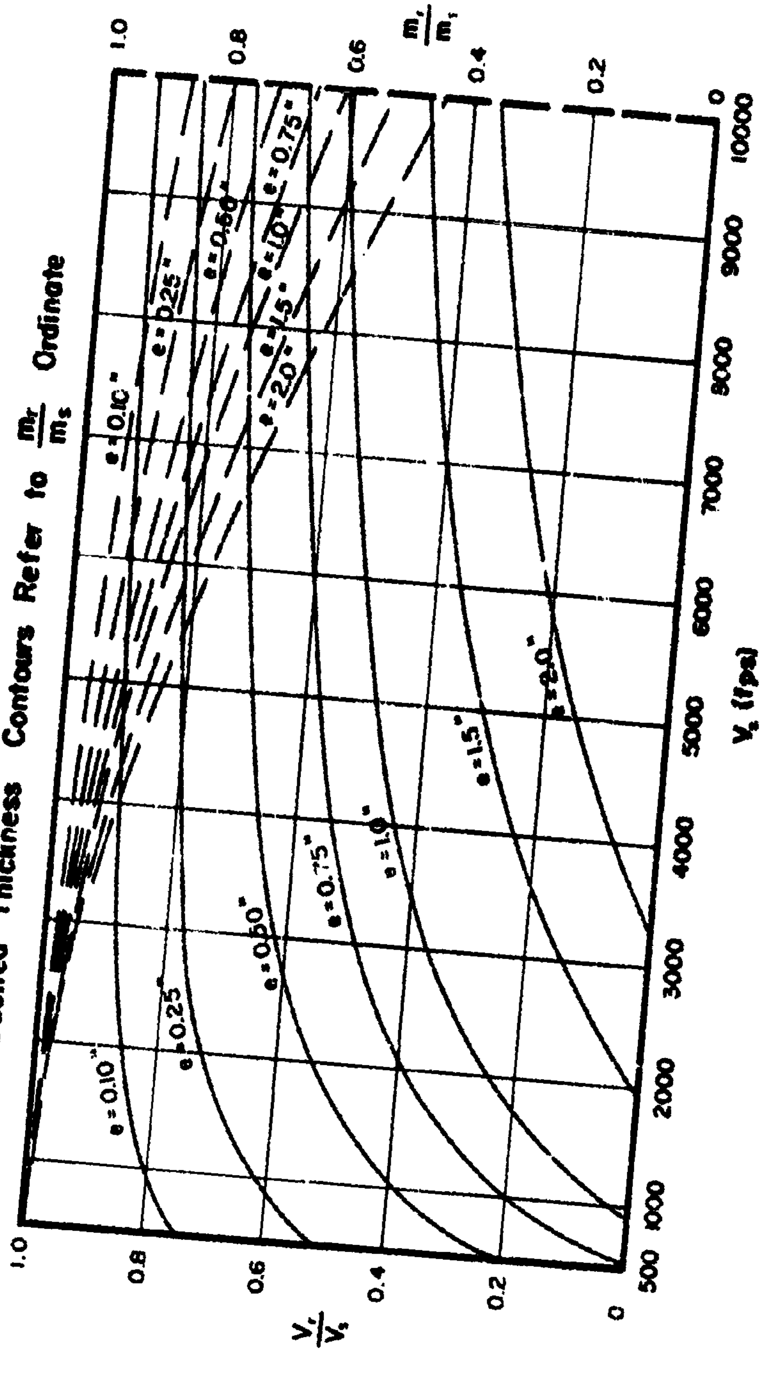

Fig. 49

$\frac{V_r}{V_s}$ and $\frac{m_r}{m_s}$ vs V_s for Selected Target Thicknesses

Target: Lexan

Obliquity: 70°

Fragment Size: 300 grains

Dashed Thickness Contours Refer to $\frac{m_r}{m_s}$ Ordinate

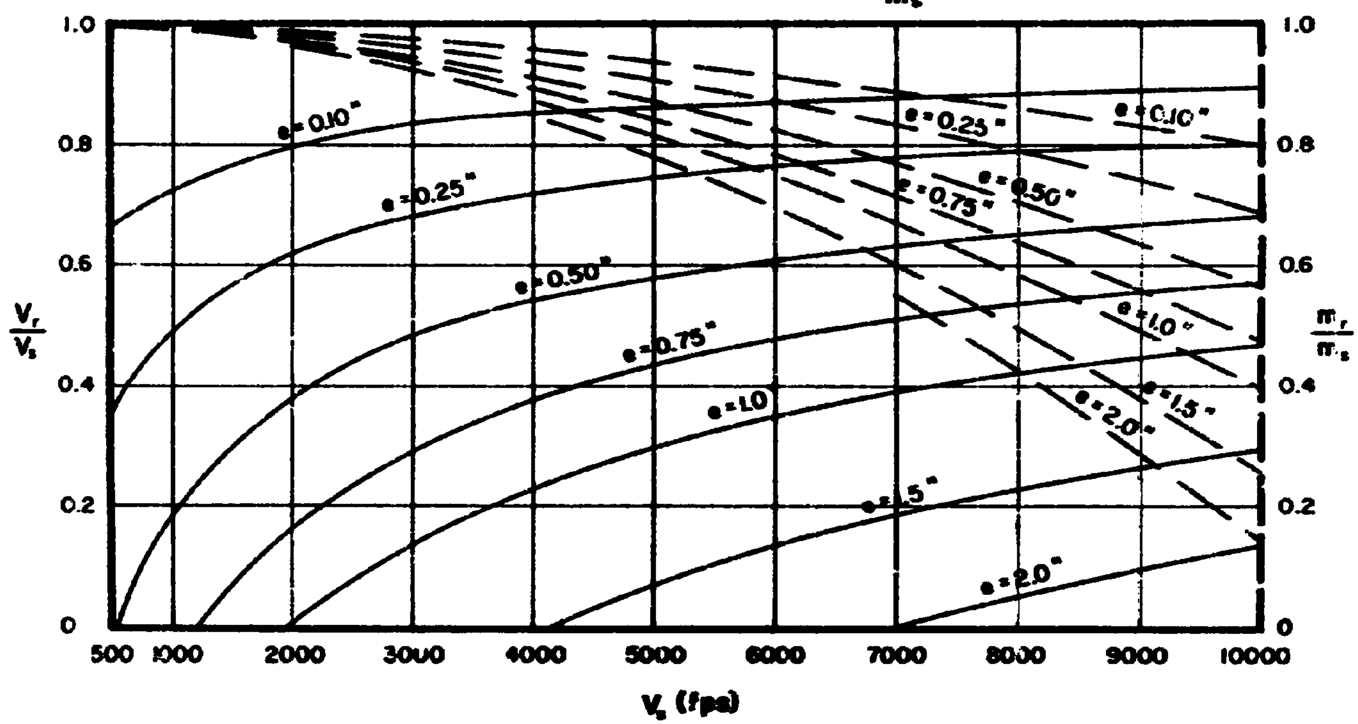

Fig. 50

$\frac{V_r}{V_s}$ and $\frac{m_r}{m_s}$ vs V_s for Selected Target Thicknesses

Target: Plexiglas, as Cast

Obliquity: 0°

Fragment Size: 30 grains

Dashed Thickness Contours Refer to $\frac{m_r}{m_s}$ Ordinate

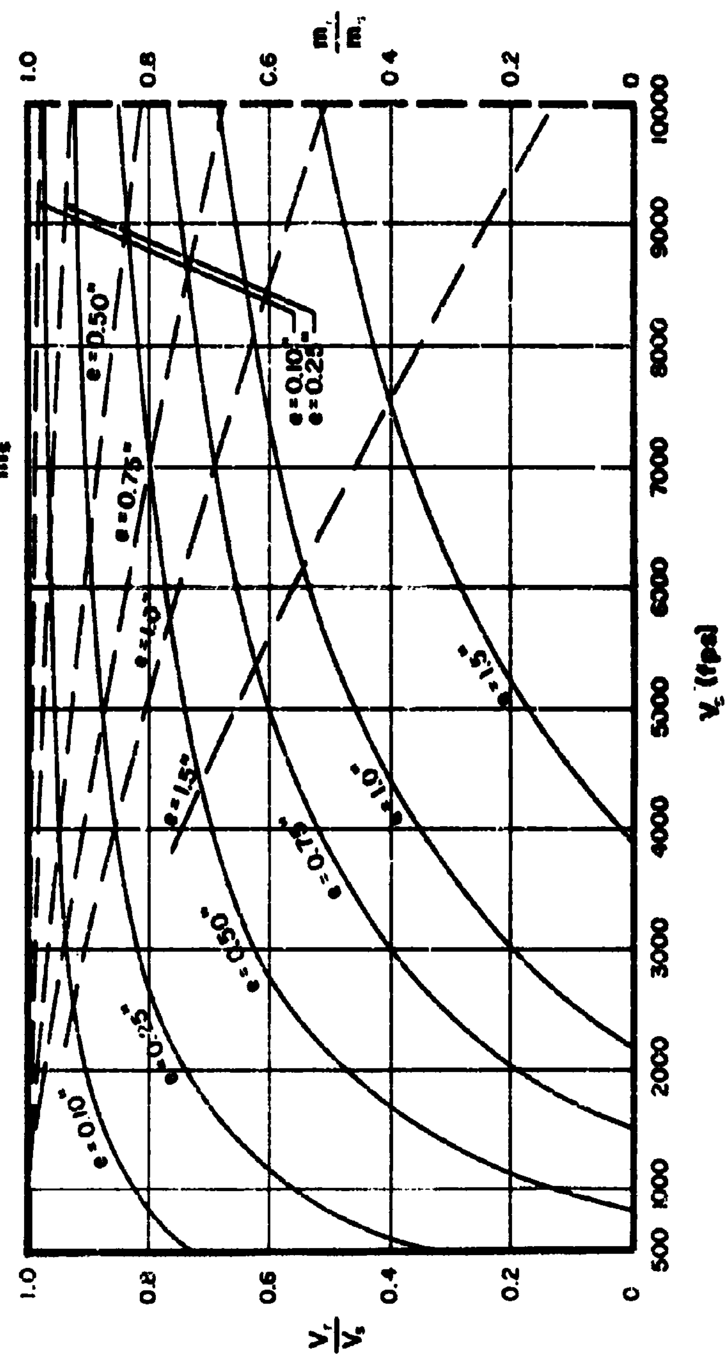

Fig. 51

$\frac{V_r}{V_s}$ and $\frac{m_r}{m_s}$ vs V_s for Selected Target Thicknesses

Target: Plexiglas, as Cast

Obliquity: 60°

Fragment Size: 30 grains

Dashed Thickness Contours Refer to $\frac{m_r}{m_s}$ Ordinate

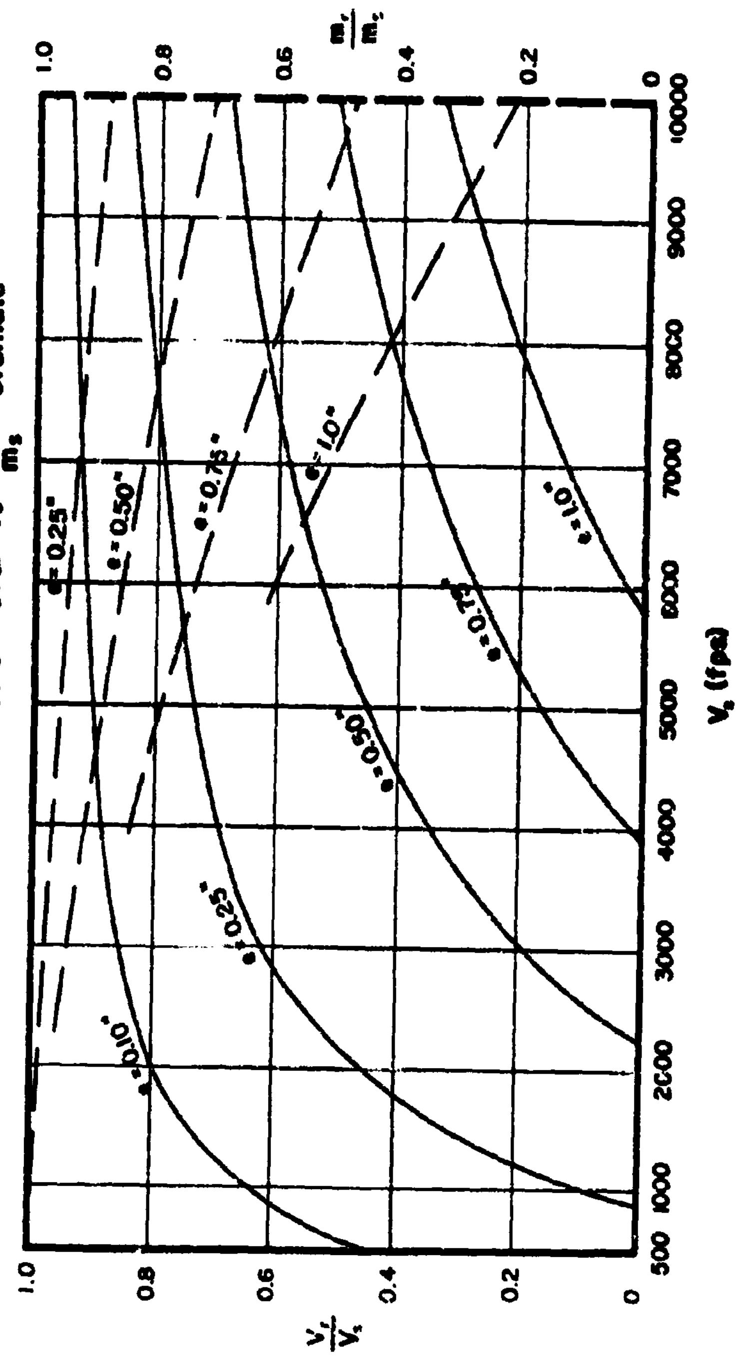

Fig. 52

$\frac{V_r}{V_s}$ and $\frac{m_r}{m_s}$ vs V_s for Selected Target Thicknesses

Target: Plexiglas, as Cast

Obliquity: 70°

Fragment Size: 30 grains

Dashed Thickness Contours Refer to $\frac{m_r}{m_s}$ Ordinate

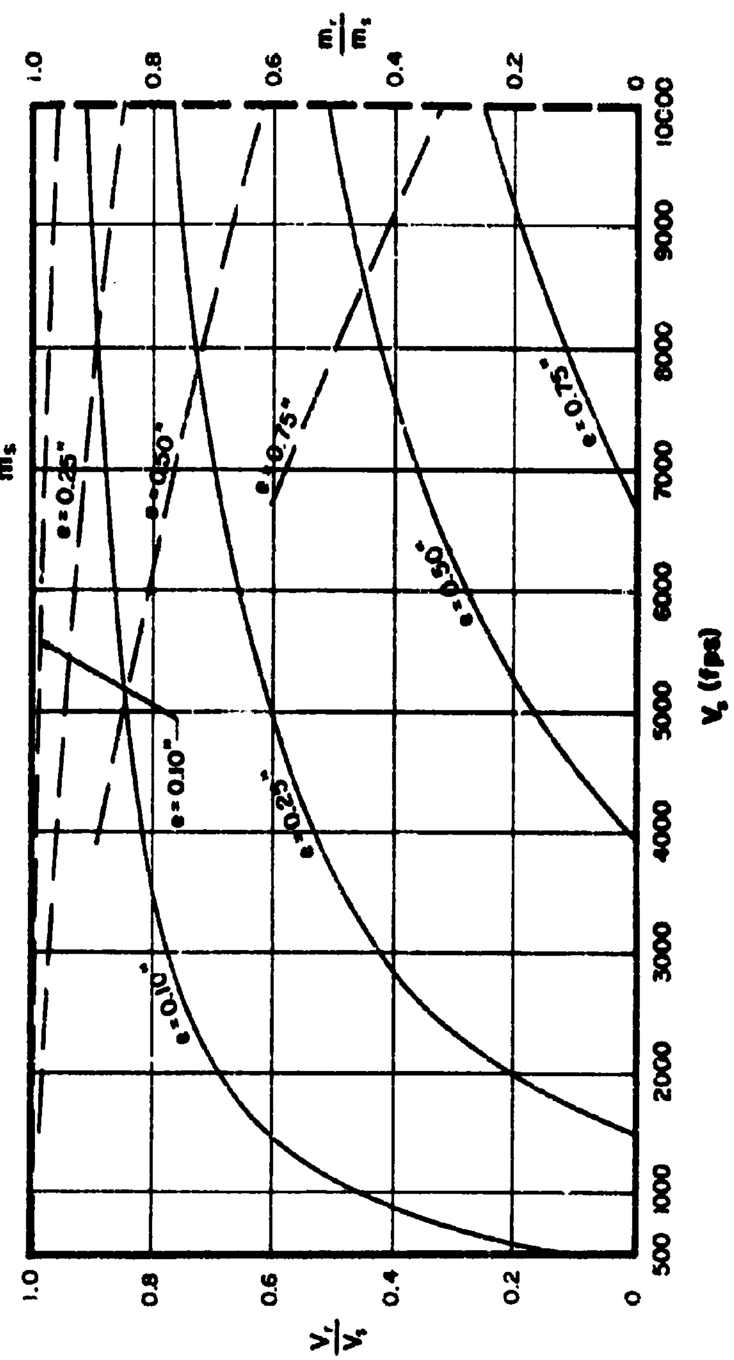

Fig. 53

CONFIDENTIAL

$\frac{V_r}{V_s}$ and $\frac{m_r}{m_s}$ vs V_s for Selected Target Thicknesses

Target: Plexiglas, as Cast

Obliquity: 0°

Fragment Size: 100 grains

Dashed Thickness Contours Refer to $\frac{m_r}{m_s}$ Ordinate

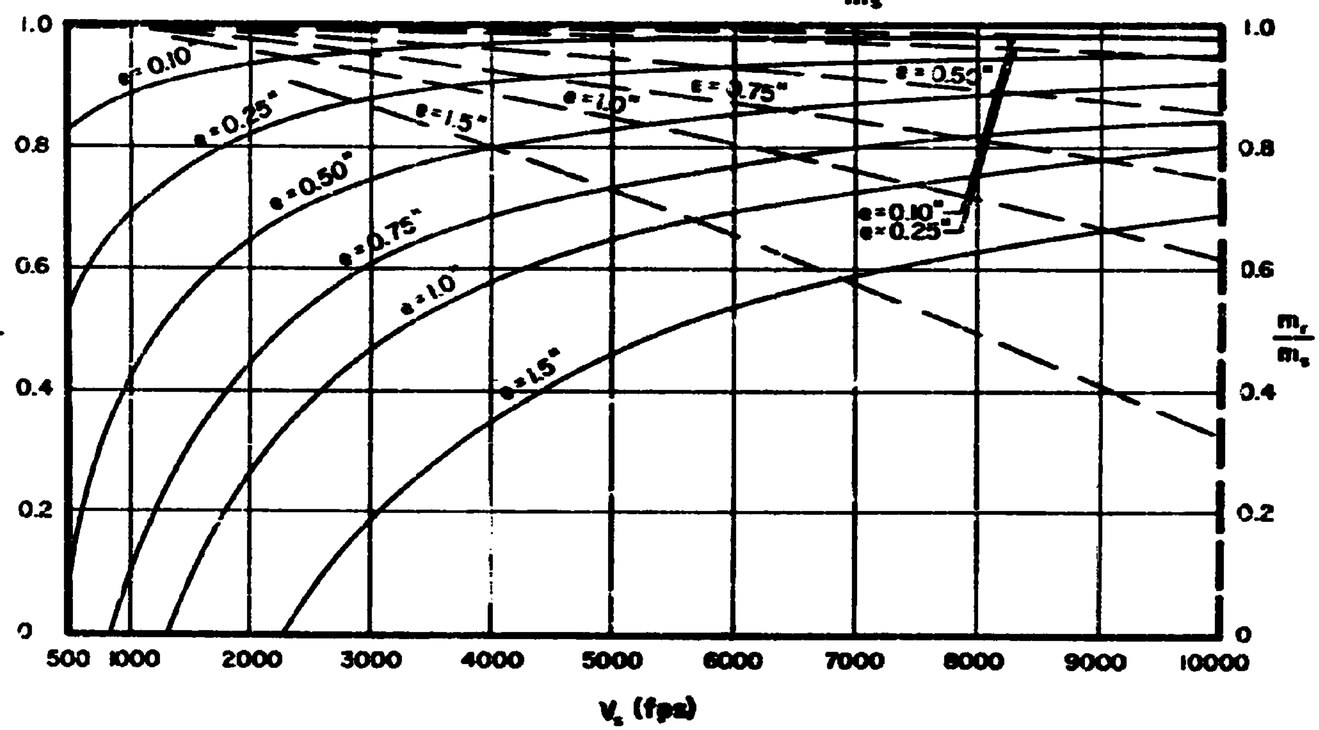

Fig. 54

CONFIDENTIAL

$\frac{V_r}{V_s}$ and $\frac{m_r}{m_s}$ vs V_s for Selected Target Thicknesses

Target: Plexiglas, as Cast

Obliquity: 60°

Fragment Size: 100 grains

Dashed Thickness Contours Refer to $\frac{m_r}{m_s}$ Ordinate

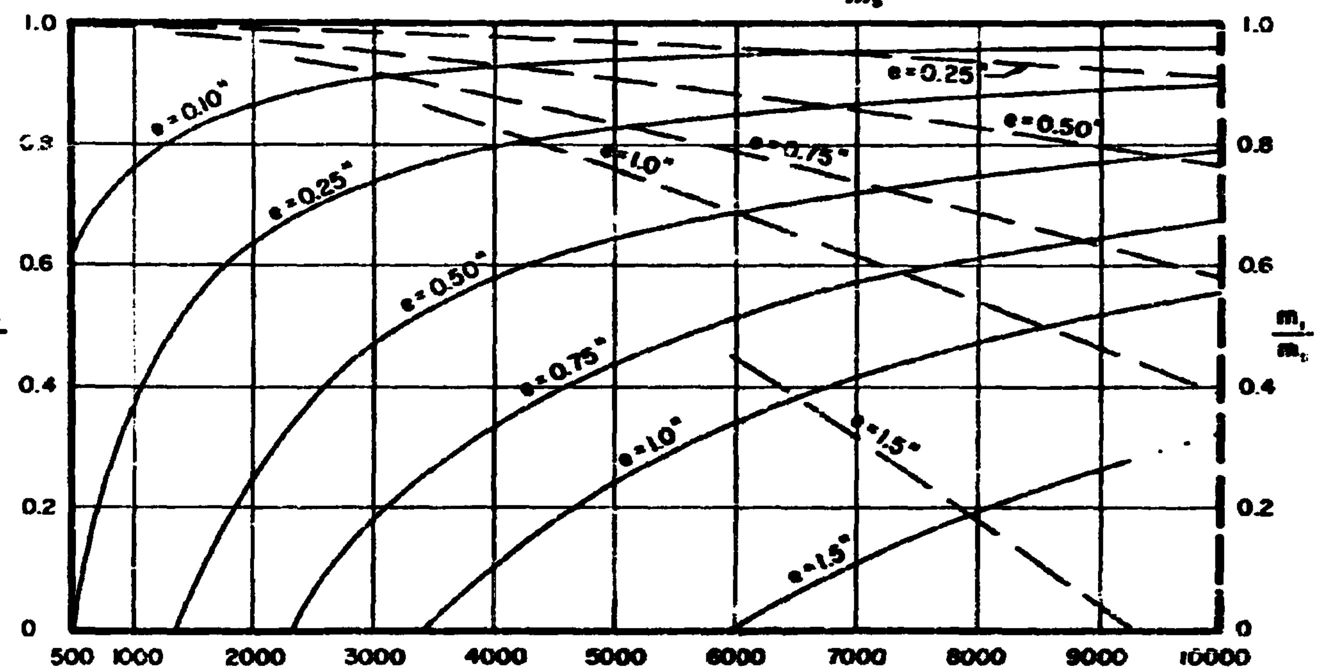

Fig. 55

$\frac{V_r}{V_s}$ and $\frac{m_r}{m_s}$ vs V_s for Selected Target Thicknesses

Target: Plexiglas, as Cast

Obliquity: 70°

Fragment Size: 100 grains

Dashed Thickness Contours Refer to $\frac{m_r}{m_s}$ Ordinate

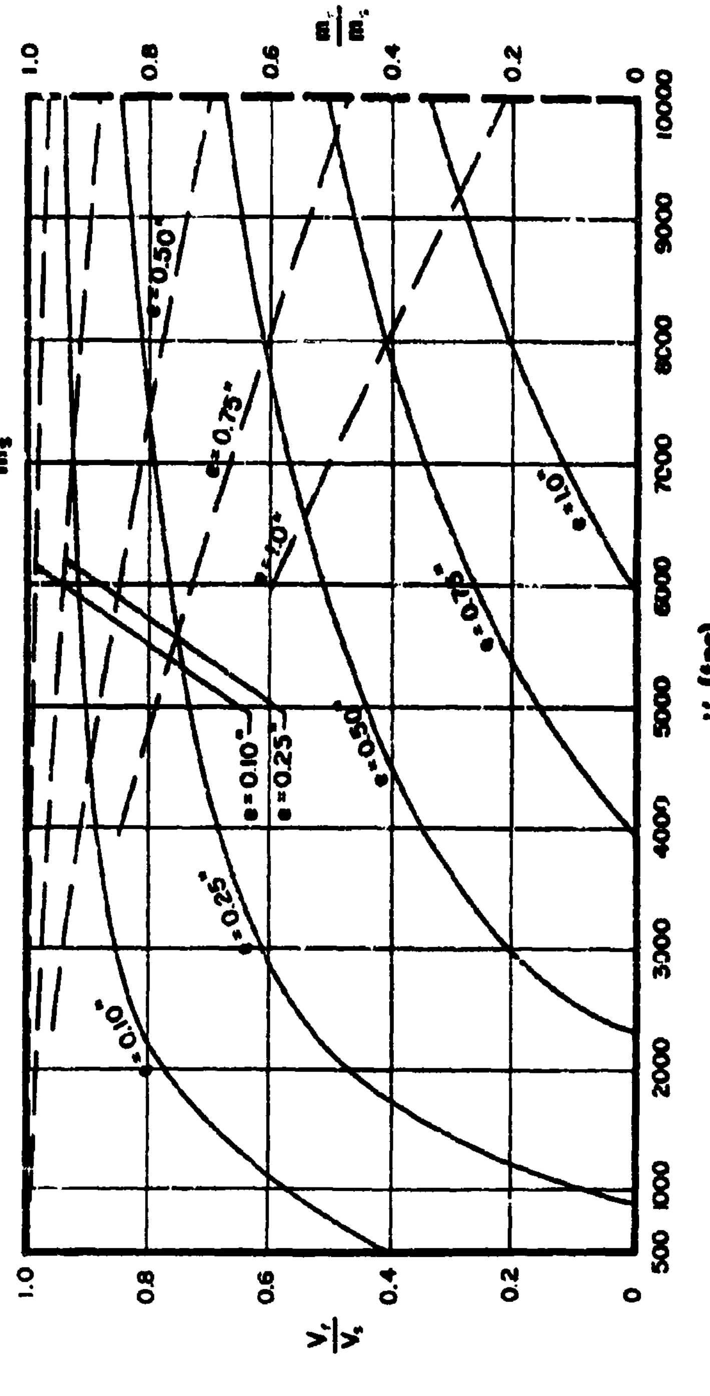

Fig. 56

$\frac{V_r}{V_s}$ and $\frac{m_r}{m_s}$ vs V_s for Selected Target Thicknesses

Target: Plexiglas, as Cast

Obliquity: 0°

Fragment Size: 300 grains

Dashed Thickness Contours Refer to $\frac{m_r}{m_s}$ Ordinate

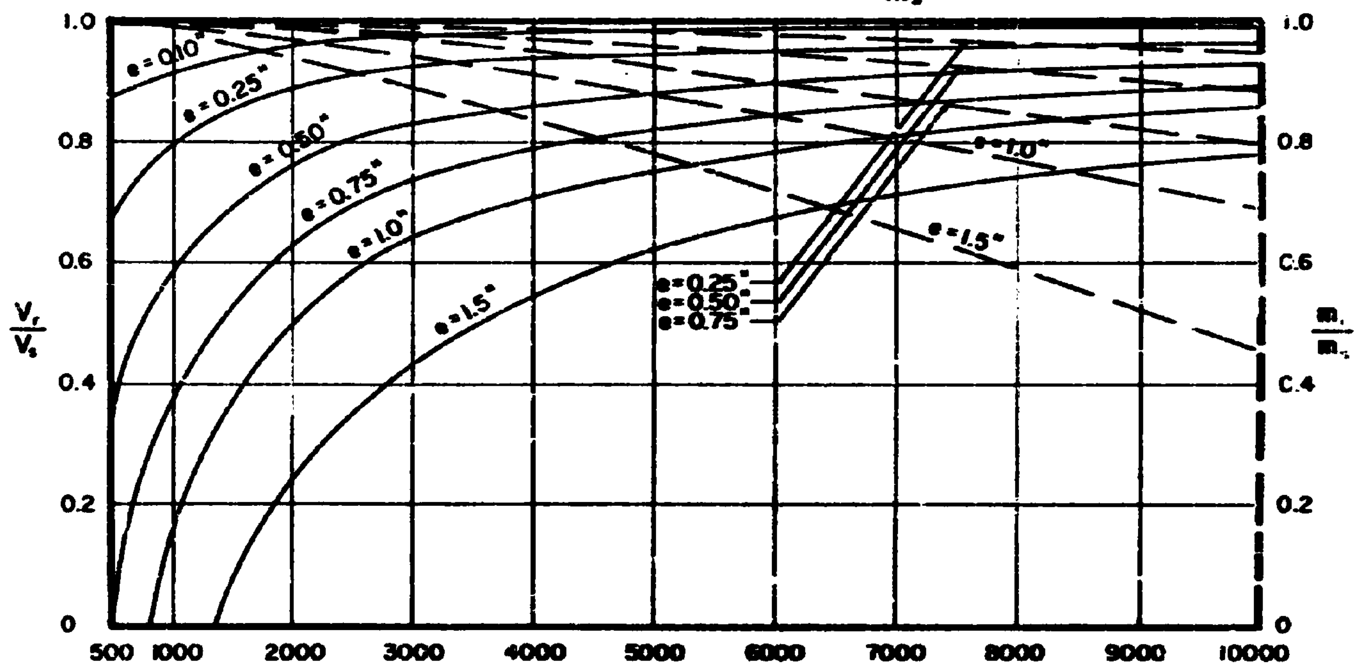

Fig. 57

$\frac{V_r}{V_s}$ and $\frac{m_r}{m_s}$ vs V_s for Selected Target Thicknesses

Target: Plexiglas, as Cast

Obliquity: 60°

Fragment Size: 300 grains

Dashed Thickness Contours Refer to $\frac{m_r}{m_s}$ Ordinate

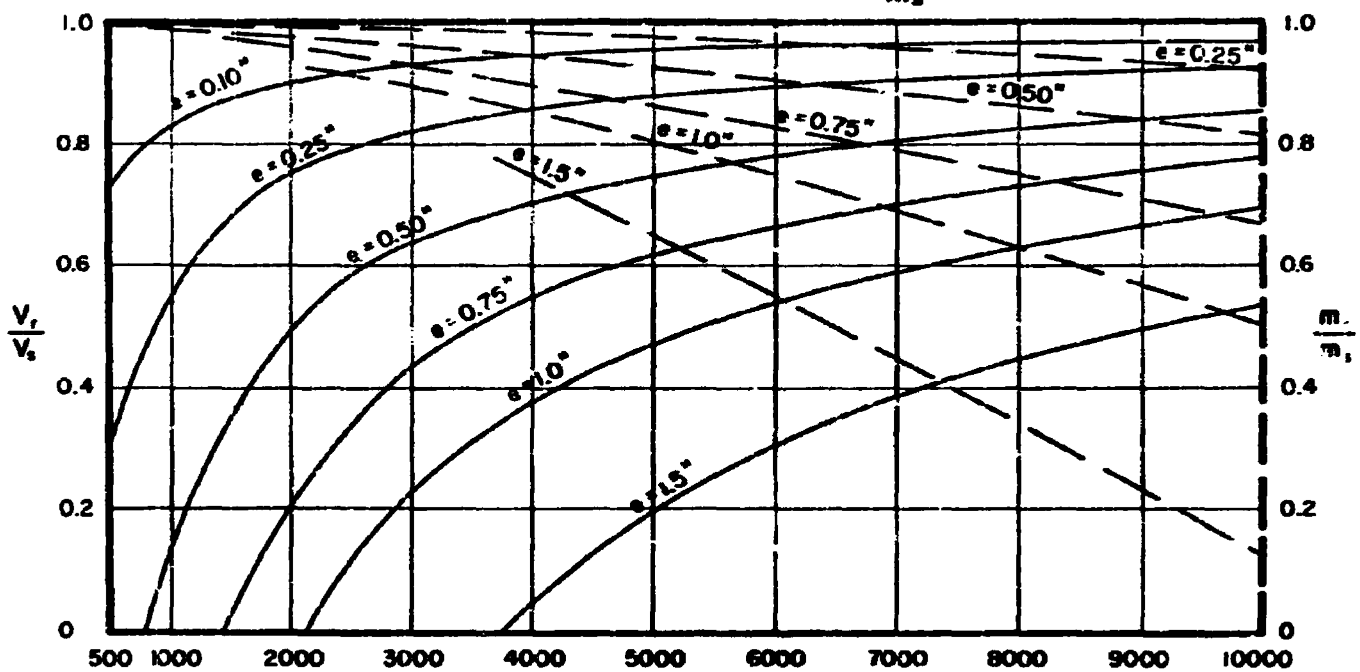

V_s (fps)

Fig. 58

$\frac{V_r}{V_s}$ and $\frac{m_r}{m_s}$ vs V_s for Selected Target Thicknesses

Target: Plexiglas, as Cast

Obliquity: 70°

Fragment Size: 300 grains

Dashed Thickness Contours Refer to $\frac{m_r}{m_s}$ Ordinate

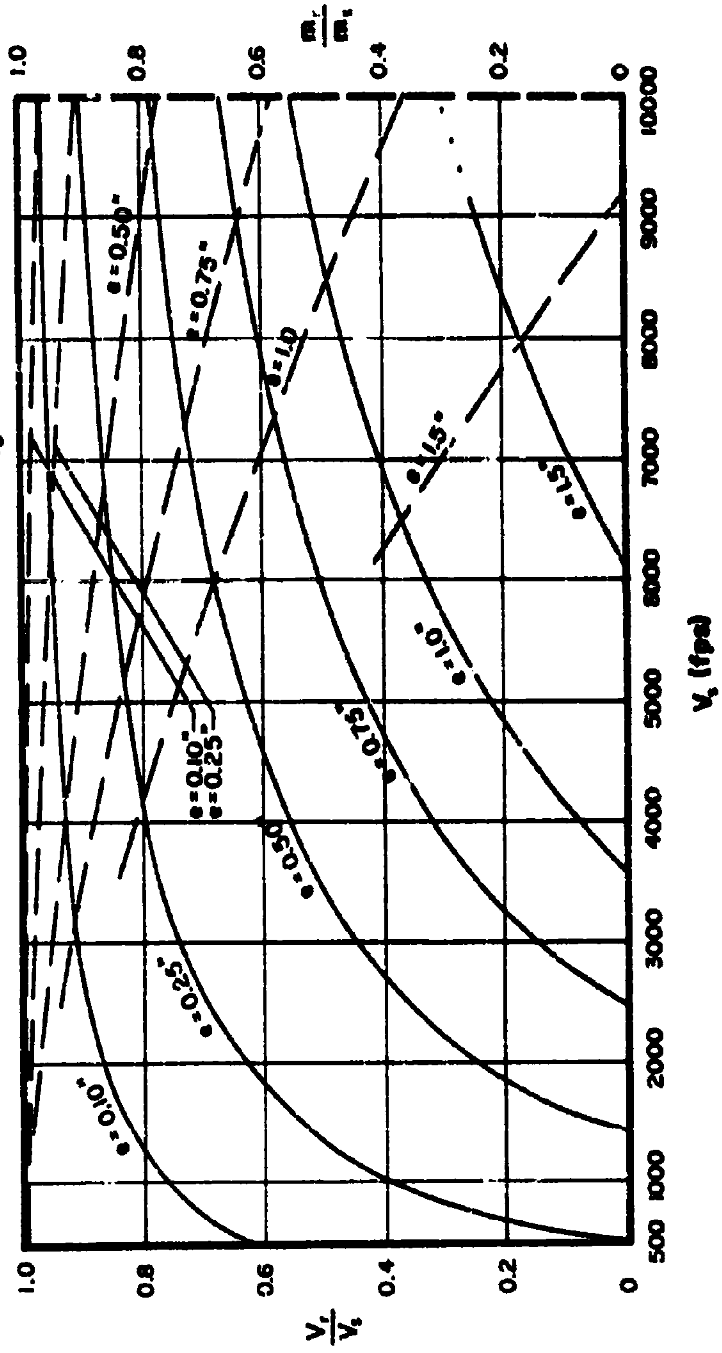

Fig. 59

$\frac{V_r}{V_s}$ and $\frac{m_r}{m_s}$ vs V_s for Selected Target Thicknesses

Target: Stretched Plexiglas

Obliquity: 0°

Fragment Size: 30 grains

Dashed Thickness Contours Refer to $\frac{m_r}{m_s}$ Ordinate

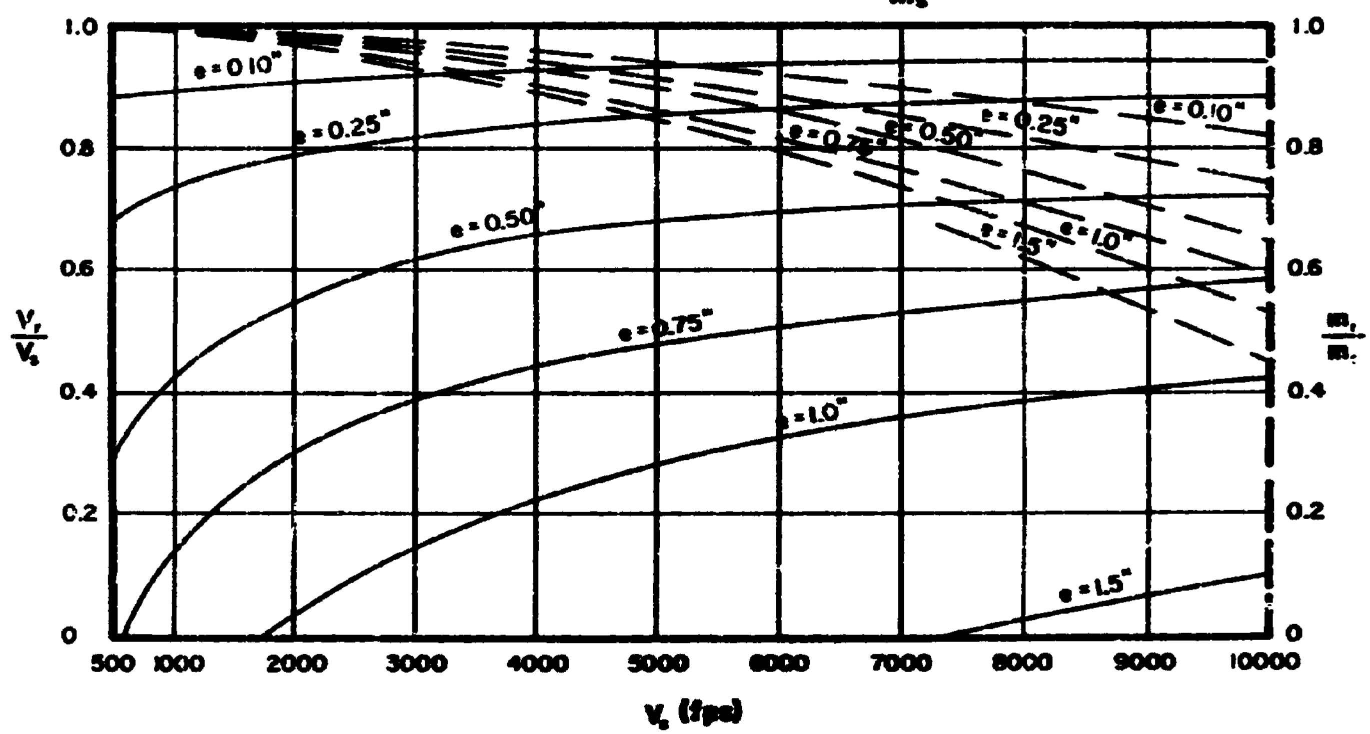

Fig. 60

$\frac{V_r}{V_s}$ and $\frac{m_r}{m_s}$ vs V_s for Selected Target Thicknesses

Target: Stretched Plexiglas

Obliquity: 60°

Fragment Size: 30 grains

Dashed Thickness Contours Refer to $\frac{m_r}{m_s}$ Ordinate

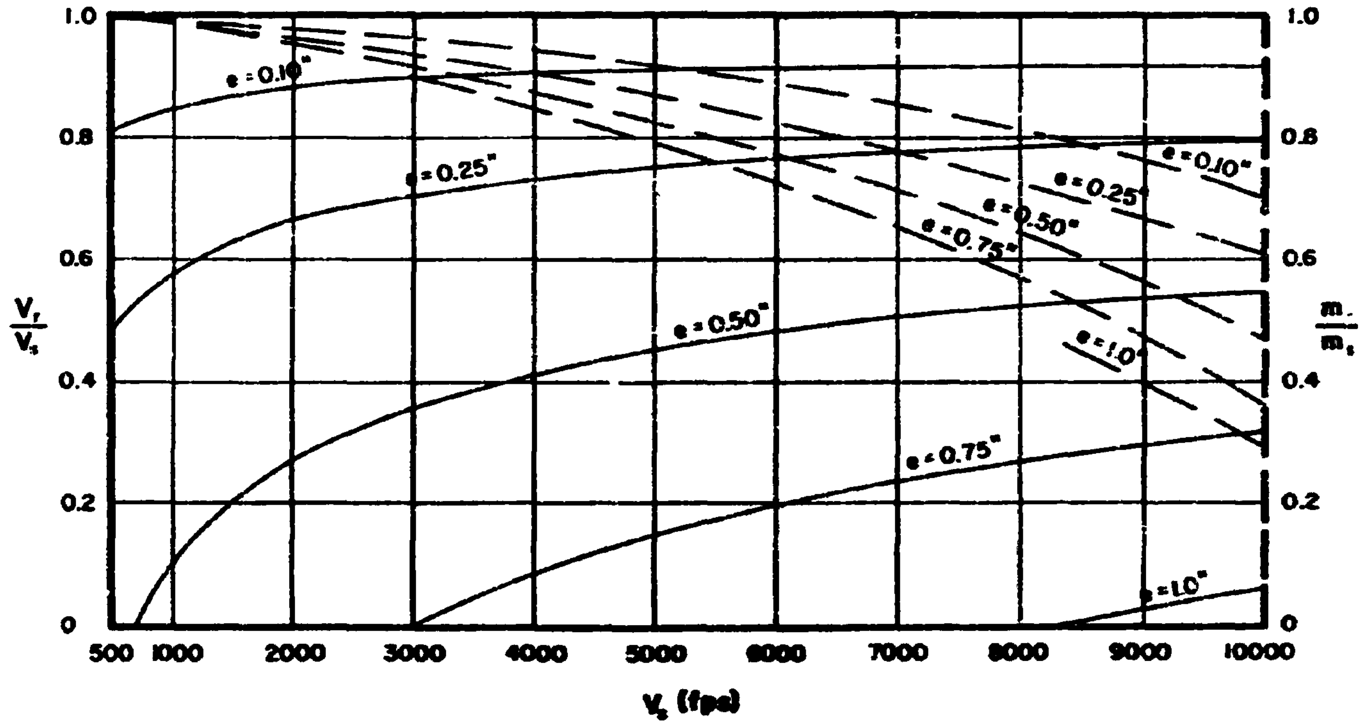

Fig. 61

$\frac{V_r}{V_s}$ and $\frac{m_r}{m_s}$ vs V_s for Selected Target Thicknesses

Target: Stretched Plexiglas

Obliquity: 70°

Fragment Size: 30 grains

Dashed Thickness Contours Refer to $\frac{m_r}{m_s}$ Ordinate

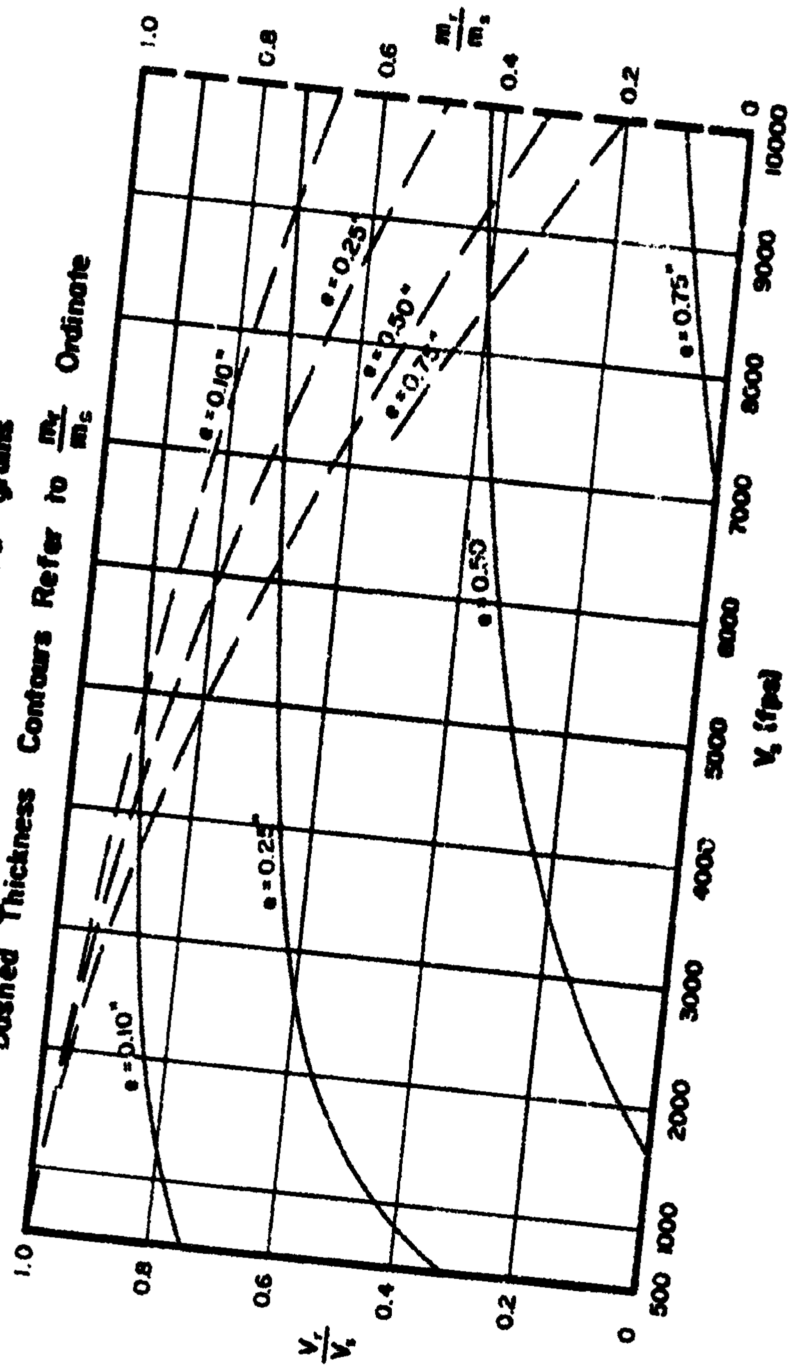

Fig. 62

$\frac{V_r}{V_s}$ and $\frac{m_r}{m_s}$ vs V_s for Selected Target Thicknesses

Target: Stretched Plexiglas

Obliquity: 0°

Fragment Size: 100 grains

Dashed Thickness Contours Refer to $\frac{m_r}{m_s}$ Ordinate

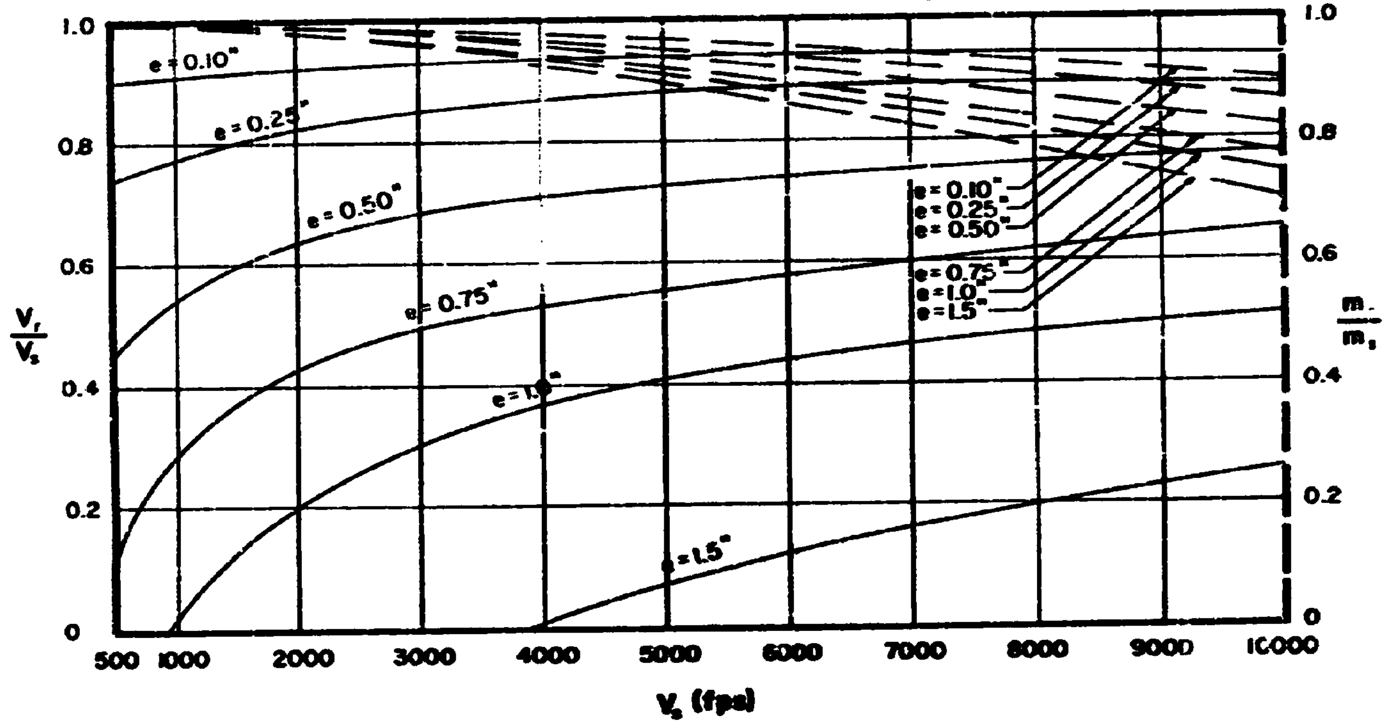

Fig. 63

$\frac{V_r}{V_s}$ and $\frac{m_r}{m_s}$ vs V_s for Selected Target Thicknesses

Target: Stretched Plexiglas

Obliquity: 60°

Fragment Size: 100 grains

Dashed Thickness Contours Refer to $\frac{m_r}{m_s}$ Ordinate

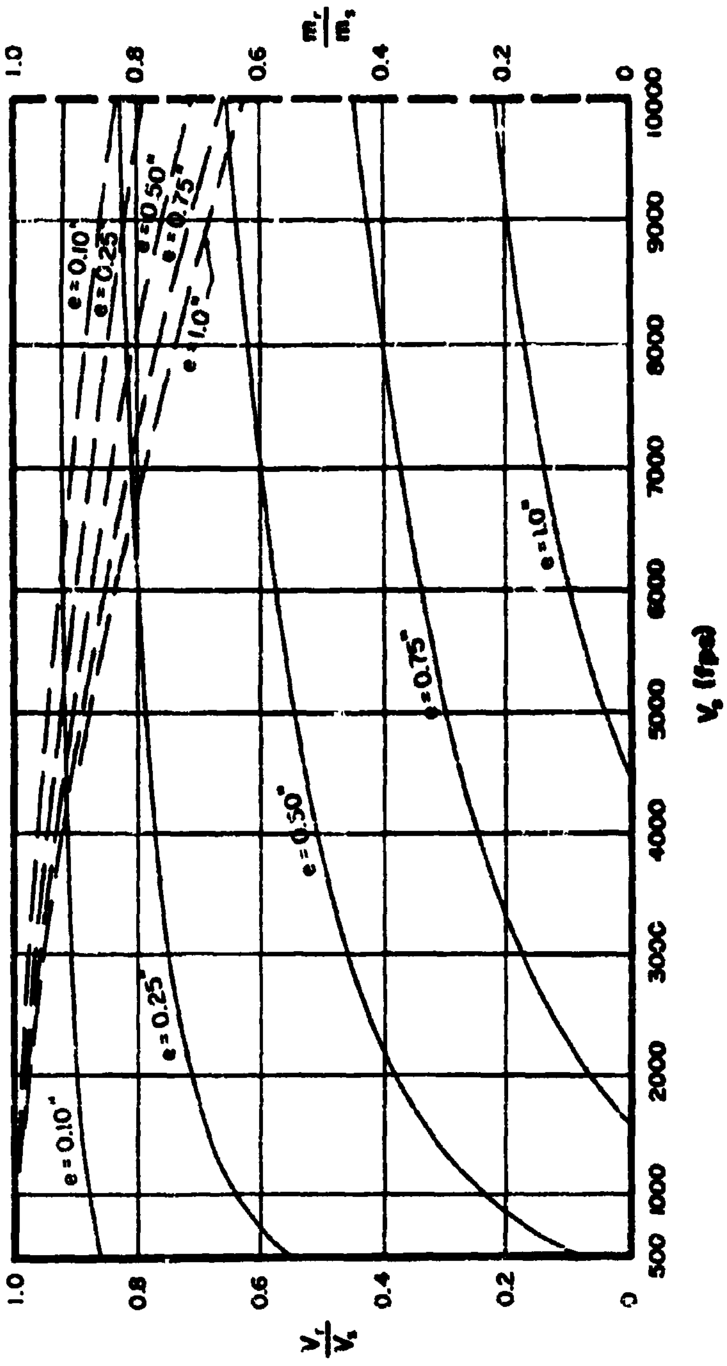

Fig. 64

$\frac{V_r}{V_s}$ and $\frac{m_r}{m_s}$ vs V_s for Selected Target Thicknesses

Target: Stretched Plexiglas

Obliquity: 70°

Fragment Size: 100 grains

Dashed Thickness Contours Refer to $\frac{m_r}{m_s}$ Ordinate

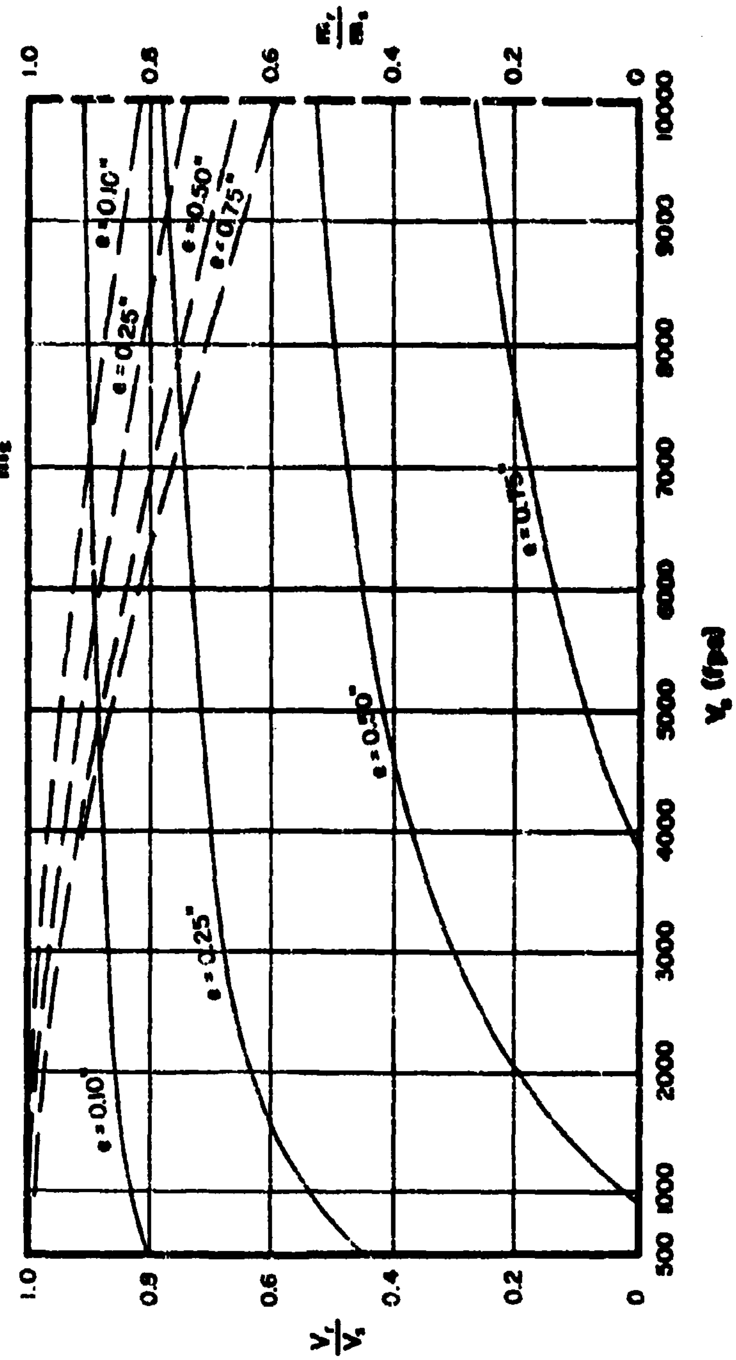

Fig. 65

$\frac{V_r}{V_s}$ and $\frac{m_r}{m_s}$ vs V_s for Selected Target Thicknesses

Target: Stretched Plexiglas

Obliquity: 0°

Fragment Size: 300 grains

Dashed Thickness Contours Refer to $\frac{m_r}{m_s}$ Ordinate

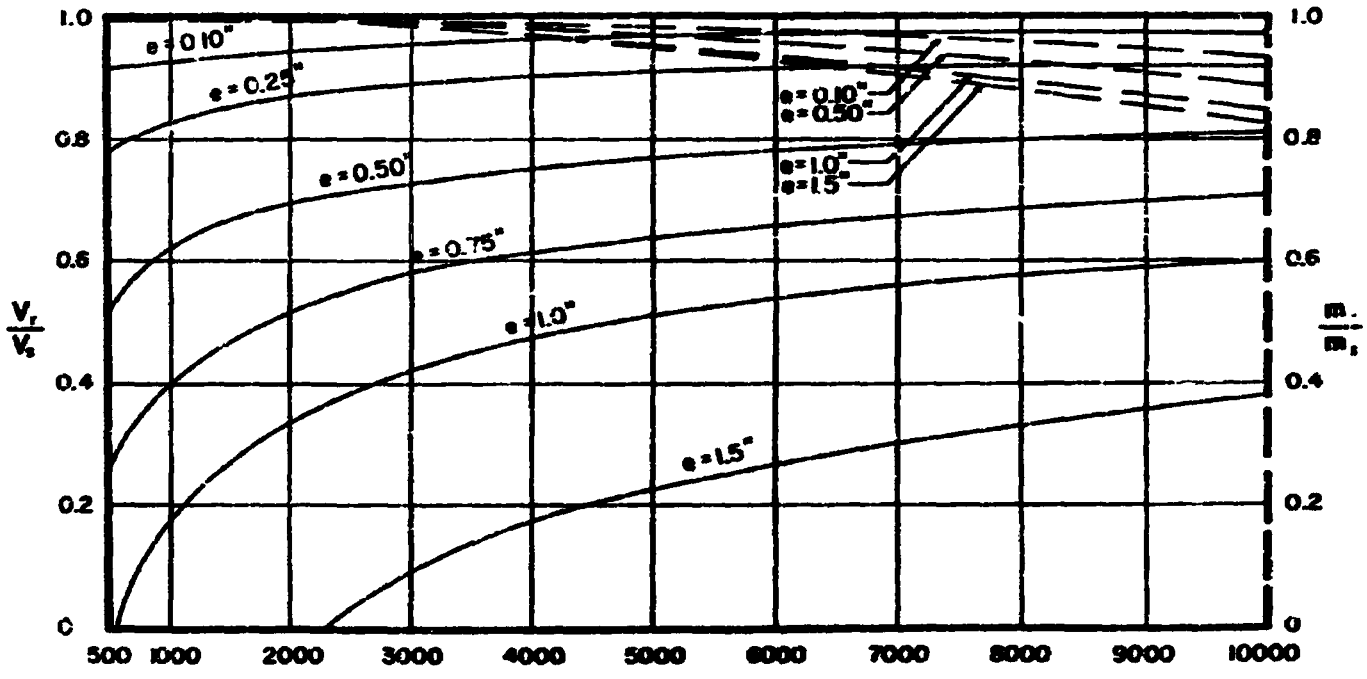

Fig. 66

$\frac{V_r}{V_s}$ and $\frac{m_r}{m_s}$ vs V_s for Selected Target Thicknesses

Target: Stretched Plexiglas

Obliquity: 60°

Fragment Size: 300 grains

Dashed Thickness Contours Refer to $\frac{m_r}{m_s}$ Ordinate

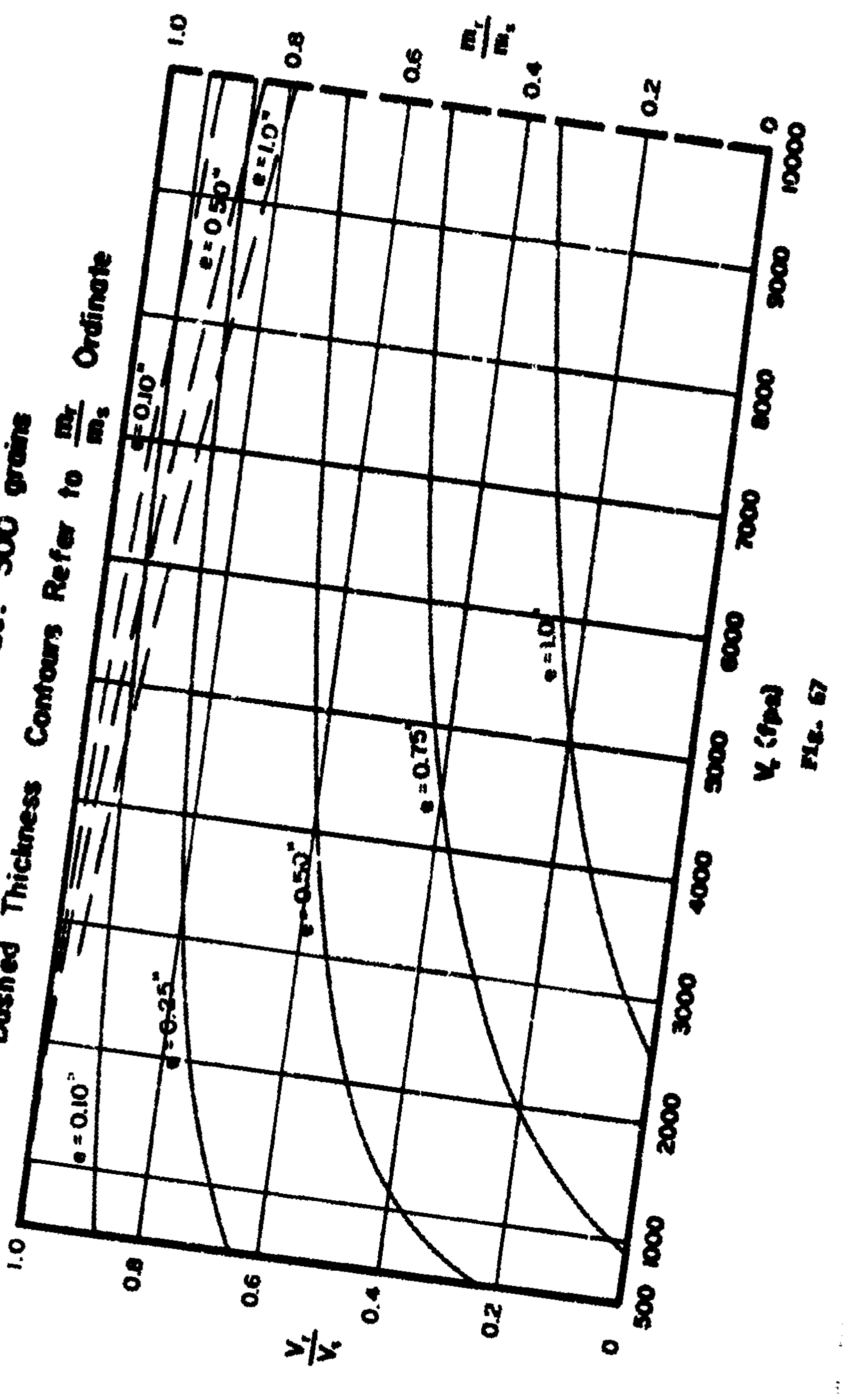

Fig. 67

$\frac{V_r}{V_s}$ and $\frac{m_r}{m_s}$ vs V_s for Selected Target Thicknesses

Target: Stretched Plexiglas

Obliquity: 70°

Fragment Size: 300 grains

Dashed Thickness Contours Refer to $\frac{m_r}{m_s}$ Ordinate

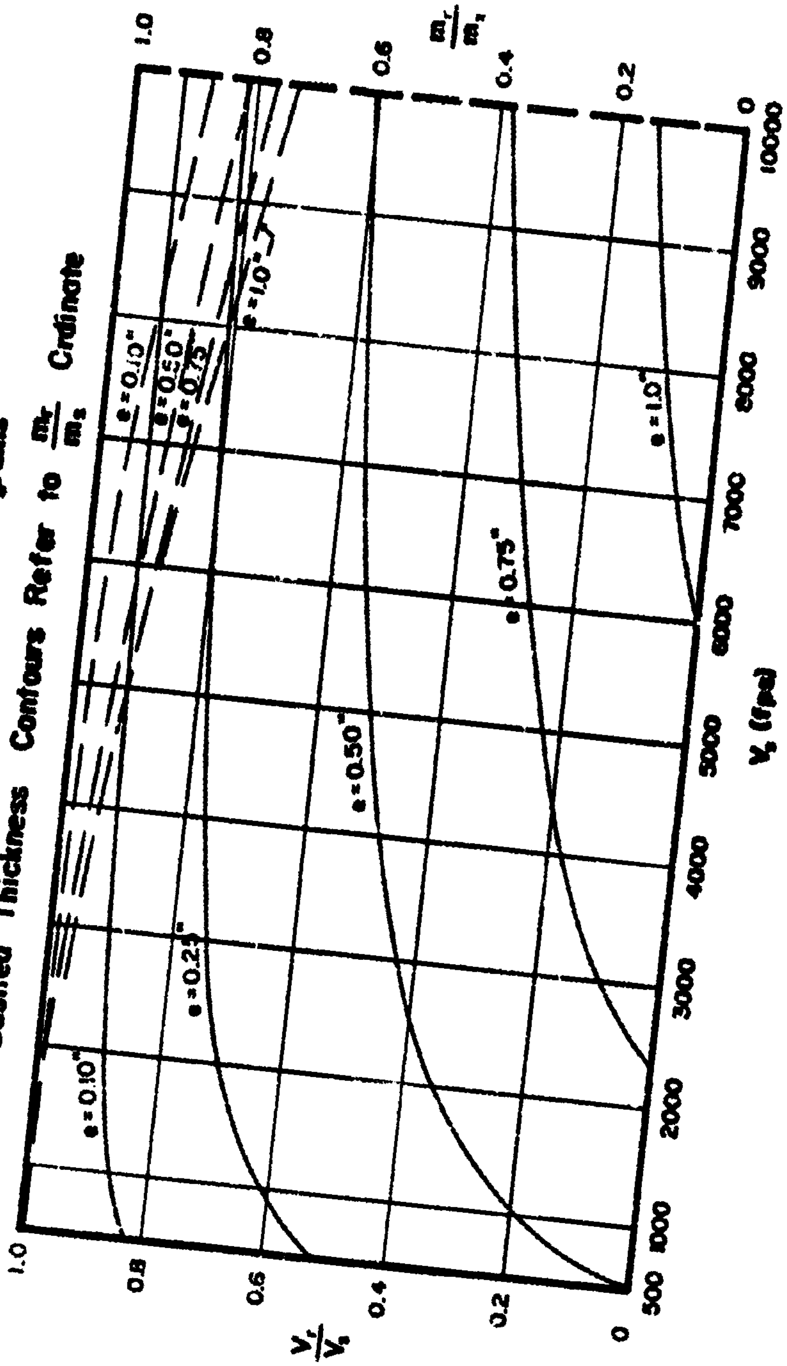

Fig. 68

$\frac{V_r}{V_s}$ and $\frac{m_r}{m_s}$ vs V_s for Selected Target Thicknesses

Target: Doron

Obliquity: 0°

Fragment Size: 30 grains

Dashed Thickness Contours Refer to $\frac{m_r}{m_s}$ Ordinate

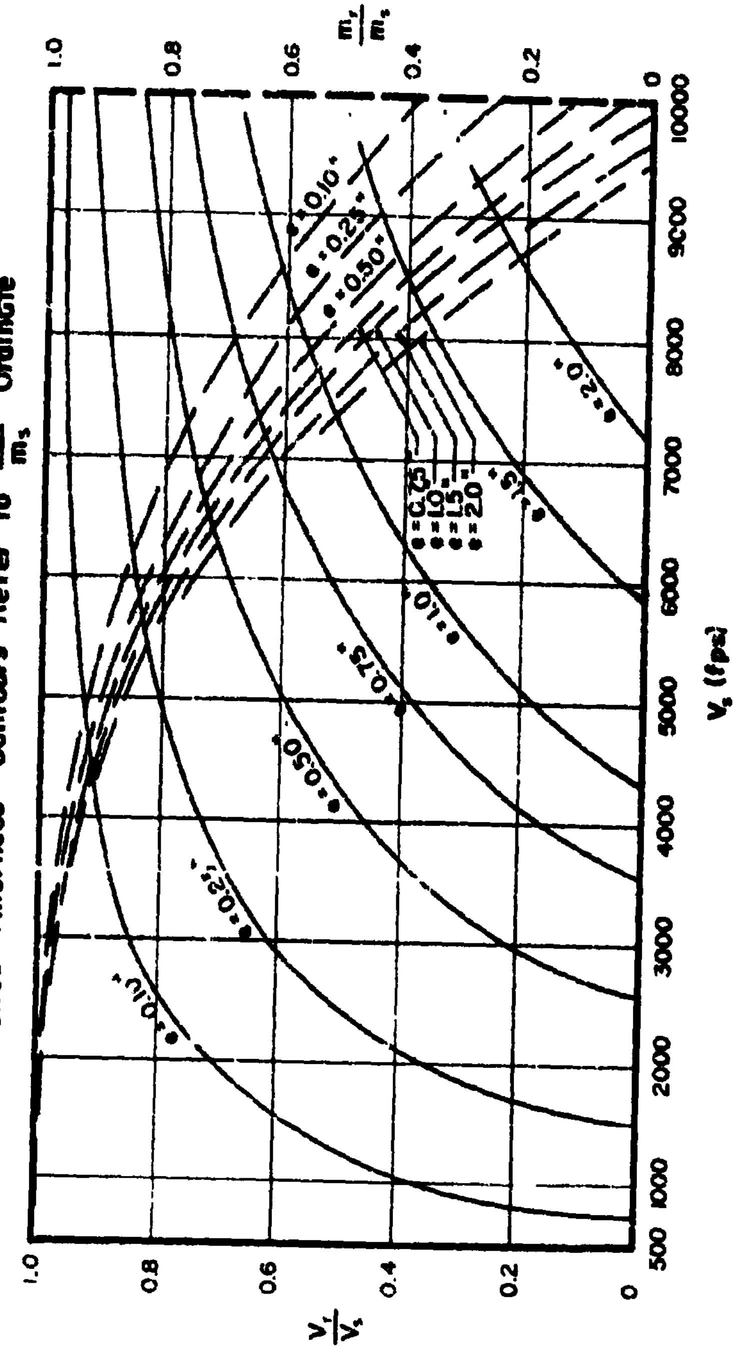

Fig. 69

$\frac{V_r}{V_s}$ and $\frac{m_r}{m_s}$ vs V_s for Selected Target Thicknesses

Target: Doron

Obliquity: 60°

Fragment Size: 30 grains

Dashed Thickness Contours Refer to $\frac{m_r}{m_s}$ Ordinate

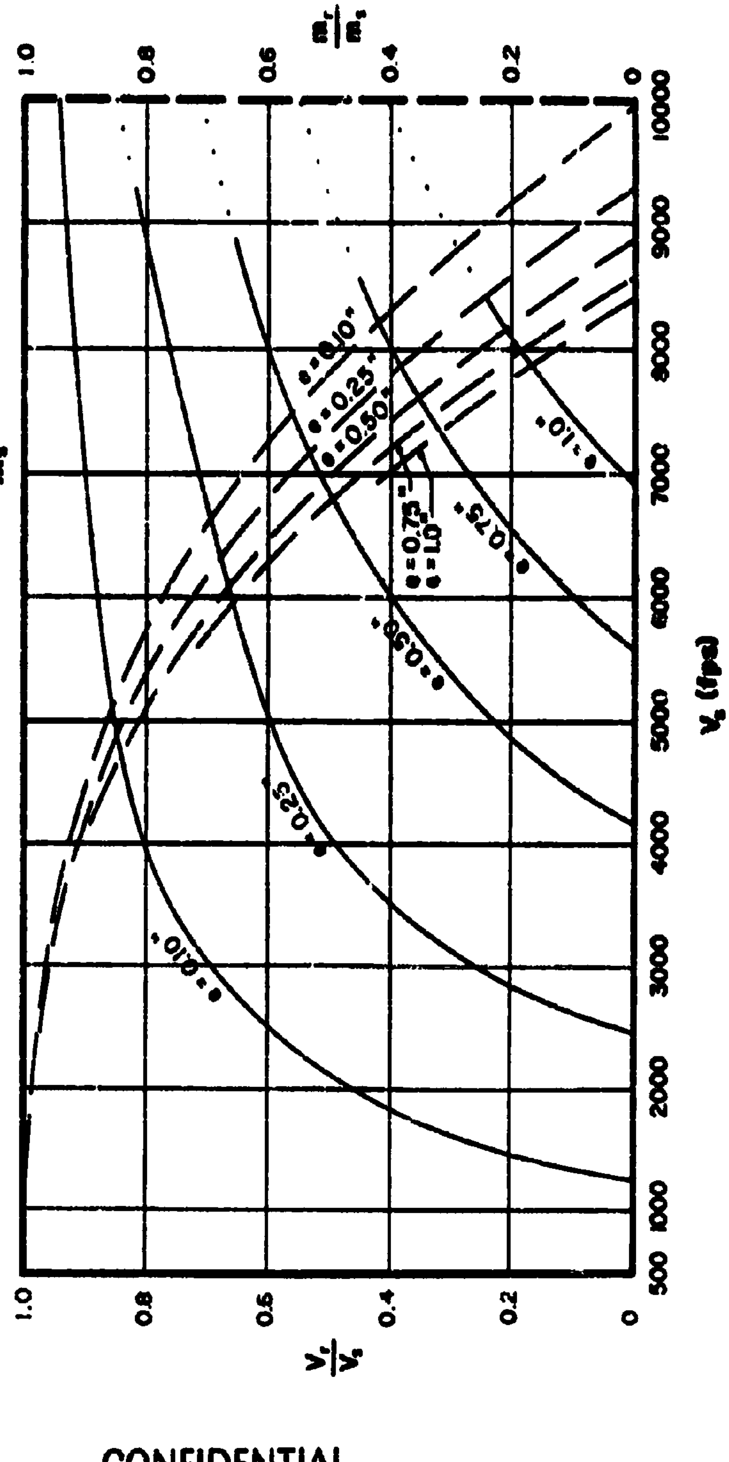

Fig. 70

$\frac{V_r}{V_s}$ and $\frac{m_r}{m_s}$ vs V_s for Selected Target Thicknesses

Target: Doron

Obliquity: 70°

Fragment Size: 30 grains

Dashed Thickness Contours Refer to $\frac{m_r}{m_s}$ Ordinate

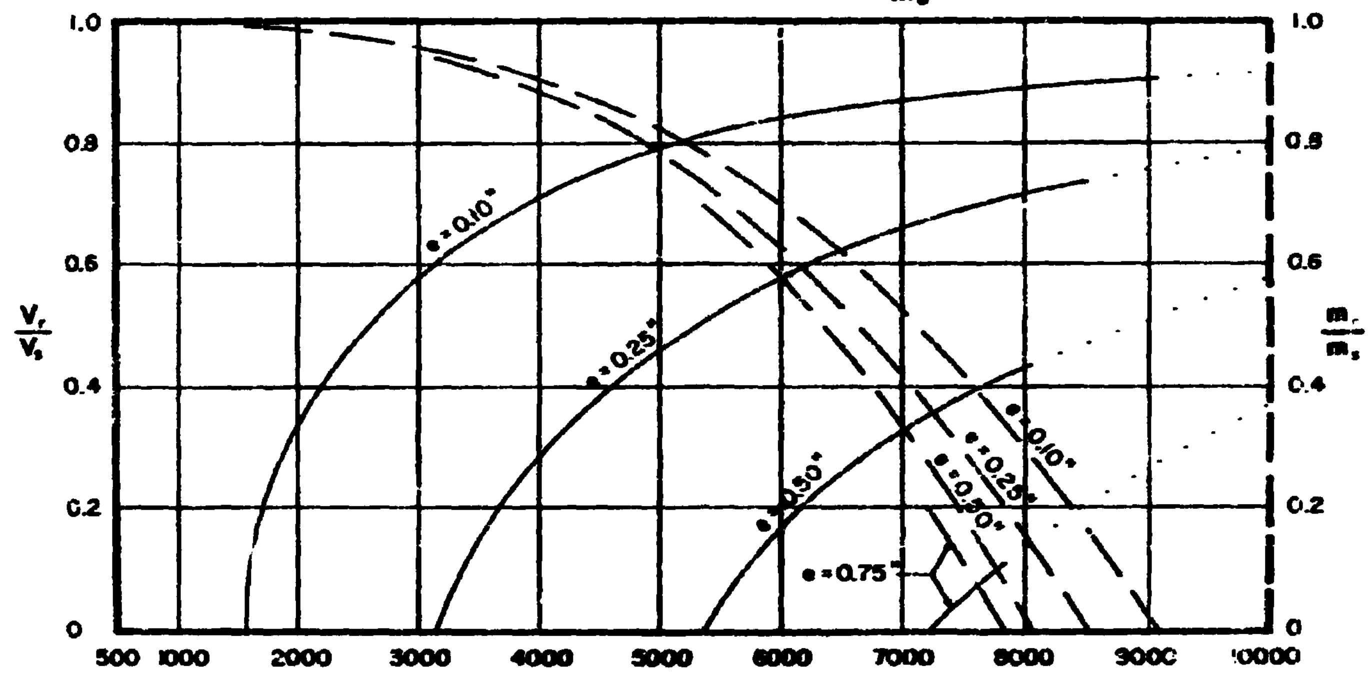

Fig. 71

$\frac{V_r}{V_s}$ and $\frac{m_r}{m_s}$ vs V_s for Selected Target Thicknesses

Target: Doron

Obliquity: 0°

Fragment Size: 100 grains

Dashed Thickness Contours Refer to $\frac{m_r}{m_s}$ Ordinate

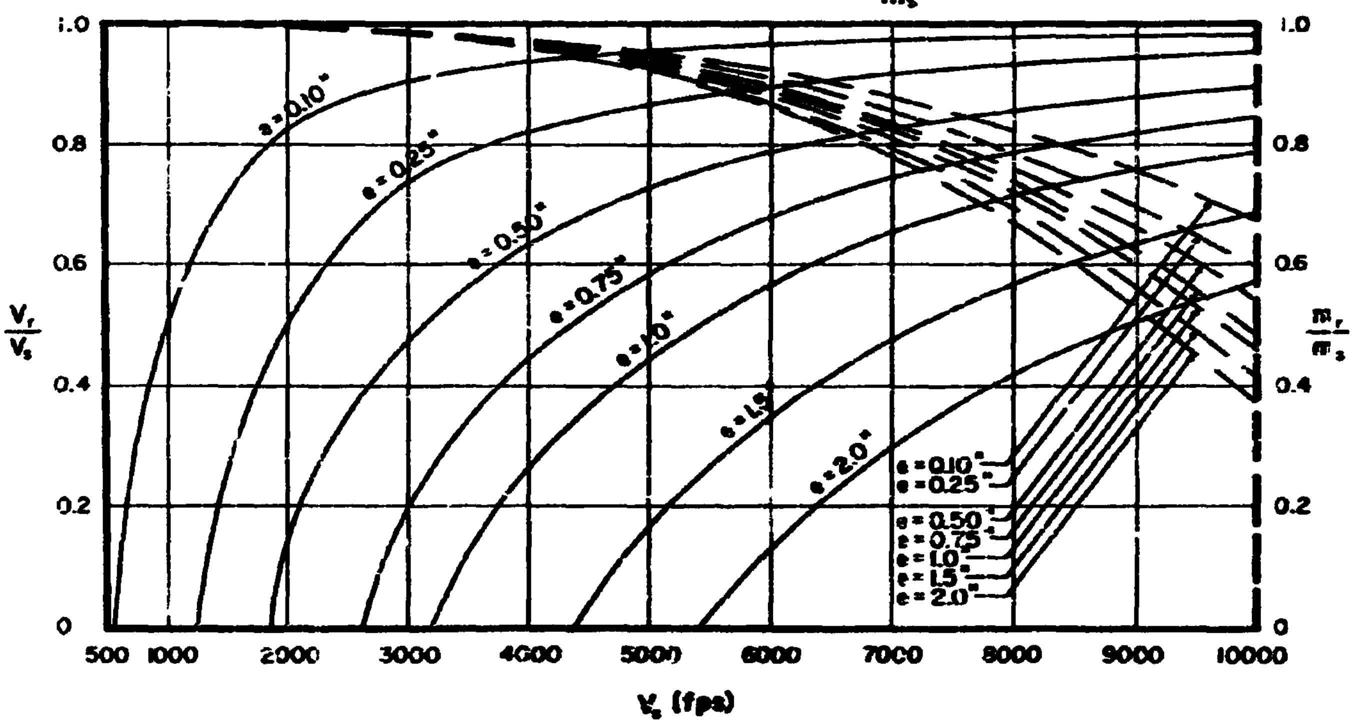

Fig. 72

$\frac{V_r}{V_s}$ and $\frac{m_r}{m_s}$ vs V_s for Selected Target Thicknesses

Target: Doron

Obliquity: 60°

Fragment Size: 100 grains

Dashed Thickness Contours Refer to $\frac{m_r}{m_s}$ Ordinate

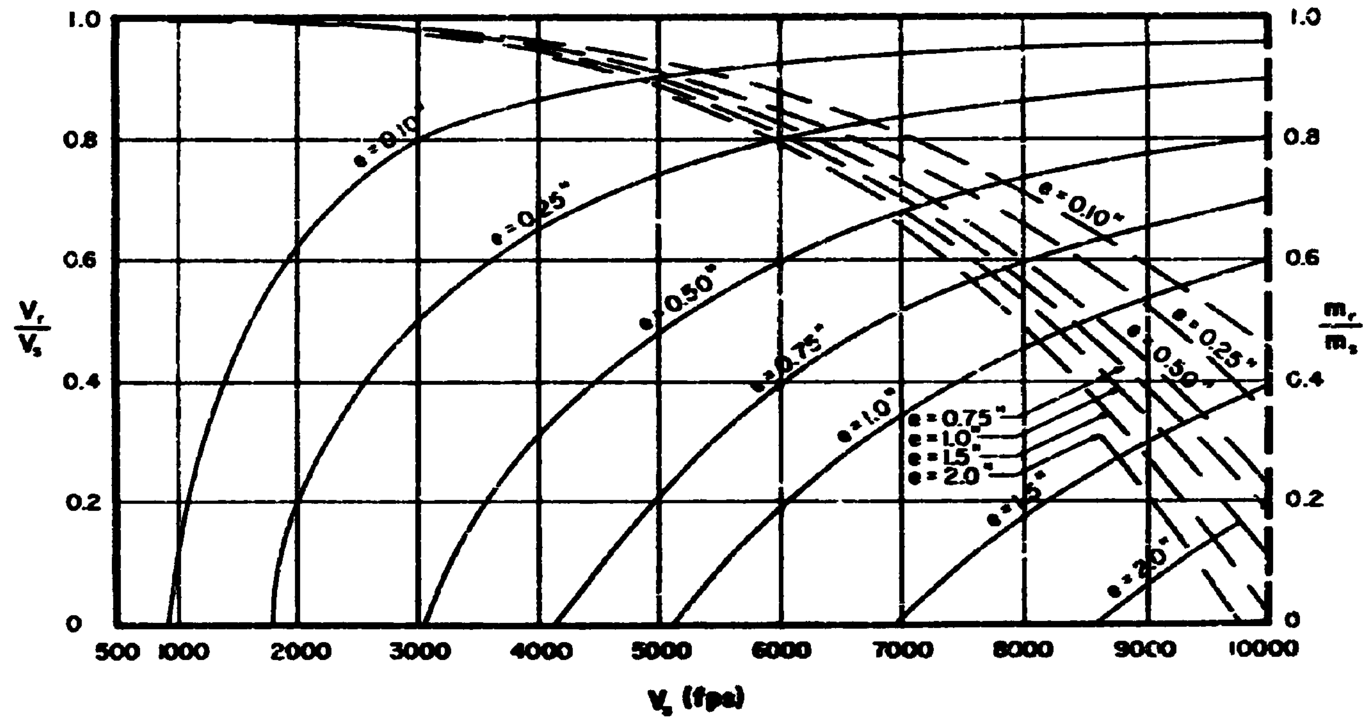

Fig. 73

$\frac{V_r}{V_s}$ and $\frac{m_r}{m_s}$ vs V_s for Selected Target Thicknesses

Target: Doron

Obliquity: 70°

Fragment Size: 100 grains

Dashed Thickness Contours Refer to $\frac{m_r}{m_s}$ Ordinate

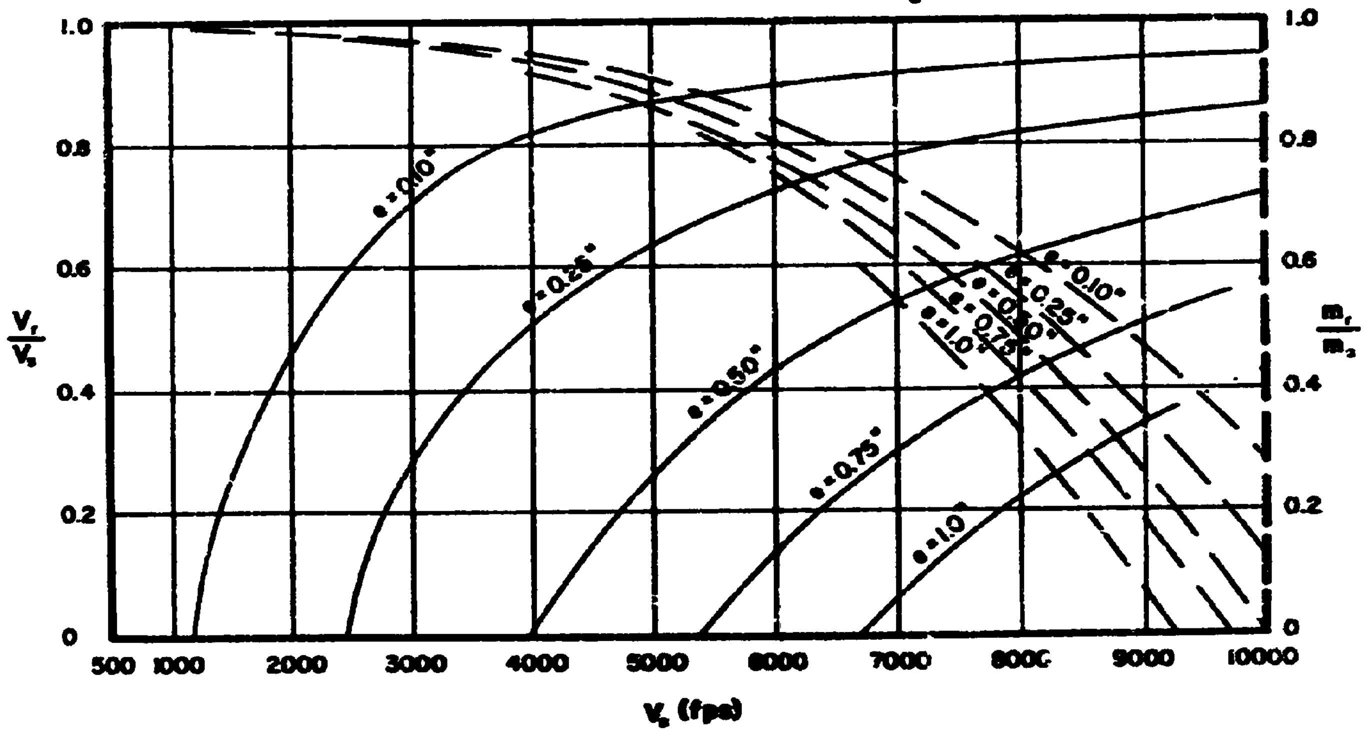

Fig. 74

$\frac{V_r}{V_s}$ and $\frac{m_r}{m_s}$ vs V_s for Selected Target Thicknesses

Target: Doron

Obliquity: 0°

Fragment Size: 300 grains

Dashed Thickness Contours Refer to $\frac{m_r}{m_s}$ Ordinate

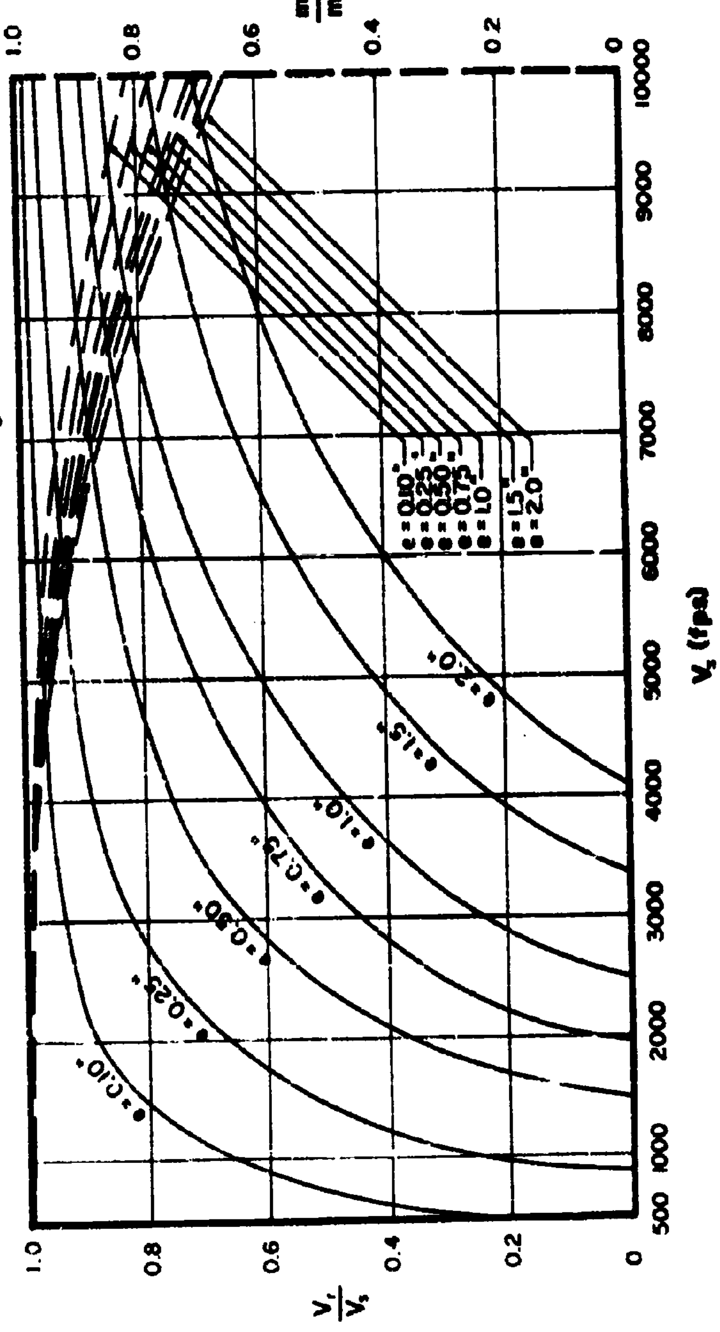

Fig. 75

$\frac{V_r}{V_s}$ and $\frac{m_r}{m_s}$ vs V_s for Selected Target Thicknesses

Target: Doron

Obliquity: 60°

Fragment Size: 300 grains

Dashed Thickness Contours Refer to $\frac{m_r}{m_s}$ Ordinate

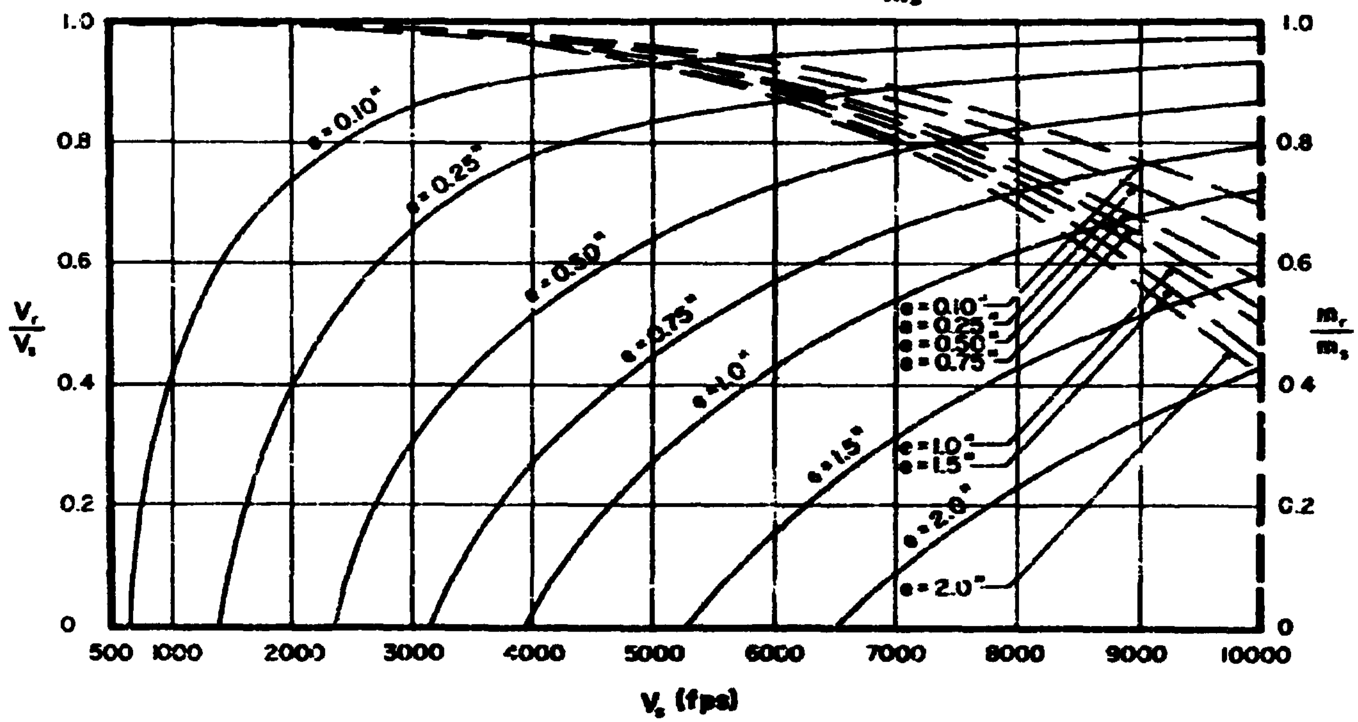

Fig. 76

$\frac{V_r}{V_s}$ and $\frac{m_r}{m_s}$ vs V_s for Selected Target Thicknesses

Target: Doron

Obliquity: 70°

Fragment Size: 300 grains

Dashed Thickness Contours Refer to $\frac{m_r}{m_s}$ Ordinate

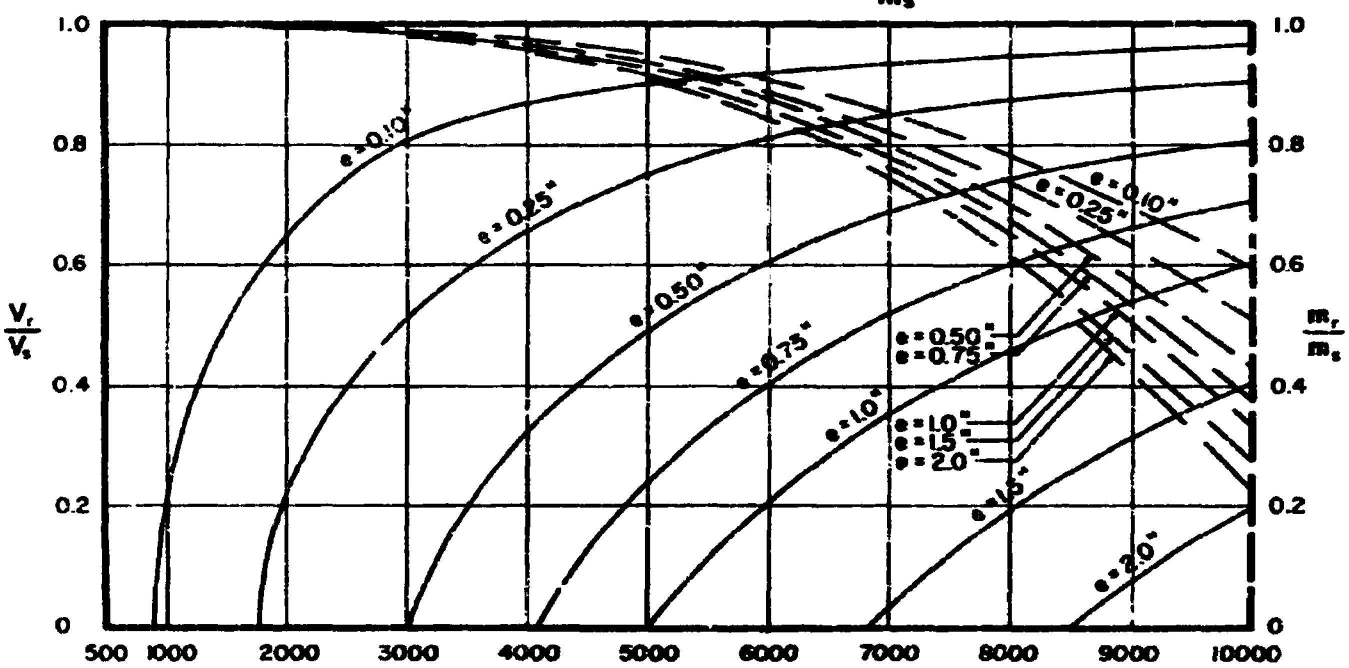

Fig. 77

$\frac{V_r}{V_s}$ and $\frac{m_r}{m_s}$ vs V_s for Selected Target Thicknesses

Target: Bullet-Resistant Glass

Obliquity: 0°

Fragment Size: 30 grains

Dashed Thickness Contours Refer to $\frac{m_r}{m_s}$ Ordinate

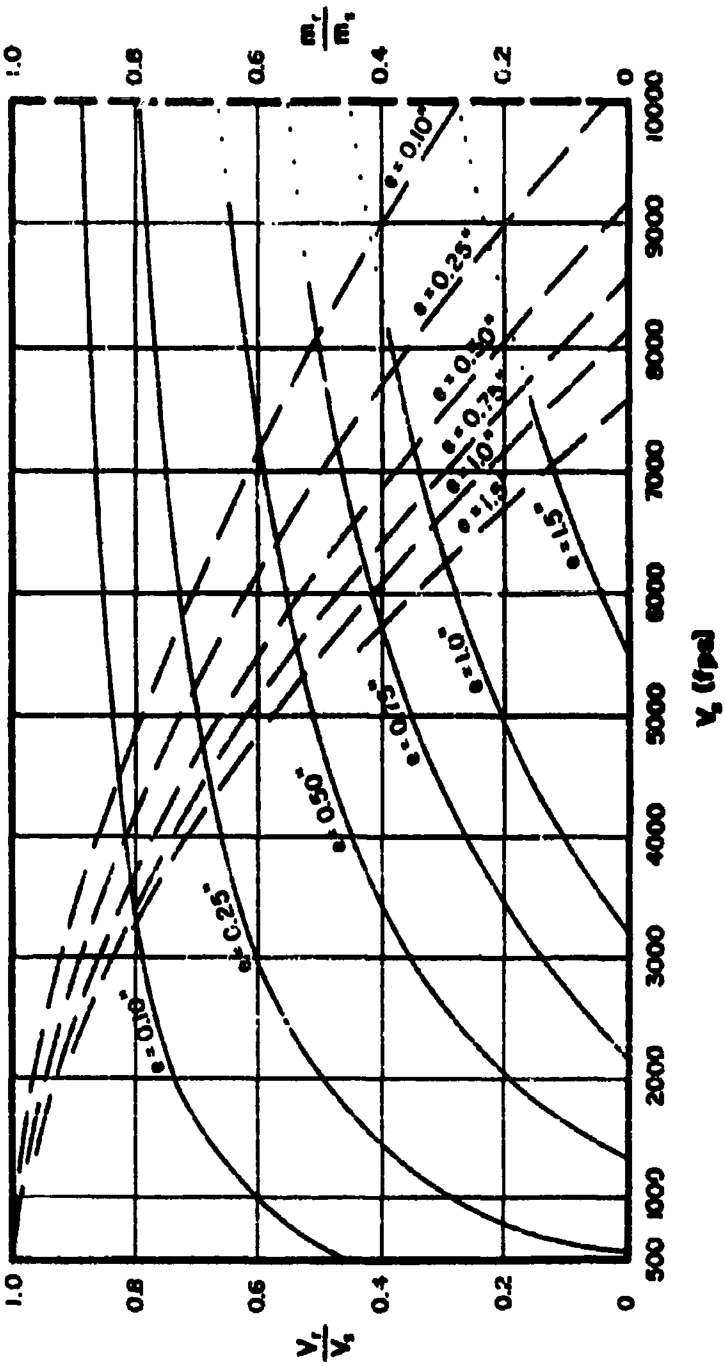

Fig. 78

$\frac{V_r}{V_s}$ and $\frac{m_r}{m_s}$ vs V_s for Selected Target Thicknesses

Target: Bullet-Resistant Glass

Obliquity: 60°

Fragment Size: 30 grains

Dashed Thickness Contours Refer to $\frac{m_r}{m_s}$ Ordinate

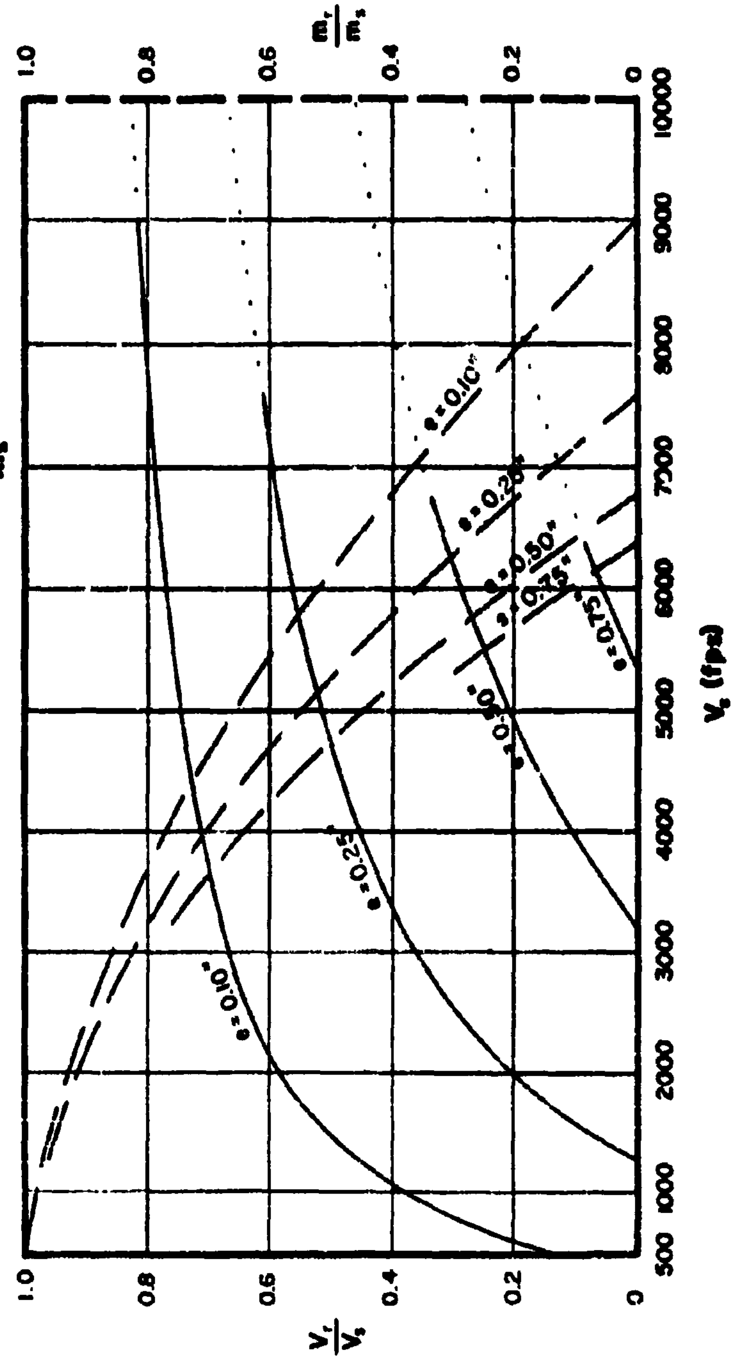

Fig. 79

$\frac{V_r}{V_s}$ and $\frac{m_r}{m_s}$ vs V_s for Selected Target Thicknesses

Target: Bullet-Resistant Glass

Obliquity: 70°

Fragment Size: 30 grains

Dashed Thickness Contours Refer to $\frac{m_r}{m_s}$ Ordinate

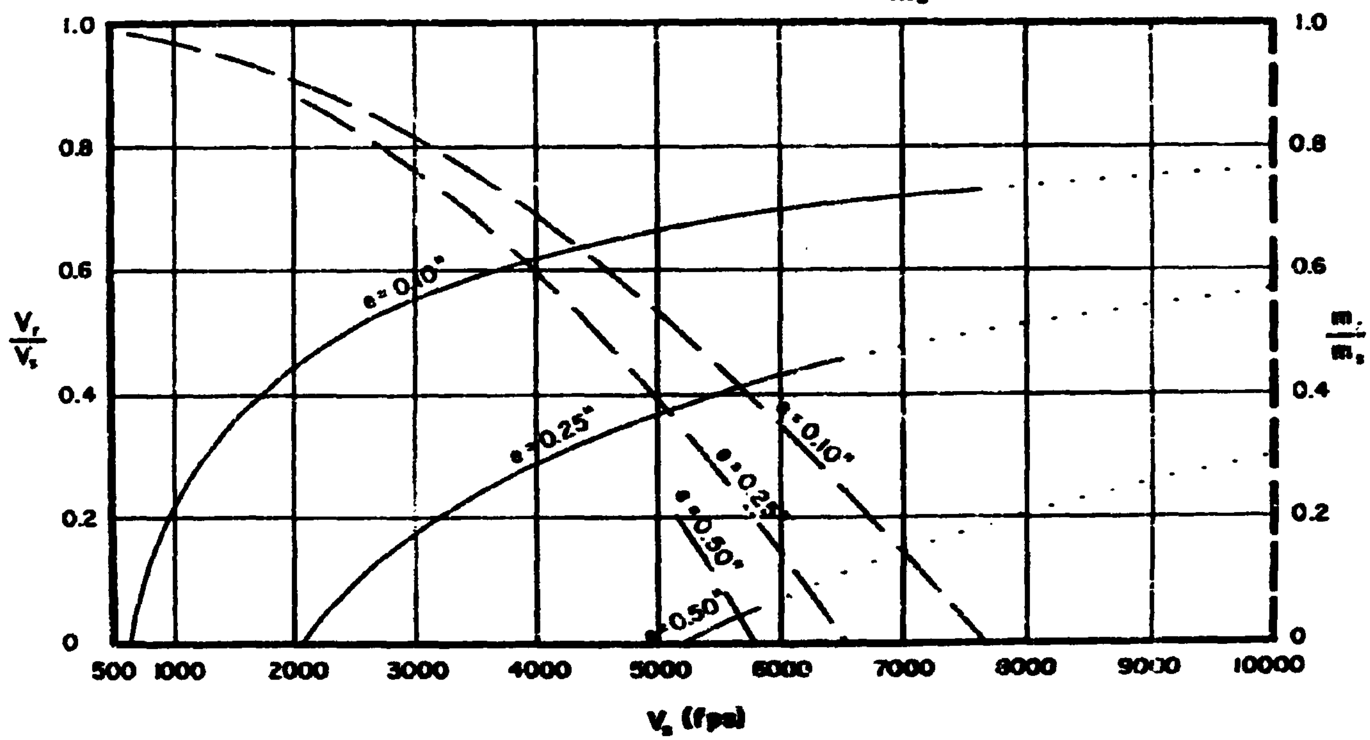

Fig. 80

$\frac{V_r}{V_s}$ and $\frac{m_r}{m_s}$ vs V_s for Selected Target Thicknesses

Target: Bullet-Resistant Glass

Obliquity: 0°

Fragment Size: 100 grains

Dashed Thickness Contours Refer to $\frac{m_r}{m_s}$ Ordinate

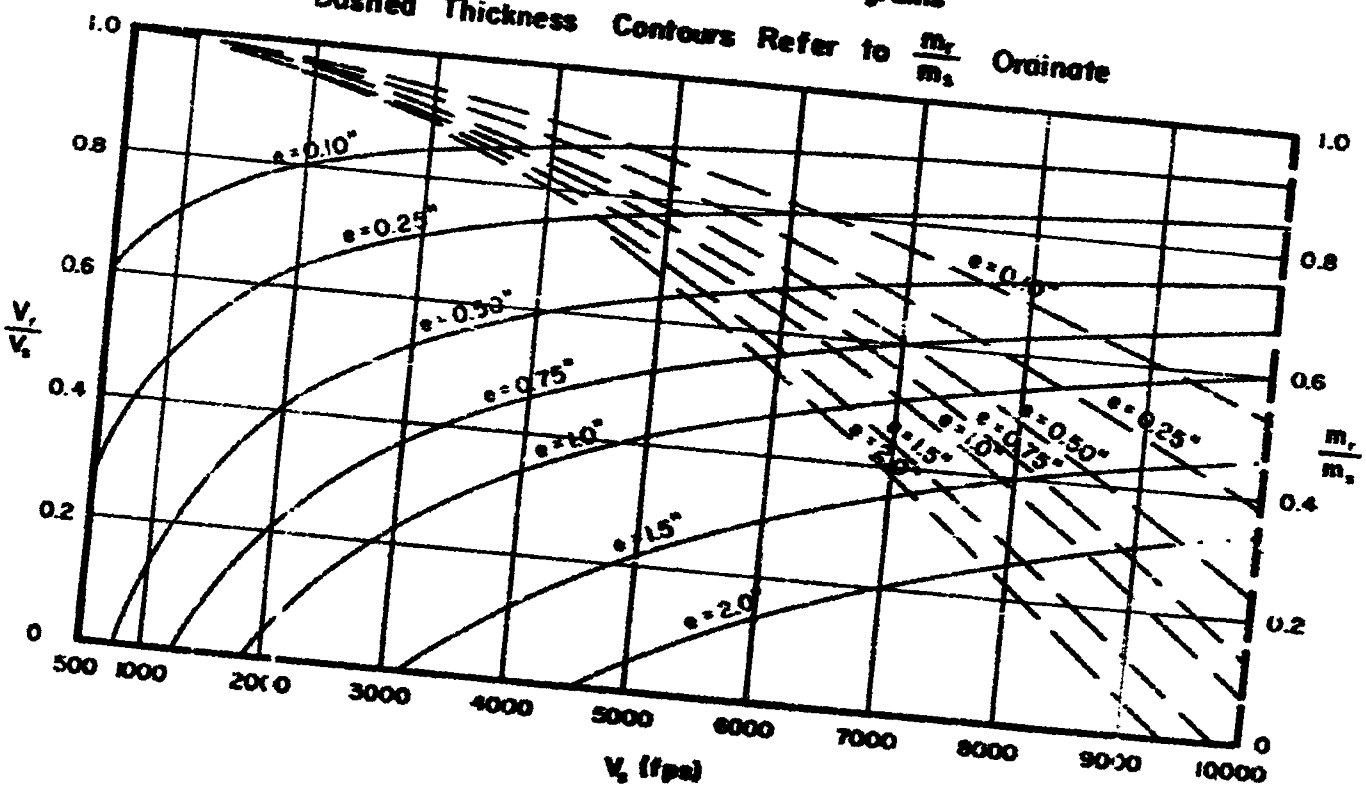

Fig. 81

$\frac{V_r}{V_s}$ and $\frac{m_r}{m_s}$ vs V_s for Selected Target Thicknesses

Target: Bullet-Resistant Glass

Obliquity: 60°

Fragment Size: 100 grains

Dashed Thickness Contours Refer to $\frac{m_r}{m_s}$ Ordinate

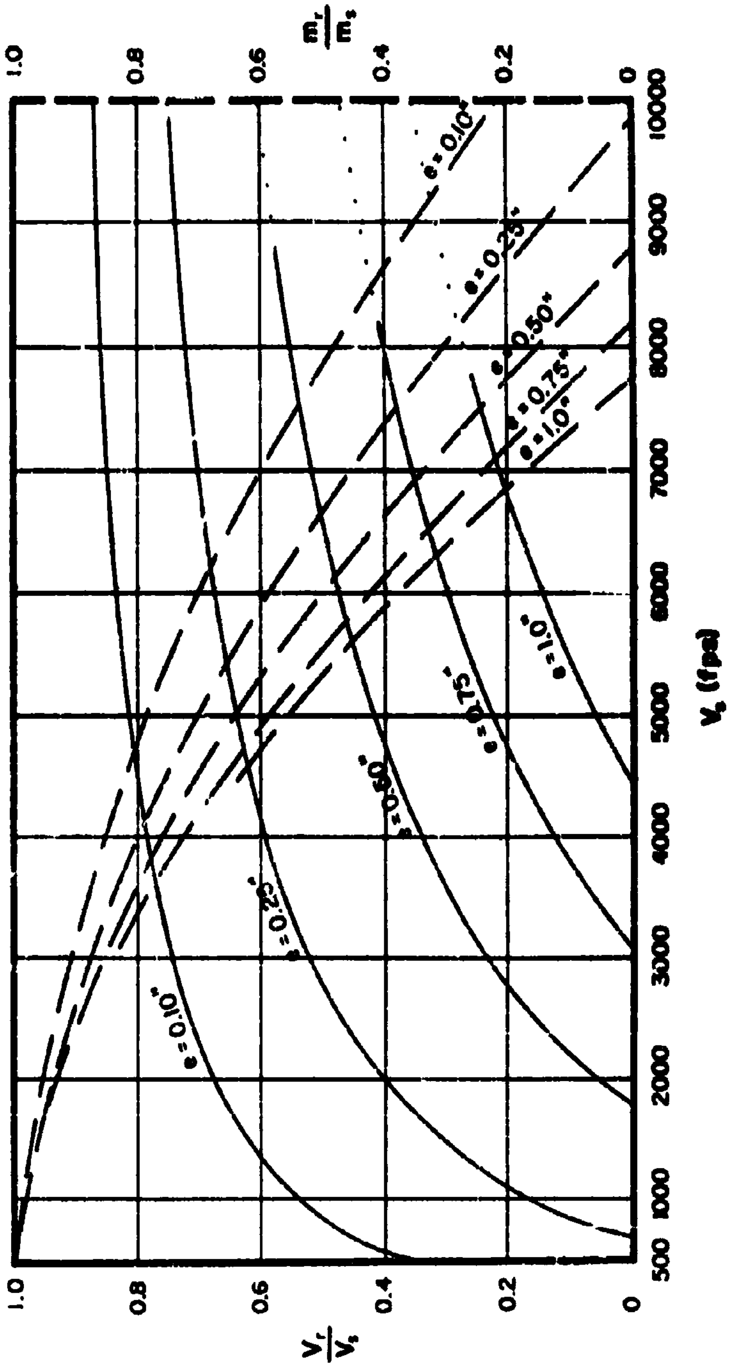

Fig. 82

$\frac{V_r}{V_s}$ and $\frac{m_r}{m_s}$ vs V_s for Selected Target Thicknesses

Target: Bullet-Resistant Glass

Obliquity: 70°

Fragment Size: 100 grains

Dashed Thickness Contours Refer to $\frac{m_r}{m_s}$ Ordinate

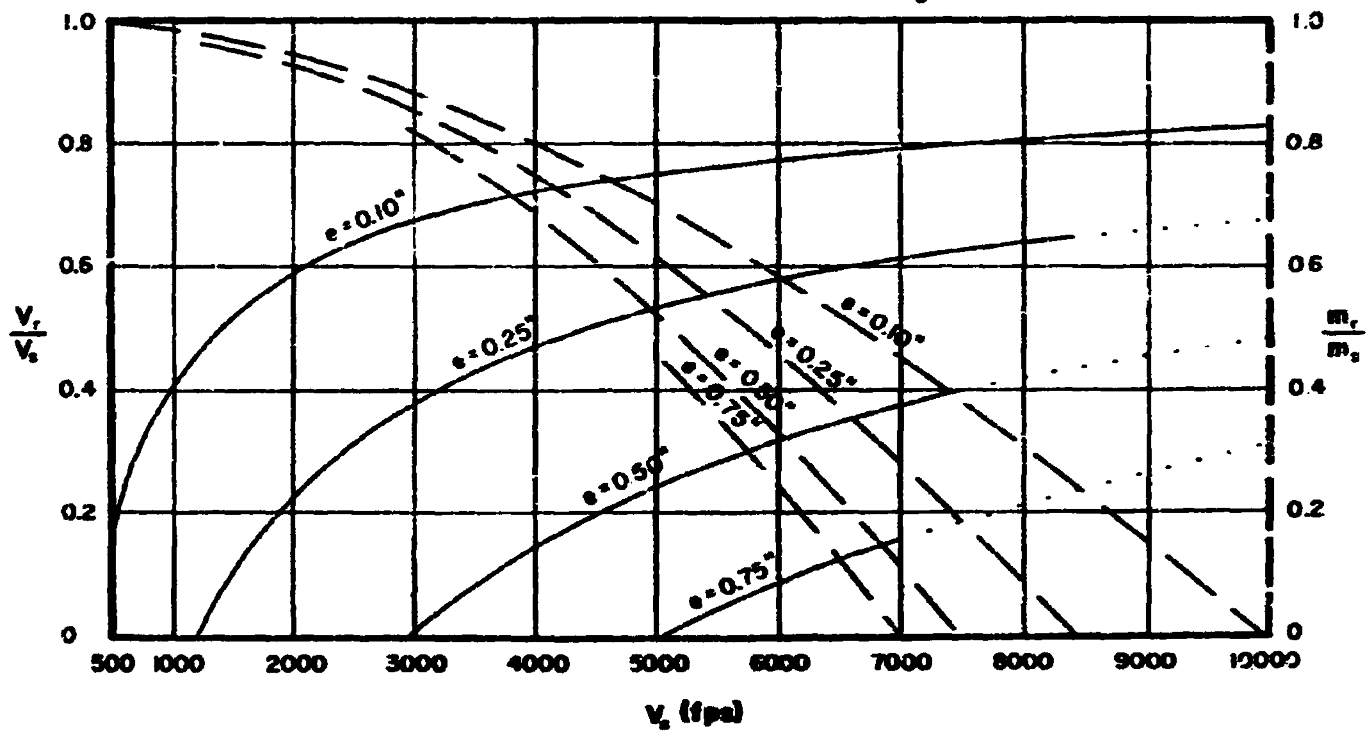

Fig. 83

$\frac{V_r}{V_s}$ and $\frac{m_r}{m_s}$ vs V_s for Selected Target Thicknesses

Target: Bullet-Resistant Glass

Obliquity: 0°

Fragment Size: 300 grains

Dashed Thickness Contours Refer to $\frac{m_r}{m_s}$ Ordinate

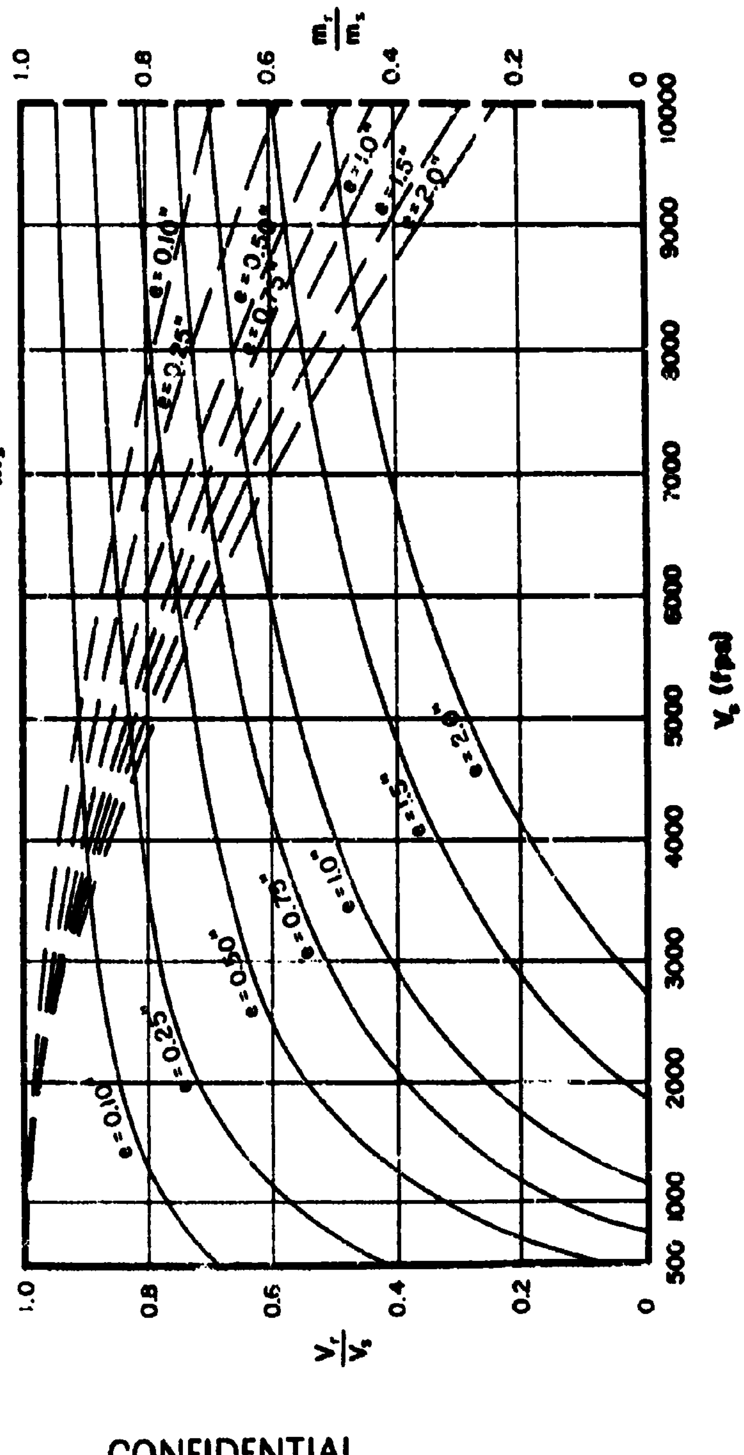

Fig. 84

$\frac{V_r}{V_s}$ and $\frac{m_r}{m_s}$ vs V_s for Selected Target Thicknesses

Target: Bullet-Resistant Glass

Obliquity: 60°

Fragment Size: 300 grains

Dashed Thickness Contours Refer to $\frac{m_r}{m_s}$ Ordinate

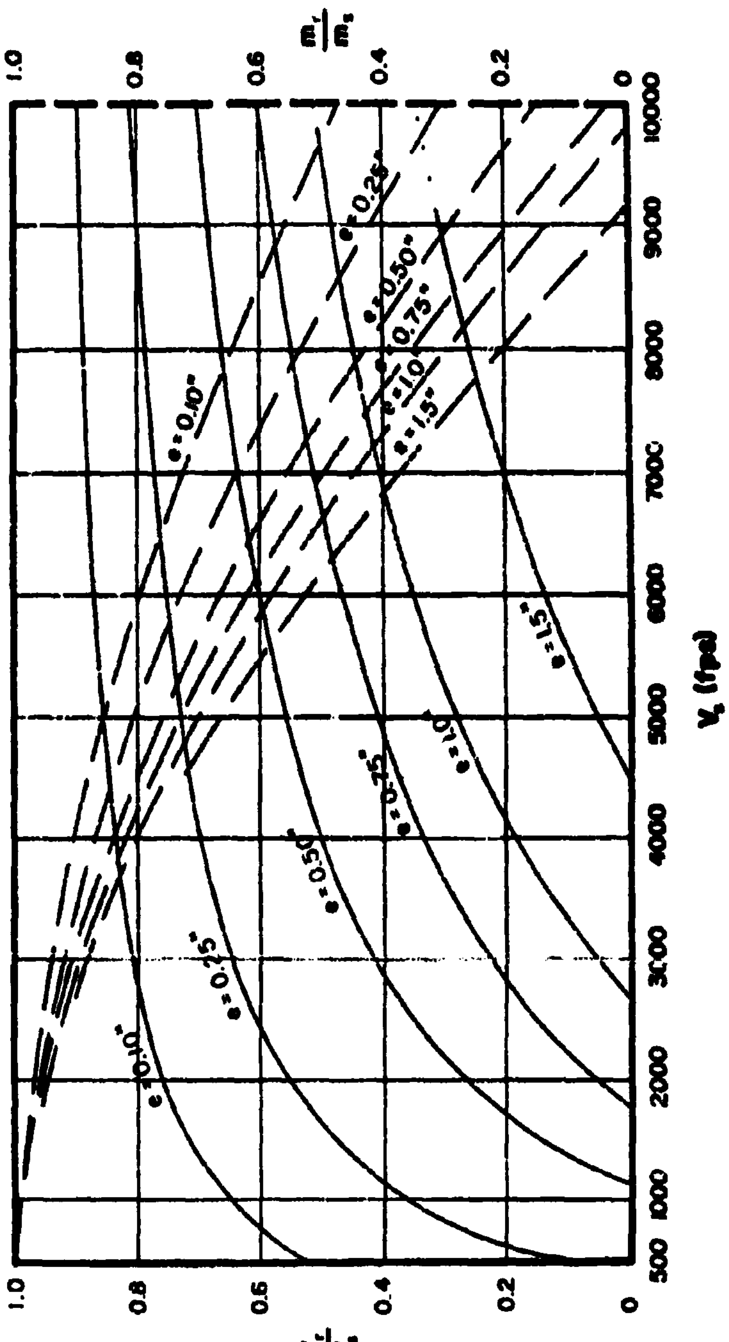

Fig. 85

$\frac{V_r}{V_s}$ and $\frac{m_r}{m_s}$ vs V_s for Selected Target Thicknesses

Target: Bullet-Resistant Glass

Obliquity: 70°

Fragment Size: 300 grains

Dashed Thickness Contours Refer to $\frac{m_r}{m_s}$ Ordinate

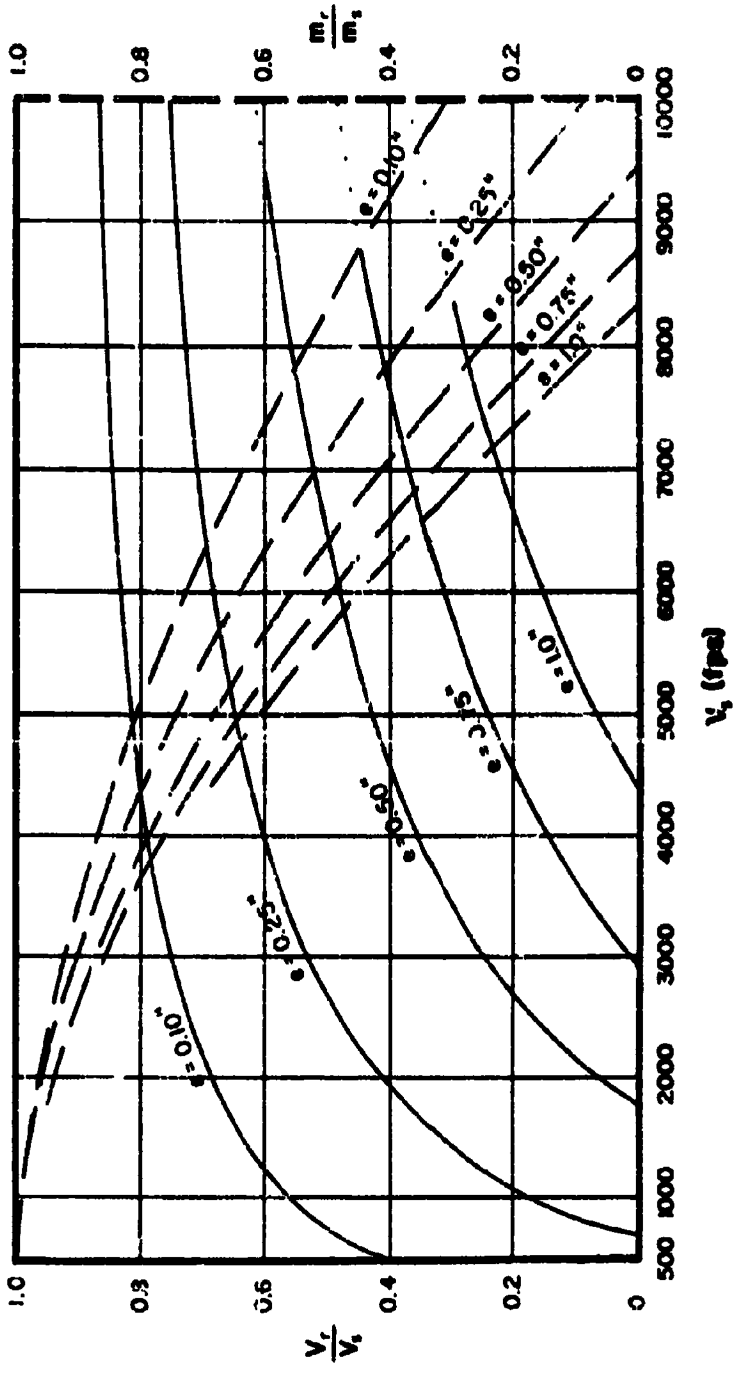

Fig. 86

Appendix C

Graph Set III: $f(m_r, V_r)$ vs E

for a Particular Combination of m_s, θ, V_s

Figs. 87-90

Note: Within this set of graphs, a contour for a particular material is shown only for those values of the abscissa for which m_r and V_r are both non-negative. Furthermore, the contours are not significantly extrapolated beyond the interval of thicknesses of target material employed in the basic BRL experiments.

$f(m_r, v_r)$ vs E

for Various Combinations of m_s, θ, and V_s

m_s = 100 grains θ = 60 degrees V_s = 6000 fps

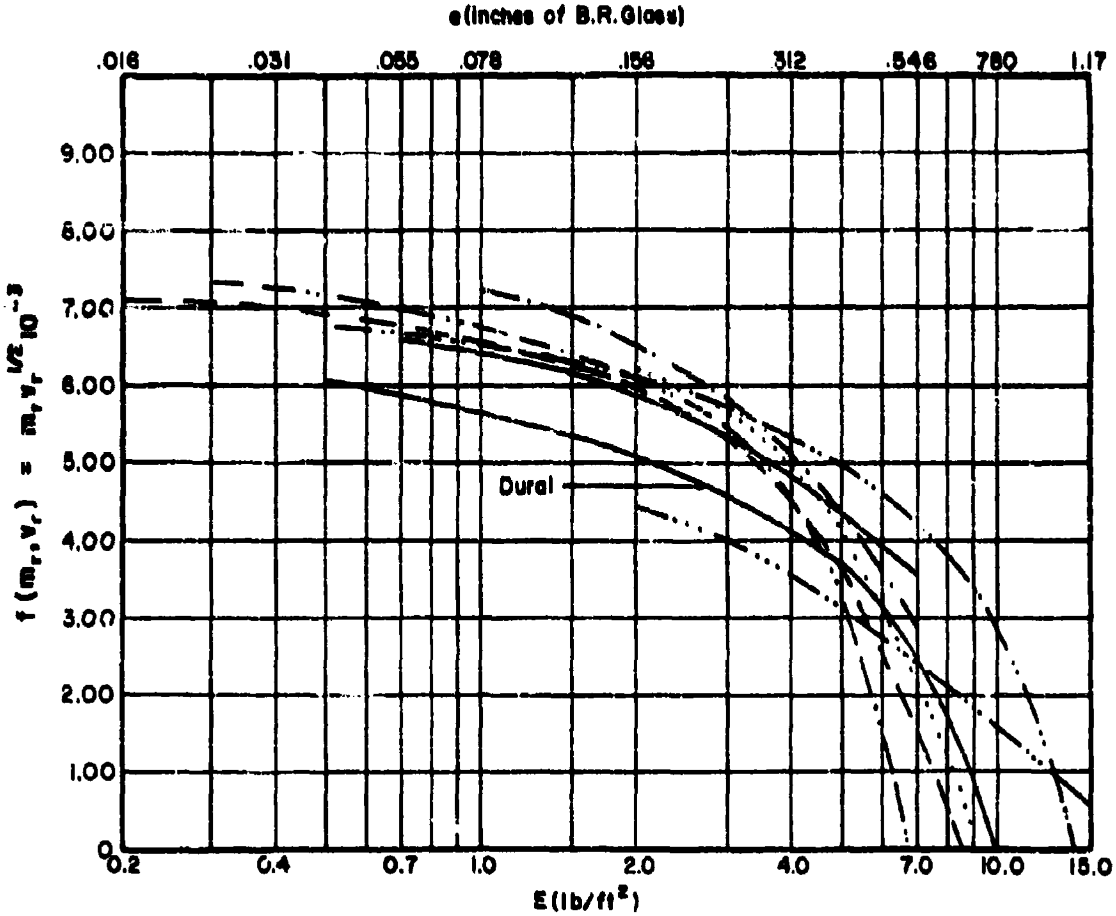

		*			*
Unbonded Nylon	– – – –	3.31	Stretched Plexiglas	– – · · – –	2.01
Bonded Nylon	·········	2.66	Doron	– · – –	1.23
Lexan	———	2.06	B. R. Glass	– · · · – · · ·	1.00
Cast Plexiglas	– · – · –	2.01			

*Ratio of Material Thickness Relative to a Unit Thickness of B.R.Glass

Fig. 87

$f(m_r, v_r)$ vs E

for Various Combinations of m_s, Θ, and V_s

m_s = 100 grains Θ = 60 degrees V_s = 6000 fps

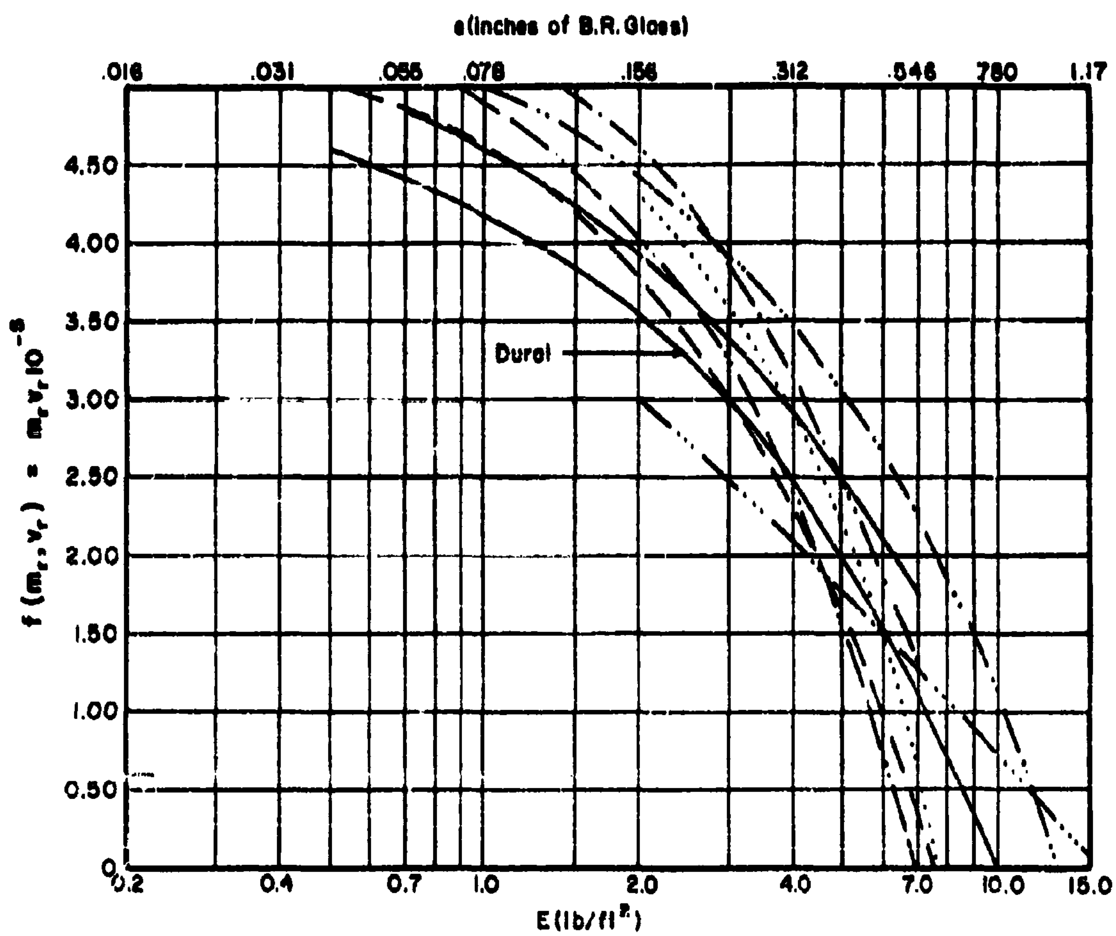

		*			*
Unbonded Nylon	----	3.31	Stretched Plexiglas	--··--	2.01
Bonded Nylon	········	2.66	Doron	-··--	1.23
Lexan	——	2.06	B. R. Glass	-···-···	1.00
Cast Plexiglas	-·-·-	2.01			

*Ratio of Material Thickness Relative to a Unit Thickness of B.R.Glass

Fig. 88

$f(m_r, v_r)$ vs E

for Various Combinations of m_s, Θ, and V_s

m_s = 100 grains Θ = 60 degrees V_s = 6000 fps

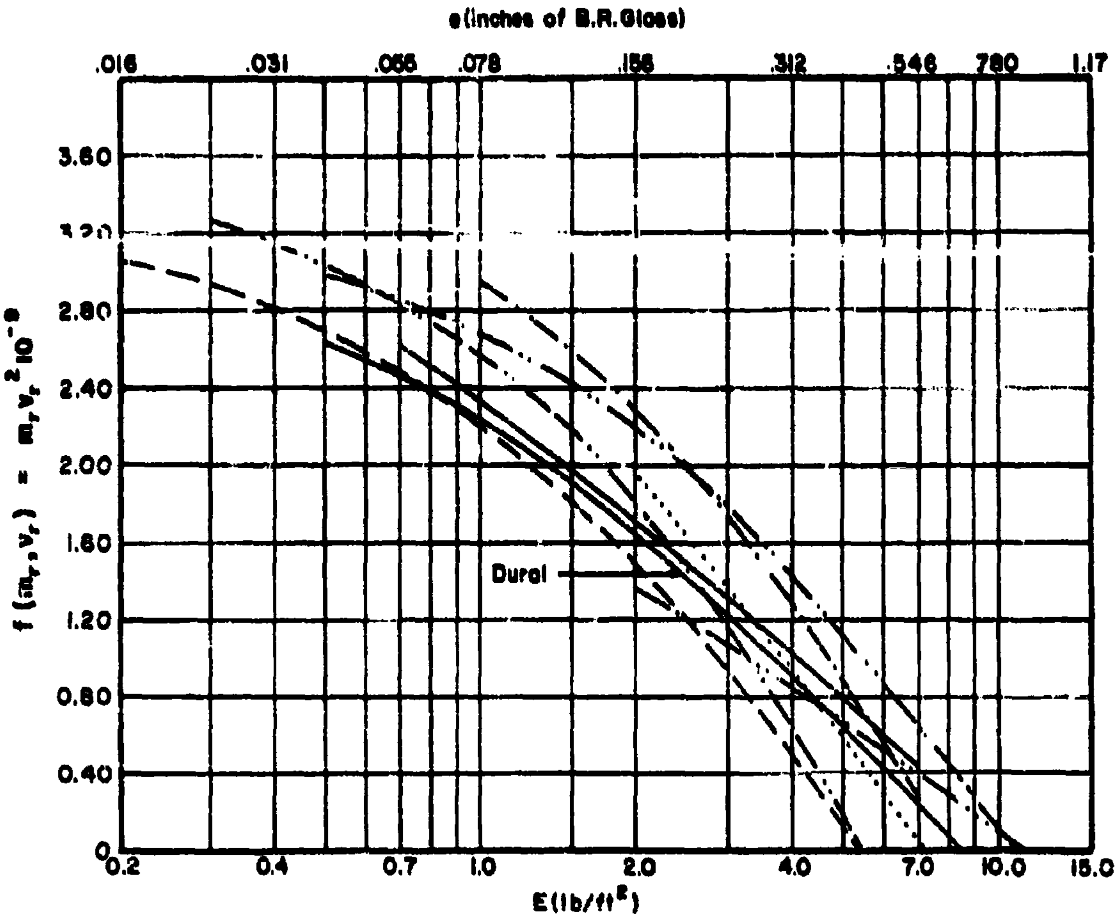

		*			*
Unbonded Nylon	– – – –	3.31	Stretched Plexiglas	—··— —	2.01
Bonded Nylon	·········	2.68	Doron	—··——··	1.23
Lexan	———	2.06	B. R. Glass	—···—··	1.00
Cast Plexiglas	—·—·—	2.01			

*Ratio of Material Thickness Relative to a Unit Thickness of B.R. Glass

Fig. 89

$f(m_r, v_r)$ vs E
for Various Combinations of m_s, Θ, and V_s

m_s = 100 grains Θ = 60 degrees V_s = 6000 fps

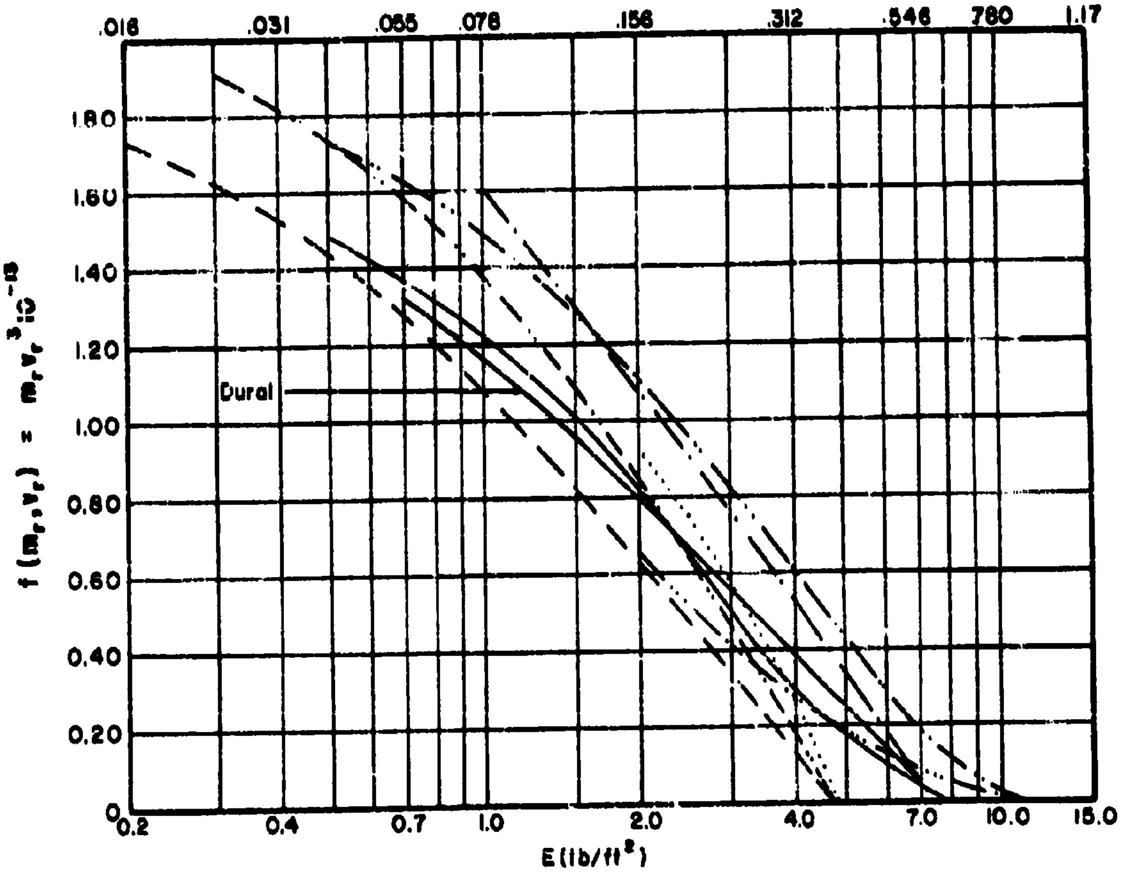

		*			*
Unbonded Nylon	– – – –	3.31	Stretched Plexiglas	– –·· – –	2.01
Bonded Nylon	·········	2.66	Doron	–··–––·–	1.23
Lexan	———	2.06	B. R. Glass	–···––	1.00
Cast Plexiglas	–·–·–	2.01			

*Ratio of Material Thickness Relative to a Unit Thickness of B.R. Glass

Fig. 90

Appendix D

Graph Set IV: e (inches of 2024T-3) vs E
for Various Combinations of m_s, θ, and V_s

Figs. 91-117

Note: The ordinate represents an estimate of the maximum thickness of calibrating material that can possibly be perforated by the largest portion of the residual fragment after the original fragment has impacted initially on one of the given targets. The assumption is made that the residual fragment strikes the calibrating material at normal impact and that, furthermore, the shape of the original fragment is retained despite any loss in weight.

On each graph in this appendix there appears a value of e_o. This value is an estimate of the maximum thickness of the calibrating material that the original fragment can perforate, assuming normal impact and no intermediate barrier.

The contours are limited on these graphs to 3.0" of 2024T-3. This represents the maximum thickness of this material that has been considered in BRL single-target firings. In fact, there is no instance to date of a perforation of 3.0" of 2024T-3 in BRL experimental work with compact fragments.

$e_{2024T-3}$ vs E
for Various Combinations of m_s, Θ, and V_s

m_s = 30 grains Θ = 0 degrees V_s = 3000 fps

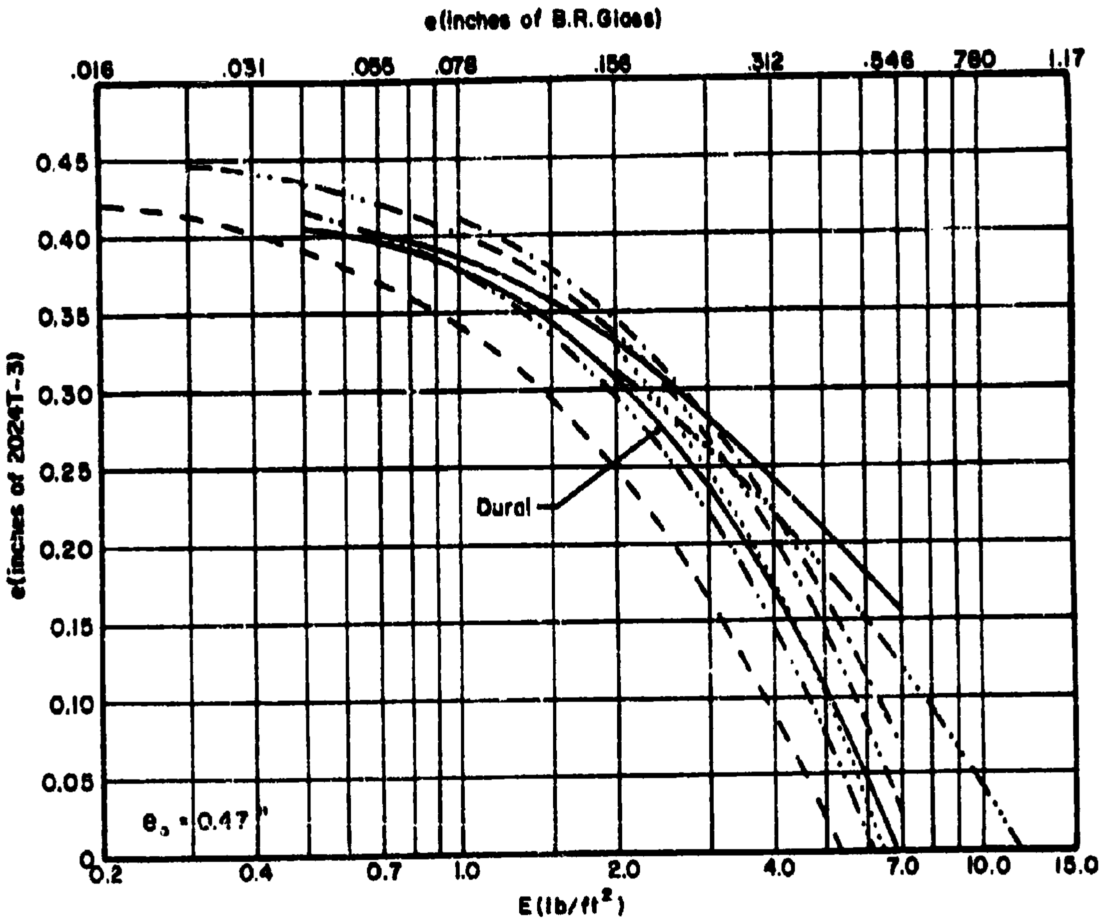

		*			*
Unbonded Nylon	----	3.31	Stretched Plexiglas	---··---	2.01
Bonded Nylon	········	2.66	Dural	--·--·--	1.23
Lexan	———	2.06	B. R. Glass	--···--···	1.00
Cast Plexiglas	--·--·--	2.01			

*Ratio of Material Thickness Relative to a Unit Thickness of B.R.Glass

Fig. 91

$e_{2024T\text{-}3}$ vs E

for Various Combinations of m_s, Θ, and V_s

m_s = 100 grains Θ = 0 degrees V_s = 3000 fps

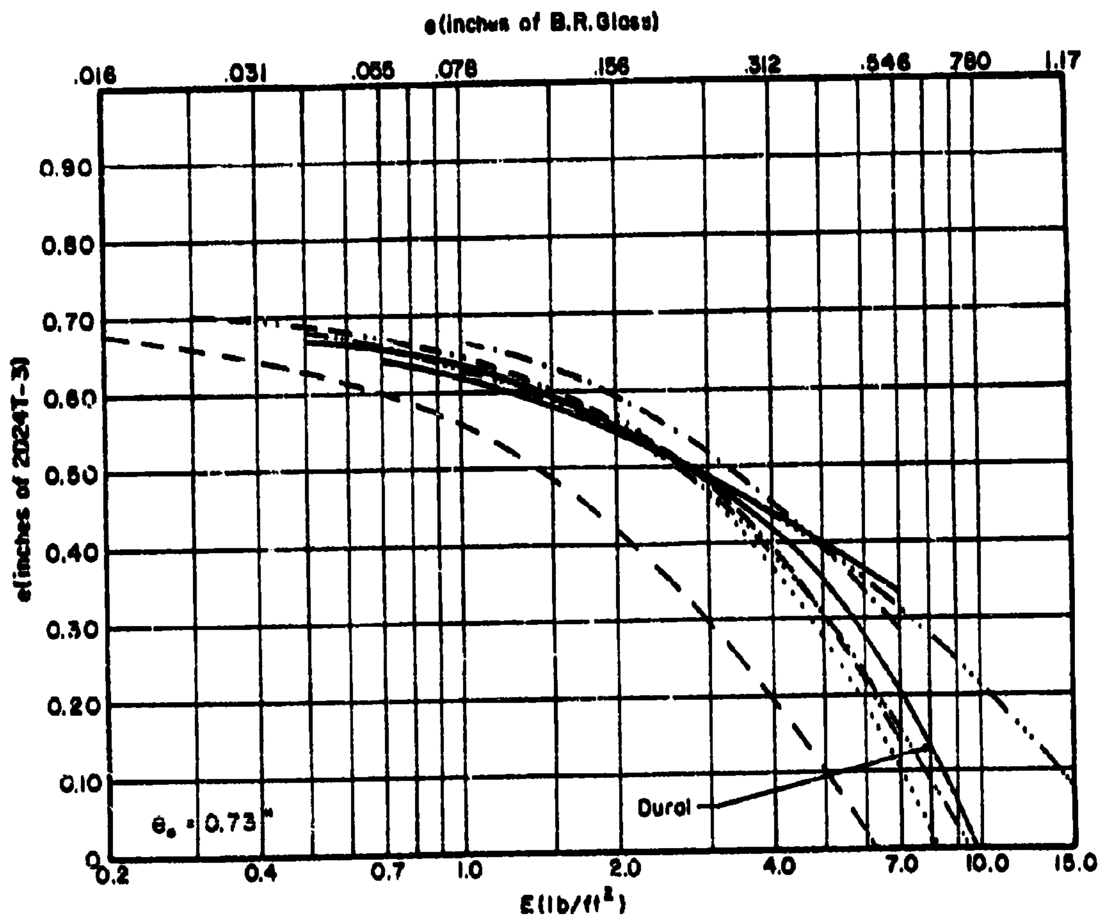

		*			*
Unbonded Nylon	— — — —	3.31	Stretched Plexiglas	— · · —	2.01
Bonded Nylon	········	2.66	Doron	— · · — · · —	1.23
Lexan	————	2.06	B. R. Glass	— · · · — · · ·	1.00
Cast Plexiglas	— · — · —	2.01			

*Ratio of Material Thickness Relative to a Unit Thickness of B.R.Glass

Fig. 92

$e_{2024T-3}$ vs E

for Various Combinations of m_s, Θ, and V_s

m_s = 300 grains Θ = 0 degrees V_s = 3000 fps

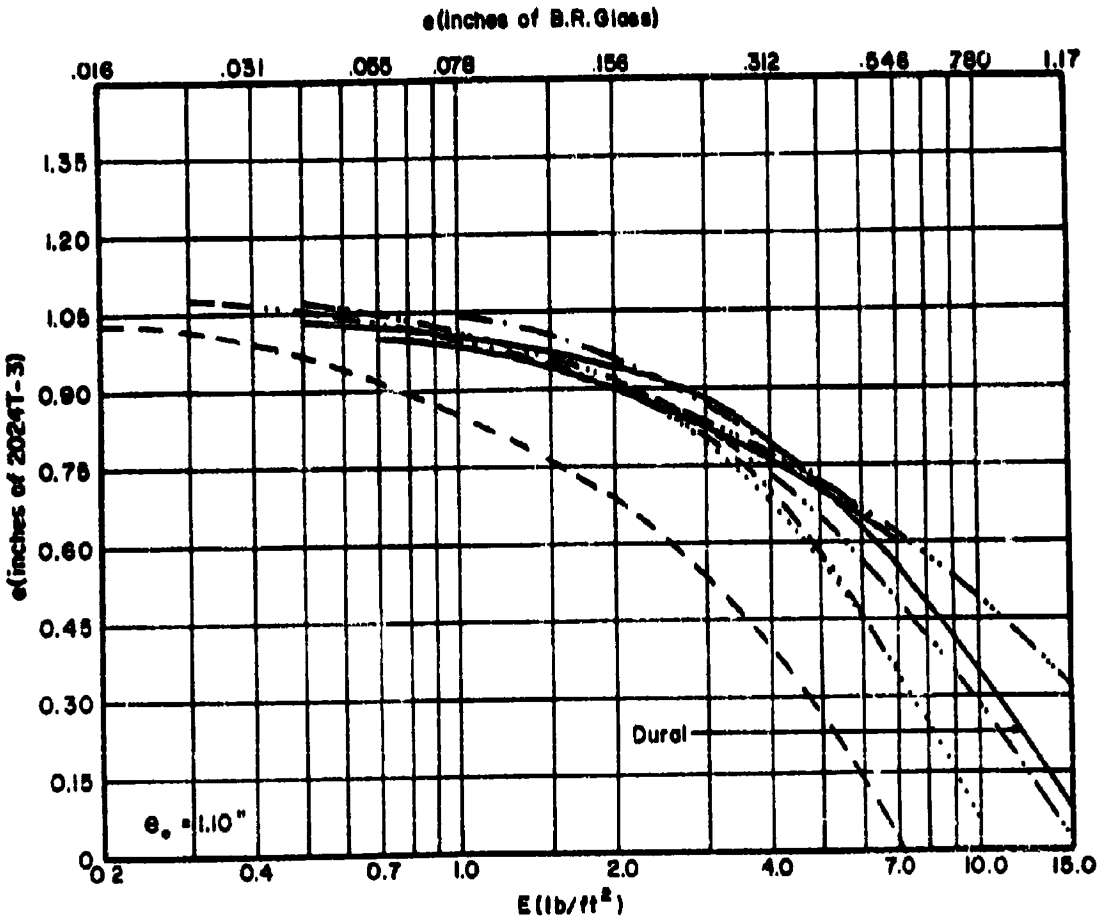

	*		*
Unbonded Nylon ----	3.31	Stretched Plexiglas	2.01
Bonded Nylon	2.66	Doron	1.23
Lexan ———	2.06	B. R. Glass	1.00
Cast Plexiglas -·-·-	2.01		

*Ratio of Material Thickness Relative to a Unit Thickness of B.R.Glass

Fig. 93

$e_{2024T-3}$ vs E

for Various Combinations of m_s, Θ, and V_s

m_s = 30 grains Θ = 60 degrees V_s = 3000 fps

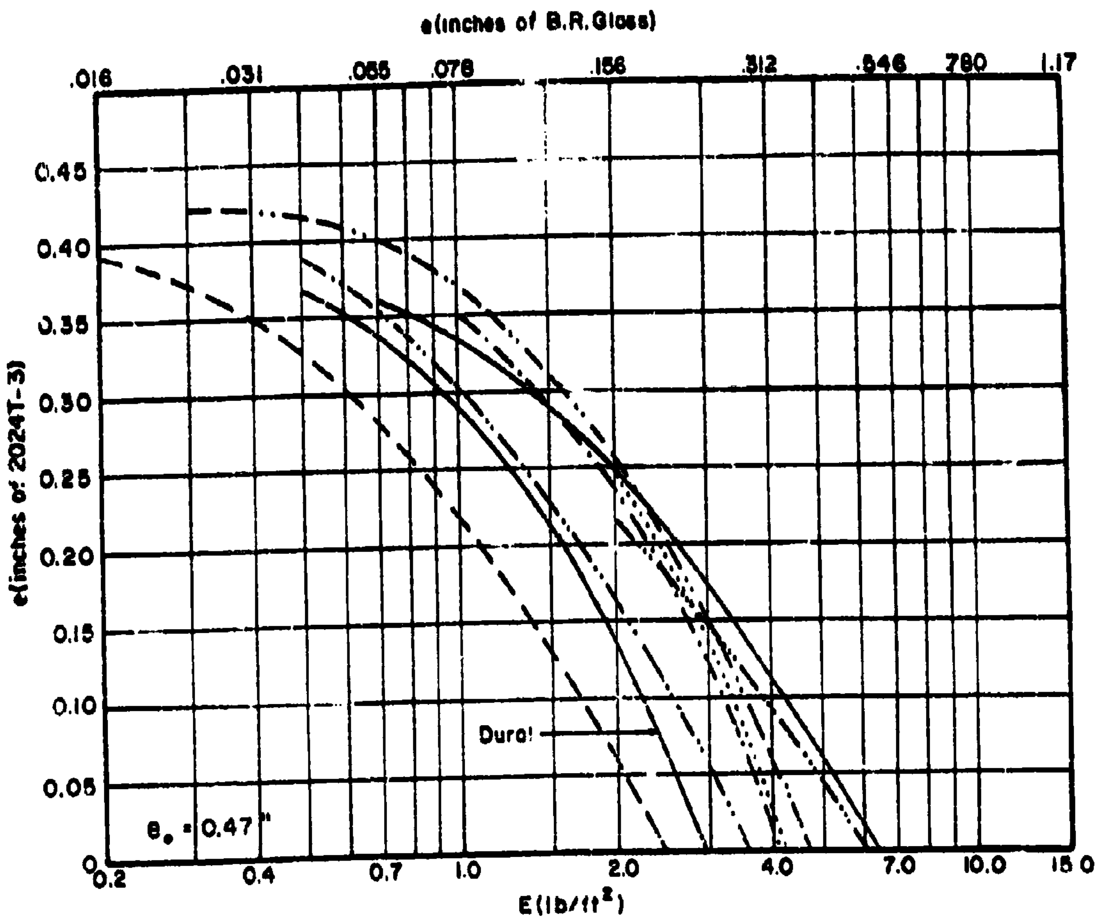

		*			*
Unbonded Nylon	----	3.31	Stretched Plexiglas	---·---	2.01
Bonded Nylon	·········	2.66	Doron	–··––··	1.23
Lexan	———	2.06	B. R. Glass	–···–··	1.00
Cast Plexiglas	–·–·–	2.01			

*Ratio of Material Thickness Relative to a Unit Thickness of B.R.Glass

Fig. 94

$e_{2024T-3}$ vs E
for Various Combinations of m_s, Θ, and V_s

m_s = 100 grains Θ = 60 degrees V_s = 3000 fps

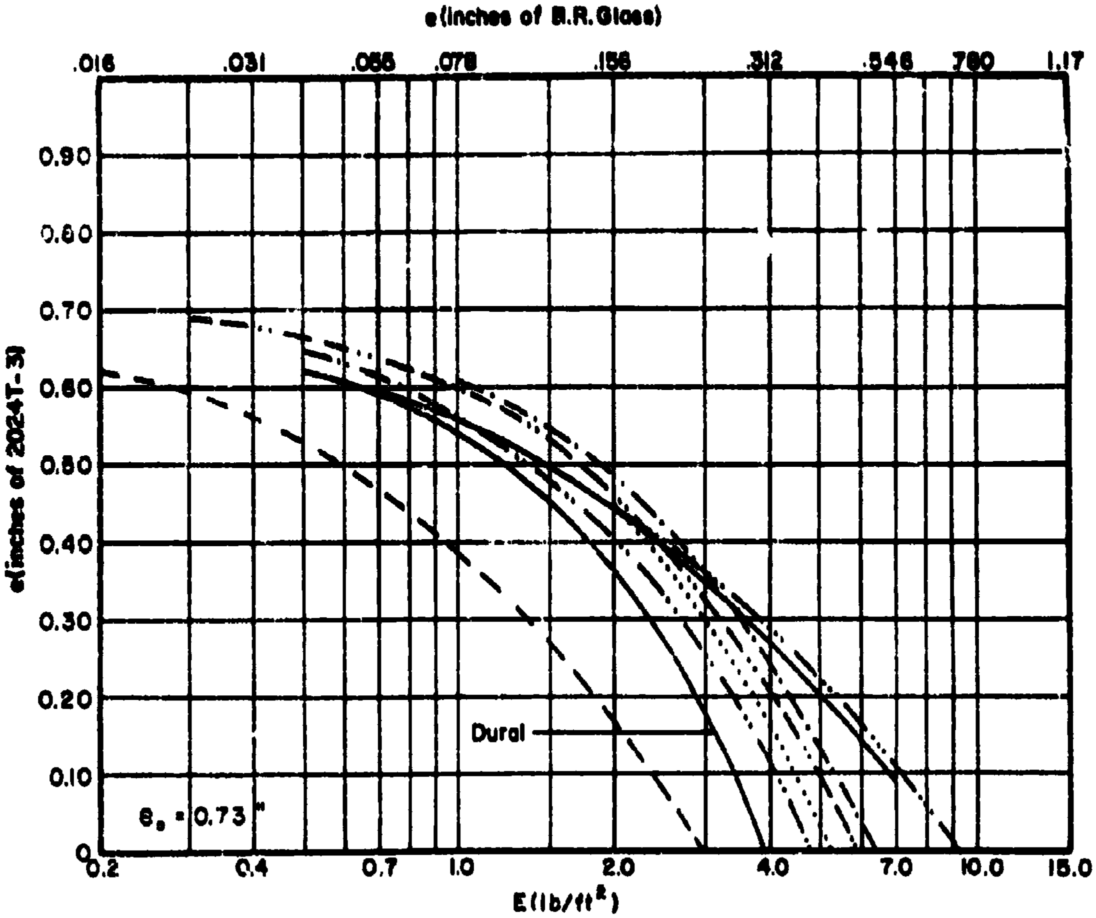

		*
Unbonded Nylon	– – – –	3.31
Bonded Nylon	········	2.66
Lexan	———	2.06
Cast Plexiglas	–·–·–	2.01
Stretched Plexiglas	–··–·–	2.01
Doron	–··––	1.23
B. R. Glass	–···–	1.00

*Ratio of Material Thickness Relative to a Unit Thickness of B.R.Glass

Fig. 95

$e_{2024T-3}$ vs E

for Various Combinations of m_s, θ, and V_s

m_s = 300 grains θ = 60 degrees V_s = 3000 fps

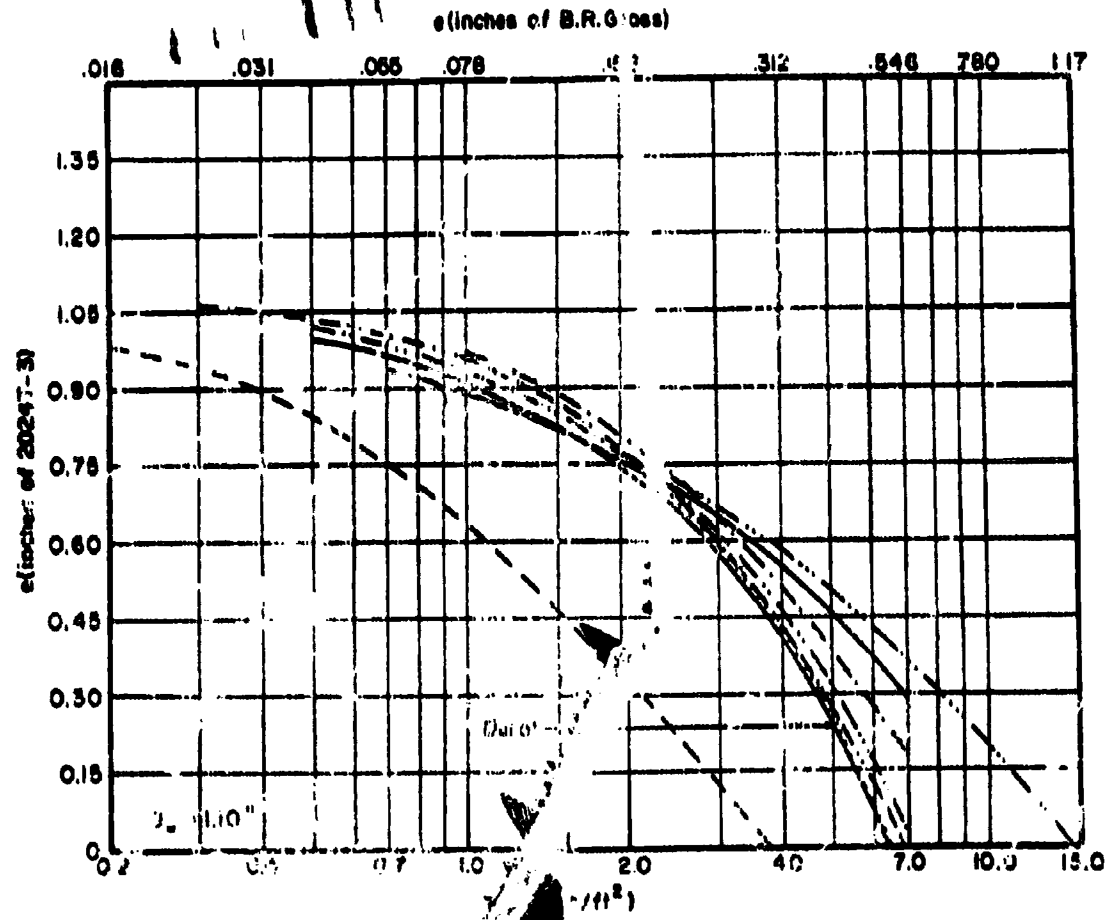

Unbonded Nylon	----	
Bonded Nylon	······	
Lexan	——	2.06
Cast Plexiglas	- - -	2.01
Stretched Plexiglas	—-··—-	2.01
Doron	—··—··	1.23
B. R. Glass	—·—···	1.00

*Ratio of Material Thickness Relative to a Unit Thickness of B.R. Glass

Fig. 96

$e_{2024T-3}$ vs E

for Various Combinations of m_s, Θ, and V_s

m_s = 30 grains Θ = 70 degrees V_s = 3000 fps

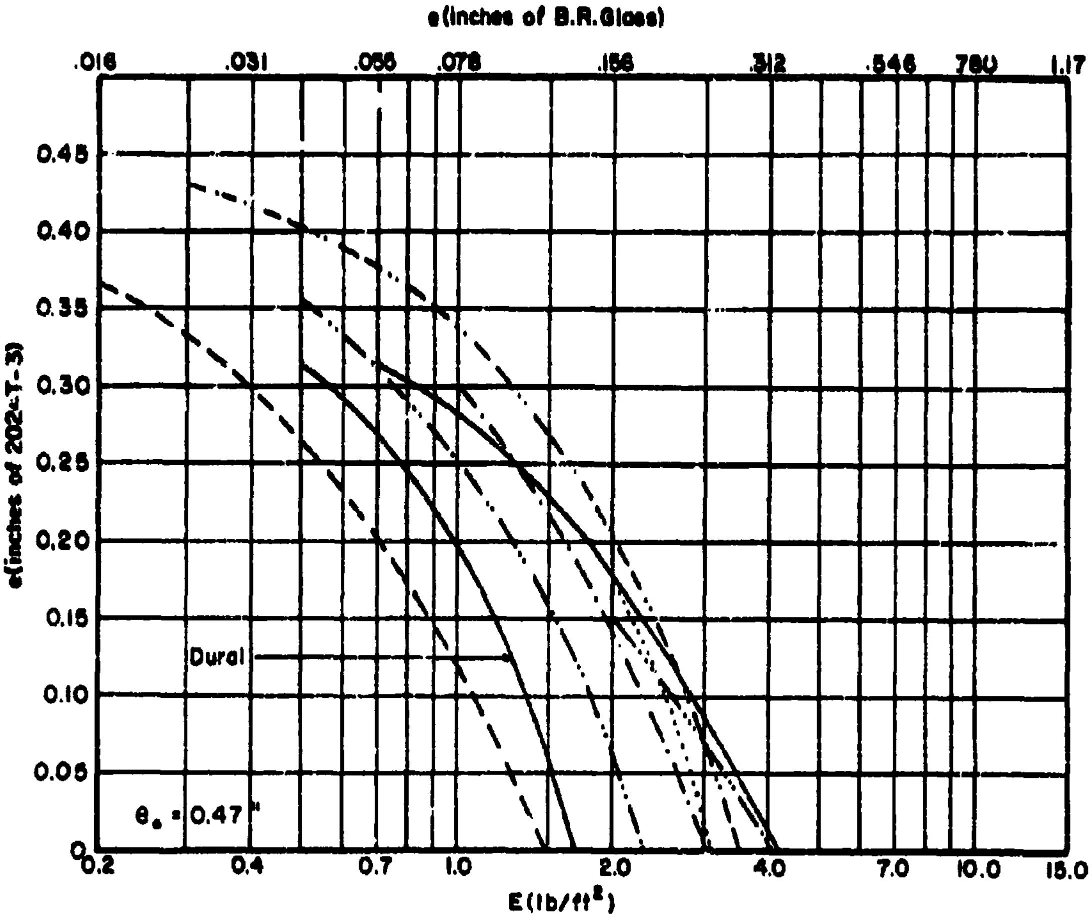

		*			*
Unbonded Nylon	– – – –	3.31	Stretched Plexiglas	– – · · – –	2.01
Bonded Nylon	··········	2.66	Doron	– · · – –	1.23
Lexan	———	2.06	B. R. Glass	– · · · –	1.00
Cast Plexiglas	– · – · –	2.01			

*Ratio of Material Thickness Relative to a Unit Thickness of B.R.Glass

Fig. 97

$e_{2024T-3}$ vs E

for Various Combinations of m_s, Θ, and V_s

m_s = 100 grains Θ = 70 degrees V_s = 3000 fps

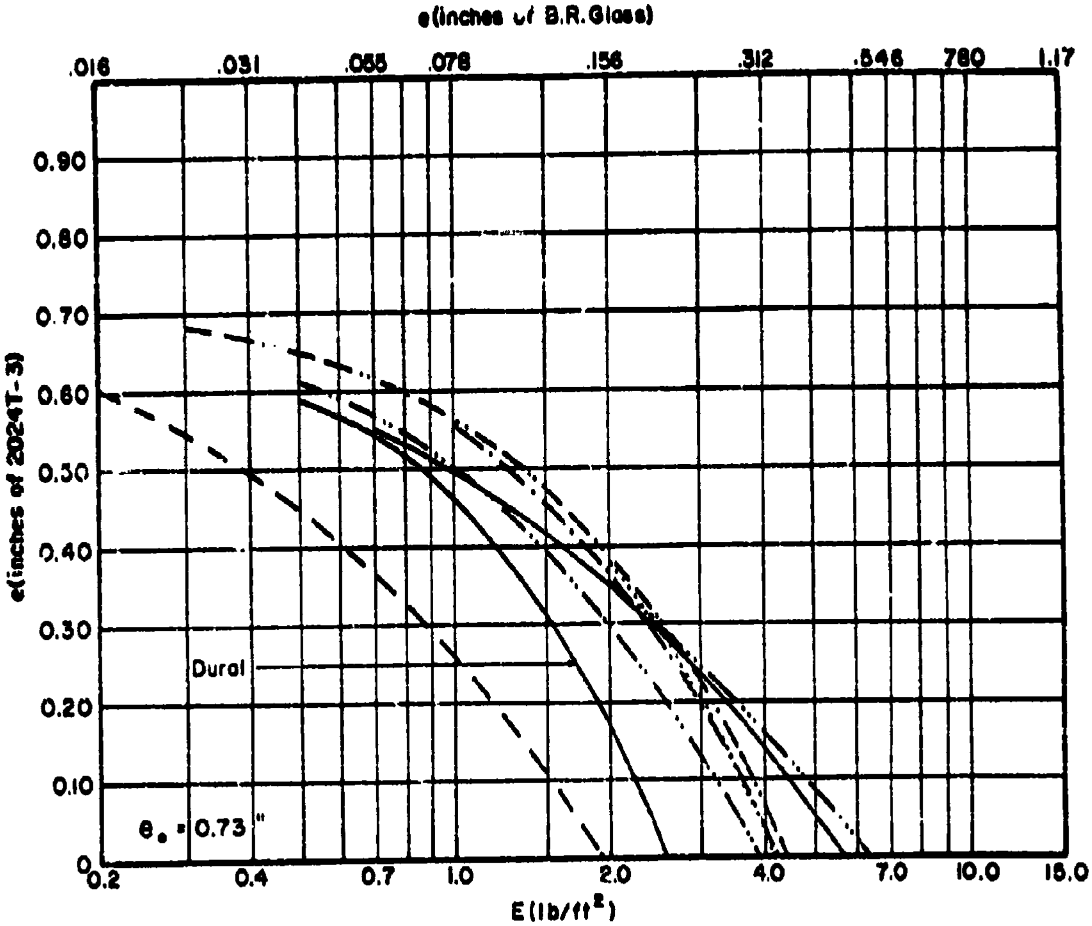

		*			*
Unbonded Nylon	----	3.31	Stretched Plexiglas	--·--	2.01
Bonded Nylon	········	2.66	Doron	--··--	1.23
Lexan	———	2.06	B. R. Glass	--···--	1.00
Cast Plexiglas	--·--·--	2.01			

*Ratio of Material Thickness Relative to a Unit Thickness of B.R.Glass

Fig. 98

$e_{2024T-3}$ vs E

for Various Combinations of m_c, Θ, and V_s

m_s = 300 grains Θ = 70 degrees V_s = 3000 fps

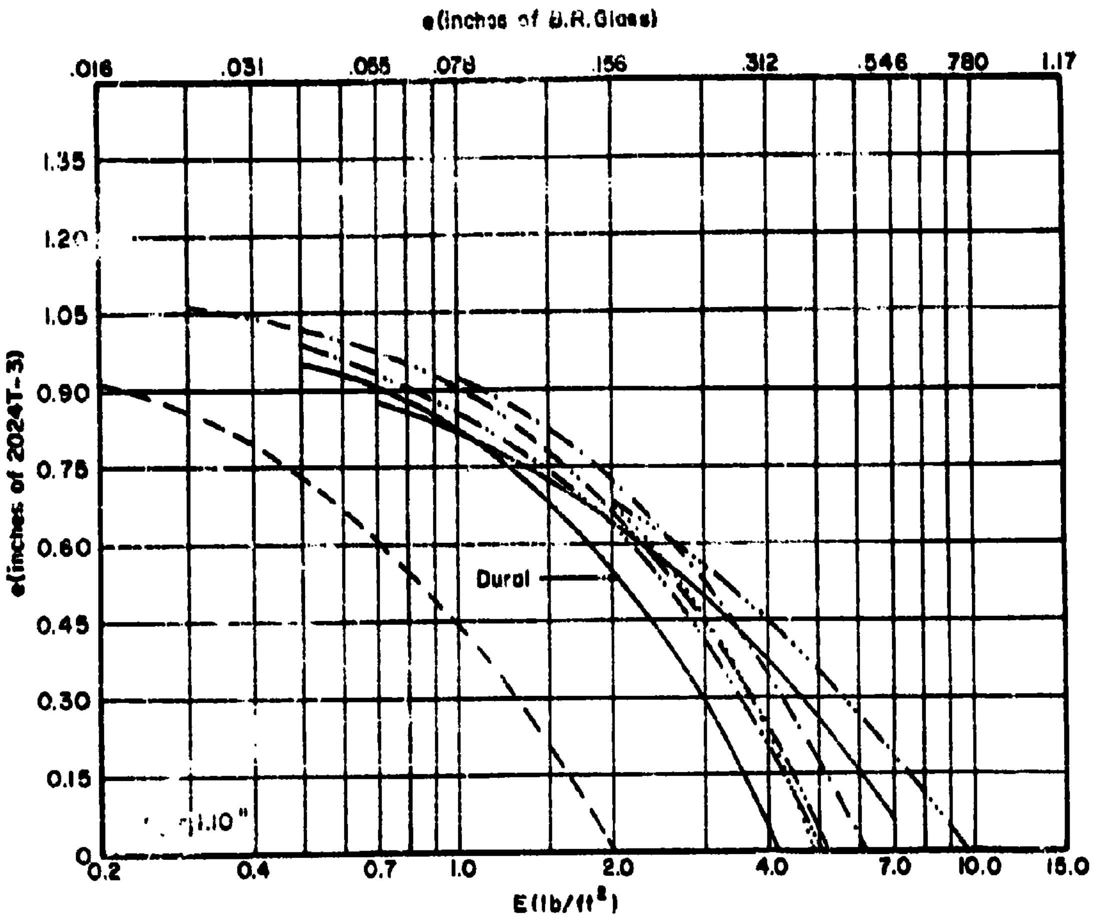

		*
Unbonded Nylon	-----	3.31
Bonded Nylon	....	2.66
Lexan	———	2.06
Cast Plexiglas	-·-·-	2.01
Stretched Plexiglas	--··--	2.01
Doron	-··--	1.23
B. R. Glass	-···-··	1.00

*Ratio of Material Thickness Relative to a Unit Thickness of B.R.Glass

Fig. 99

$e_{2024T-3}$ vs E

for Various Combinations of m_s, Θ, and V_s

m_s = 30 grains Θ = 0 degrees V_s = 6000 fps

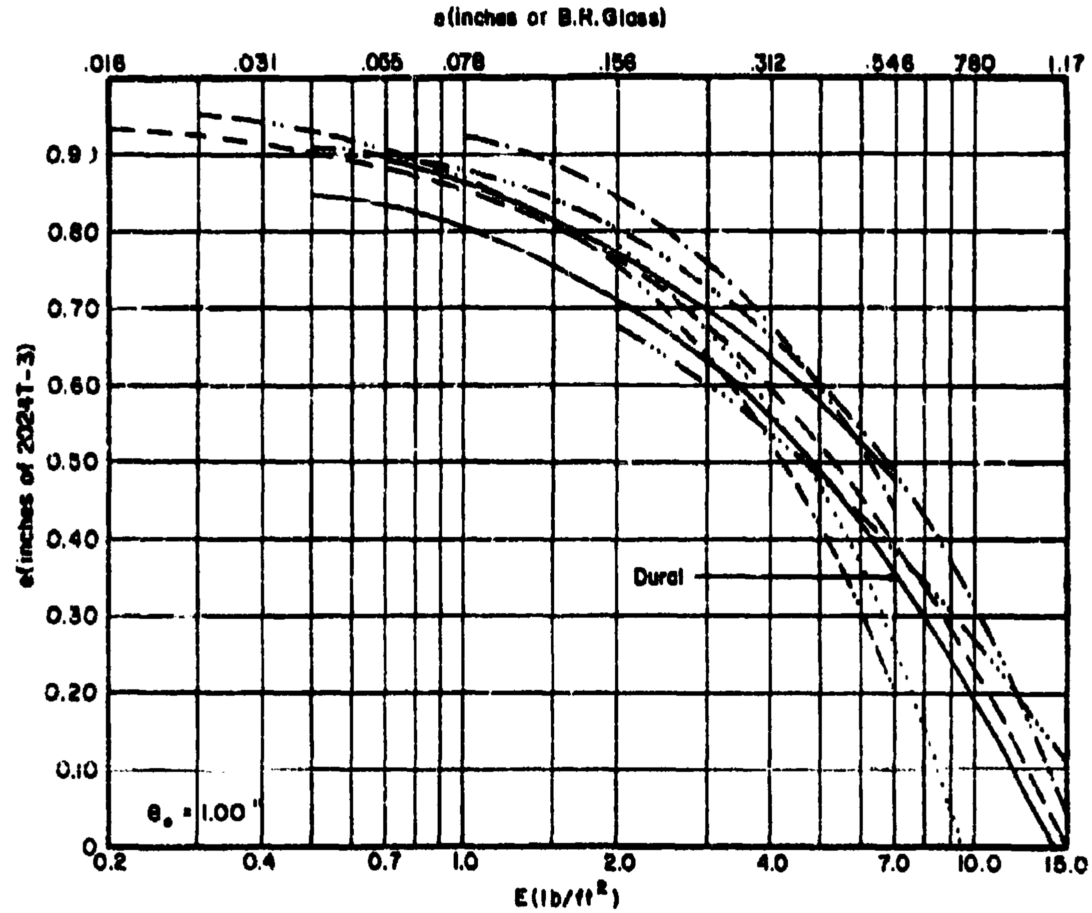

		*			*
Unbonded Nylon	– – – –	3.31	Stretched Plexiglas	— — · — —	2.01
Bonded Nylon	········	2.66	Doron	– · · – – –	1.23
Lexan	———	2.06	B. R. Glass	— · · · — · · ·	1.00
Cast Plexiglas	– · – · · –	2.01			

*Ratio of Material Thickness Relative to a Unit Thickness of B.R.Glass

Fig. 100

$e_{2024T\text{-}3}$ vs E

for Various Combinations of m_s, Θ, and V_s

m_s = 100 grains Θ = 0 degrees V_s = 6000 fps

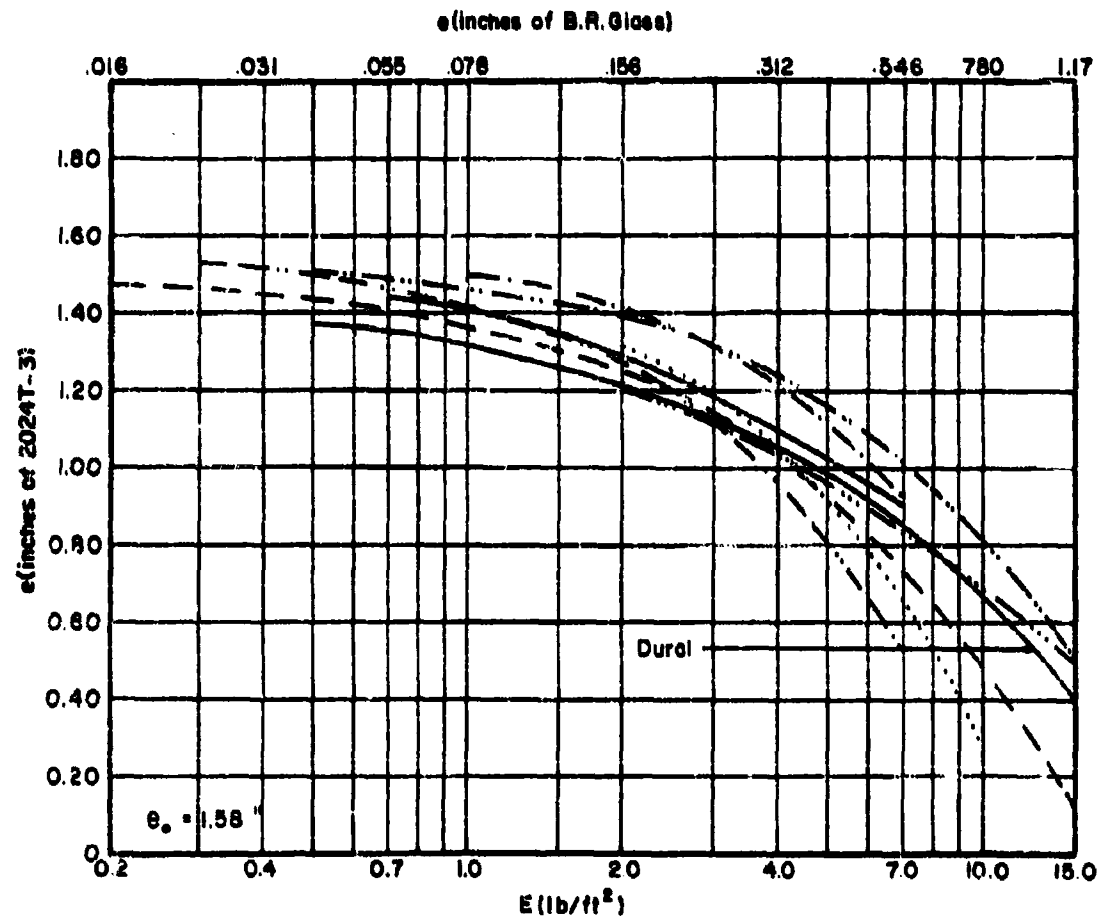

	*		*
Unbonded Nylon ----	3.31	Stretched Plexiglas —-··—	2.01
Bonded Nylon ········	2.66	Doron —··——	1.23
Lexan ———	2.06	B. R. Glass —···—	1.00
Cast Plexiglas —·—·—	2.01		

*Ratio of Material Thickness Relative to a Unit Thickness of B.R.Glass

Fig. 101

$e_{2024T-3}$ vs E

for Various Combinations of m_s, Θ, and V_s

m_s = 300 grains Θ = 0 degrees V_s = 6000 fps

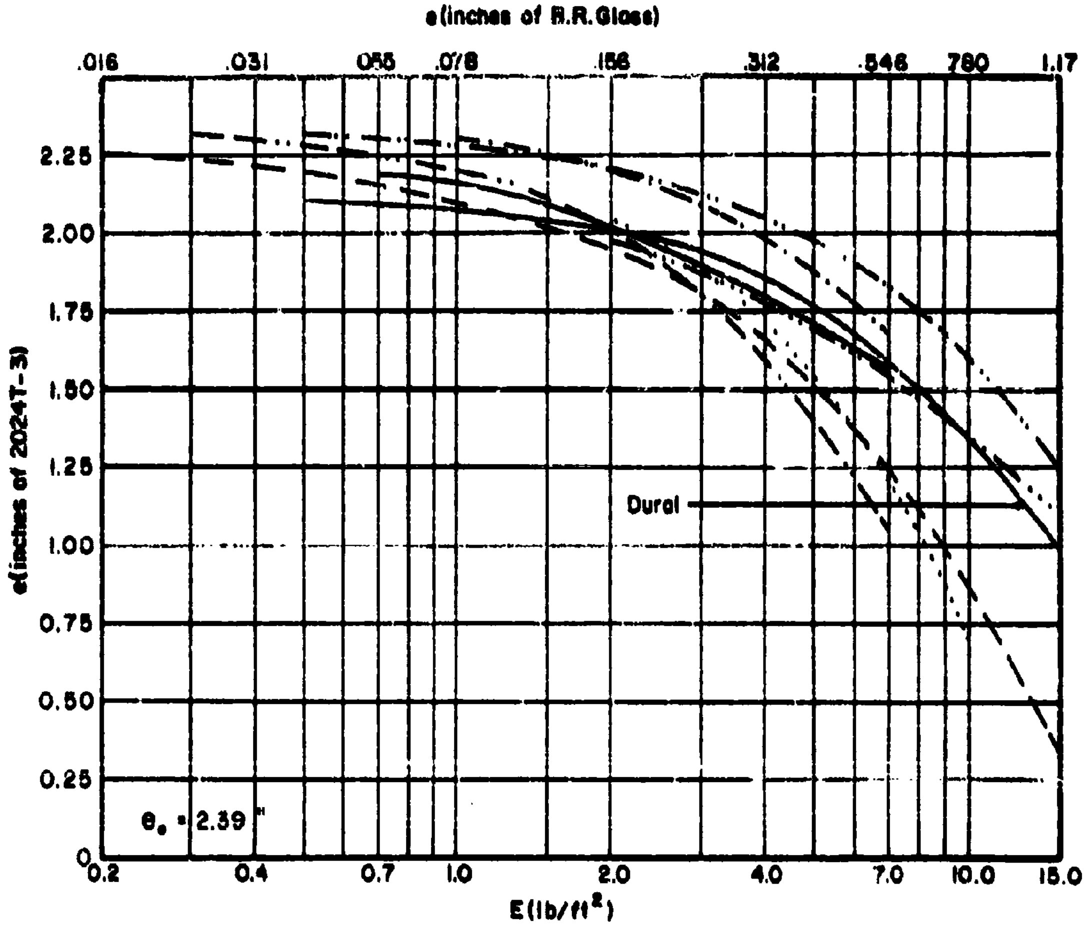

		*			*
Unbonded Nylon	----	3.31	Stretched Plexiglas	---·---	2.01
Bonded Nylon	········	2.66	Doron	--··--··-	1.23
Lexon	———	2.06	B. R. Glass	--···--···	1.00
Cast Plexiglas	--·--·-	2.01			

*Ratio of Material Thickness Relative to a Unit Thickness of B.R.Glass

Fig. 102

$e_{2024T-3}$ vs E for Various Combinations of m_s, Θ, and V_s

m_s = 30 grains Θ = 60 degrees V_s = 6000 fps

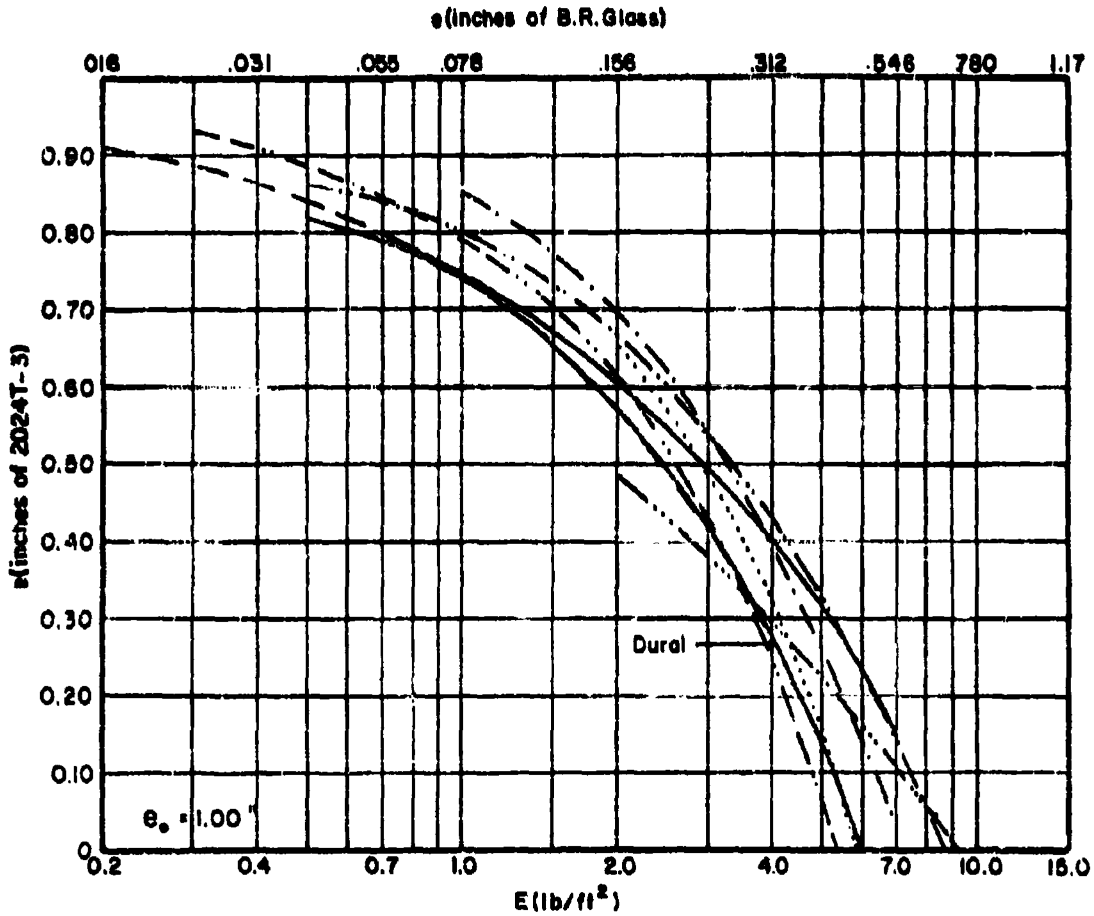

		*			*
Unbonded Nylon	----	3.31	Stretched Plexiglas	---··--	2.01
Bonded Nylon	········	2.66	Doron	-··-··-	1.23
Lexan	———	2.06	B. R. Glass	-···-···	1.00
Cast Plexiglas	-·-·-	2.01			

*Ratio of Material Thickness Relative to a Unit Thickness of B.R.Glass

Fig. 103

$e_{2024T-3}$ vs E

for Various Combinations of m_s, Θ, and V_s

m_s = 100 grains Θ = 60 degrees V_s = 6000 fps

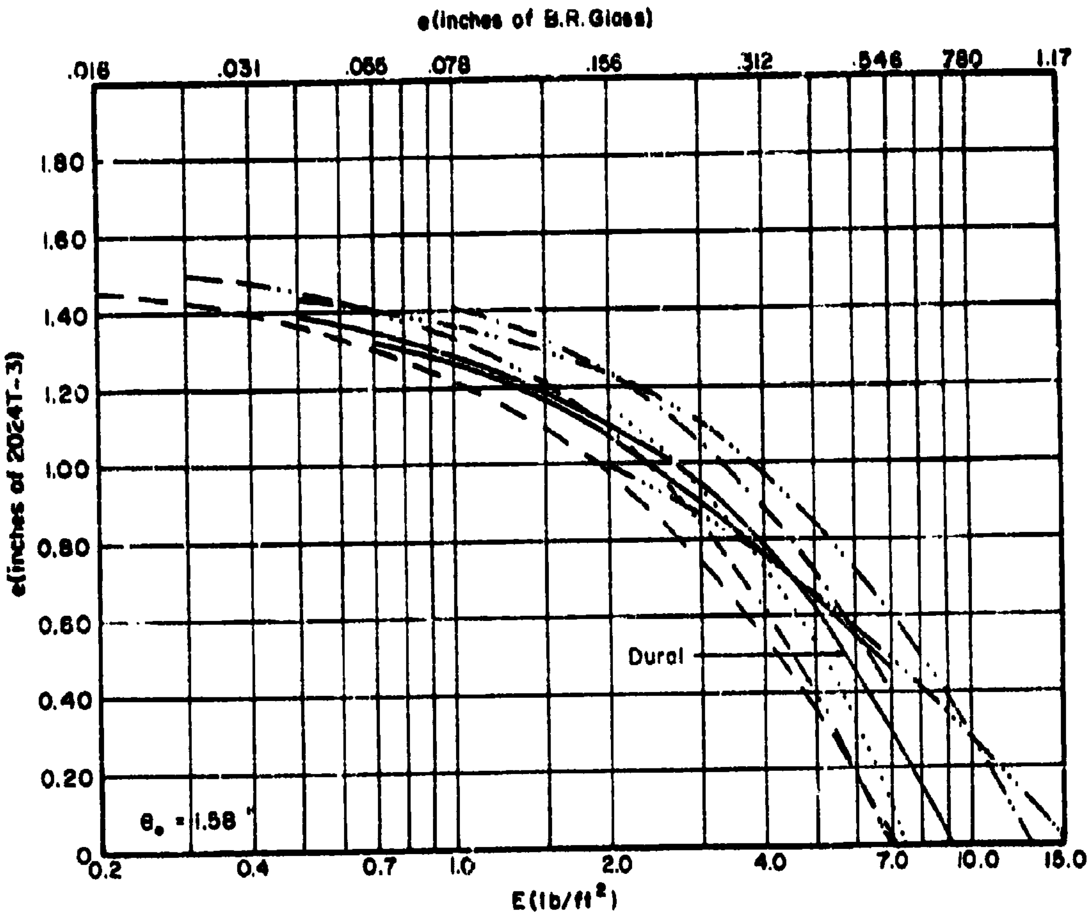

		*			*
Unbonded Nylon	----	3.31	Stretched Plexiglas	—··—	2.01
Bonded Nylon	········	2.66	Doron	—··——	1.23
Lexan	———	2.06	B. R. Glass	—···—···	1.00
Cast Plexiglas	—·—·—	2.01			

*Ratio of Material Thickness Relative to a Unit Thickness of B.R.Glass

Fig. 104

$e_{2024T-3}$ vs E
for Various Combinations of m_s, Θ, and V_s

m_s = 300 grains Θ = 60 degrees V_s = 6000 fps

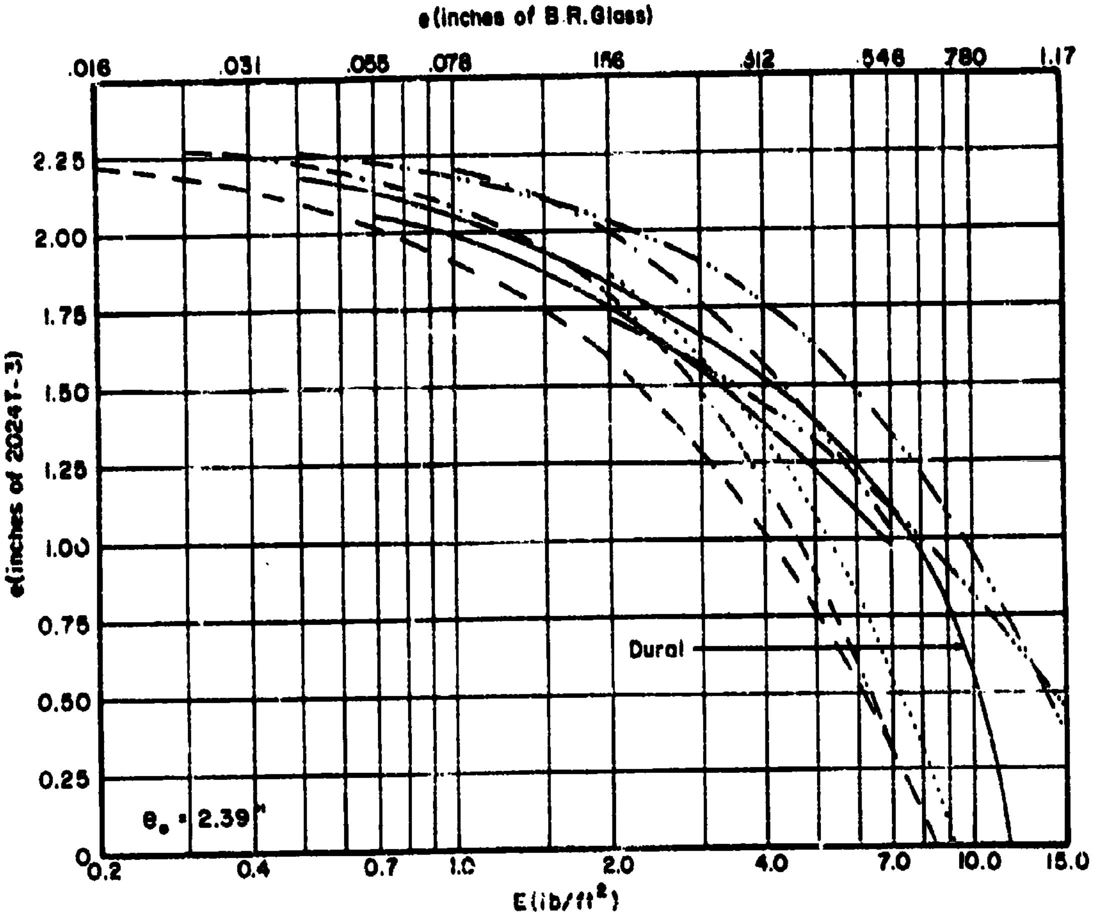

		*			*
Unbonded Nylon	– – – –	3.31	Stretched Plexiglas	– – · – –	2.01
Bonded Nylon	·········	2.66	Doron	– · · – –	1.23
Lexan	———	2.06	B. R. Glass	– · · · –	1.00
Cast Plexiglas	– · – · –	2.01			

*Ratio of Material Thickness Relative to a Unit Thickness of B.R.Glass

Fig. 105

$e_{2024T-3}$ vs E

for Various Combinations of m_s, Θ, and V_s

m_s = 30 grains Θ = 70 degrees V_s = 6000 fps

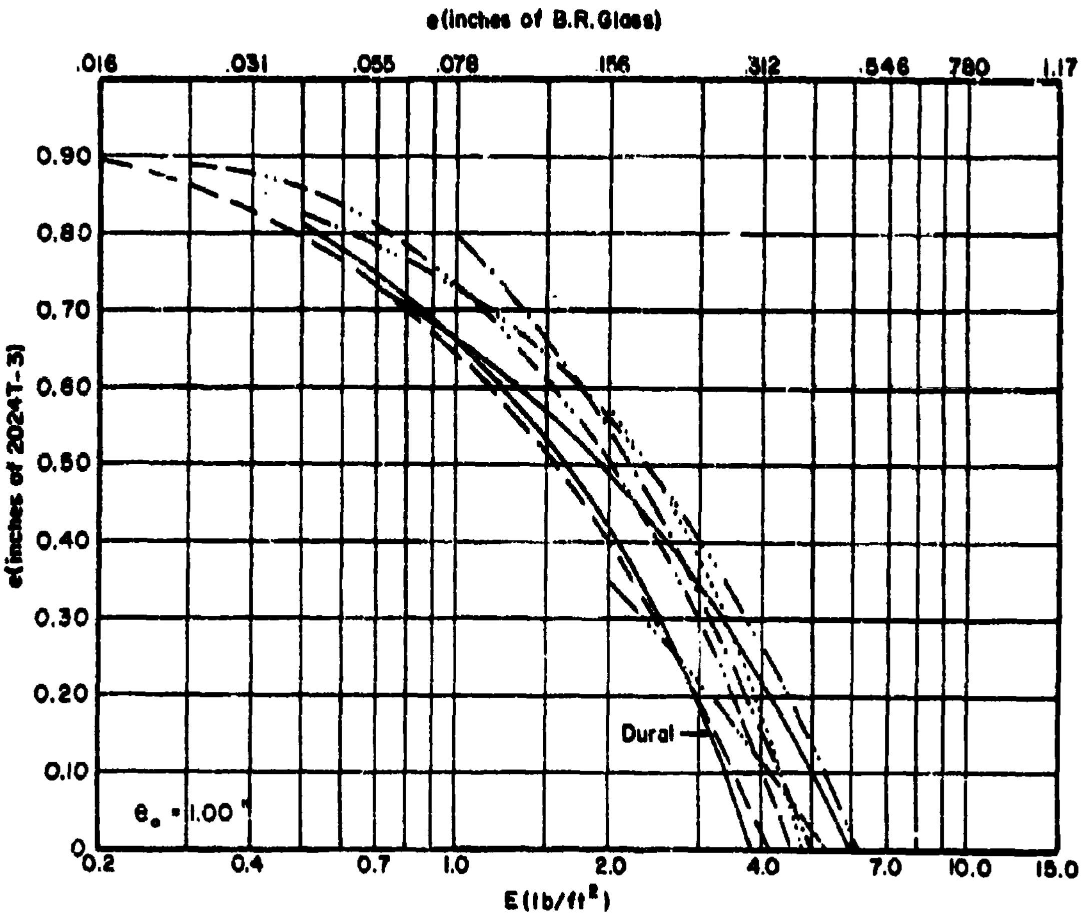

		*
Unbonded Nylon	----	3.31
Bonded Nylon	········	2.66
Lexan	———	2.06
Cast Plexiglas	-·-·-	2.01
Stretched Plexiglas	--··--	2.01
Doron	-··-·-	1.23
B. R. Glass	-···-···	1.00

*Ratio of Material Thickness Relative to a Unit Thickness of B.R.Glass

Fig. 106

$e_{2024T-3}$ vs E

for Various Combinations of m_s, Θ, and V_s

m_s = 100 grains Θ = 70 degrees V_s = 6000 fps

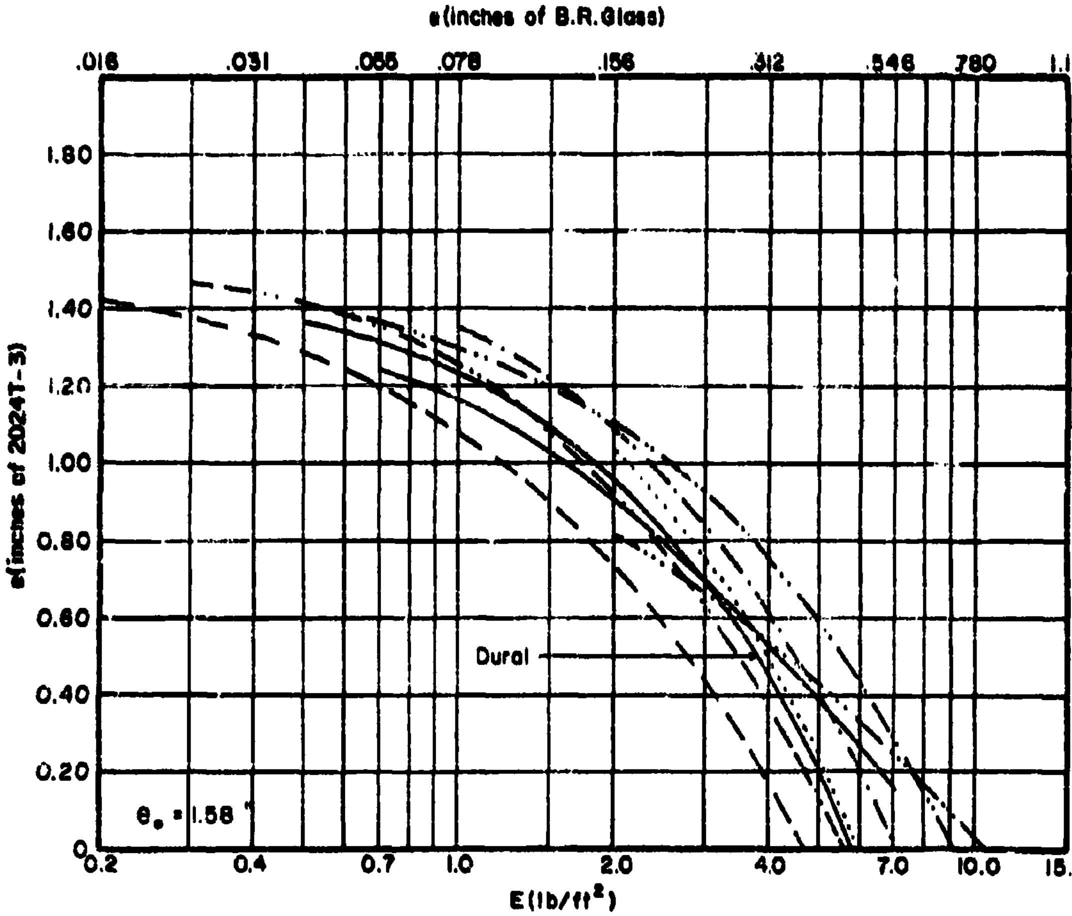

		*
Unbonded Nylon	– – – –	3.31
Bonded Nylon	·········	2.66
Lexan	———	2.06
Cast Plexiglas	– · – · –	2.01
Stretched Plexiglas	– – · · – –	2.01
Doron	– · · – – · · –	1.23
B. R. Glass	– · · · – · · ·	1.00

*Ratio of Material Thickness Relative to a Unit Thickness of B.R.Glass

Fig. 107

$e_{2024T-3}$ vs E

for Various Combinations of m_s, Θ, and V_s

m_s = 300 grains Θ = 70 degrees V_c = 6000 fps

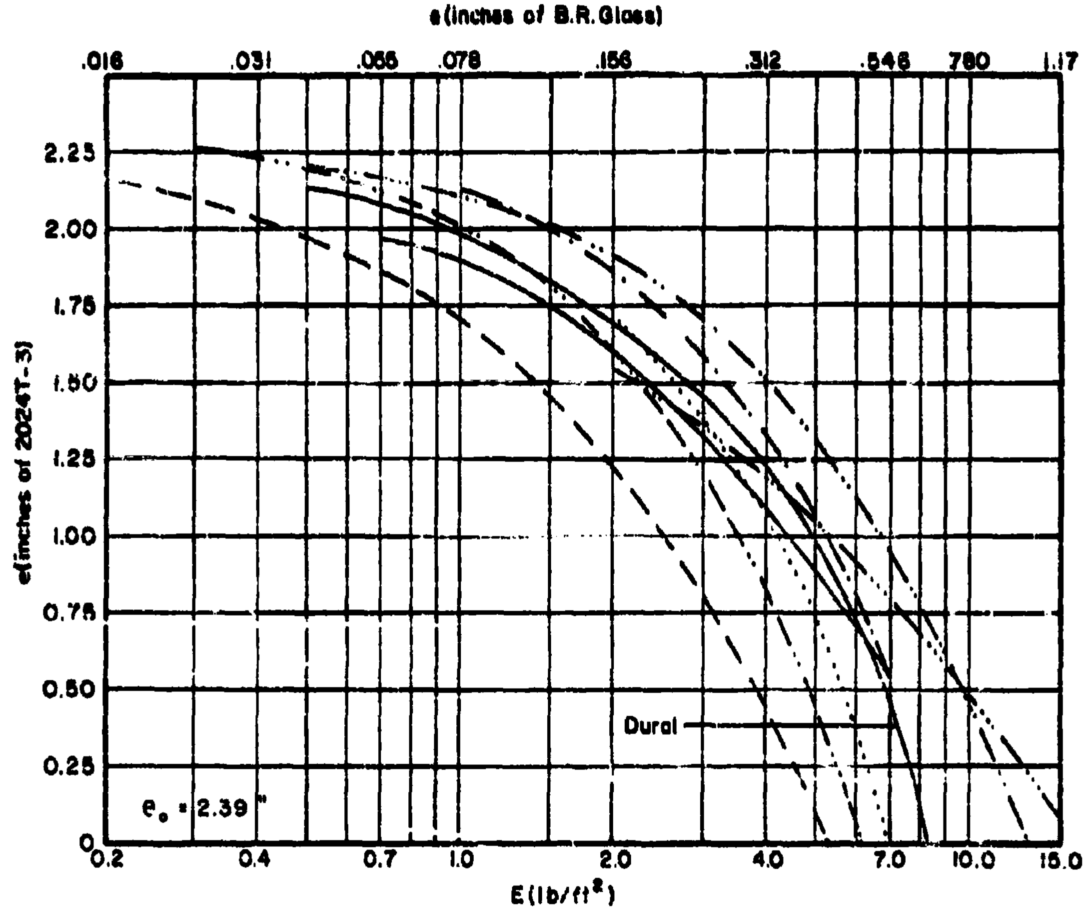

		*
Unbonded Nylon	– – – –	3.31
Bonded Nylon	·········	2.66
Lexan	———	2.06
Cast Plexiglas	–·–·–	2.01
Stretched Plexiglas	–·–··–	2.01
Doron	–··–··–	1.23
B. R. Glass	–···–···	1.00

*Ratio of Material Thickness Relative to a Unit Thickness of B.R.Glass

Fig. 108

$e_{2024T-3}$ vs E

for Various Combinations of m_s, Θ, and V_s

m_s = 30 grains Θ = 0 degrees V_s = 9000 fps

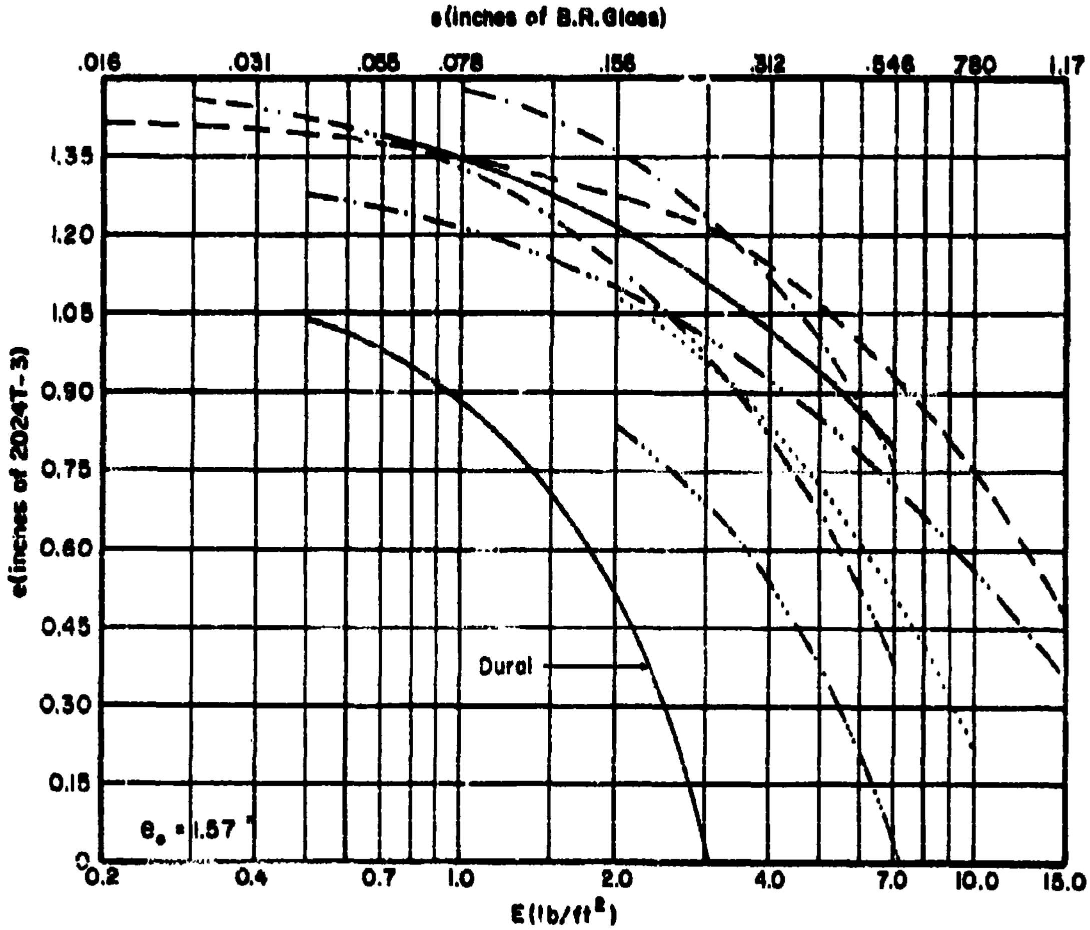

		*			*
Unbonded Nylon	----	3.31	Stretched Plexiglas	---··---	2.01
Bonded Nylon	········	2.66	Doron	-··-··-	1.23
Lexan	——	2.06	B. R. Glass	-···-···	1.00
Cast Plexiglas	-·-·-	2.01			

*Ratio of Material Thickness Relative to a Unit Thickness of B.R.Glass

Fig. 109

$e_{2024T-3}$ vs E

for Various Combinations of m_s, Θ, and V_s

m_s = 100 grains Θ = 0 degrees V_s = 9000 fps

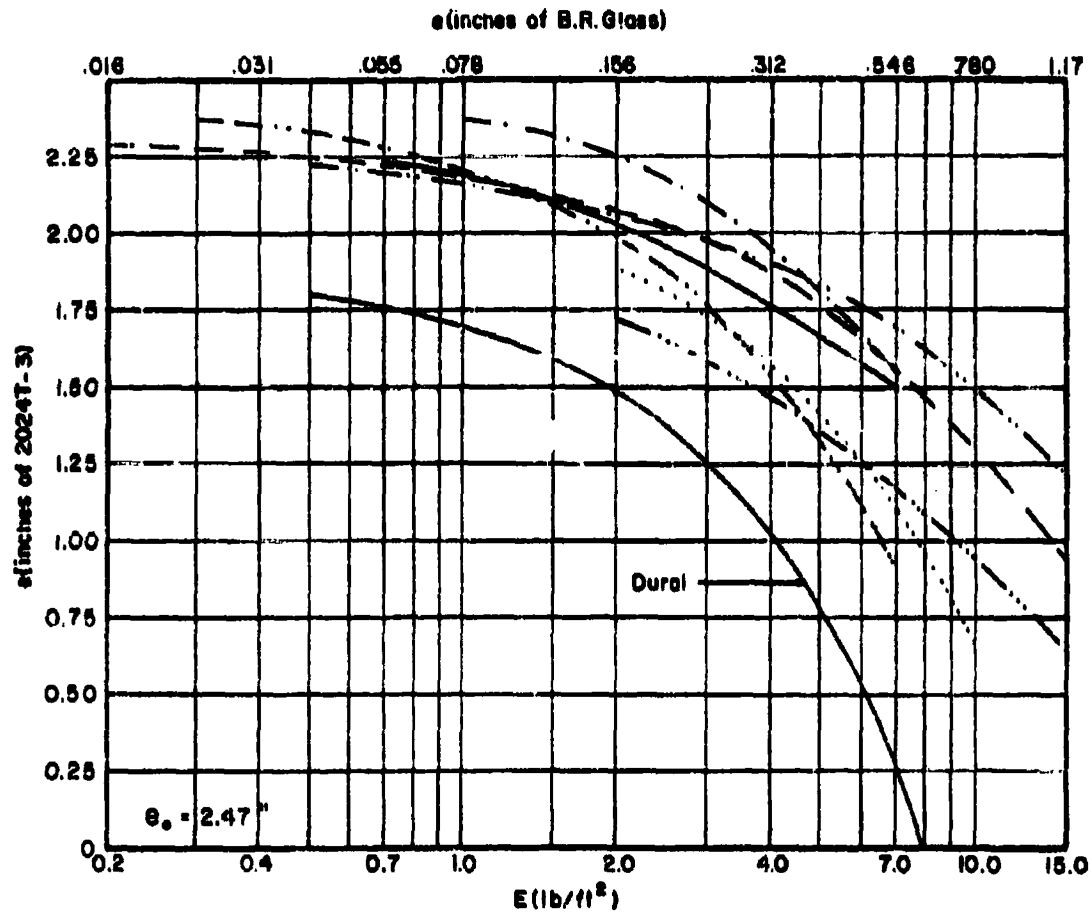

		*
Unbonded Nylon	----	3.31
Bonded Nylon	········	2.66
Lexan	———	2.06
Cast Plexiglas	-·-·-	2.01
Stretched Plexiglas	--··--	2.01
Doron	-··-··-	1.23
B. R. Glass	-···-···	1.00

*Ratio of Material Thickness Relative to a Unit Thickness of B.R.Glass

Fig. 110

$e_{2024T-3}$ vs E
for Various Combinations of m_s, Θ, and V_s

m_s = 300 grains Θ = 0 degrees V_s = 9000 fps

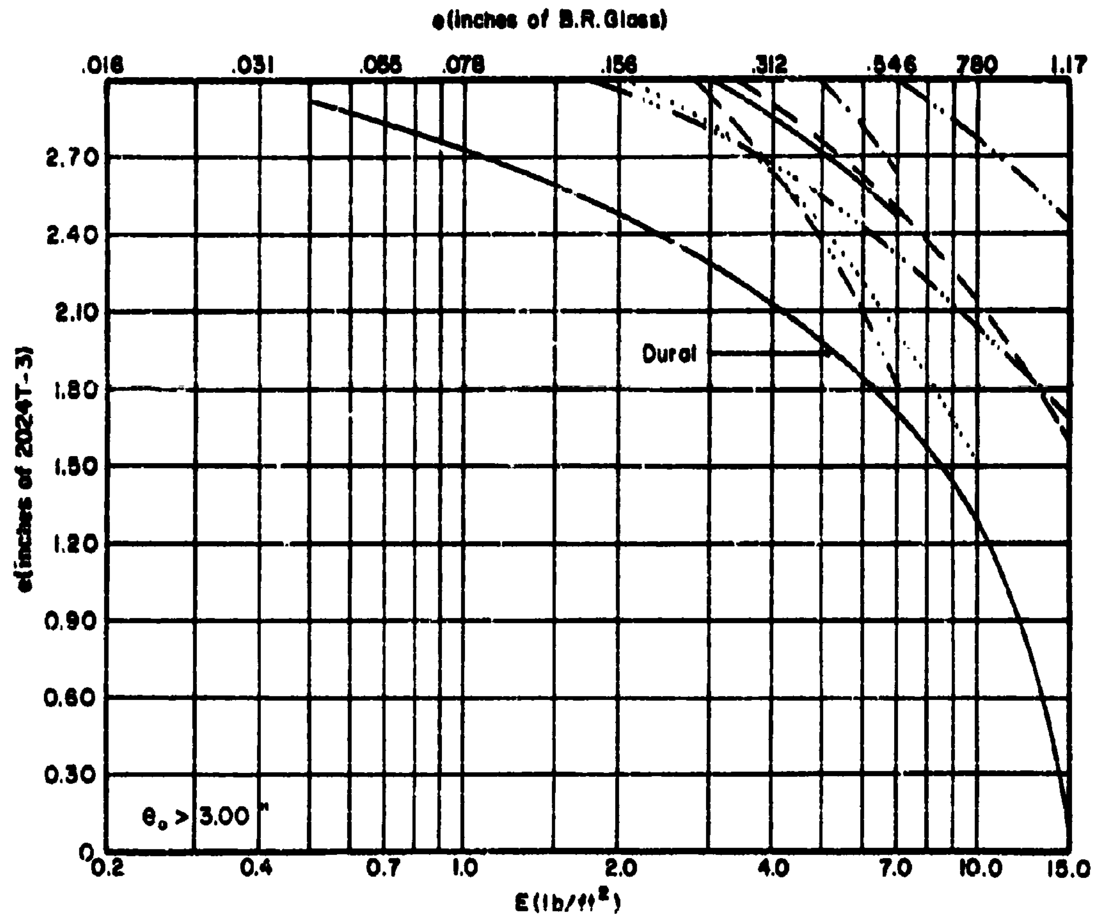

		*			*
Unbonded Nylon	– – – –	3.31	Stretched Plexiglas	—··—	2.01
Bonded Nylon	·········	2.66	Doron	—·—·—	1.23
Lexan	———	2.06	B. R. Glass	—···—	1.00
Cast Plexiglas	–·–·–	2.01			

*Ratio of Material Thickness Relative to a Unit Thickness of B.R.Glass

Fig. 111

$e_{2024T-3}$ vs E

for Various Combinations of m_s, θ, and V_s

m_s = 30 grains θ = 60 degrees V_s = 9000 fps

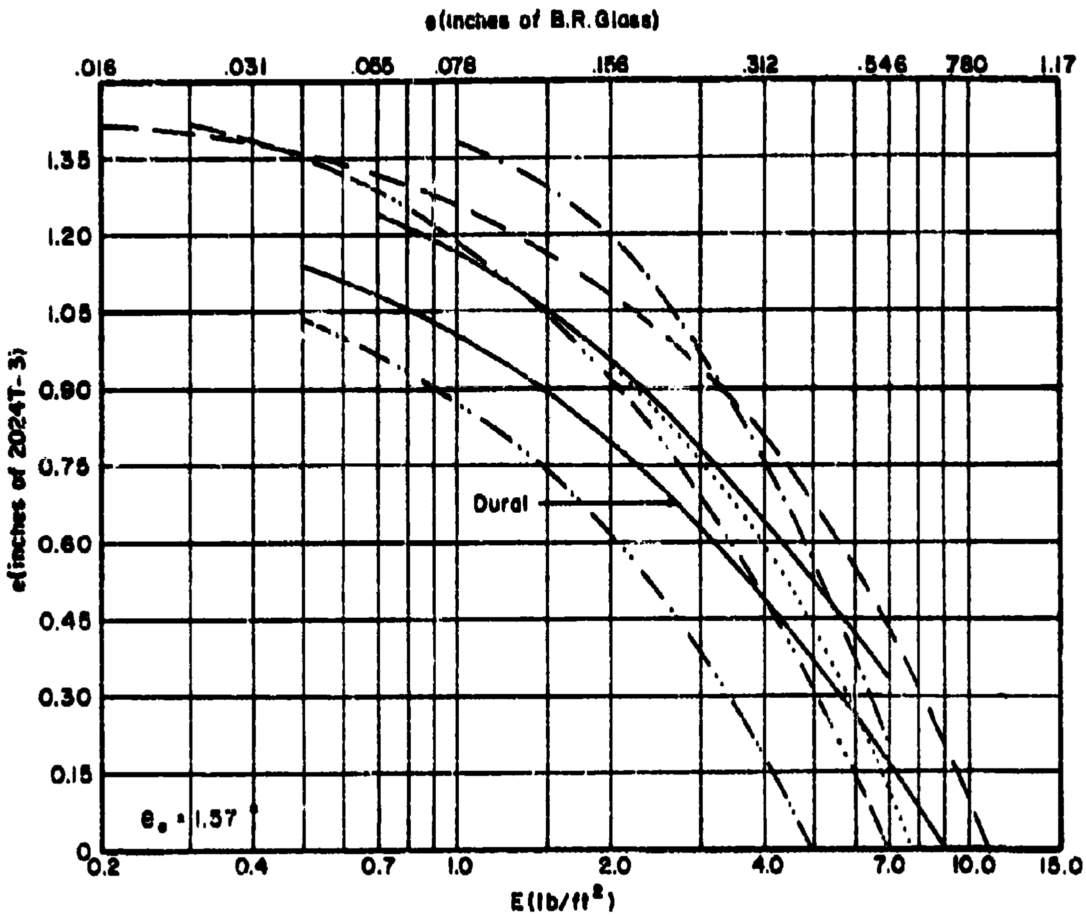

		*			*
Unbonded Nylon	– – – –	3.31	Stretched Plexiglas	– – · · – –	2.01
Bonded Nylon	·······	2.66	Doron	– · · – –	1.23
Lexan	———	2.06	B. R. Glass	– · · · –	1.00
Cast Plexiglas	– · – · –	2.01			

*Ratio of Material Thickness Relative to a Unit Thickness of B.R.Glass

Fig. 112

$e_{2024T\text{-}3}$ vs E

for Various Combinations of m_s, Θ, and V_s

m_s = 100 grains Θ = 60 degrees V_s = 9000 fps

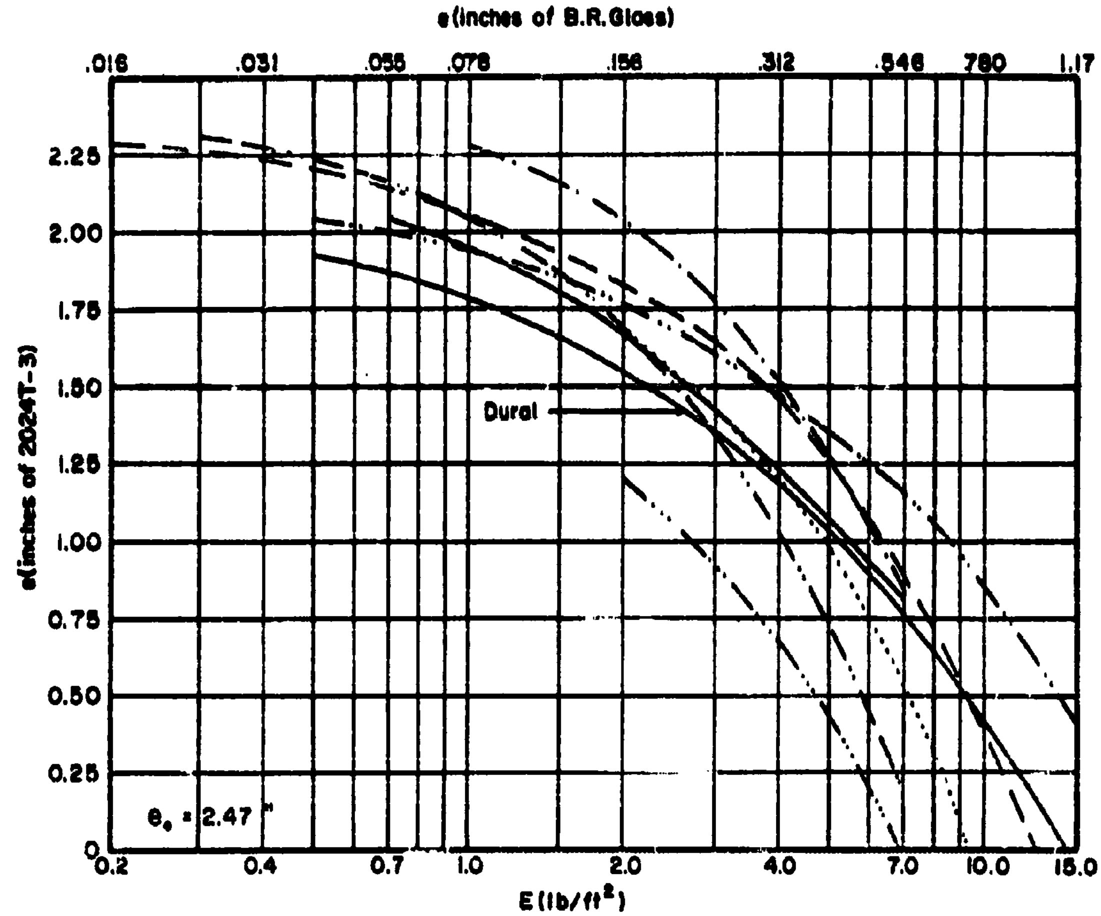

		*			*
Unbonded Nylon	– – – –	3.31	Stretched Plexiglas	— — · — —	2.01
Bonded Nylon	·········	2.66	Doron	— · · — — · ·	1.23
Lexan	————	2.06	B. R. Glass	— · · · — · · ·	1.00
Cast Plexiglas	— · — · —	2.01			

*Ratio of Material Thickness Relative to a Unit Thickness of B.R.Glass

Fig. 113

$e_{2024T\text{-}3}$ vs E

for Various Combinations of m_s, Θ, and V_s

m_s = 300 grains Θ = 60 degrees V_s = 9000 fps

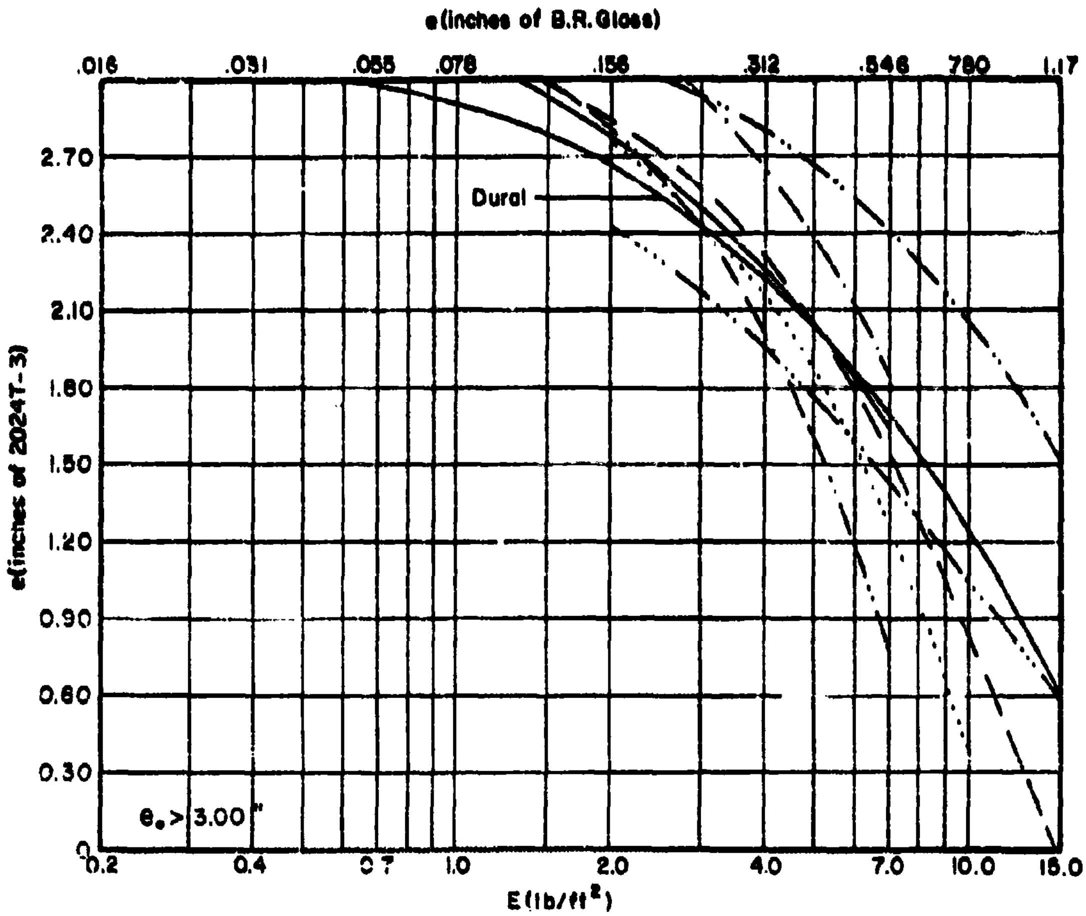

		*			*
Unbonded Nylon	– – – –	3.31	Stretched Plexiglas	— — · — —	2.01
Bonded Nylon	·········	2.66	Doron	— · · — —	1.23
Lexan	———	2.06	B. R. Glass	— · · · — · · ·	1.00
Cast Plexiglas	— · — · —	2.01			

*Ratio of Material Thickness Relative to a Unit Thickness of B.R.Glass

Fig. 114

$e_{2024T-3}$ vs E

for Various Combinations of m_s, θ, and V_s

m_s = 30 grains θ = 70 degrees V_s = 9000 fps

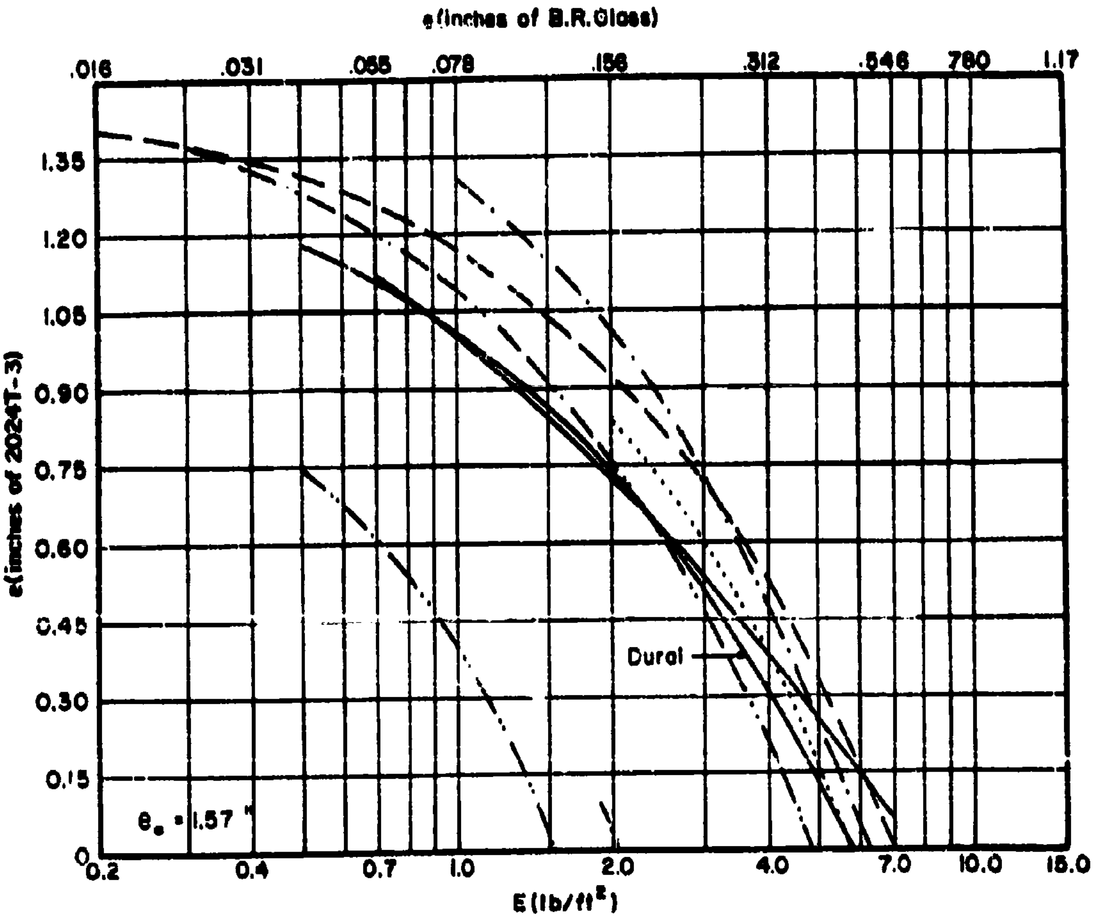

		*			*
Unbonded Nylon	– – – –	3.31	Stretched Plexiglas	– – ·· – –	2.01
Bonded Nylon	·········	2.66	Doron	– ·· —— ··	1.23
Lexan	————	2.06	B. R. Glass	– ··· —— ···	1.00
Cast Plexiglas	– · – · –	2.01			

*Ratio of Material Thickness Relative to a Unit Thickness of B.R.Glass

Fig. 115

$e_{2024T-3}$ vs E

for Various Combinations of m_s, Θ, and V_s

m_s = 100 grains Θ = 70 degrees V_s = 9000 fps

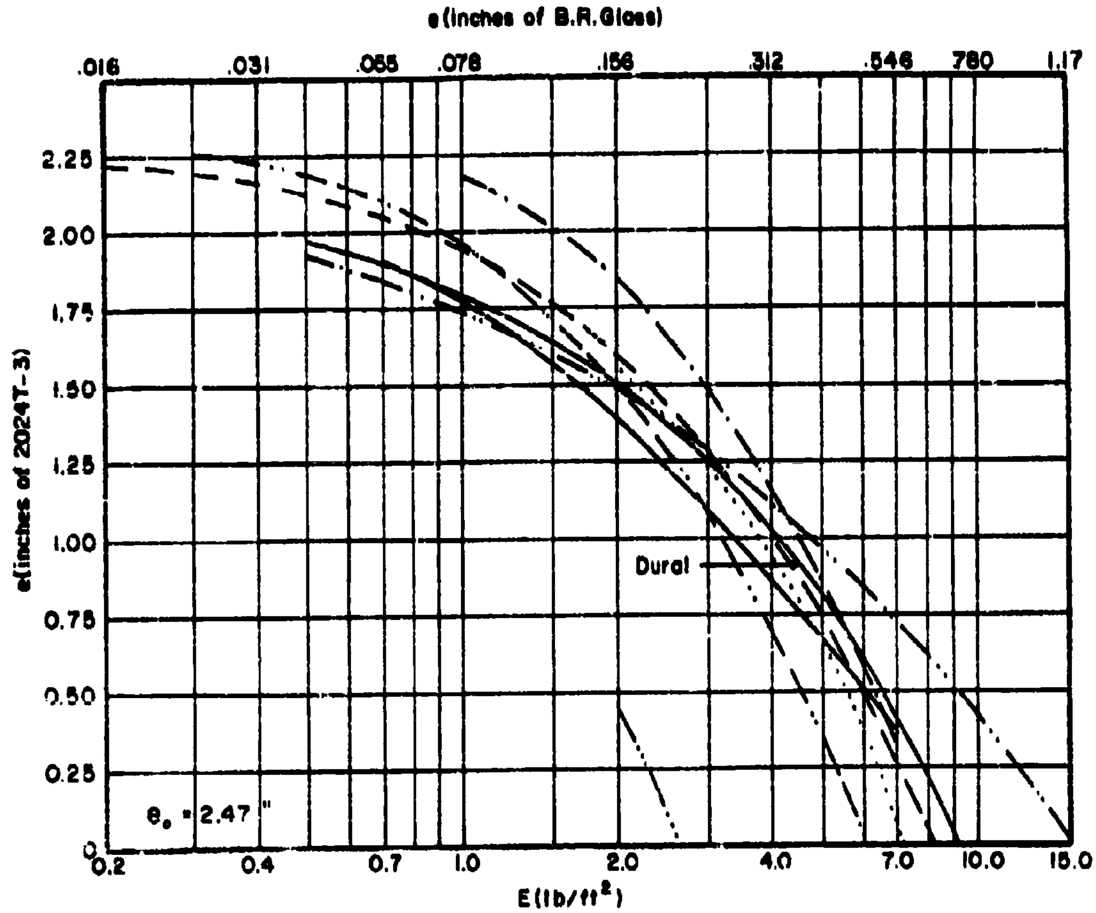

		*			*
Unbonded Nylon	– – – –	3.31	Stretched Plexiglas	— – · · – —	2.01
Bonded Nylon	·········	2.66	Doron	— · · — · · —	1.23
Lexan	———	2.06	B. R. Glass	— · · · — · · ·	1.00
Cast Plexiglas	– · – · –	2.01			

*Ratio of Material Thickness Relative to a Unit Thickness of B.R.Glass

Fig. 116

$e_{2024T-3}$ vs E
for Various Combinations of m_c, Θ, and V_s

m_s = 300 grains Θ = 70 degrees V_s = 9000 fps

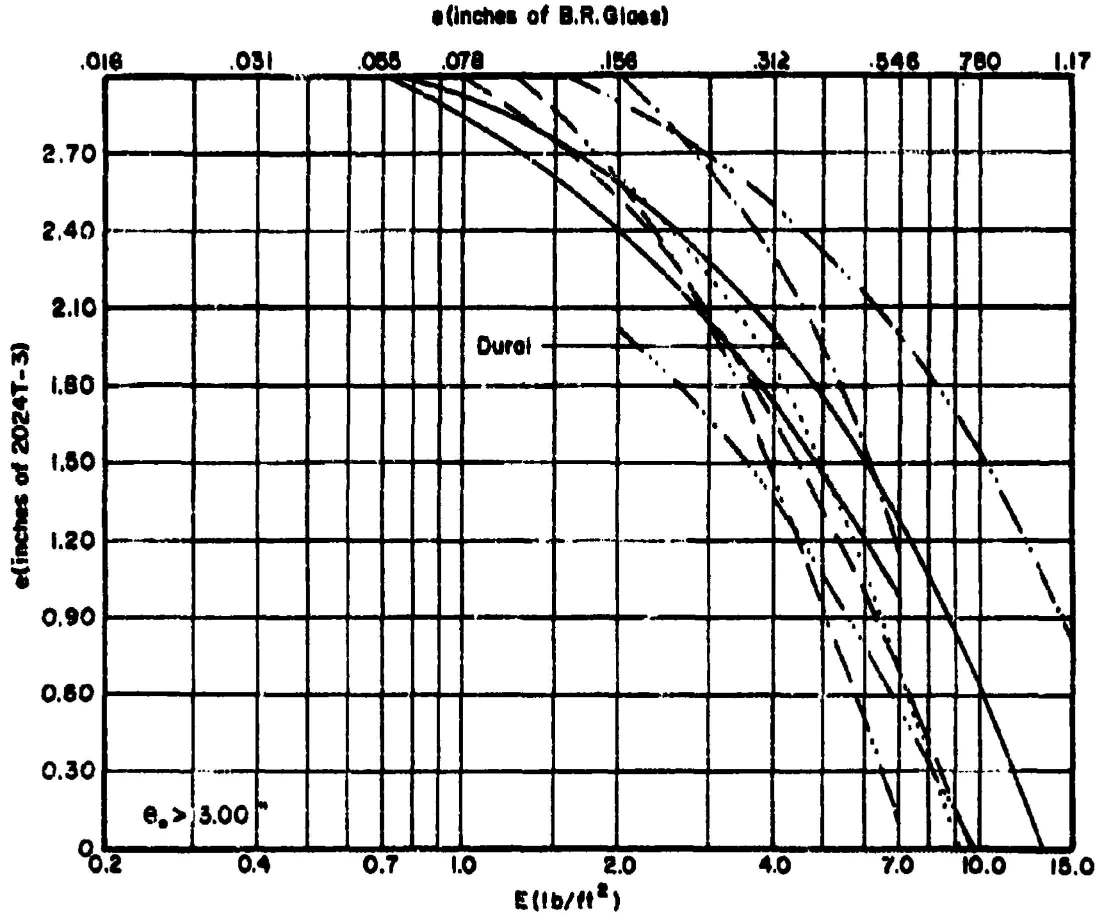

		*			*
Unbonded Nylon	– – – –	3.31	Stretched Plexiglas	– – · · – –	2.01
Bonded Nylon	·········	2.66	Doron	– · · – · · –	1.23
Lexan	———	2.06	B. R. Glass	– · · · – · · ·	1.00
Cast Plexiglas	– · – · –	2.01			

*Ratio of Material Thickness Relative to a Unit Thickness of B.R.Glass

Fig. 117

Appendix E

Graph Set V: e (inches of Maftex) vs E

for Various Combinations of m_s, θ, and V_s

Figs. 118-144

Note: The ordinate represents an estimate of the maximum thickness of calibrating material that can possibly be perforated by the largest portion of the residual fragment after the original fragment has impacted initially on one of the given targets. The assumption is made that the residual fragment strikes the calibrating material at normal impact and that, furthermore, the shape of the original fragment is retained despite any loss in weight.

On each graph in this appendix there appears a value of e_o. This value is an estimate of the maximum thickness of the calibrating material that the original fragment can perforate, assuming normal impact and no intermediate barrier.

The contours are limited on these graphs to 72" of Maftex. This represents the maximum thickness of this material that has been considered in BRL single-target firings. In fact, there is no instance to date of a penetration of more than 72" of Maftex in BRL experimental work with compact fragments.

e_{MAFTEX} vs E

for Various Combinations of m_s, Θ, and V_s

m_s = 30 grains Θ = 0 degrees V_s = 3000 fps

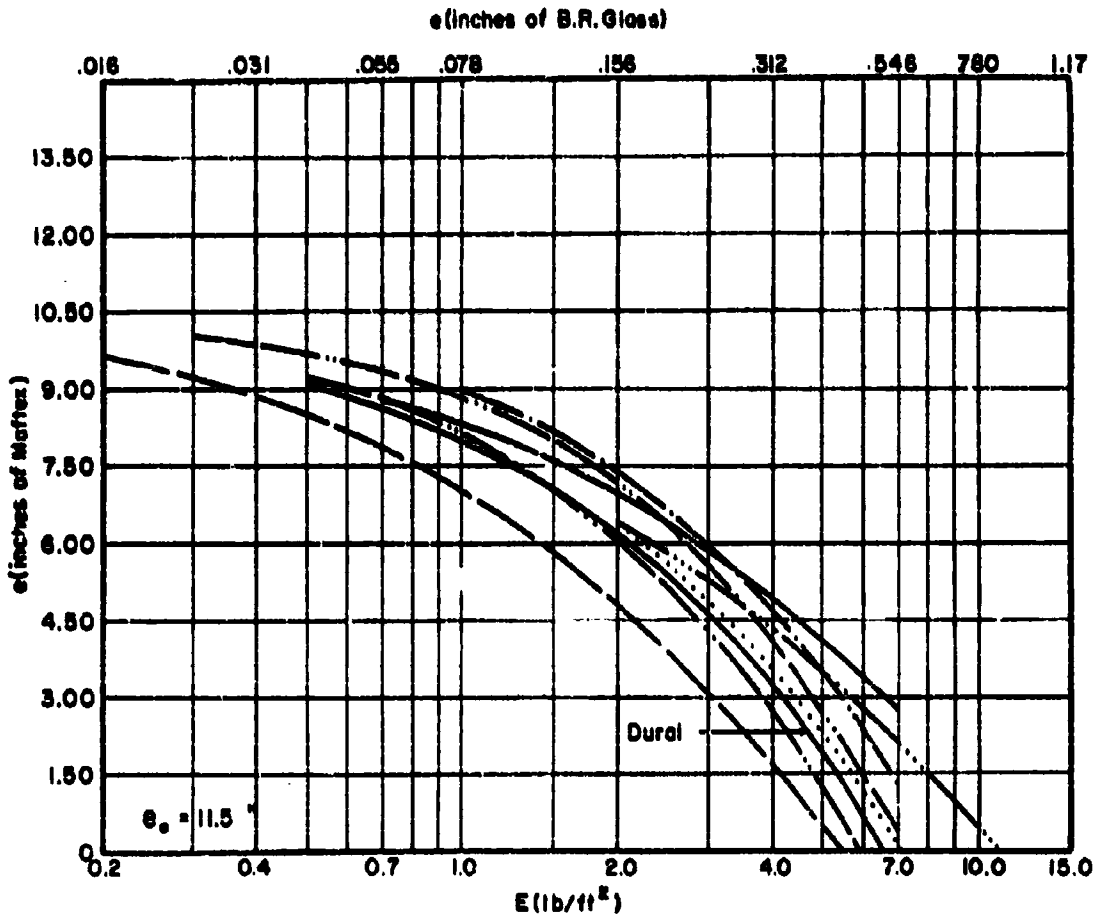

		*			*
Unbonded Nylon	----	3.31	Stretched Plexiglas	—··——	2.01
Bonded Nylon	·········	2.66	Doron	—·—·—	1.23
Lexan	———	2.06	B. R. Glass	—···—···	1.00
Cast Plexiglas	—·—·—	2.01			

*Ratio of Material Thickness Relative to a Unit Thickness of B.R.Glass

Fig. 118

e_{MAFTEX} VS E
for Various Combinations of m_s, Θ, and V_s

m_s = 100 grains Θ = 0 degrees V_s = 3000 fps

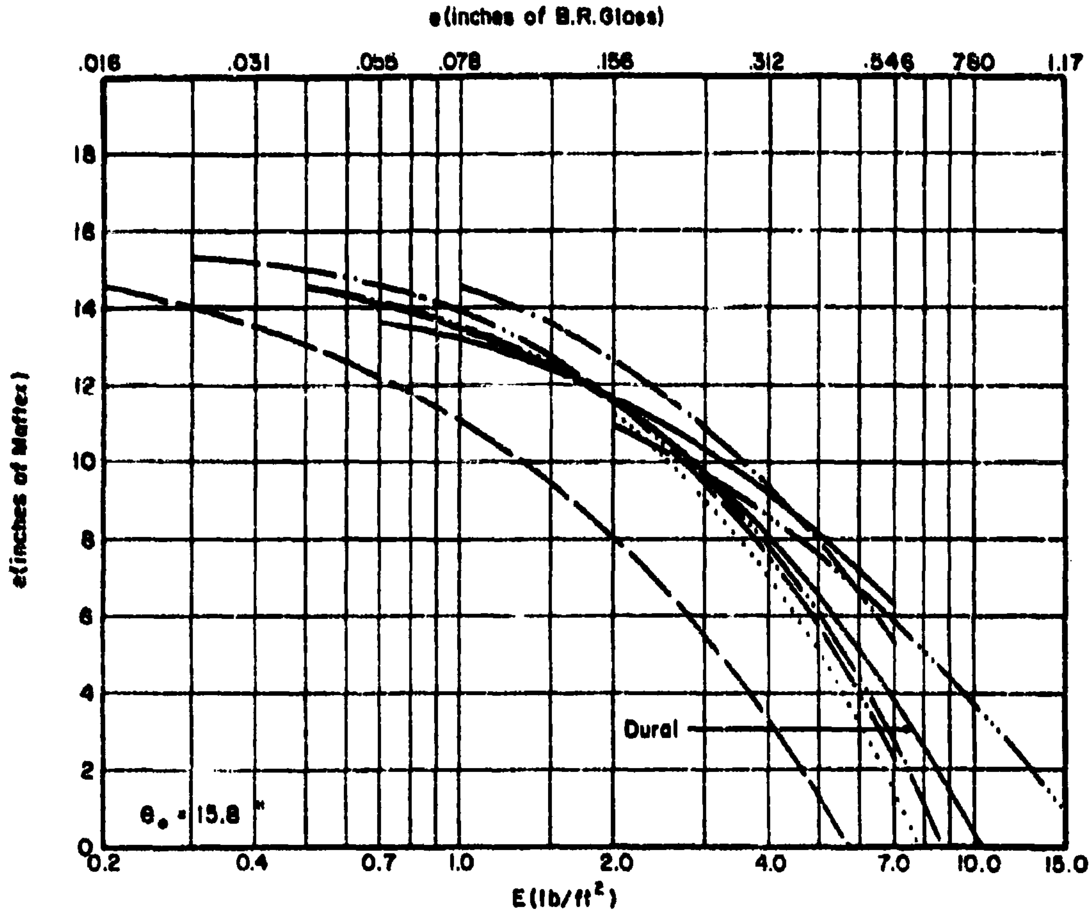

		*
Unbonded Nylon	– – – –	3.31
Bonded Nylon	········	2.66
Lexan	———	2.06
Cast Plexiglas	–·–·–	2.01
Stretched Plexiglas	–··–·–	2.01
Doron	–··–··–	1.23
B. R. Glass	–···–···	1.00

*Ratio of Material Thickness Relative to a Unit Thickness of B.R.Glass

Fig. 119

e_{MAFTEX} vs E
for Various Combinations of m_s, Θ, and V_s

m_s = 300 grains Θ = 0 degrees V_s = 3000 fps

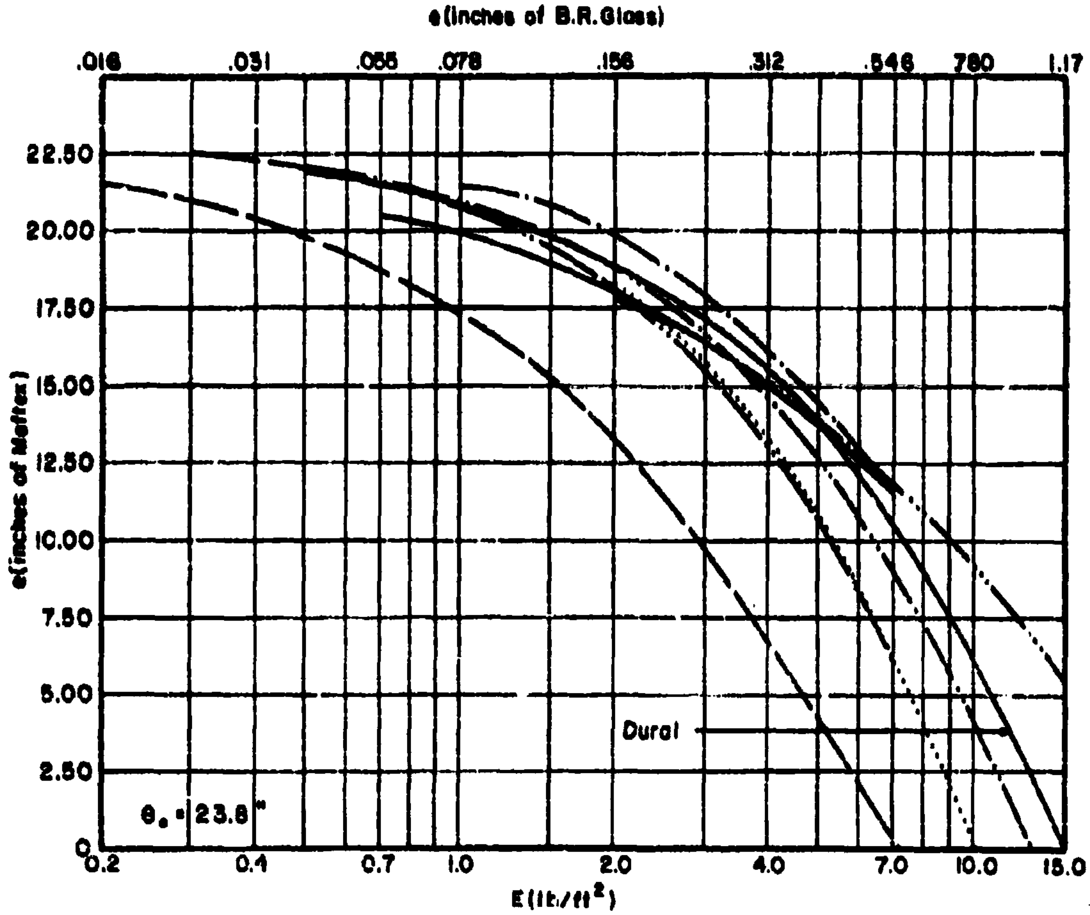

		*
Unbonded Nylon	– – – –	3.31
Bonded Nylon	....	2.66
Lexan	———	2.06
Cast Plexiglas	–·–·–	2.01
Stretched Plexiglas	——··——	2.01
Doron	—··——·	1.23
B. R. Glass	—···—···	1.00

*Ratio of Material Thickness Relative to a Unit Thickness of B.R.Glass

Fig. 120

e_{MAFTEX} vs E

for Various Combinations of m_s, Θ, and V_s

m_s = 30 grains Θ = 60 degrees V_s = 3000 fps

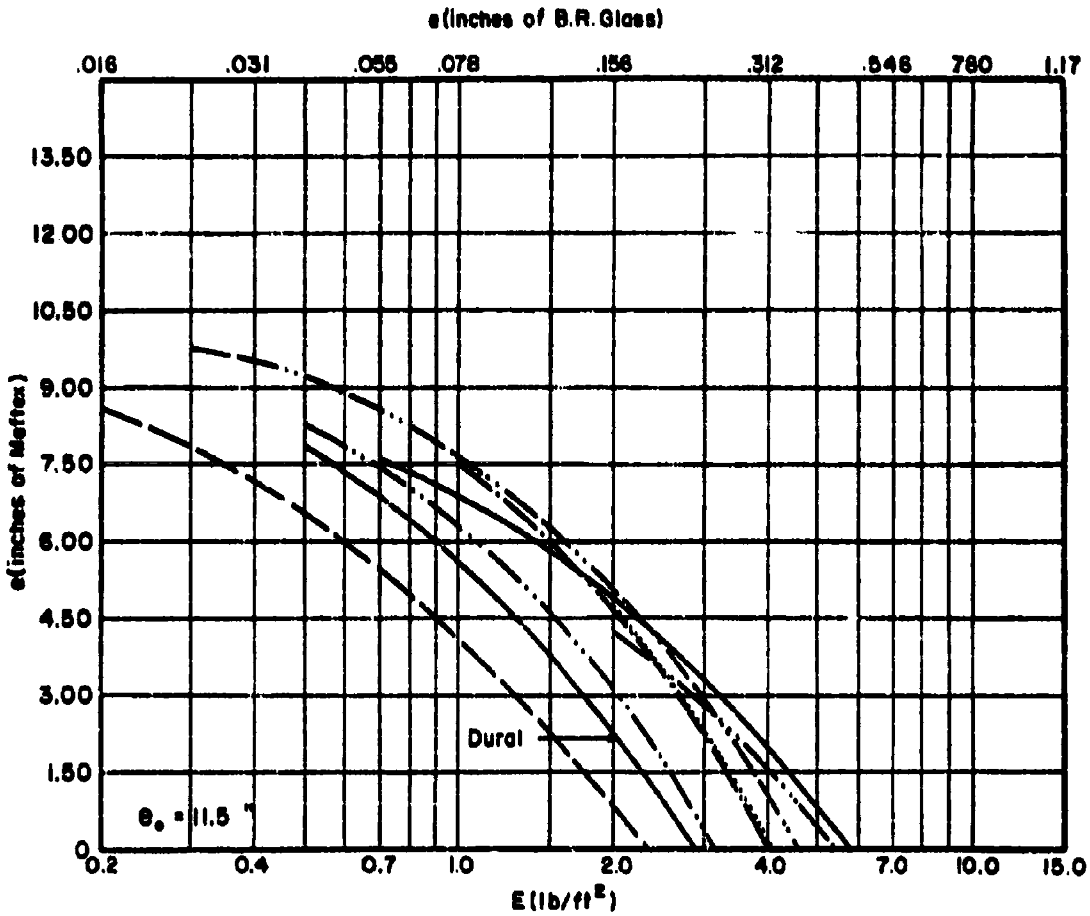

		*			*
Unbonded Nylon	----	3.31	Stretched Plexiglas	--·--	2.01
Bonded Nylon	········	2.66	Doron	-··-··	1.23
Lexan	———	2.06	B. R. Glass	-···-···	1.00
Cast Plexiglas	-·-·-	2.01			

*Ratio of Material Thickness Relative to a Unit Thickness of B.R.Glass

Fig. 121

e_{MAFTEX} vs E
for Various Combinations of m_s, Θ, and V_s

m_s = 100 grains Θ = 60 degrees V_s = 3000 fps

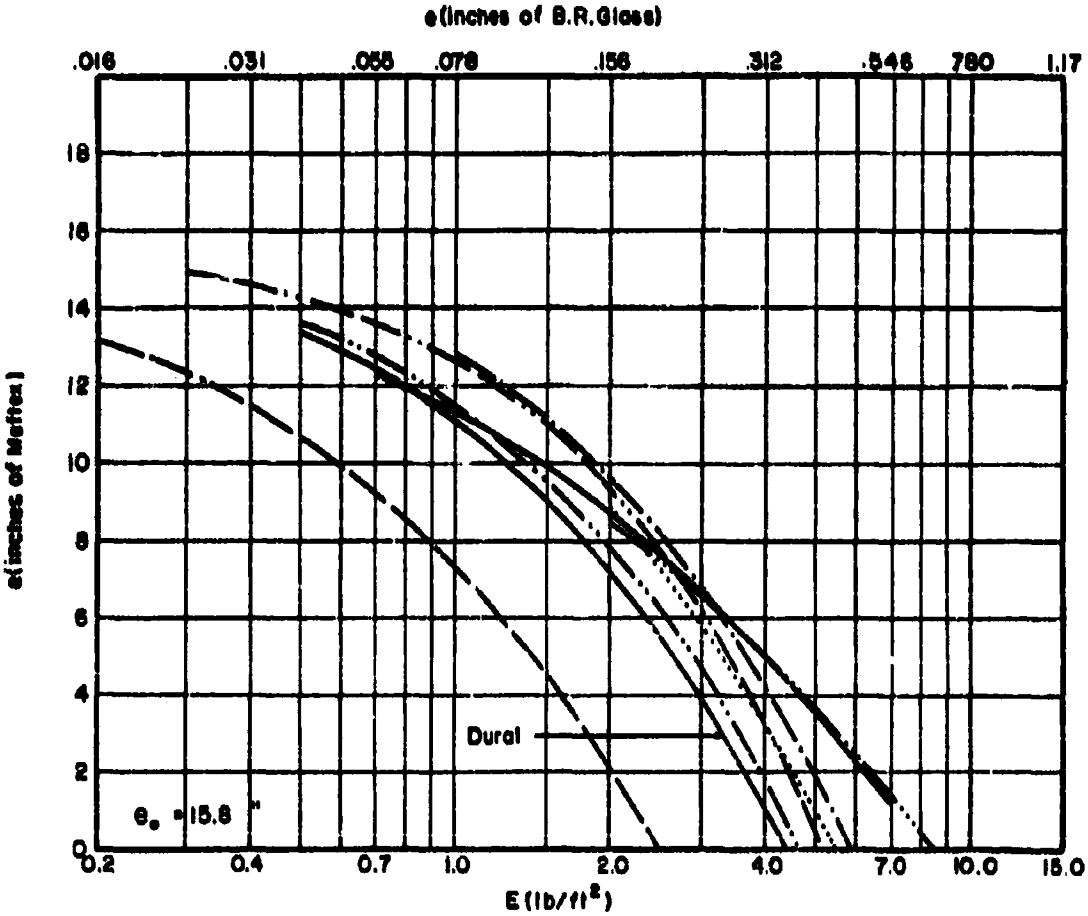

		*			*
Unbonded Nylon	– – – –	3.31	Stretched Plexiglas	– – ·· – –	2.01
Bonded Nylon	·········	2.66	Doron	– ·· – ·· –	1.23
Lexan	———	2.06	B. R. Glass	– ··· – ···	1.00
Cast Plexiglas	– · – · –	2.01			

*Ratio of Material Thickness Relative to a Unit Thickness of B.R.Glass

Fig. 122

e_{MAFTEX} vs E

for Various Combinations of m_s, Θ, and V_s

m_s = 300 grains Θ = 60 degrees V_s = 3000 fps

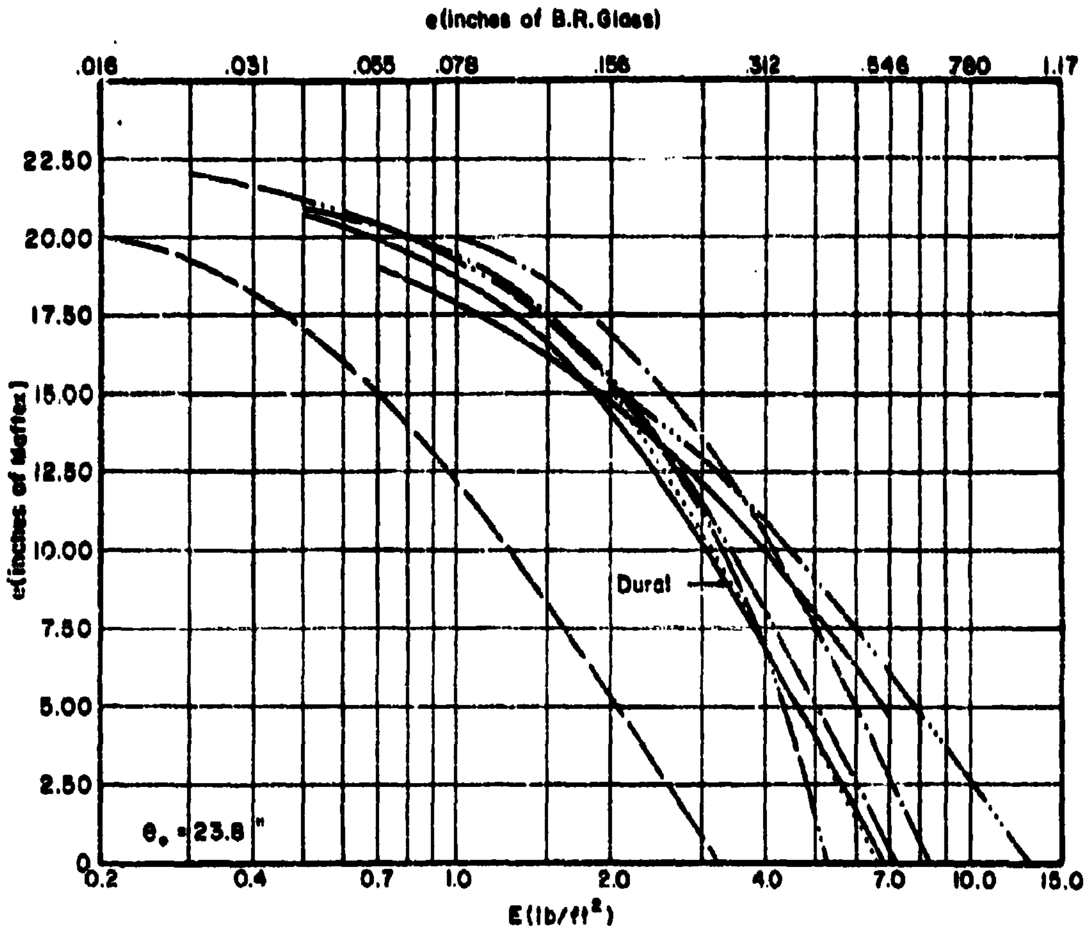

		*			*
Unbonded Nylon	----	3.31	Stretched Plexiglas	--·-·--	2.01
Bonded Nylon	········	2.66	Doron	--·-·--	1.23
Lexan	———	2.06	B. R. Glass	--··--	1.00
Cast Plexiglas	-·-·-	2.01			

*Ratio of Material Thickness Relative to a Unit Thickness of B.R.Glass

Fig. 123

e_{MAFTEX} vs E

for Various Combinations of m_s, Θ, and V_s

m_s = 30 grains Θ = 70 degrees V_s = 3000 fps

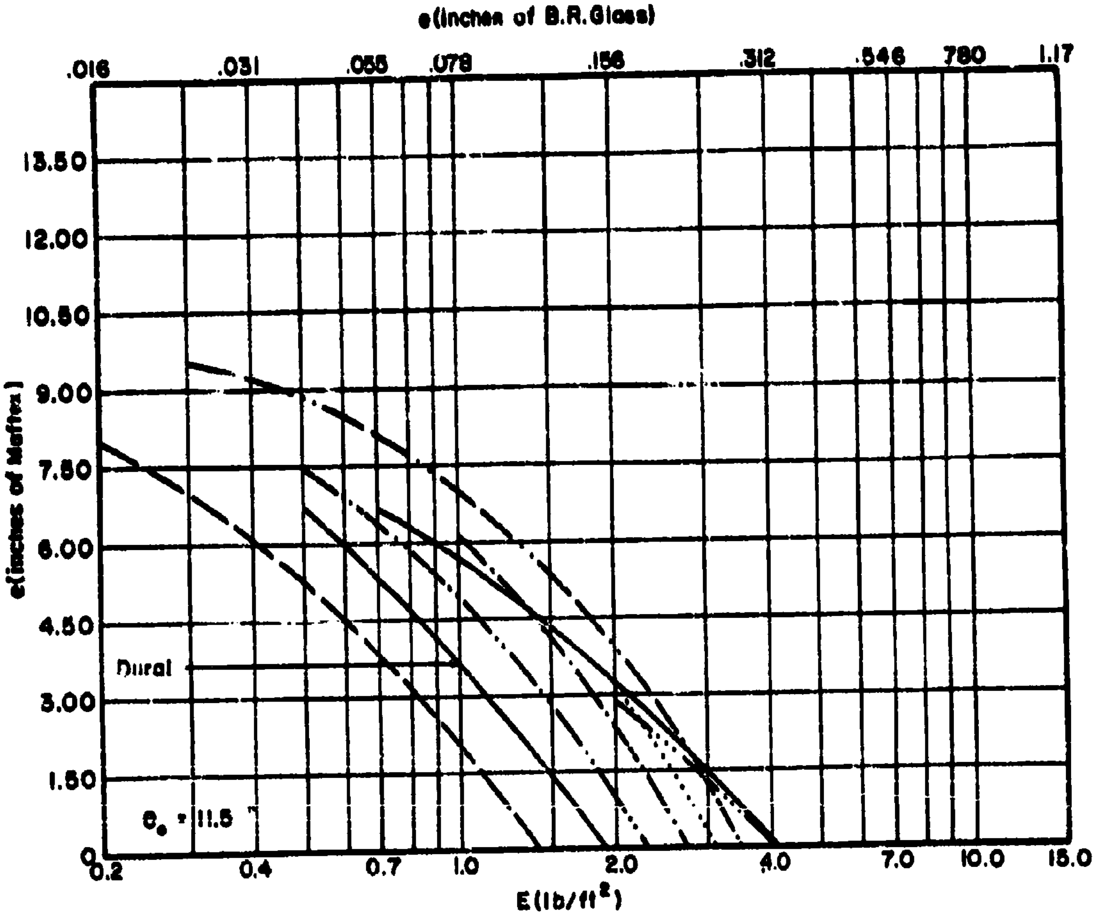

		*			*
Unbonded Nylon	– – – –	3.31	Stretched Plexiglas	— — · · — —	2.01
Bonded Nylon	....	2.66	Doron	— · · — —	1.23
Lexan	———	2.06	B. R. Glass	— · · · — · · ·	1.00
Cast Plexiglas	— · — · —	2.01			

*Ratio of Material Thickness Relative to a Unit Thickness of B.R.Glass

Fig. 124

e_{MAFTEX} vs E
for Various Combinations of m_s, θ, and V_s

m_s = 100 grains θ = 70 degrees V_s = 3000 fps

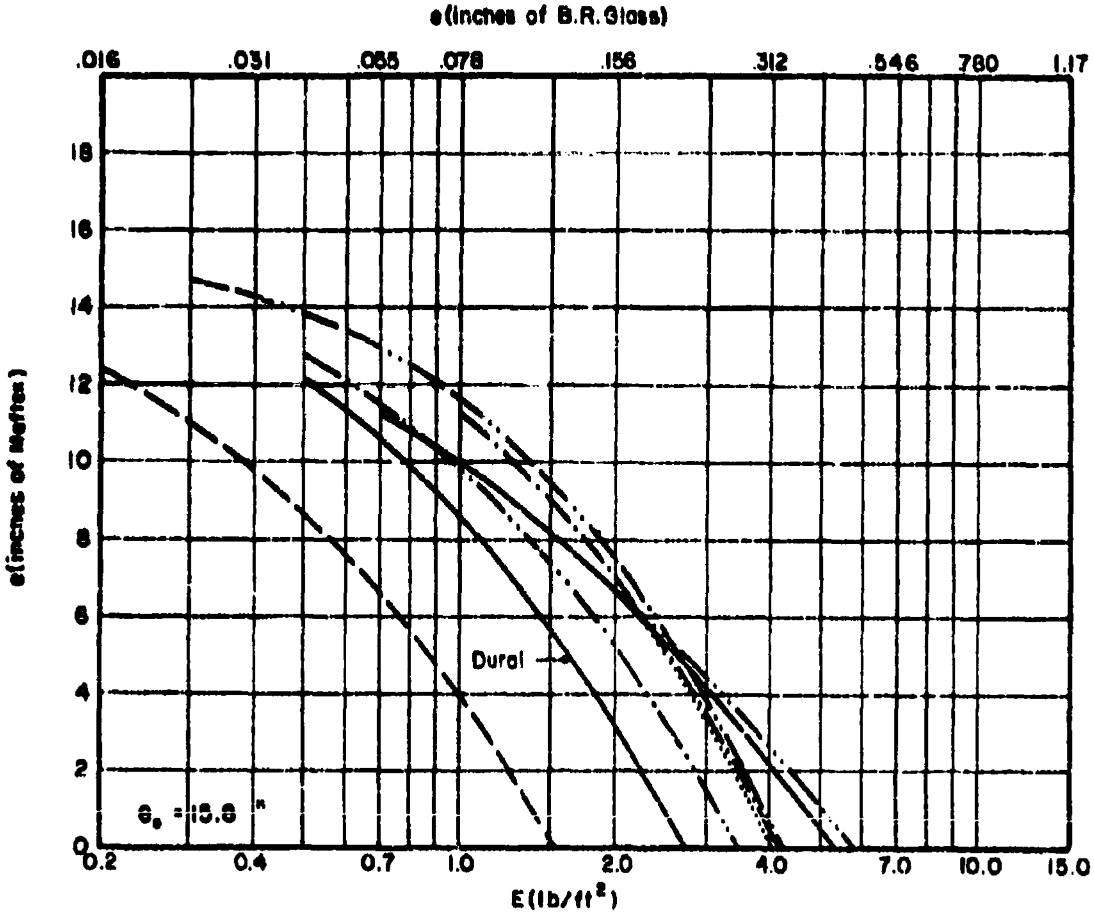

		*			*
Unbonded Nylon	– – – –	3.31	Stretched Plexiglas	– – · · – –	2.01
Bonded Nylon	·········	2.66	Doron	– · · – –	1.23
Lexan	———	2.06	B. R. Glass	– · · · –	1.00
Cast Plexiglas	– · – · –	2.01			

*Ratio of Material Thickness Relative to a Unit Thickness of B.R.Glass

Fig. 125

e_{MAFTEX} vs E

for Various Combinations of m_s, Θ, and V_s

m_s = 300 grains Θ = 70 degrees V_s = 3000 fps

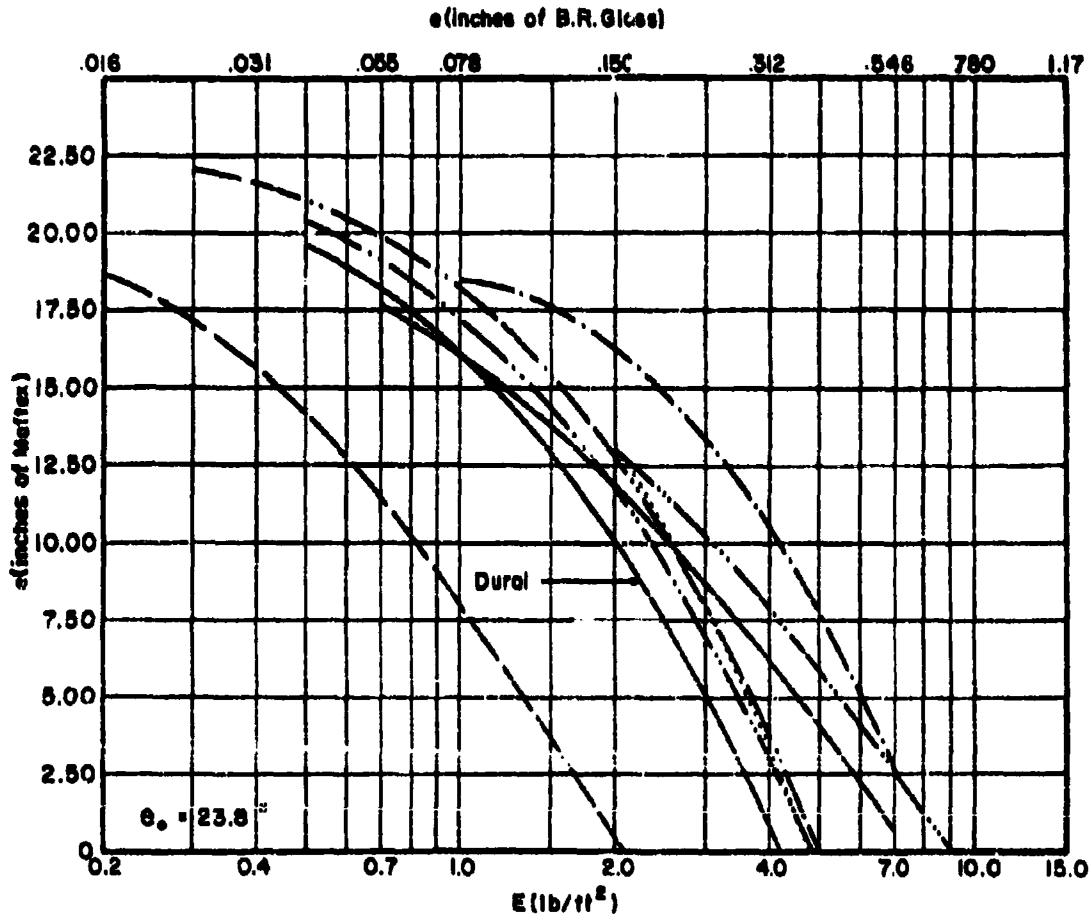

		*
Unbonded Nylon	– – – –	3.31
Bonded Nylon	....	2.66
Lexan	————	2.06
Cast Plexiglas	–·–·–	2.01
Stretched Plexiglas	––··––	2.01
Doron	–··–··	1.23
B. R. Glass	–···–···	1.00

*Ratio of Material Thickness Relative to a Unit Thickness of B.R.Glass

Fig. 126

e_{MAFTEX} VS E

for Various Combinations of m_s, Θ, and V_s

m_s = 30 grains Θ = 0 degrees V_s = 6000 fps

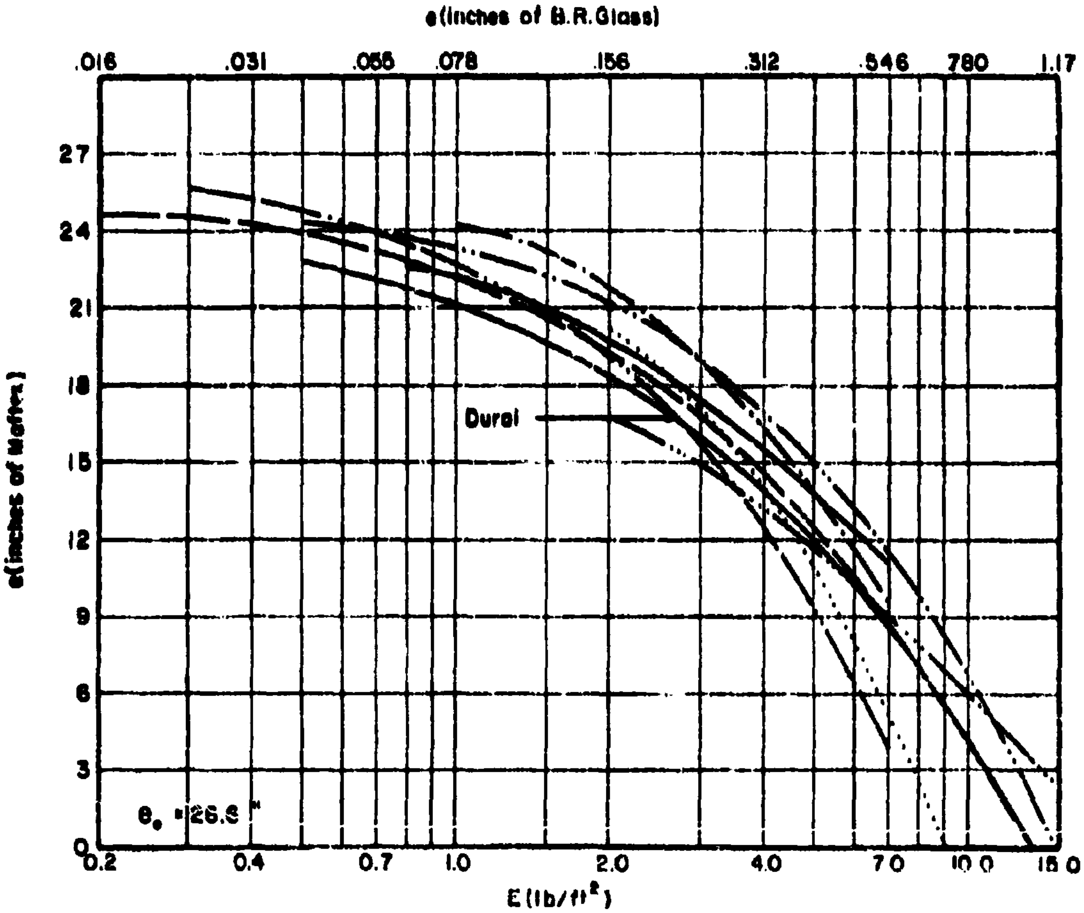

		*			*
Unbonded Nylon	— — — —	3.31	Stretched Plexiglas	— — · · — —	2.01
Bonded Nylon	·········	2.66	Doron	— · · — —	1.23
Lexan	————	2.06	B. R. Glass	— · · · —	1.00
Cast Plexiglas	— · — · —	2.01			

*Ratio of Material Thickness Relative to a Unit Thickness of B.R.Glass

Fig. 127

e_{MAFTEX} vs E

for Various Combinations of m_s, θ, and V_s

m_s = 100 grains θ = 0 degrees V_s = 6000 fps

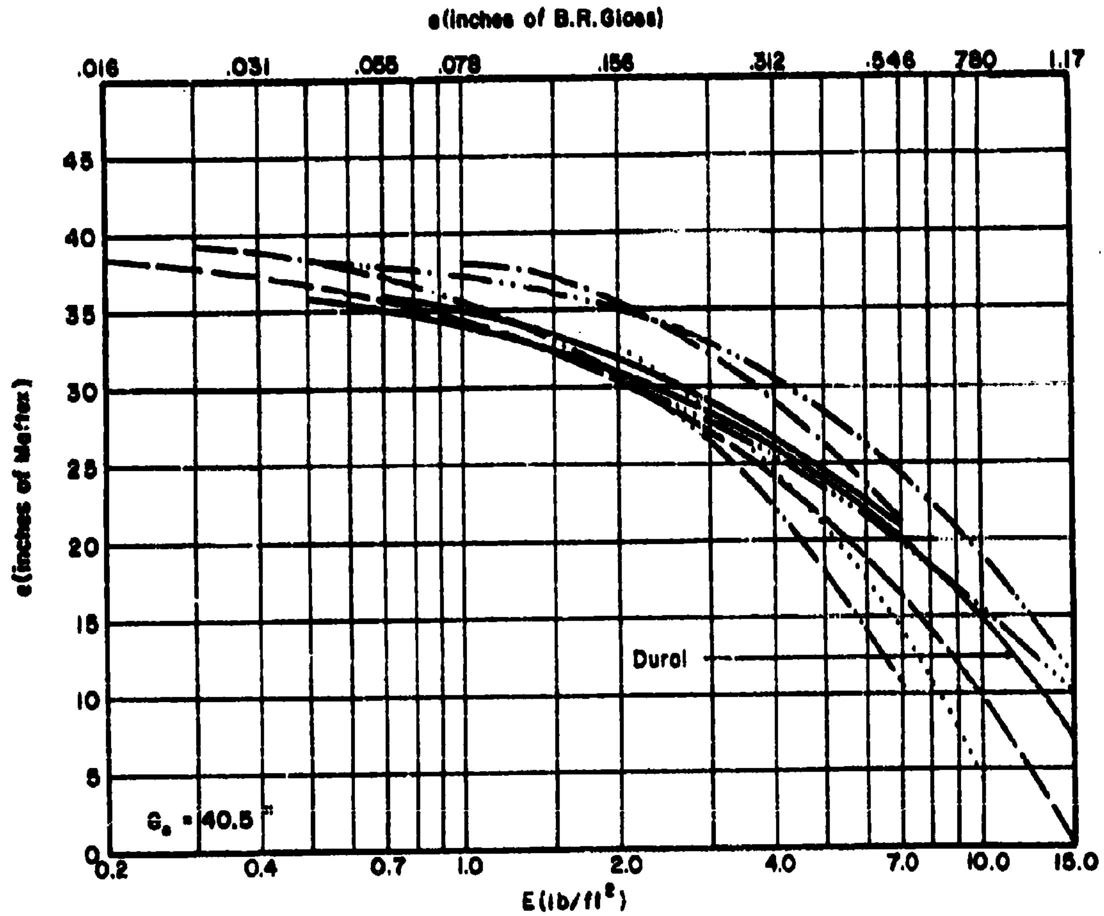

		*			*
Unbonded Nylon	----	3.31	Stretched Plexiglas	—-··-—	2.01
Bonded Nylon	·········	2.66	Doron	—··—·—	1.23
Lexan	———	2.06	B. R. Glass	—···—··	1.00
Cast Plexiglas	—·—·—	2.01			

*Ratio of Material Thickness Relative to a Unit Thickness of B.R.Glass

Fig. 128

e_{MAFTEX} VS E

for Various Combinations of m_s, Θ, and V_s

m_s = 300 grains Θ = 0 degrees V_s - 6000 fps

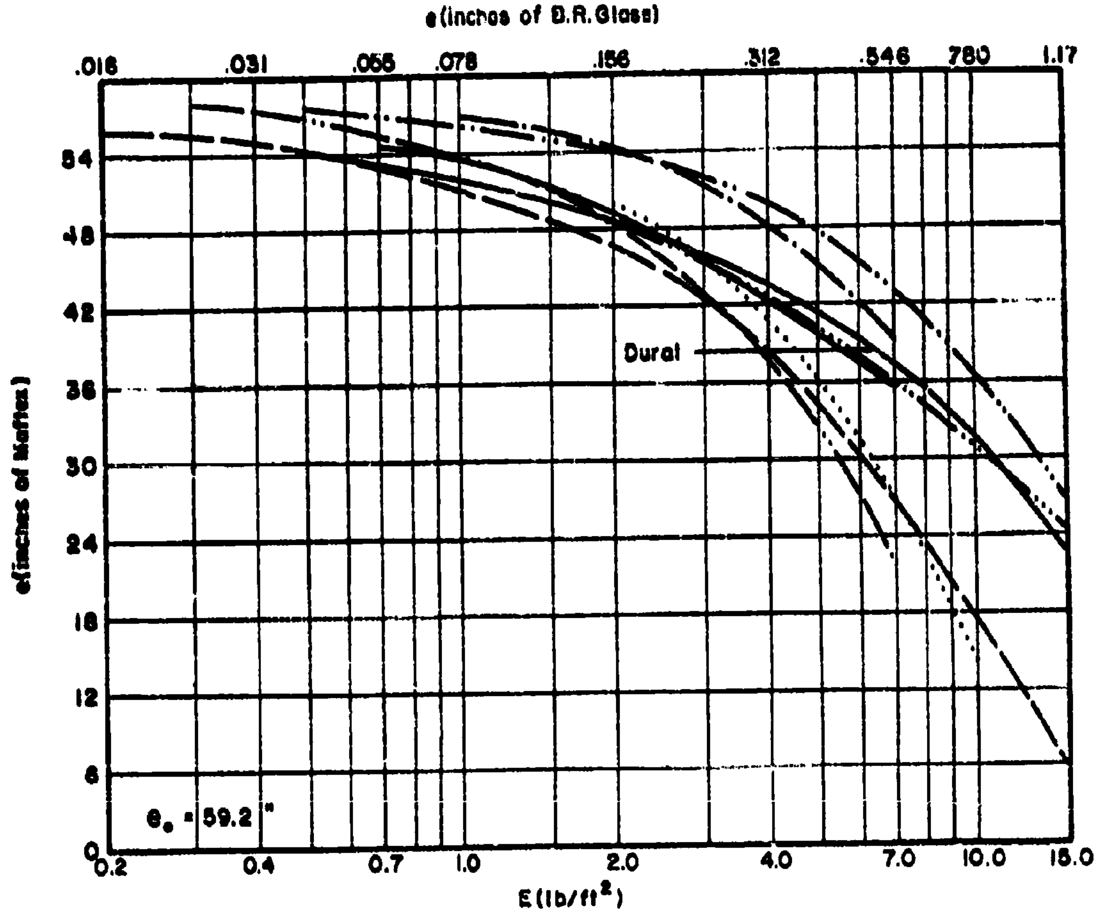

		*			*
Unbonded Nylon	– – – –	3.31	Stretched Plexiglas	— · · —	2.01
Bonded Nylon	·········	2.66	Doron	— · · — —	1.23
Lexan	———	2.06	B. R. Glass	- · · · · —	1.00
Cast Plexiglas	— · — · —	2.01			

*Ratio of Material Thickness Relative to a Unit Thickness of B.R.Glass

Fig. 129

e_{MAFTEX} vs E

for Various Combinations of m_s, Θ, and V_s

m_s = 30 grains Θ = 60 degrees V_s = 6000 fps

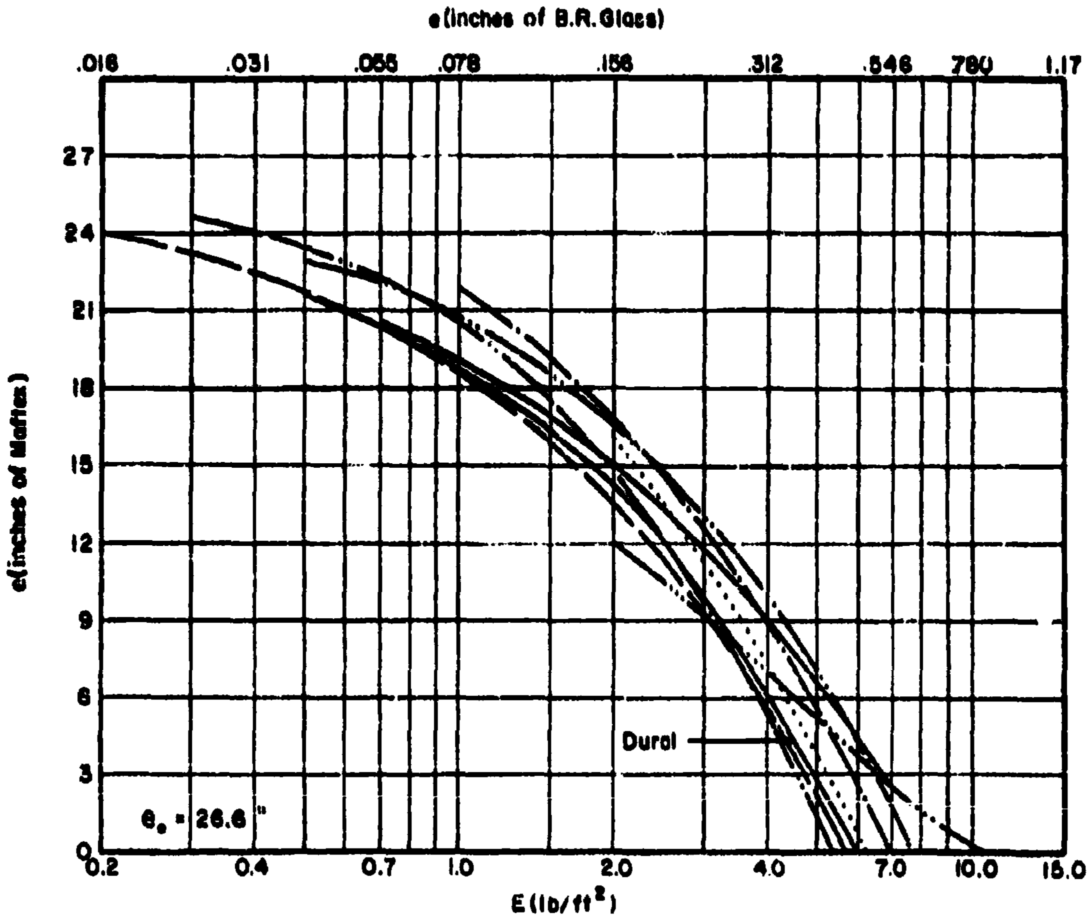

		*			*
Unbonded Nylon	— — - —	3.31	Stretched Plexiglas	— — ·· — —	2.01
Bonded Nylon	....	2.66	Doron	— ·· — —	1.23
Lexan	————	2.06	B. R. Glass	— ··· — — ···	1.00
Cast Plexiglas	— · — · —	2.01			

*Ratio of Material Thickness Relative to a Unit Thickness of B.R.Glass

Fig. 130

e_{MAFTEX} vs E
for Various Combinations of m_s, Θ, and V_s

m_s = 100 grains Θ = 60 degrees V_s = 6000 fps

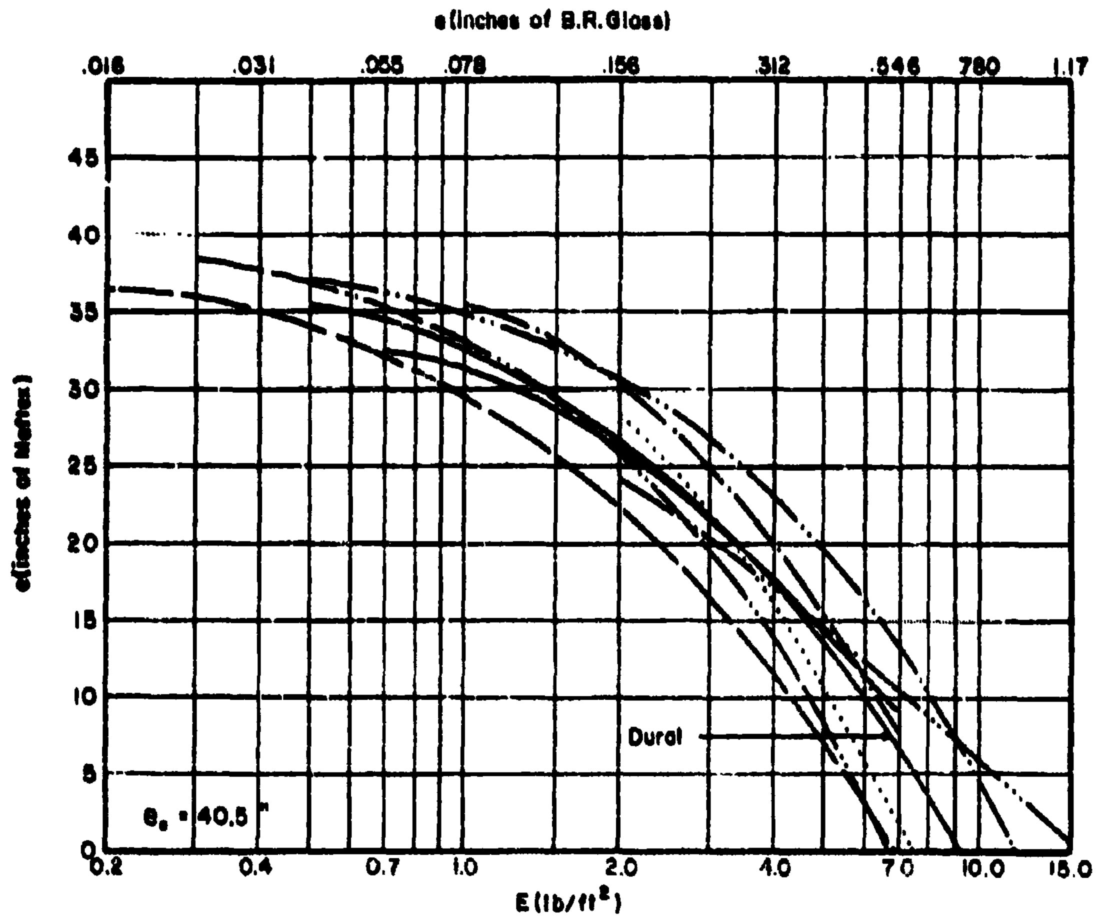

		*			*
Unbonded Nylon	– – – –	3.31	Stretched Plexiglas	– – · · – –	2.01
Bonded Nylon	·········	2.66	Doron	– · · – · · –	1.23
Lexan	———	2.06	B. R. Glass	– · · · – · · ·	1.00
Cast Plexiglas	– · – · –	2.01			

*Ratio of Material Thickness Relative to a Unit Thickness of B.R.Glass

Fig. 131

e_{MAFTEX} vs E

for Various Combinations of m_s, Θ, and V_s

m_s = 300 grains Θ = 60 degrees V_s = 6000 fps

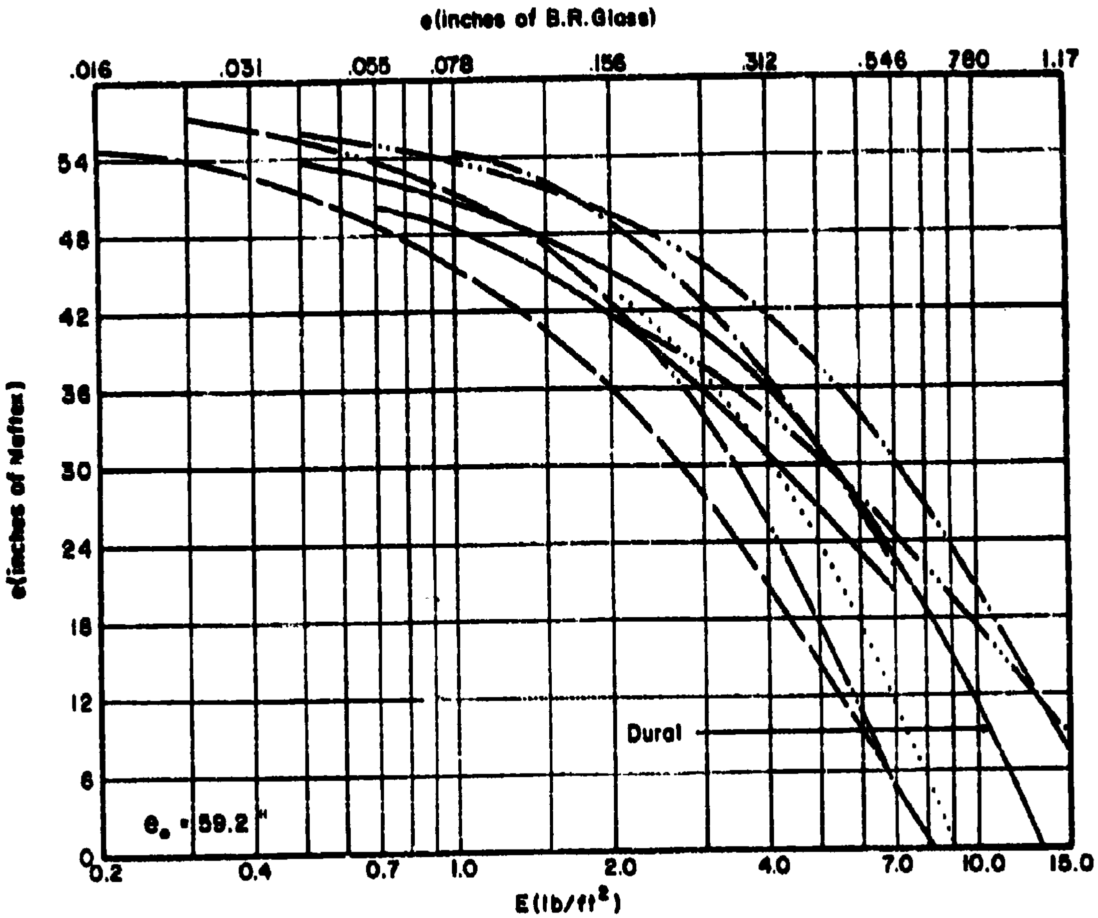

		*			*
Unbonded Nylon	— — — —	3.31	Stretched Plexiglas	—··——	2.01
Bonded Nylon	·········	2.66	Doron	—··——··	1.23
Lexan	———	2.06	B. R. Glass	—···—···	1.00
Cast Plexiglas	—·—·—	2.01			

*Ratio of Material Thickness Relative to a Unit Thickness of B.R.Glass

Fig. 132

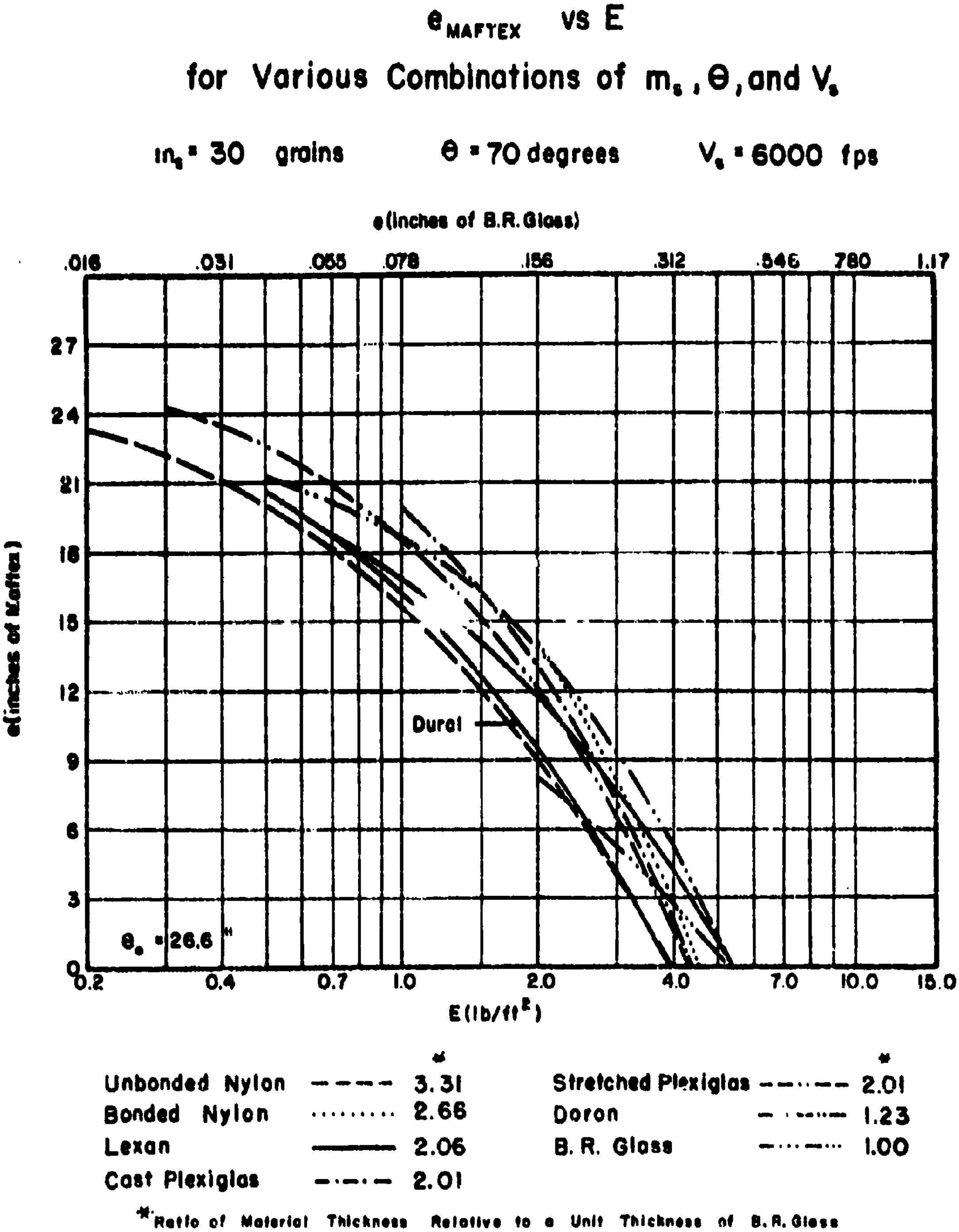
e_{MAFTEX} vs E
for Various Combinations of m_s, Θ, and V_s
m_s = 30 grains
Θ = 70 degrees
V_s = 6000 fps
e(inches of B.R.Glass)
.016
.031
.055
.078
.156
.312
.546
.780
1.17
e(inches of Maftex)
27
24
21
18
15
12
9
6
3
0
Dural
e_o = 26.6"
0.2
0.4
0.7
1.0
2.0
4.0
7.0
10.0
15.0
E(lb/ft²)
Unbonded Nylon 3.31
Bonded Nylon 2.66
Lexan 2.06
Cast Plexiglas 2.01
Stretched Plexiglas 2.01
Doron 1.23
B. R. Glass 1.00
*Ratio of Material Thickness Relative to a Unit Thickness of B.R.Glass

Fig. 133

e_{MAFTEX} vs E

for Various Combinations of m_s, Θ, and V_s

m_s = 100 grains Θ = 70 degrees V_c = 6000 fps

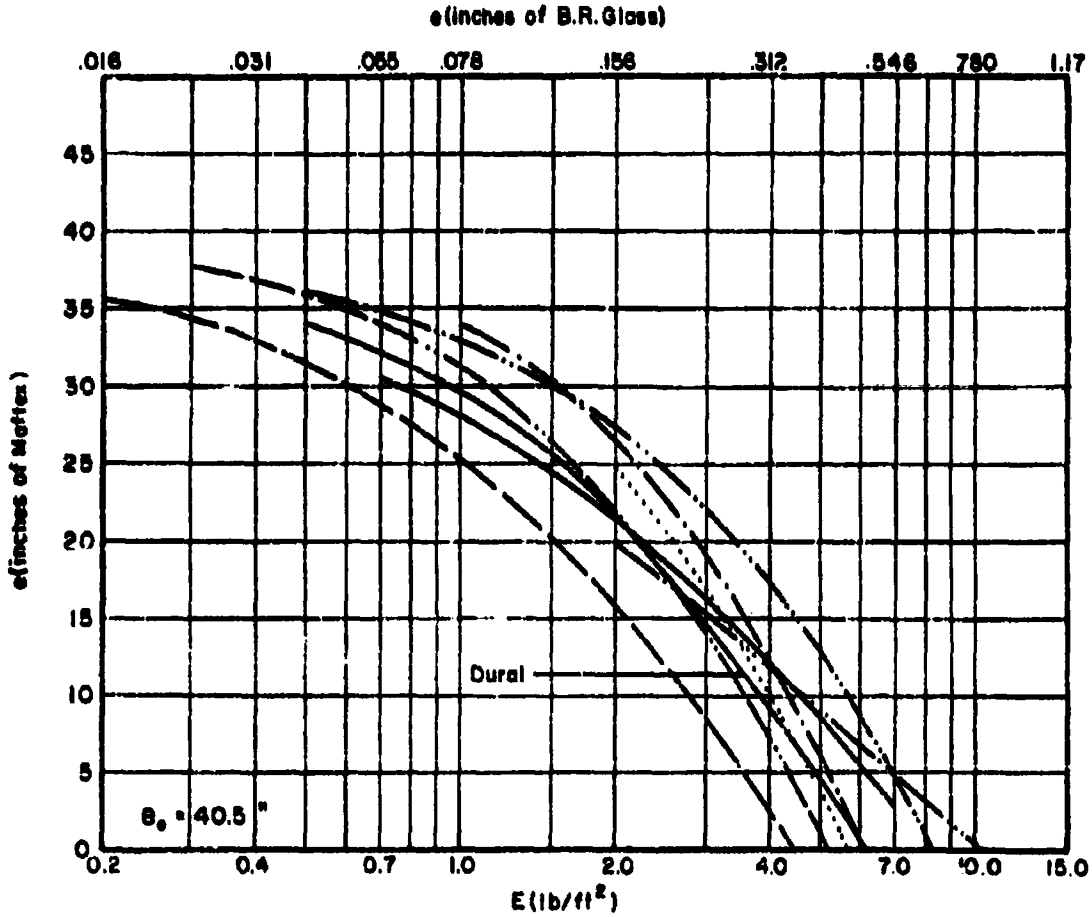

		*			*
Unbonded Nylon	----	3.31	Stretched Plexiglas	——··——	2.01
Bonded Nylon	········	2.66	Doron	—··—·—	1.23
Lexan	———	2.06	B. R. Glass	—···—···	1.00
Cast Plexiglas	—·—·—	2.01			

*Ratio of Material Thickness Relative to a Unit Thickness of B.R.Glass

Fig. 134

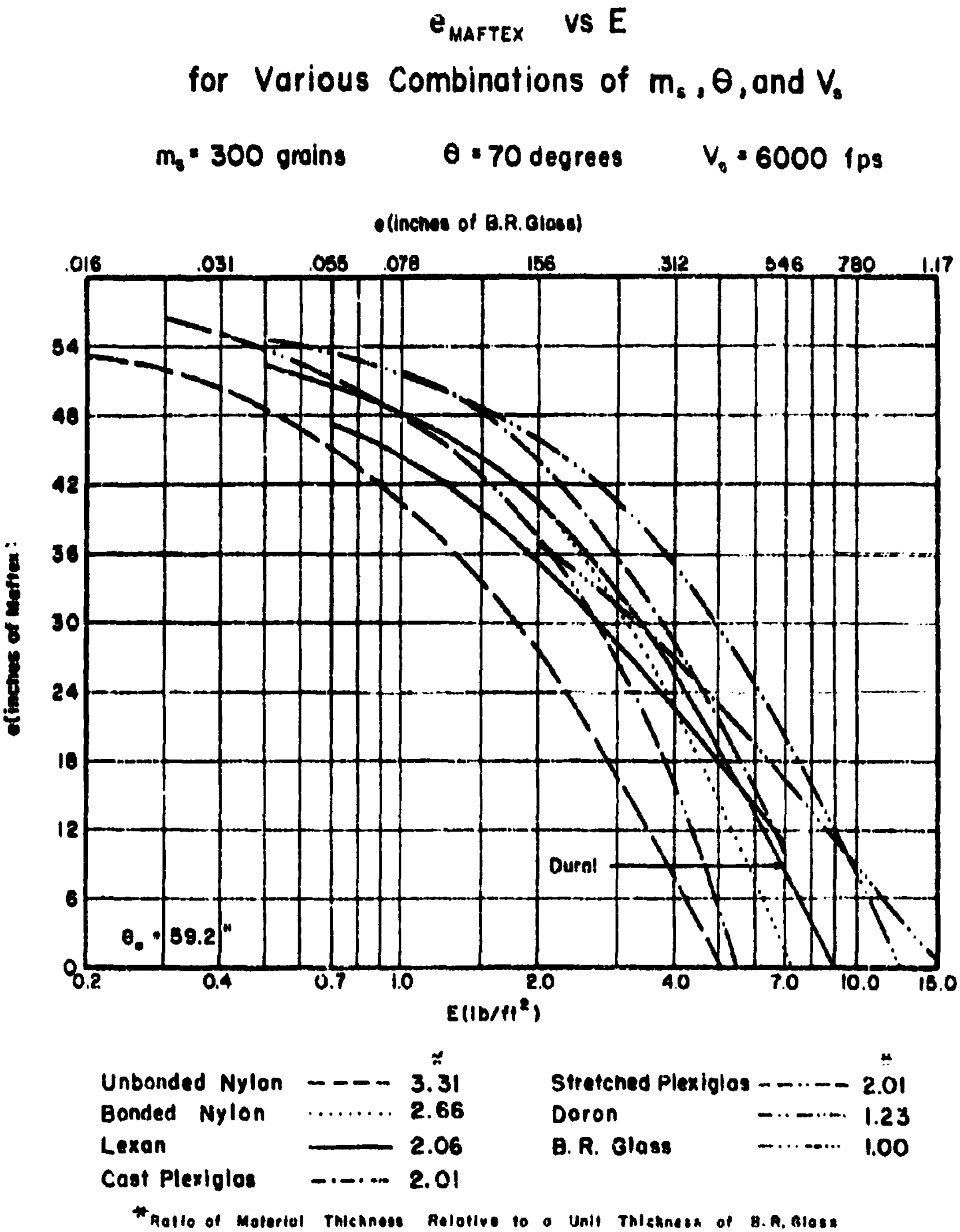
e_{MAFTEX} vs E
for Various Combinations of m_s, θ, and V_s
m_s = 300 grains
θ = 70 degrees
V_0 = 6000 fps
e(inches of B.R. Glass)
.016
.031
.055
.078
.156
.312
.546
.780
1.17
e(inches of Maftex)
54
48
42
36
30
24
18
12
6
0
θ₀ = 59.2°
Durnl
0.2
0.4
0.7
1.0
2.0
4.0
7.0
10.0
15.0
E(lb/ft²)
Unbonded Nylon 3.31
Bonded Nylon 2.66
Lexan 2.06
Cast Plexiglas 2.01
Stretched Plexiglas 2.01
Doron 1.23
B. R. Glass 1.00
*Ratio of Material Thickness Relative to a Unit Thickness of B.R. Glass

Fig. 135

e_{MAFTEX} vs E

for Various Combinations of m_s, Θ, and V_s

m_s = 30 grains Θ = 0 degrees V_s = 9000 fps

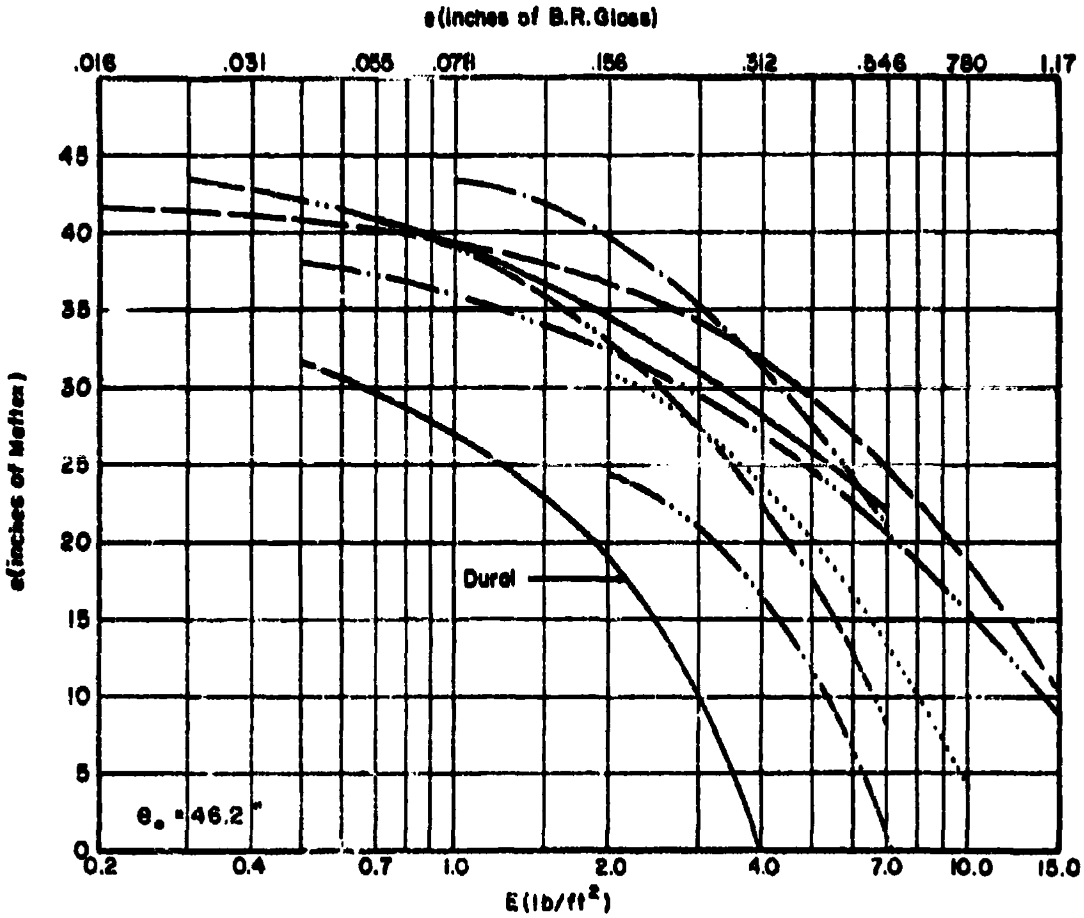

		*
Unbonded Nylon	-----	3.31
Bonded Nylon	....	2.66
Lexan	———	2.06
Cast Plexiglas	-·-·-	2.01
Stretched Plexiglas	--··--	2.01
Doron	-··—··	1.23
B. R. Glass	-···-···	1.00

*Ratio of Material Thickness Relative to a Unit Thickness of B.R.Glass

Fig. 136

e_{MAFTEX} VS E for Various Combinations of m_t, Θ, and V_s

m_t = 100 grains Θ = 0 degrees V_s = 9000 fps

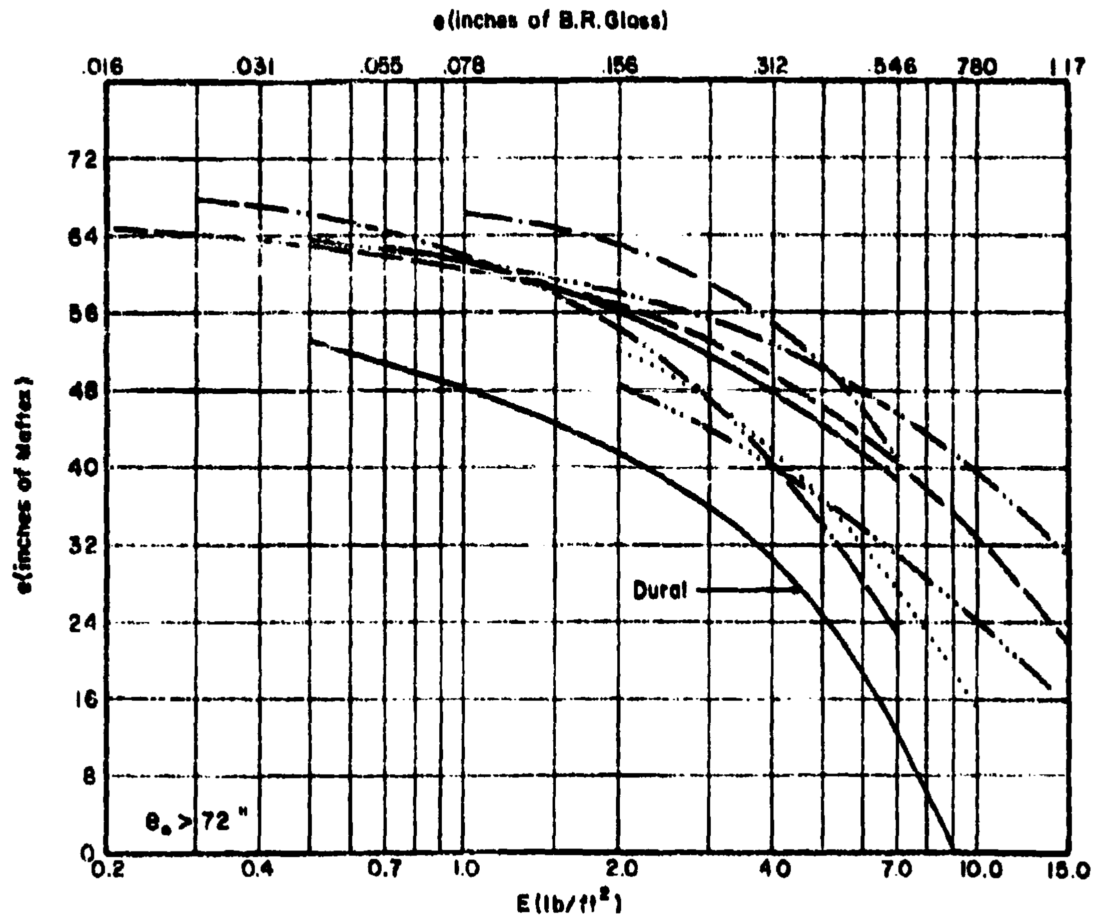

		*			*
Unbonded Nylon	— — — —	3.31	Stretched Plexiglas	— — · · — —	2.01
Bonded Nylon	· · · · · · · ·	2.66	Doron	— · · — · · —	1.23
Lexan	————	2.06	B.R Glass	— · · · — —	1.00
Cast Plexiglas	— · — · —	2.01			

*Ratio of Material Thickness Relative to a Unit Thickness of B.R. Glass

Fig. 137

e_{MAFTEX} vs E

for Various Combinations of m_s, θ, and V_s

m_s = 300 grains θ = 0 degrees V_s = 9000 fps

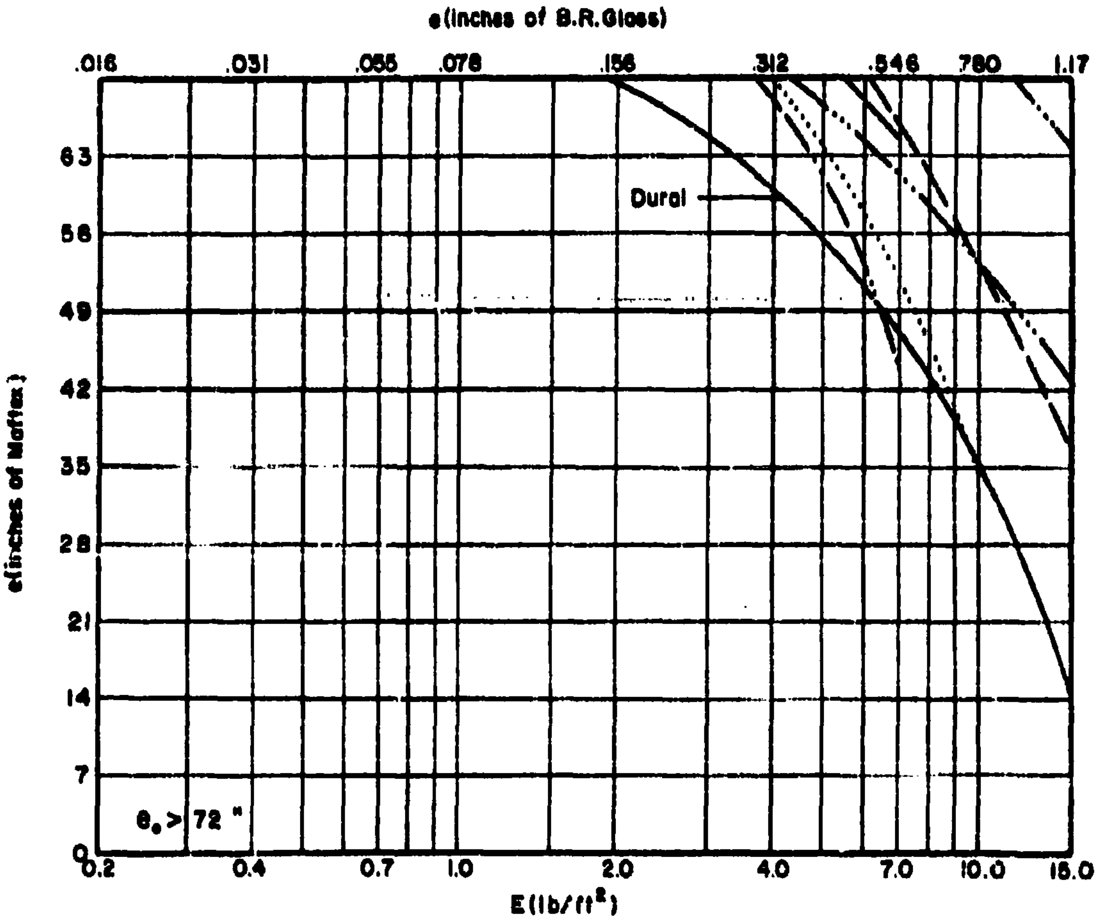

		*			*
Unbonded Nylon	----	3.31	Stretched Plexiglas	——··——	2.01
Bonded Nylon	·········	2.66	Doron	—··———	1.23
Lexan	———	2.06	B. R. Glass	—···—··	1.00
Cast Plexiglas	—·—·—	2.01			

*Ratio of Material Thickness Relative to a Unit Thickness of B.R.Glass

Fig. 138

CONFIDENTIAL

e_{MAFTEX} vs E

for Various Combinations of m_s, θ, and V_s

m_s = 30 grains θ = 60 degrees V_s = 9000 fps

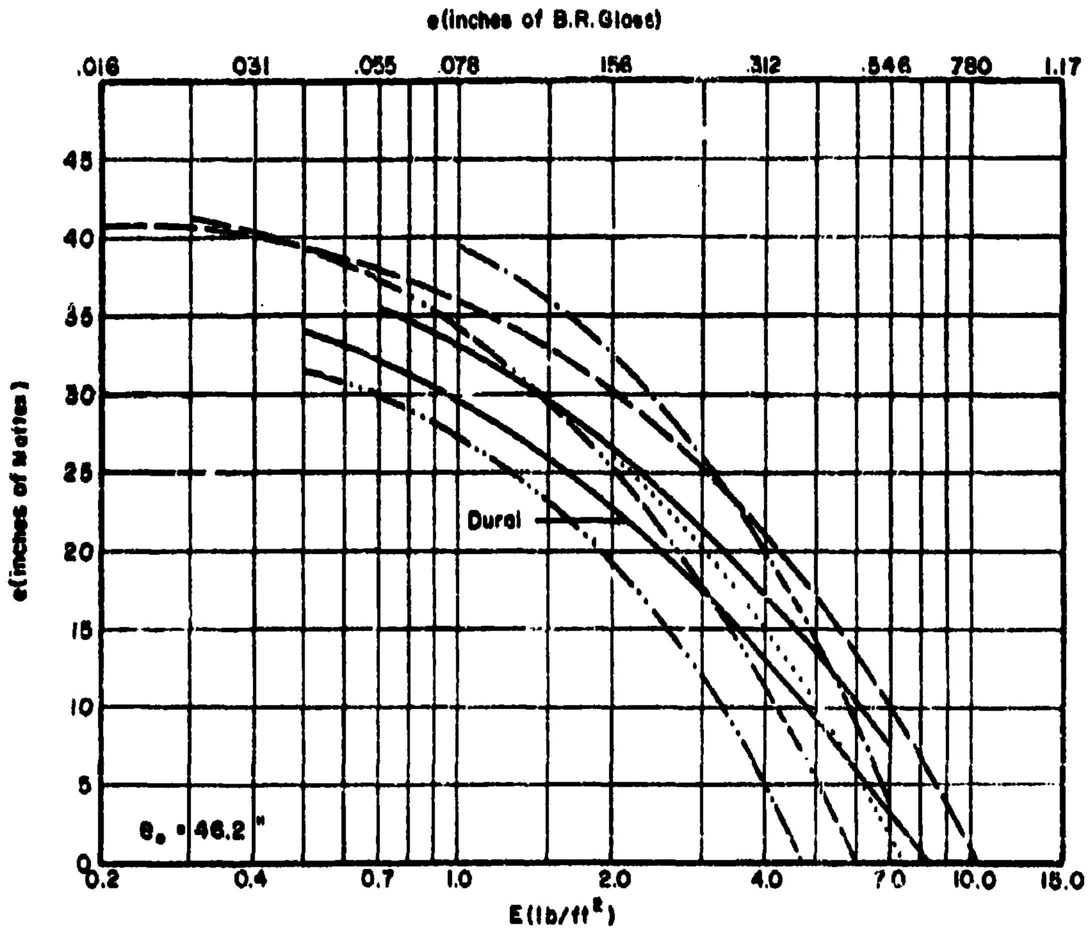

		*			*
Unbonded Nylon	– – – –	3.31	Stretched Plexiglas	–– – · · – –	2.01
Bonded Nylon	········	2.66	Doron	– · · ——	1.23
Lexan	———	2.06	B. R. Glass	– · · · —— ····	1.00
Cast Plexiglas	– · – · –	2.01			

*Ratio of Material Thickness Relative to a Unit Thickness of B.R.Glass

Fig. 139

CONFIDENTIAL

e_{MAFTEX} vs E
for Various Combinations of m_s, Θ, and V_s

m_s = 100 grains   Θ = 60 degrees V_s = 9000 fps

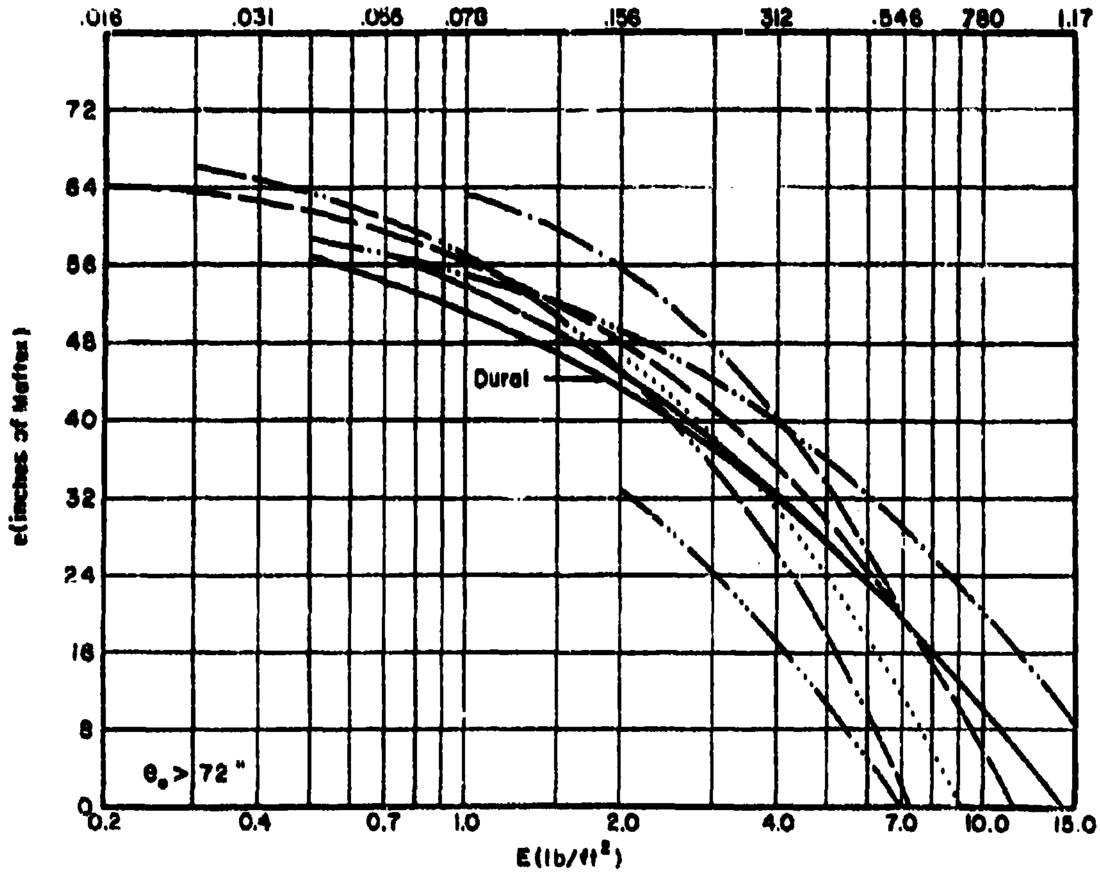

		*			*
Unbonded Nylon	— - — —	3.31	Stretched Plexiglas	— — ·· — —	2.01
Bonded Nylon	·········	2.66	Doron	— ·· — —	1.23
Lexan	———	2.06	B. R. Glass	— ··· —	1.00
Cast Plexiglas	— · — · —	2.01			

*Ratio of Material Thickness Relative to a Unit Thickness of B.R.Glass

Fig. 140

e_{MAFTEX} vs E
for Various Combinations of m_s, θ, and V_s

m_s = 300 grains θ = 60 degrees V_s = 9000 fps

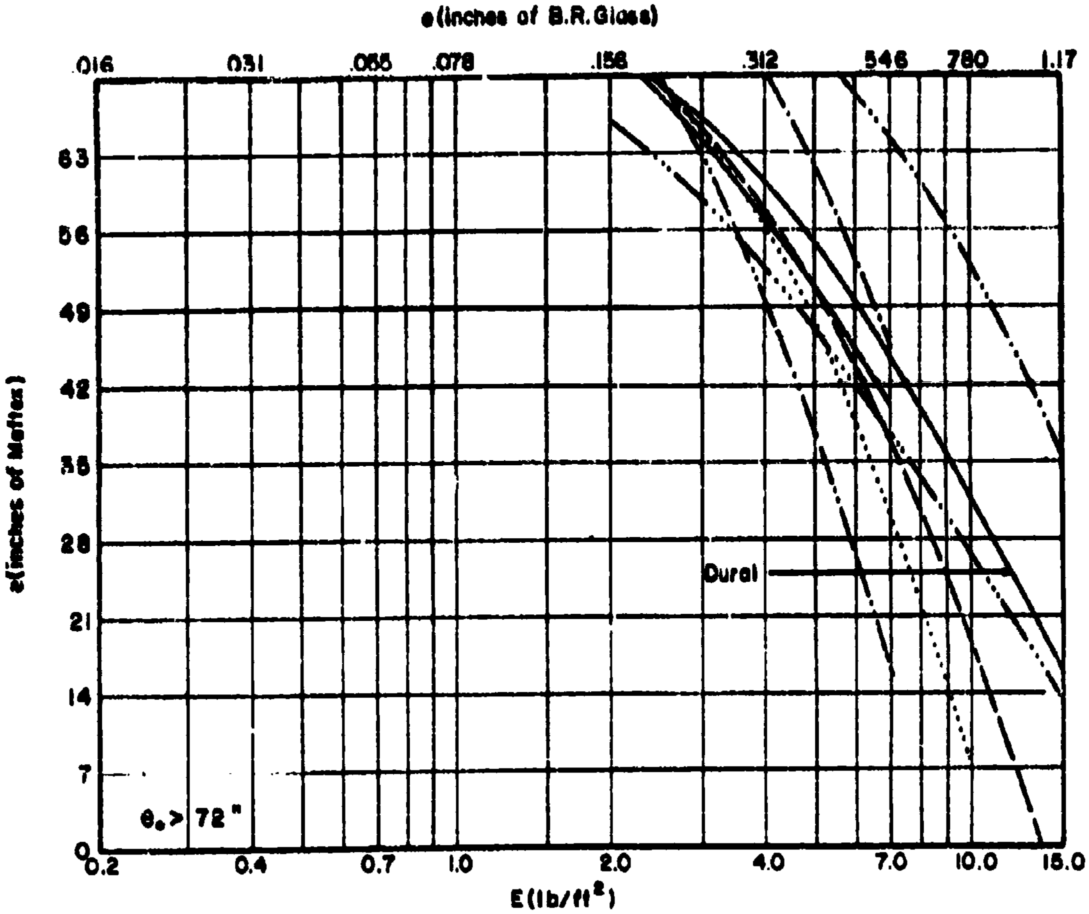

		*
Unbonded Nylon	----	3.31
Bonded Nylon	·········	2.66
Lexan	———	2.06
Cast Plexiglas	-·-·-	2.01
Stretched Plexiglas	---·--	2.01
Doron	-··--	1.23
B. R. Glass	-···-···	1.00

*Ratio of Material Thickness Relative to a Unit Thickness of B.R.Glass

Fig. 141

e_{MAFTEX} vs E

for Various Combinations of m_s, Θ, and V_s

m_s = 30 grains Θ = 70 degrees V_s = 9000 fps

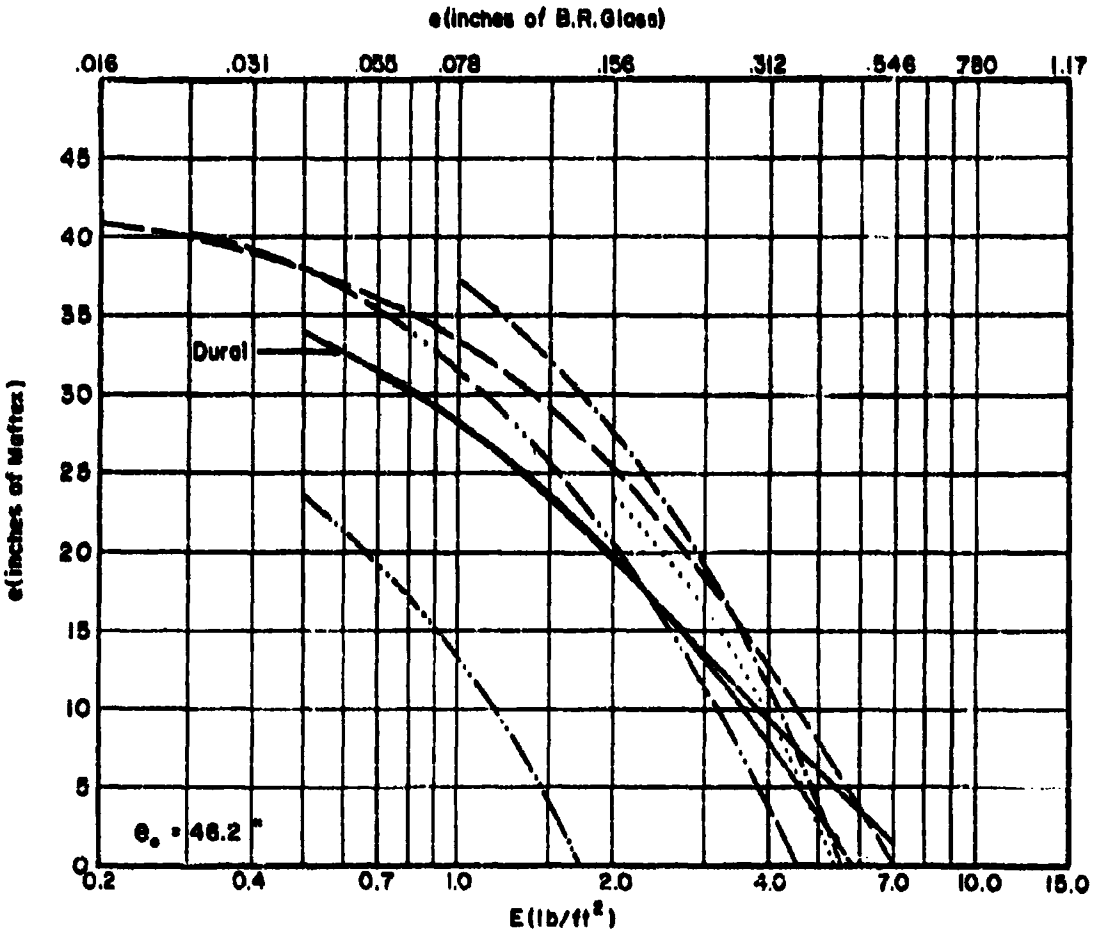

		*
Unbonded Nylon	– – – –	3.31
Bonded Nylon	········	2.66
Lexan	———	2.06
Cast Plexiglas	–·–·–	2.01
Stretched Plexiglas	——··——	2.01
Doron	—··———	1.23
B. R. Glass	—···—···	1.00

*Ratio of Material Thickness Relative to a Unit Thickness of B.R.Glass

Fig. 142

e_{MAFTEX} vs E

for Various Combinations of m_s, Θ, and V_s

m_s = 100 grains Θ = 70 degrees V_s = 9000 fps

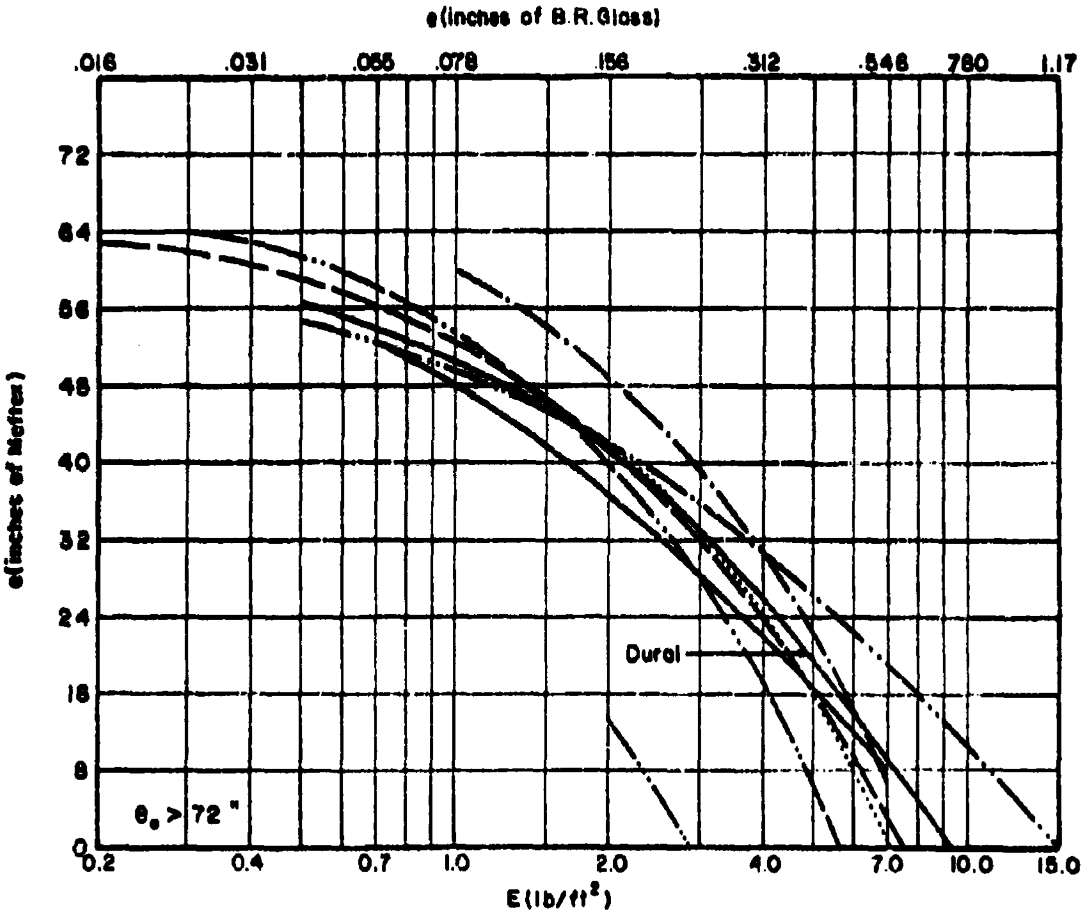

		*			*
Unbonded Nylon	– – – –	3.31	Stretched Plexiglas	– – ·· – –	2.01
Bonded Nylon	·········	2.66	Doron	– ·· – – ·· –	1.23
Lexan	———	2.06	B. R. Glass	– ··· – – ···	1.00
Cast Plexiglas	– · – · –	2.01			

*Ratio of Material Thickness Relative to a Unit Thickness of B.R.Glass

Fig. 143

e_{MAFTEX} vs E

for Various Combinations of m_s, Θ, and V_s

m_s = 300 grains Θ = 70 degrees V_s = 9000 fps

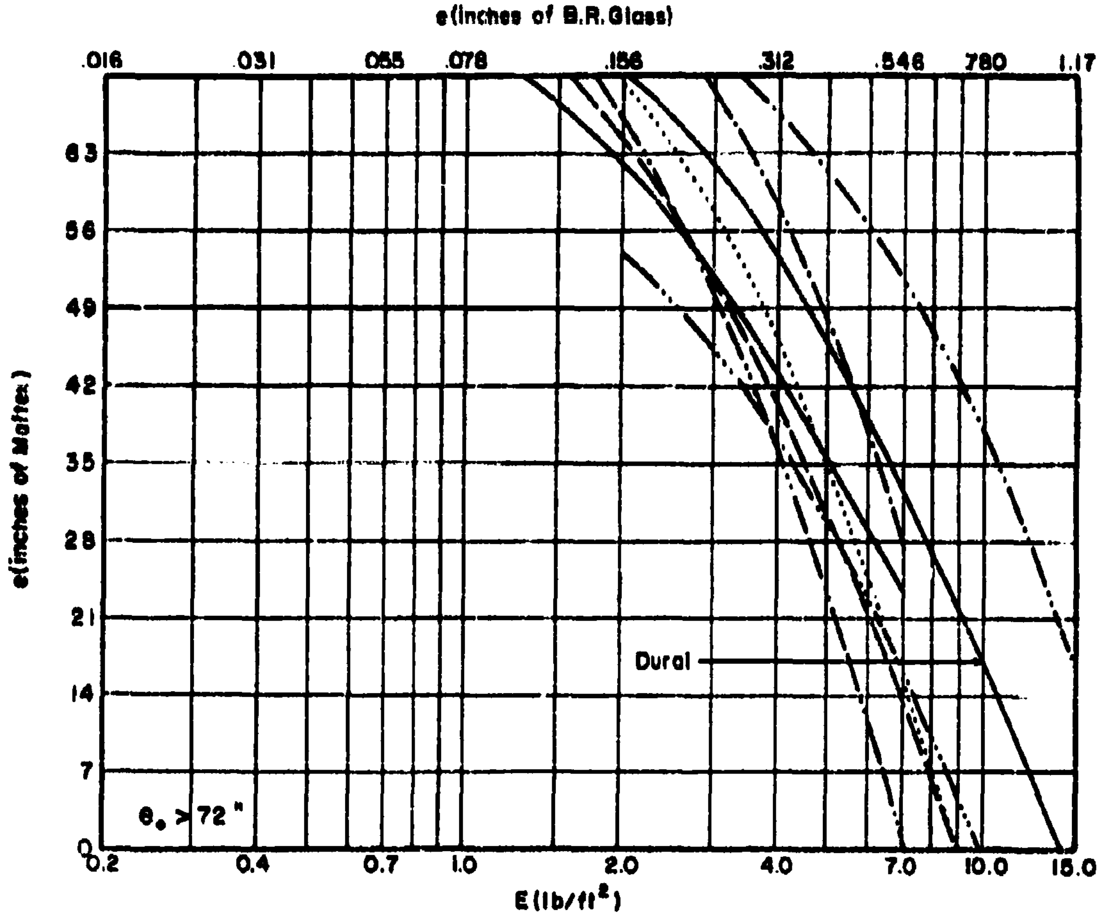

		*			*
Unbonded Nylon	– – – –	3.31	Stretched Plexiglas	—··—·—	2.01
Bonded Nylon	········	2.66	Doron	—··—·—	1.23
Lexon	———	2.06	B. R. Glass	—···—	1.00
Cast Plexiglas	—·—·—	2.01			

*Ratio of Material Thickness Relative to a Unit Thickness of B.R.Glass

Fig. 144

Appendix F

Graph Set VI: V_o versus E for Various Combinations of m_s and θ

Figs. 145-153

V_o vs E for Various Combinations of m_s and Θ

Θ : 0° m_s : 30 grains

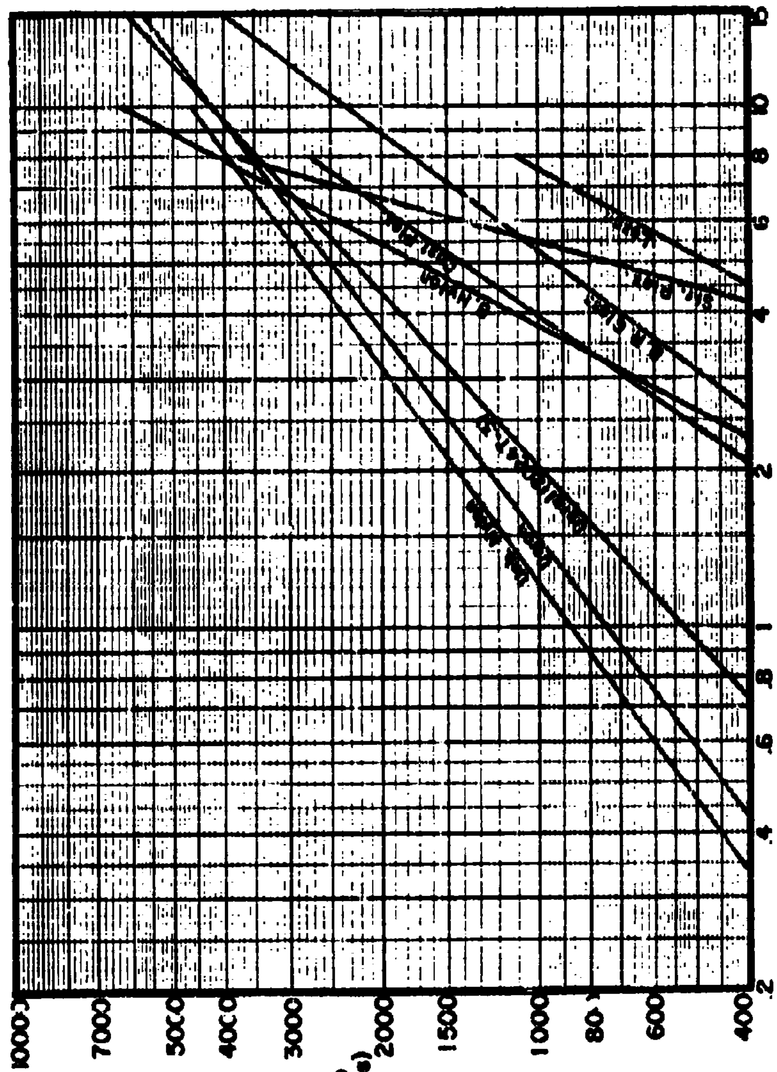

E (lb/ft²)

Fig. 145

V_0 vs E for Various Combinations of m_s and Θ

Θ : 0° m_s : 100 grains

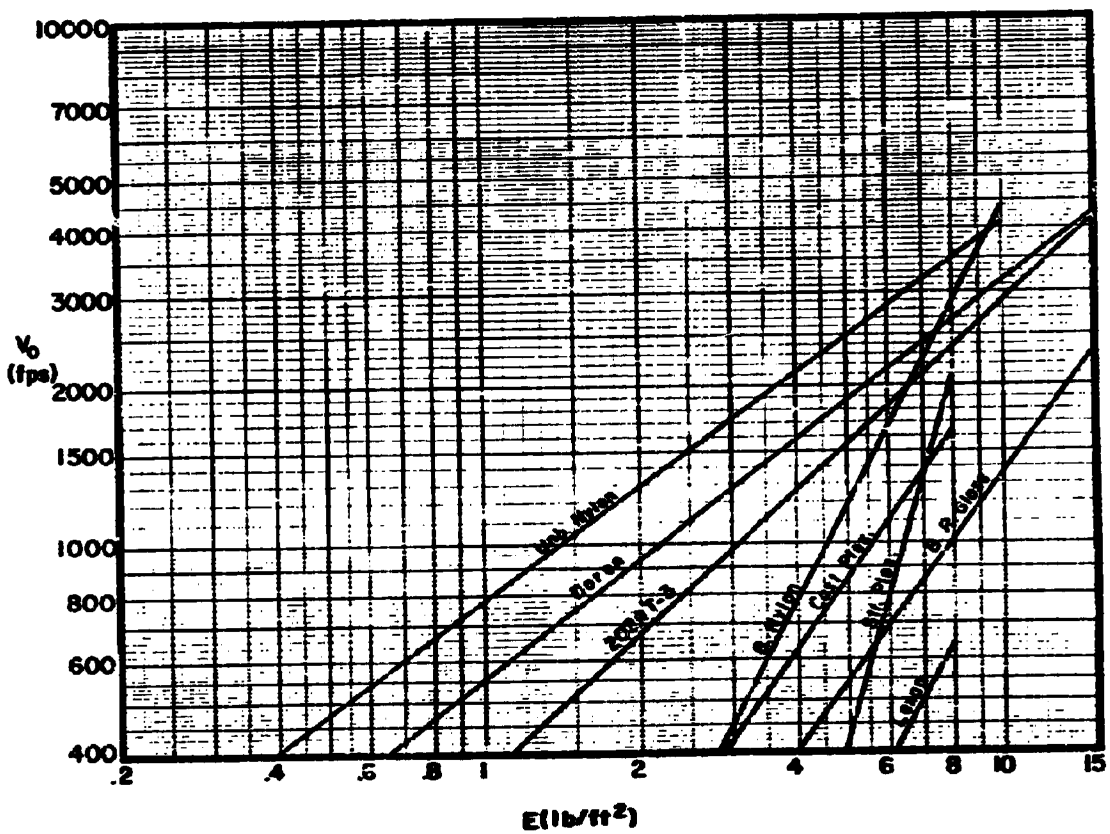

Fig. 146

V_0 vs E for Various Combinations of m_s and Θ

Θ : 0°　　　m_s : 300 grains

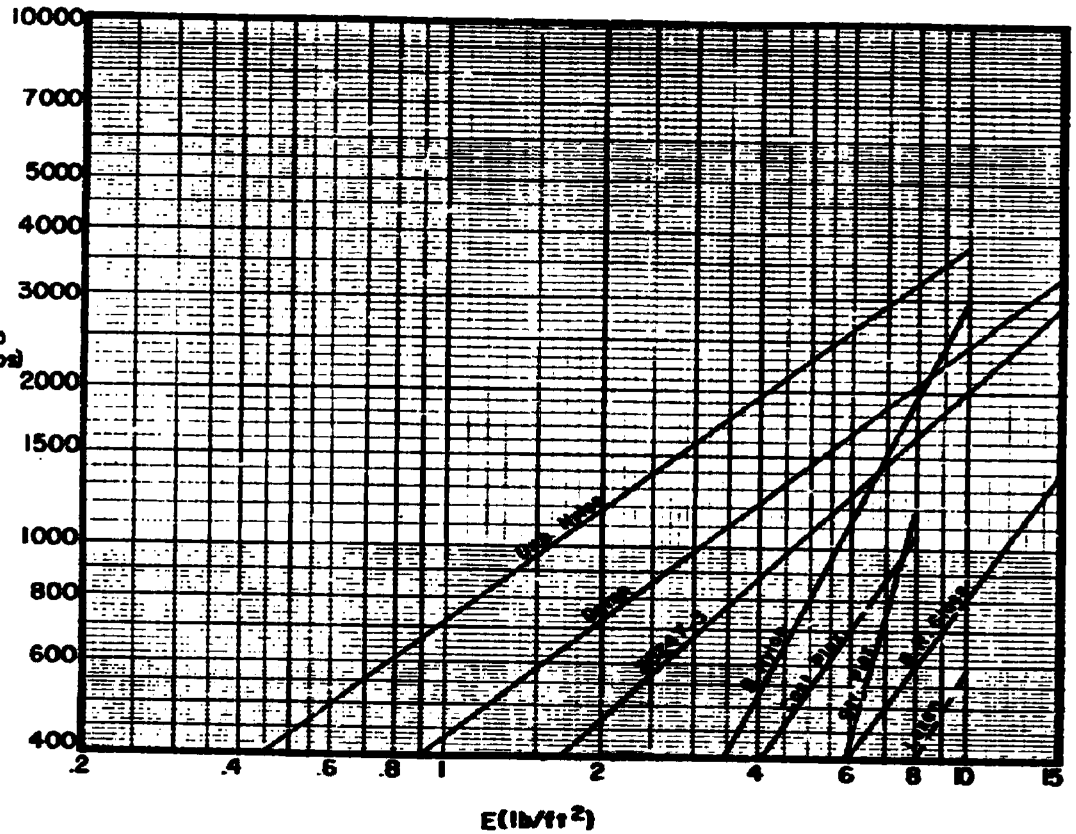

Fig. 147

V_o vs E for Various Combinations of m_s and θ

θ : 60° m_s : 30 grains

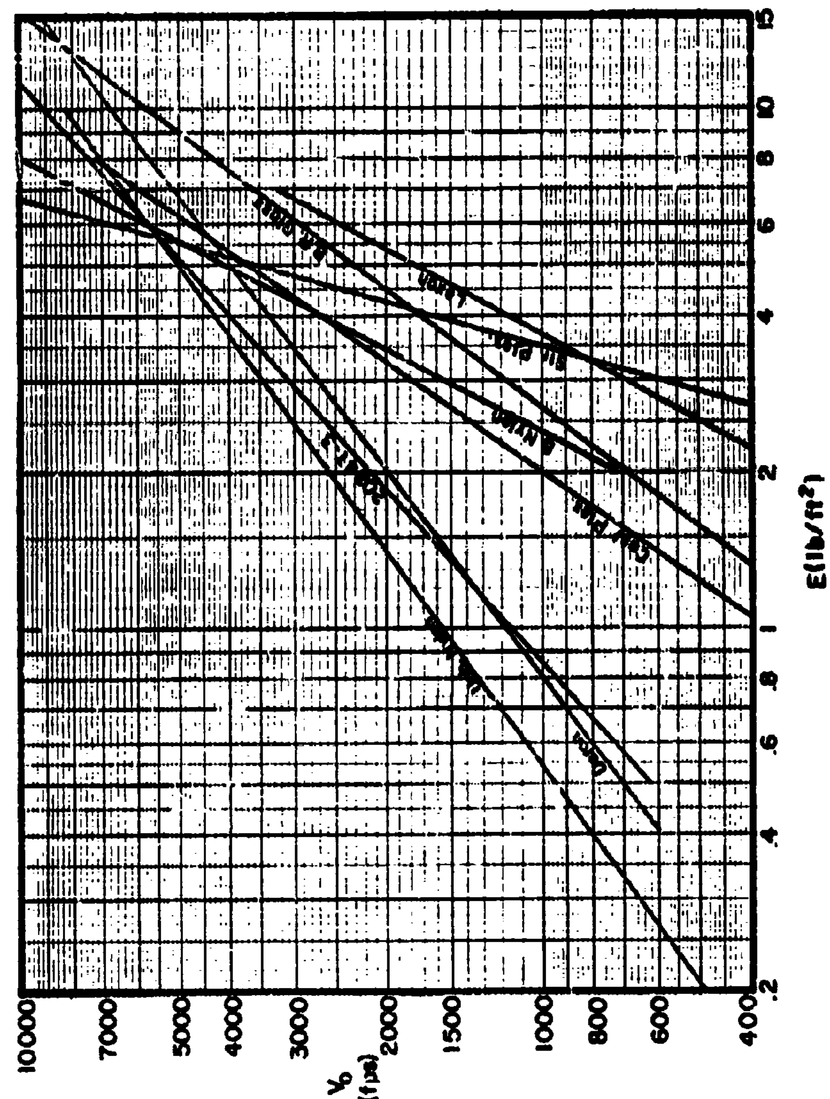

Fig. 148

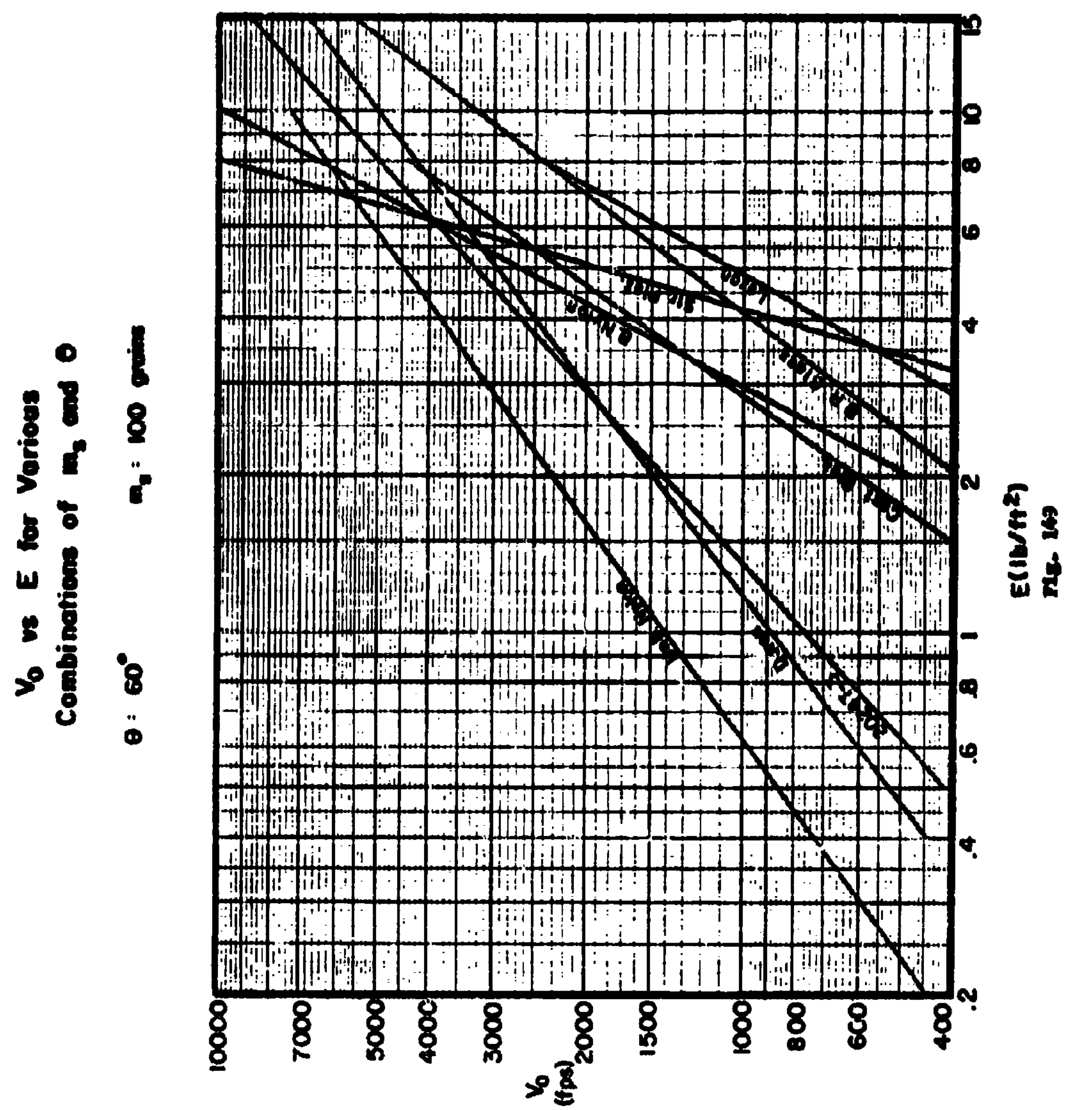
V_o vs E for Various
Combinations of m_s and Θ
Θ : 60°
m_s : 100 grains
V_o (fps)
10000
7000
5000
4000
3000
2000
1500
1000
800
600
400
.2
.4
.6
.8
1
2
4
6
8
10
15
E(lb/ft²)

Fig. 143

V_o vs E for Various Combinations of m_s and θ

θ : 60° m_s : 300 grains

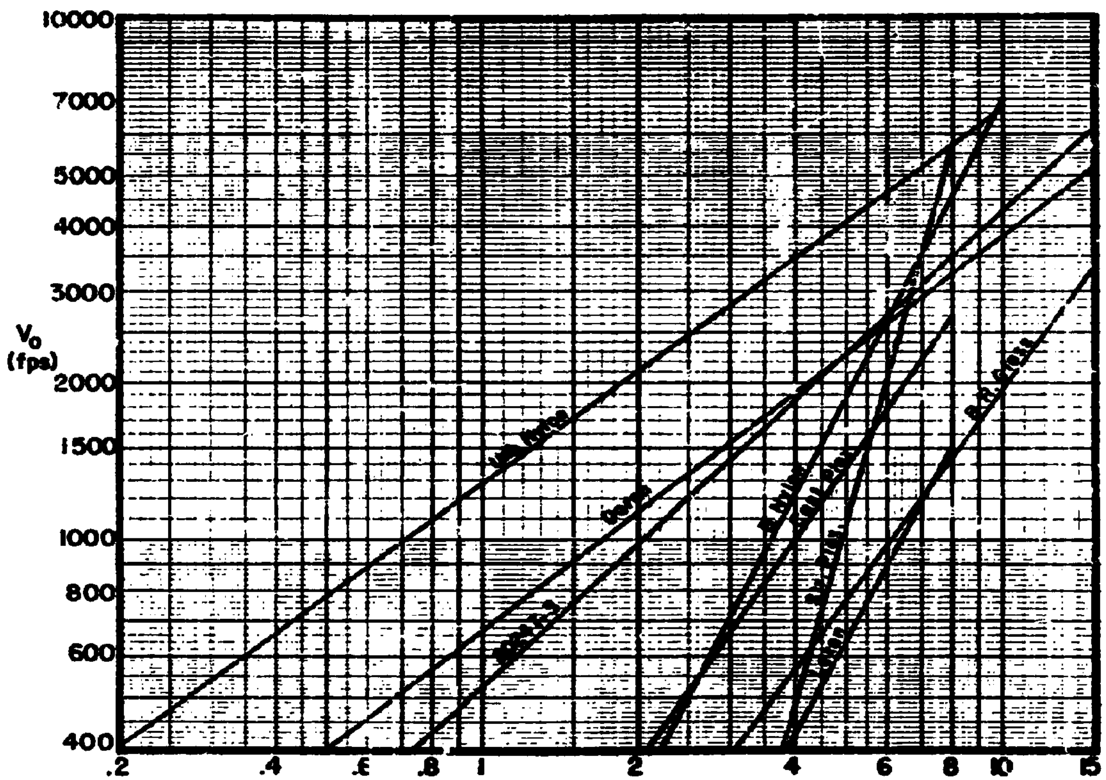

E(lb/ft²)

Fig. 158

V_o vs E for Various Combinations of m_s and θ

θ : 70° m_s : 30 grains

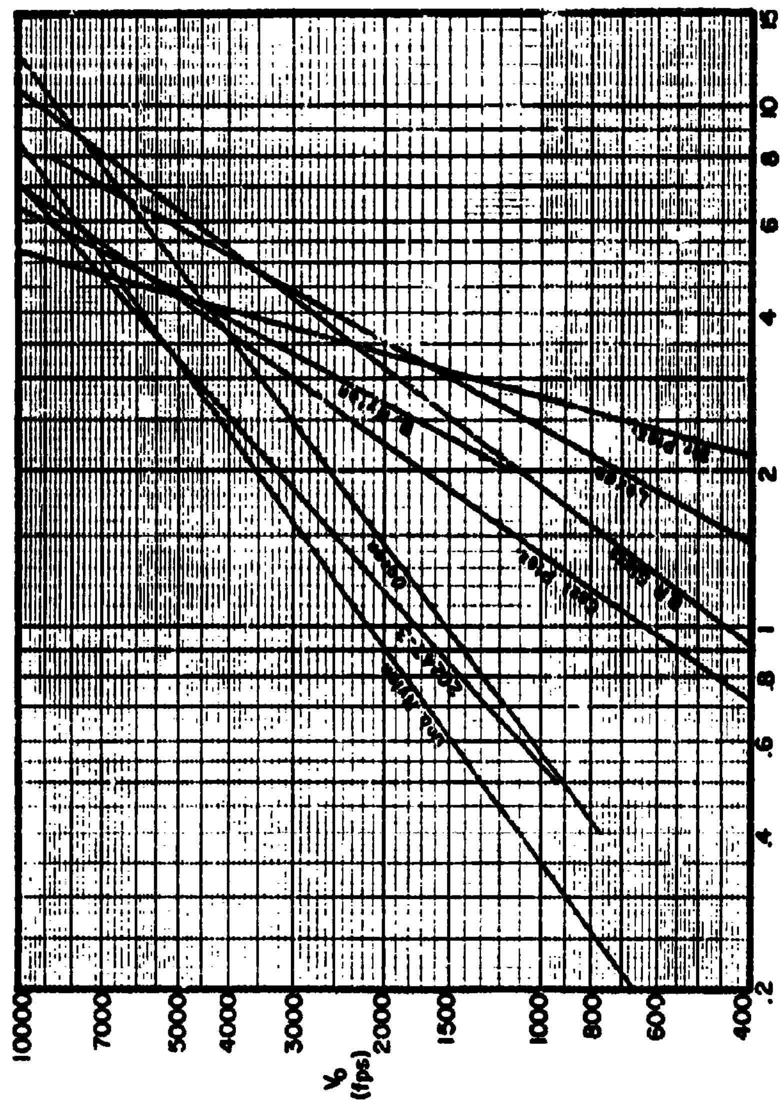

E(lb/ft²)

Fig. 151

V_0 vs E for Various Combinations of m_s and θ

θ : 70° m_s : 100 grains

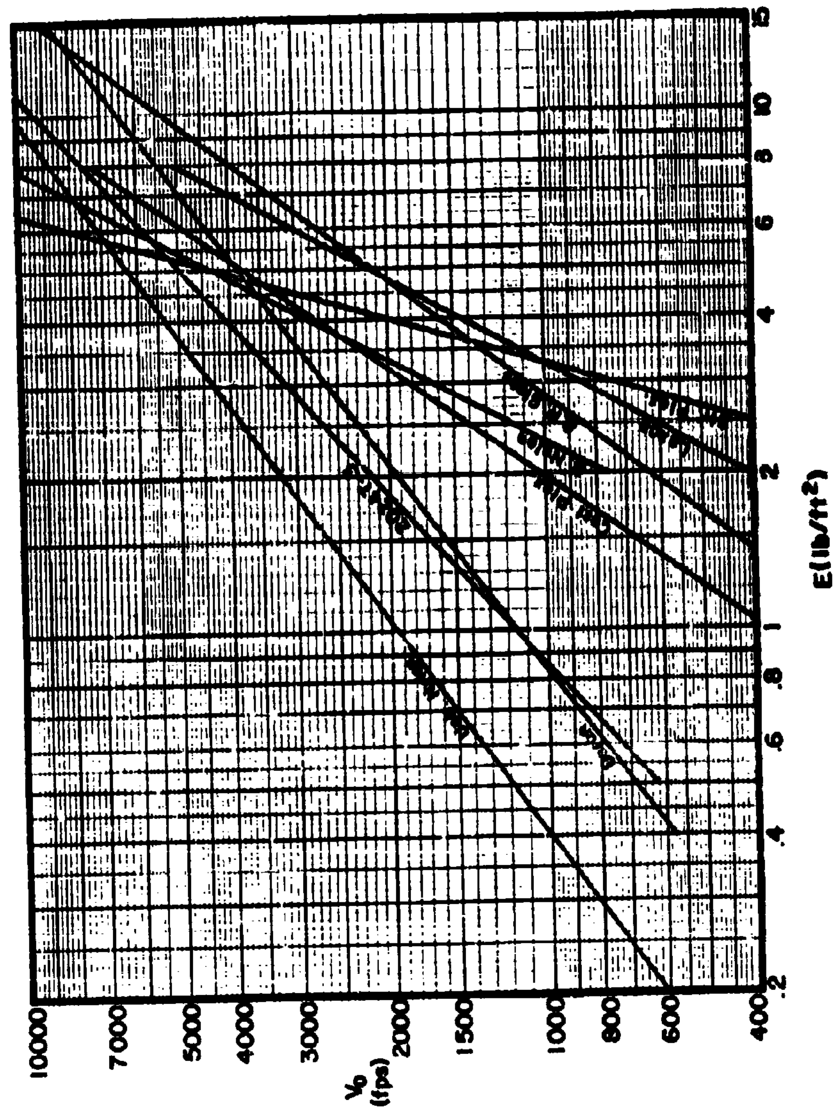

Fig. 152

V_o vs E for Various Combinations of m_s and θ

θ : 70° m_s : 300 grains

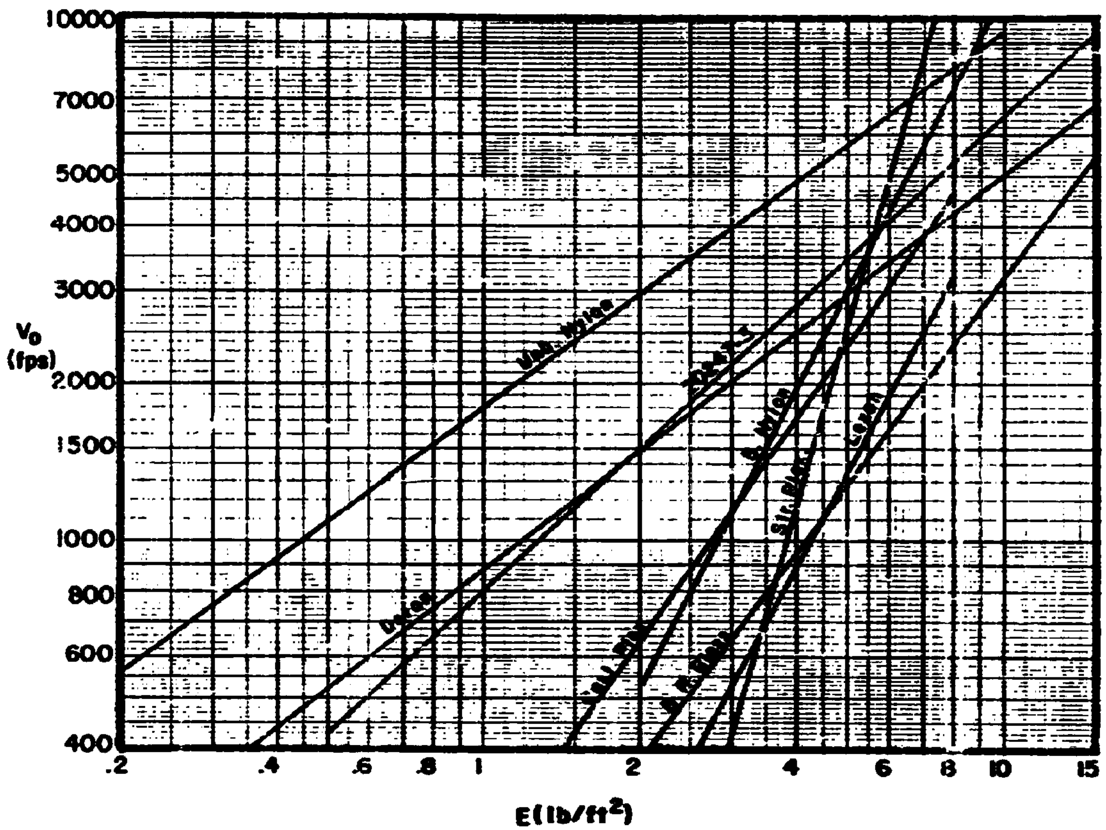

Fig. 153

Appendix G

Graph Set VII: Impact Conditions for Fragment Shatter

Figs. 154-158

Note: No graphs for Bonded and Unbonded Nylon appear within this Graph Set. The limitations of the experimental data for these materials were such that extreme cases of fragment break-up are not in evidence. Still higher striking velocities would be needed to produce the break-up data necessary to warrant predictions of impact conditions on this material for which the fragment will shatter.

Impact Conditions For Fragment Shatter

Target Material: Lexan
Shatter Criterion: $c' = m_r/m_s$ = 0 ------ Extrapolated

Notes:
1) Thickness contours shown only where perforation is anticipated.
2) Blocked area shows main region of experimentation.

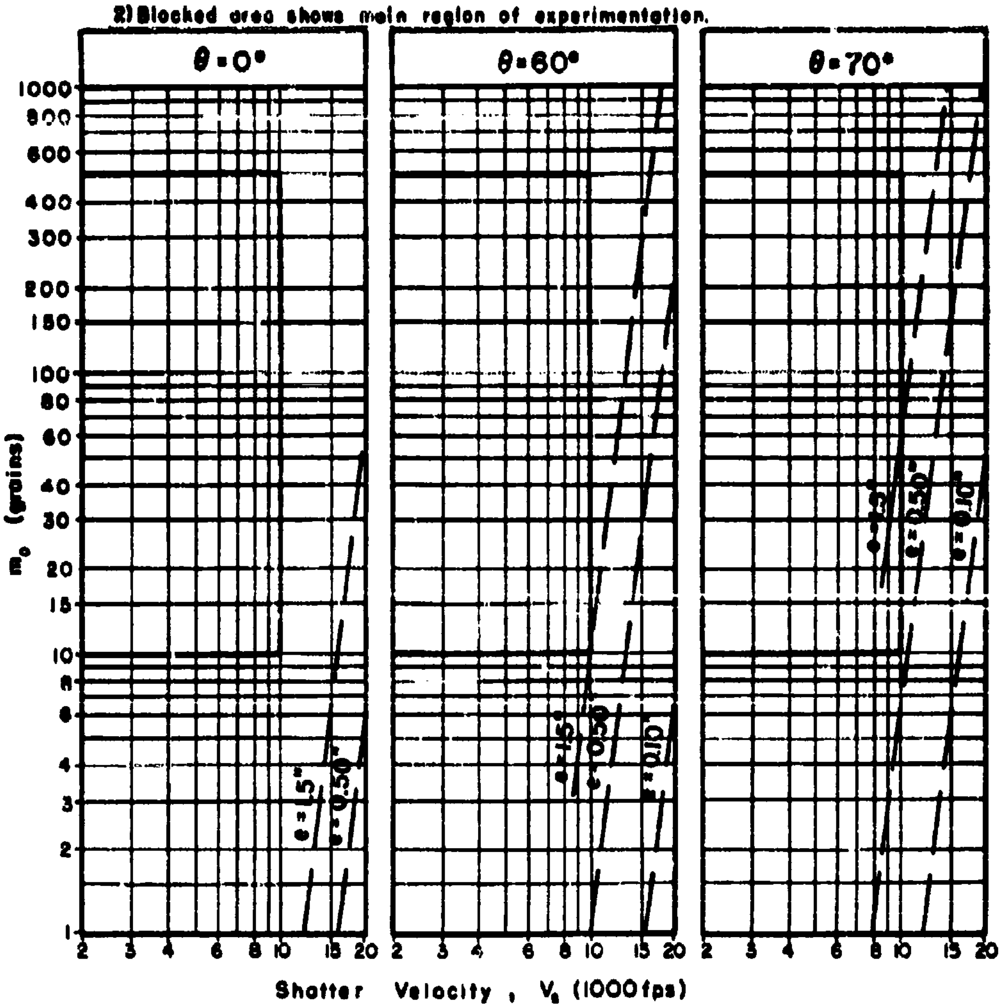

Fig. 154

Impact Conditions For Fragment Shatter

Target Material: Plexiglas, as Cast
Shatter Criterion: $c' = m_r/m_s$ = 0 ----- Extrapolated

Notes:
1) Thickness contours shown only where perforation is anticipated.
2) Blocked area shows main region of experimentation.

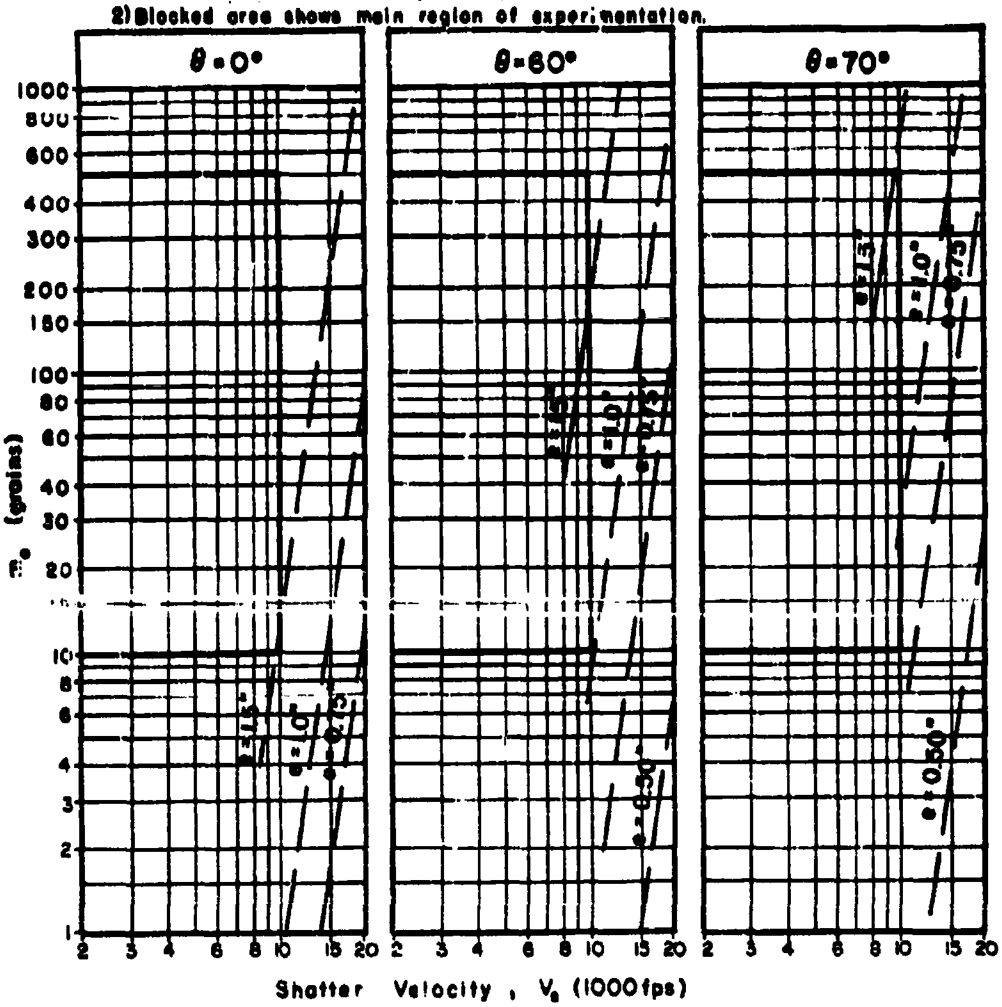

Fig.155

Impact Conditions For Fragment Shatter

Target Material: Stretched Plexiglas
Shatter Criterion: $c' = m_r/m_s$ = 0 ----- Extrapolated

Notes:
1) Thickness contours shown only where perforation is anticipated.
2) Blocked area shows main region of experimentation.

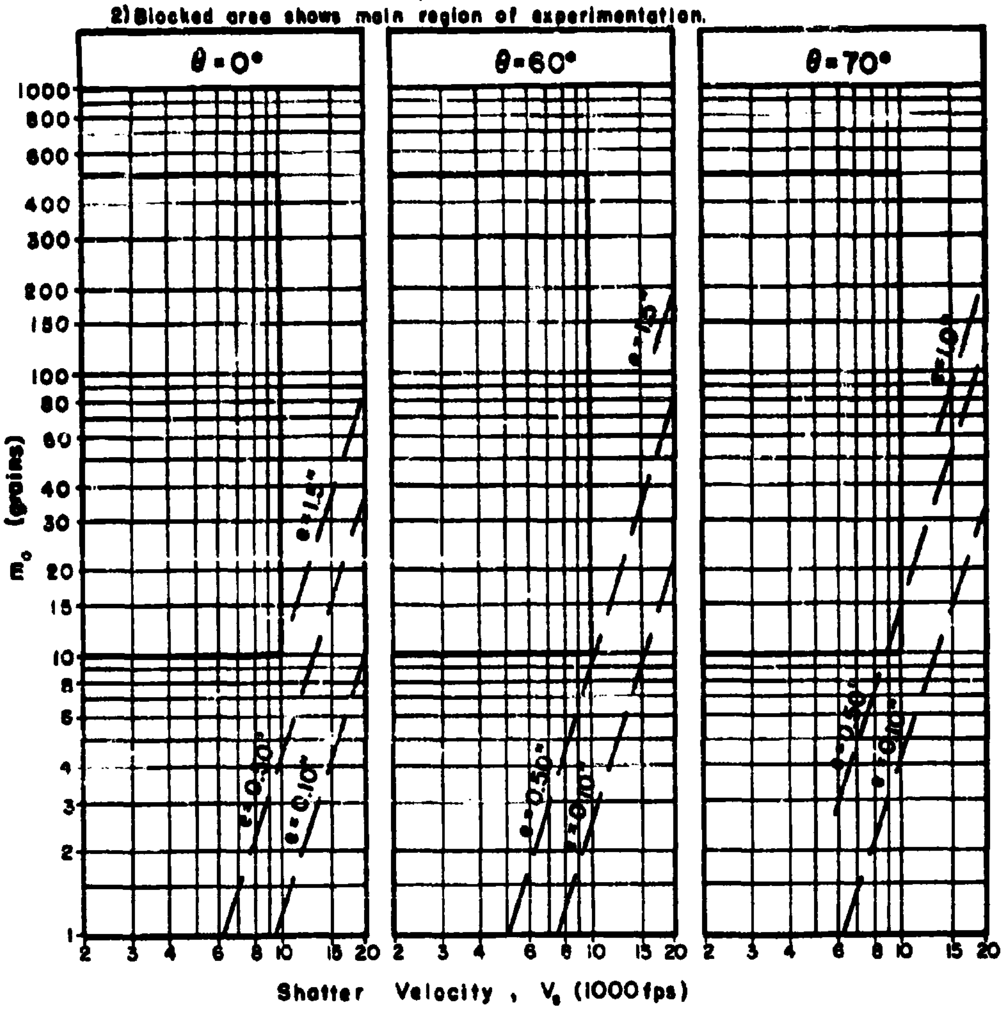

Fig. 156

Impact Conditions For Fragment Shatter

Target Material: Doron
Shatter Criterion: $c' = m_r/m_e = 0$ ----- Extrapolated

Notes:
1) Thickness contours shown only where perforation is anticipated.
2) Blocked area shows main region of experimentation.

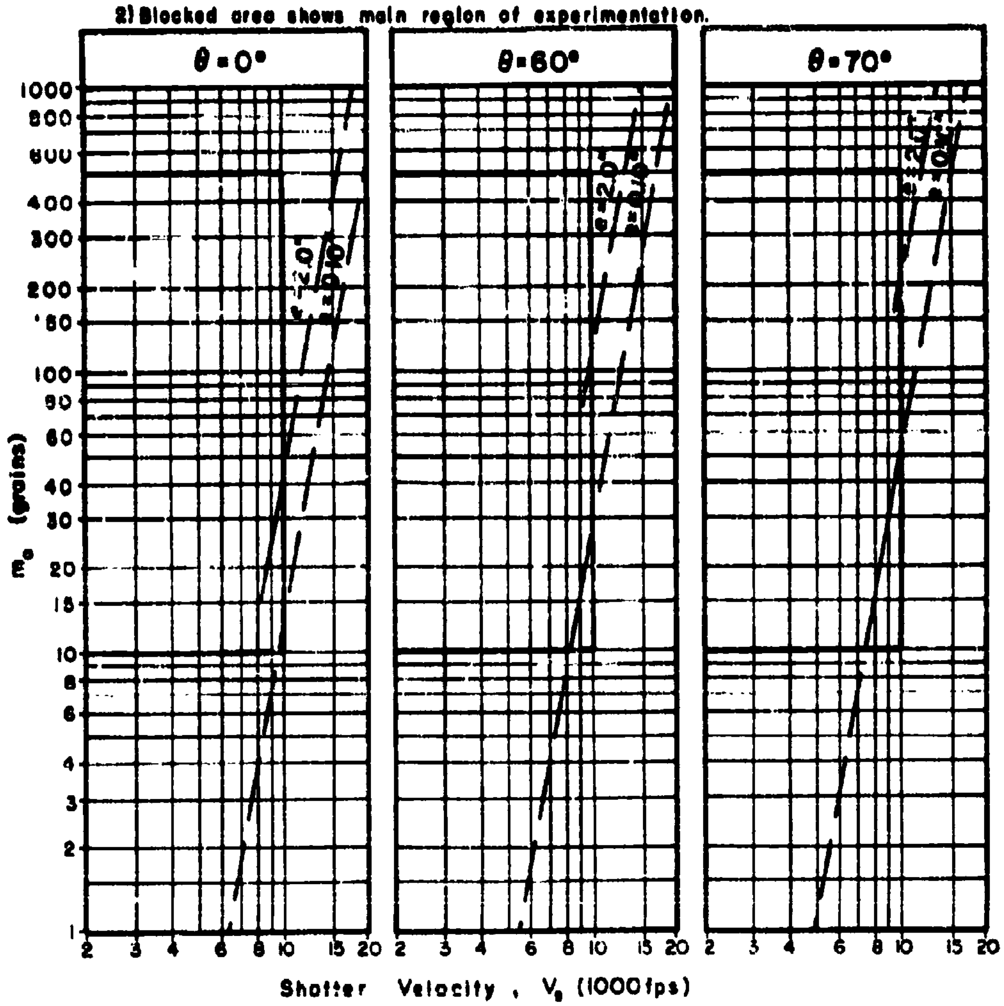

Fig. 157

Impact Conditions For Fragment Shatter

Target Material: Bullet-Resistant Glass
Shatter Criterion: $c' = m_r/m_e$ = 0 ----- Extrapolated

Notes:
1) Thickness contours shown only where perforation is anticipated.
2) Blocked area shows main region of experimentation.

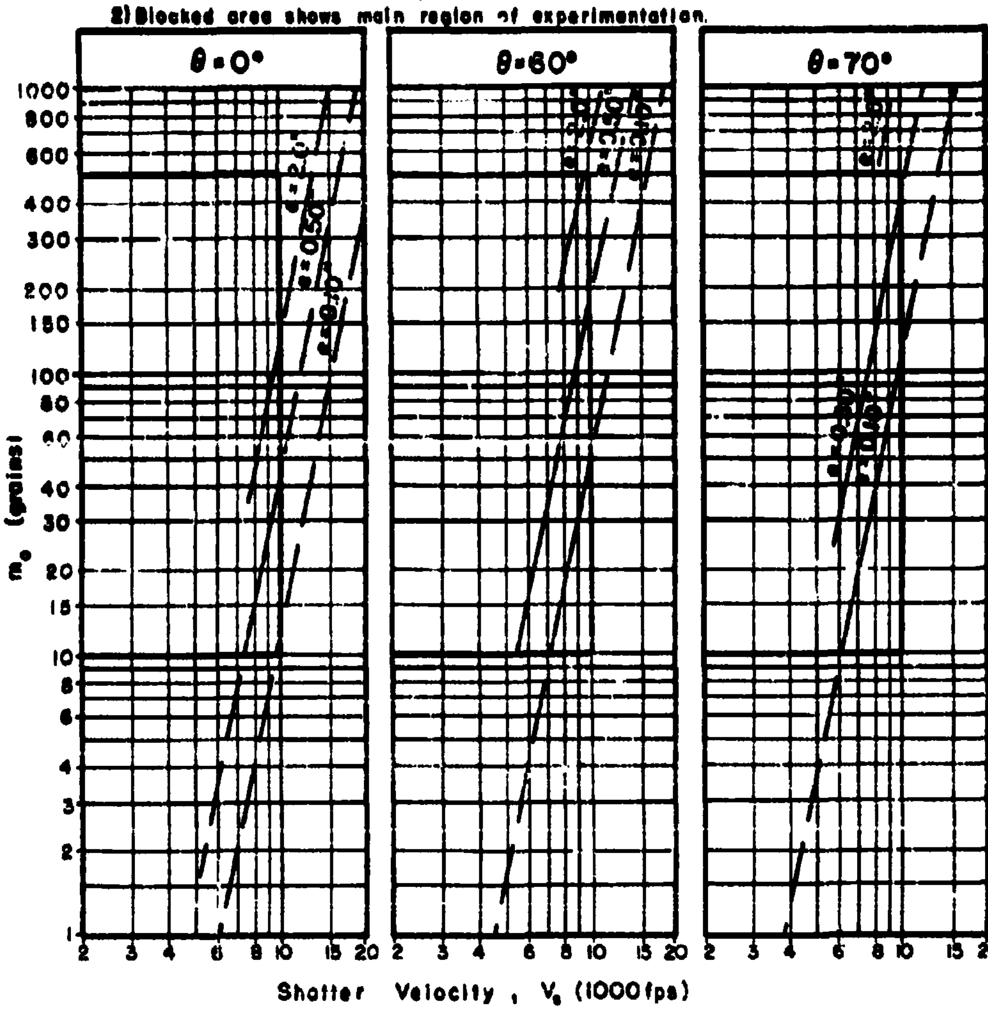

Fig. 158

Appendix H

Photographs of Targets After Impact

Figs. 159 - 176

TABLE XII

Impact Conditions Corresponding to Photographs

Figure No.	Target Material	BRL Rd. No.	e (inches)	m_s (grains)	θ (degrees)	V_s (fps)	V_r (fps)	m_r (grains)	Hole Size (in^2)
159-160	Nylon	13	0.34	5	60	8000	3855	4.5	—
161-162	Lexan	10	1.0	240	70	5257	2619	—	—
163-164	Lexan	22	1.0	30	0	8947	5442	25.5	0.08
165-166	Stretched Plexiglas	128	0.93	5	0	5300	1010	4.9	—
167-168	Stretched Plexiglas	129	0.93	5	0	5196	2094	4.9	—
169-170	Stretched Plexiglas	130	0.908	60	70	7950	1708	0.4	—
171-172	Doron	110	0.27	240	70	4125	—	—	—
173-174	Bullet-Resistant Glass	107	0.5	60	70	8740	3566	—	0.196
175-176	Bullet-Resistant Glass	110	1.6	240	60	3575	—	—	3.19

Nylon

Fig. 159

Nylon

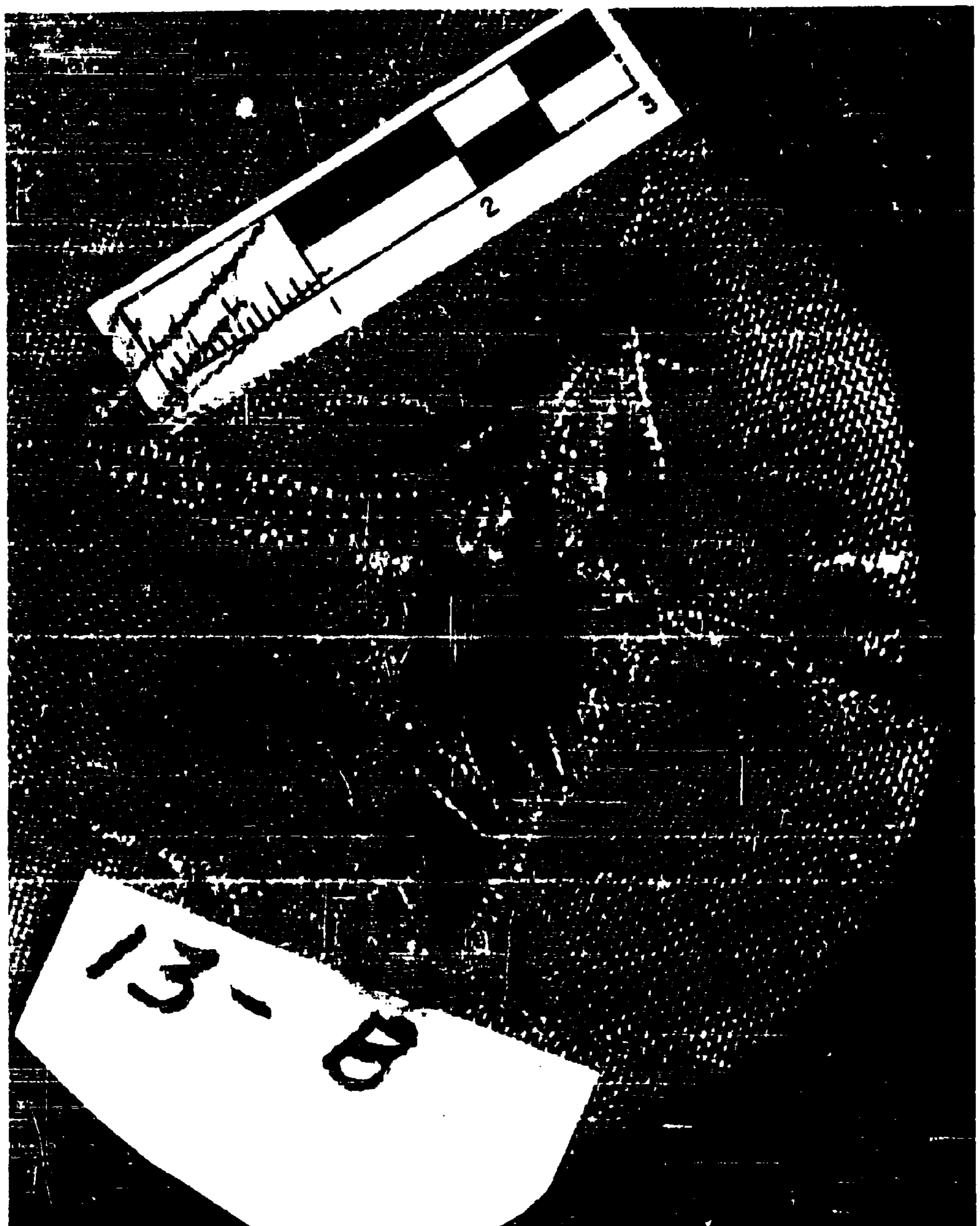

Fig. 160

Lexan

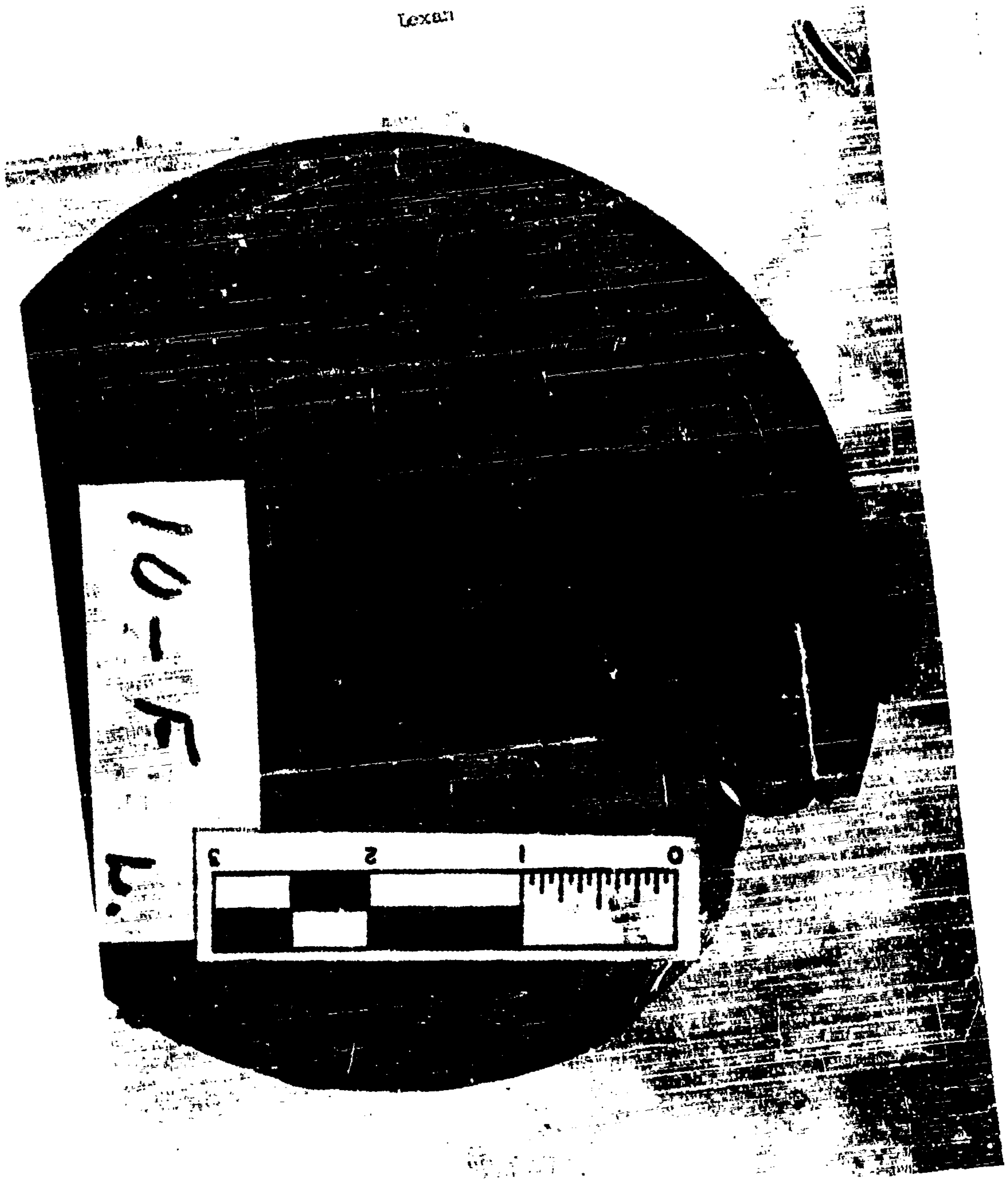

Fig. 161

Lexan

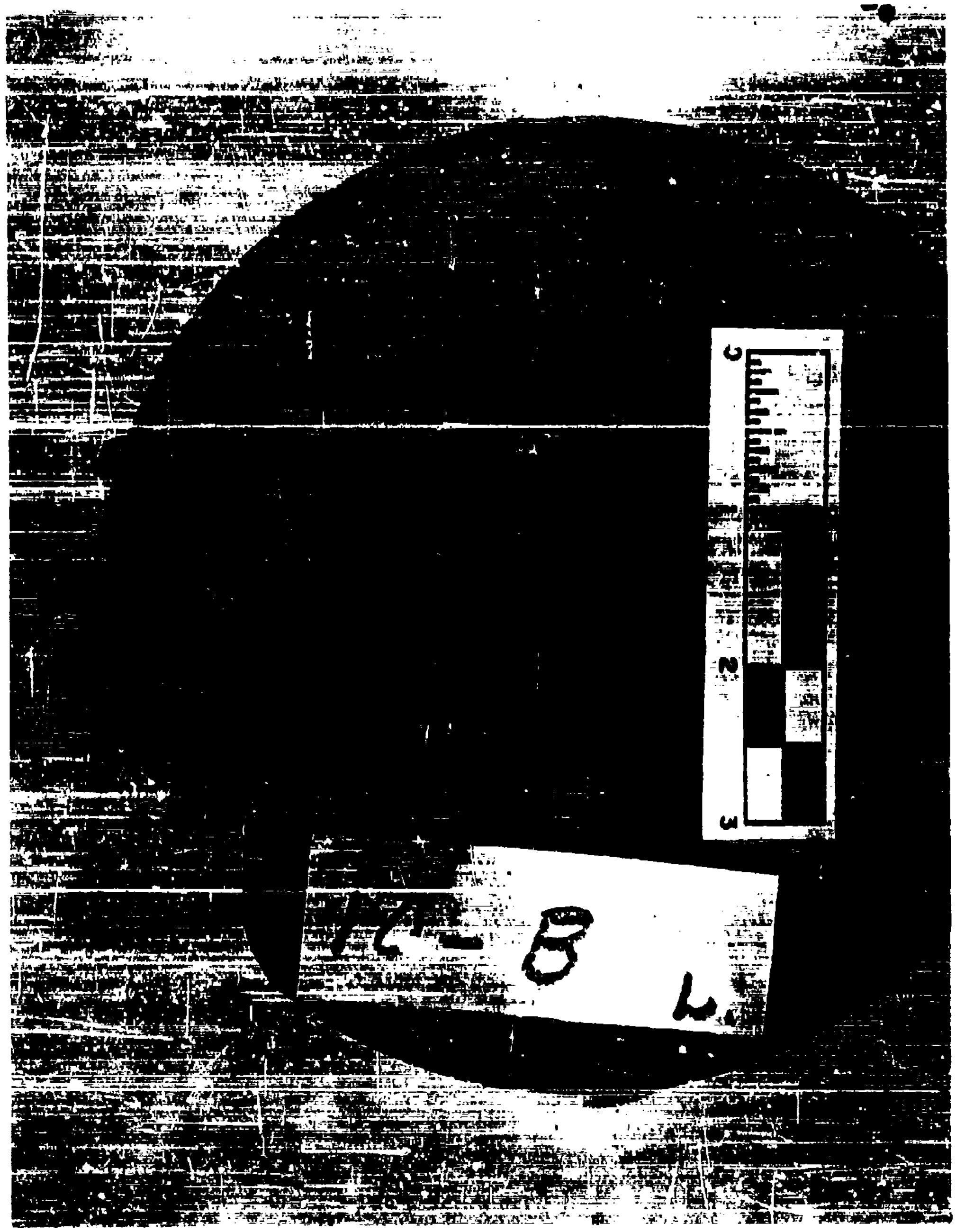

Fig. 162

Lexan

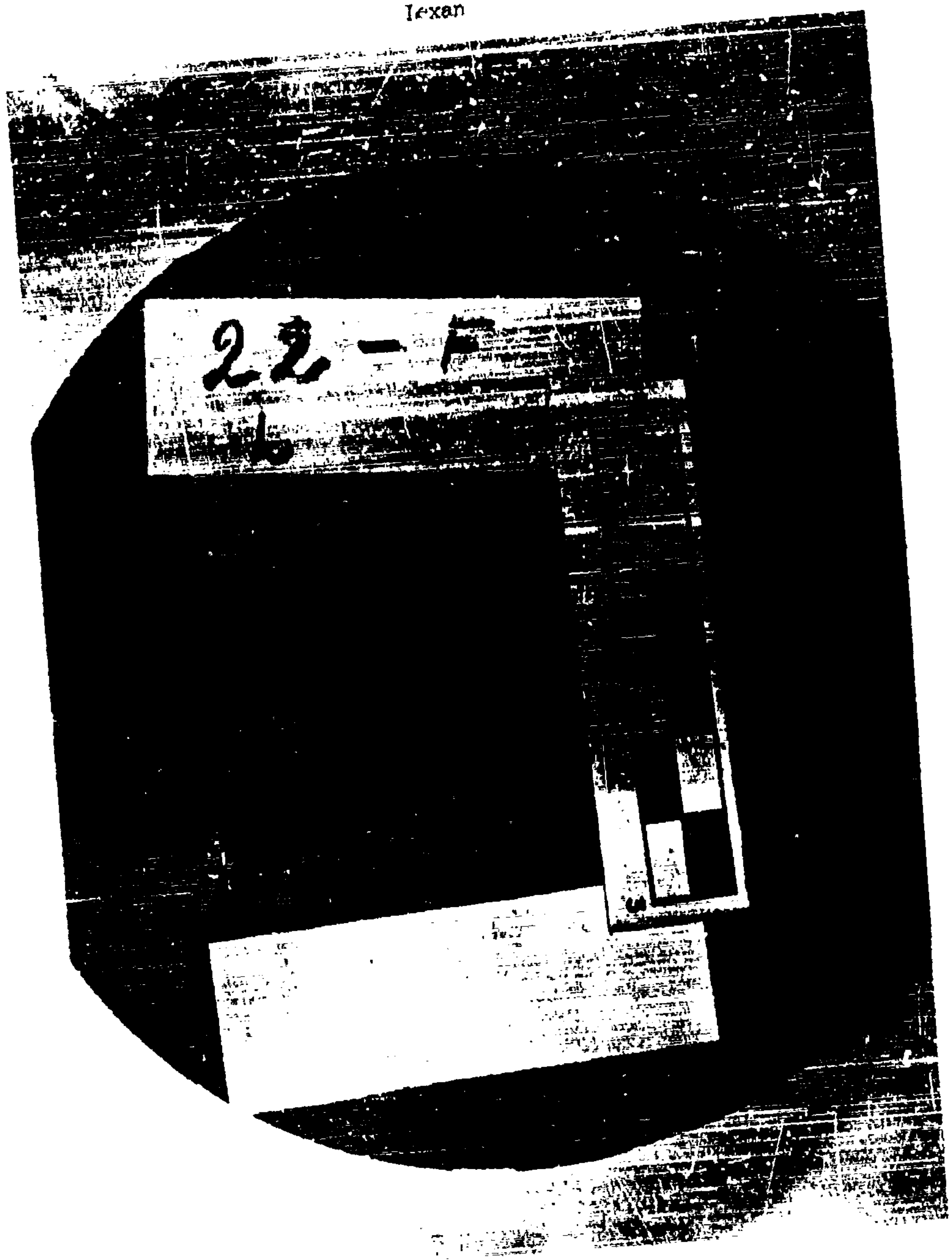

Fig. 163

Lexan

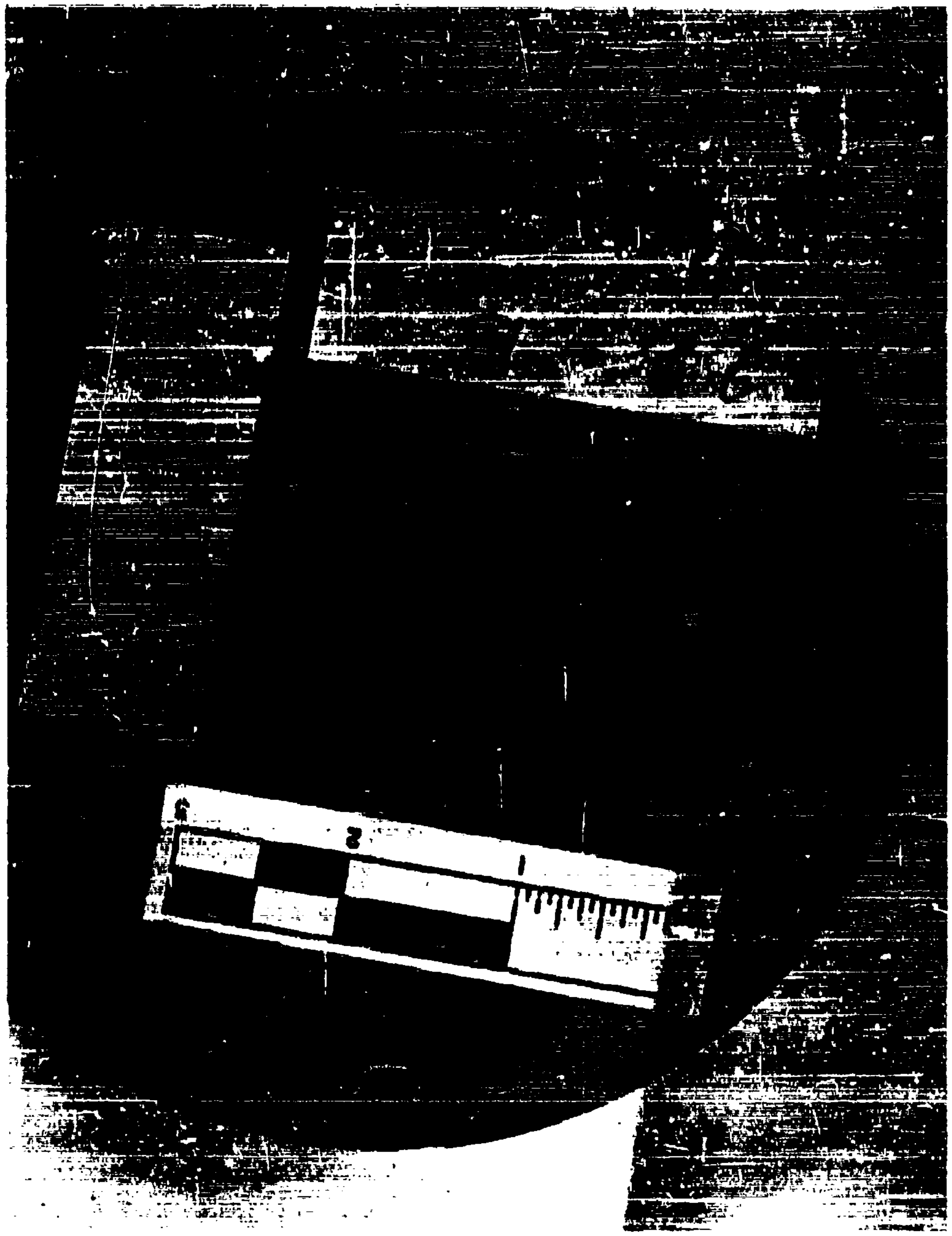

Fig. 104

Stretched Plexiglas

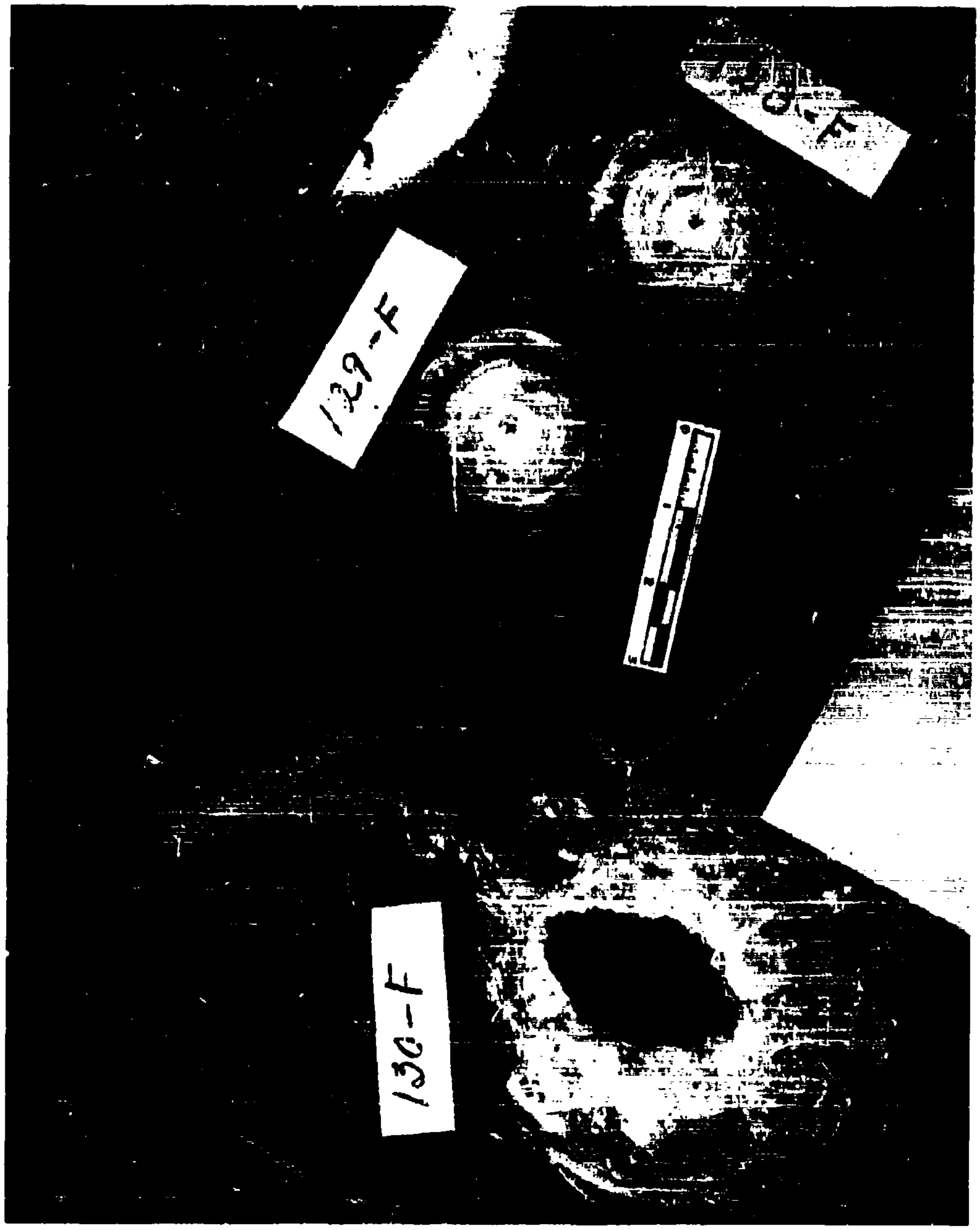

Figs. 165, 166, 167

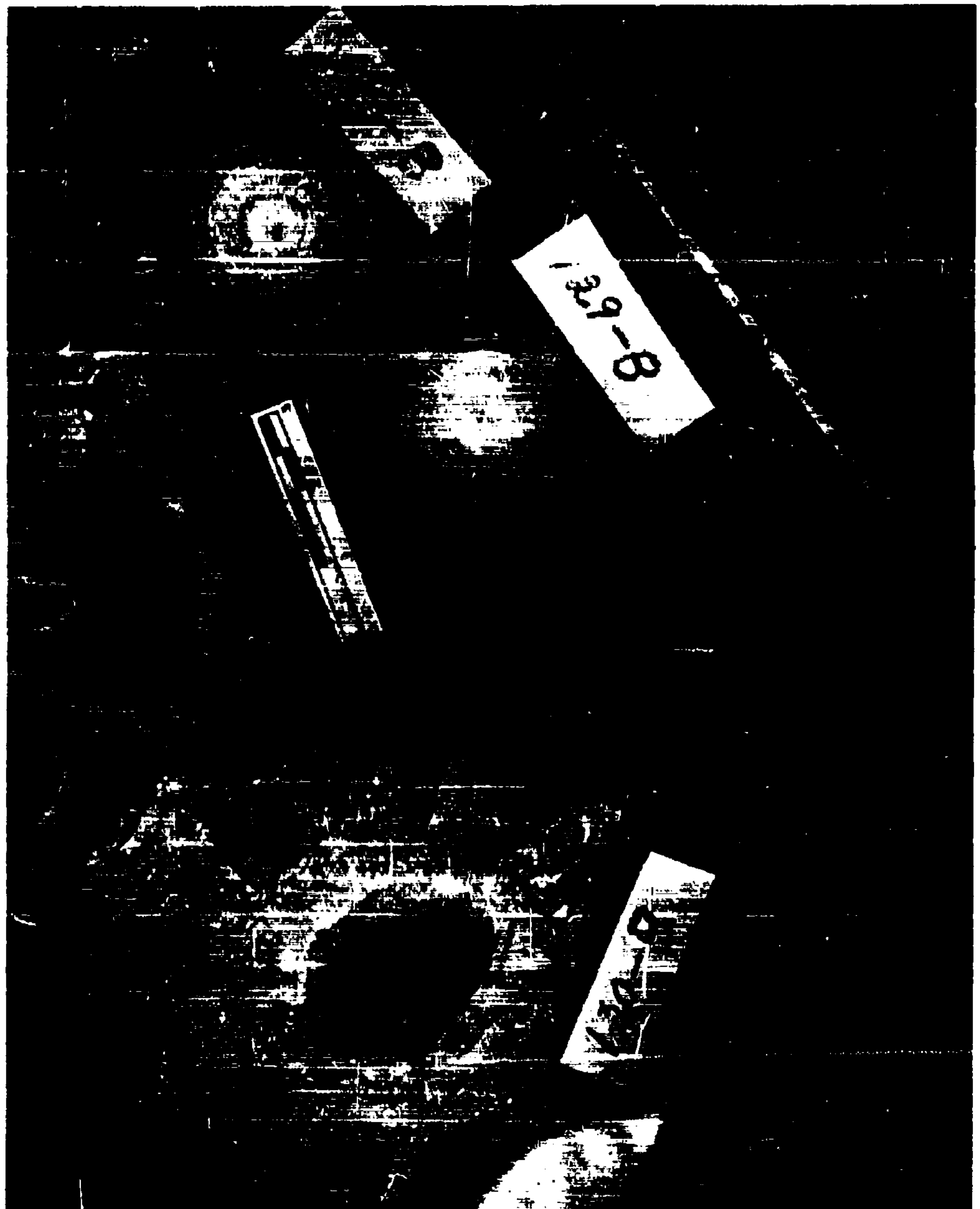

Figs. 168, 169, 170

Fig. 171

Fig. 172

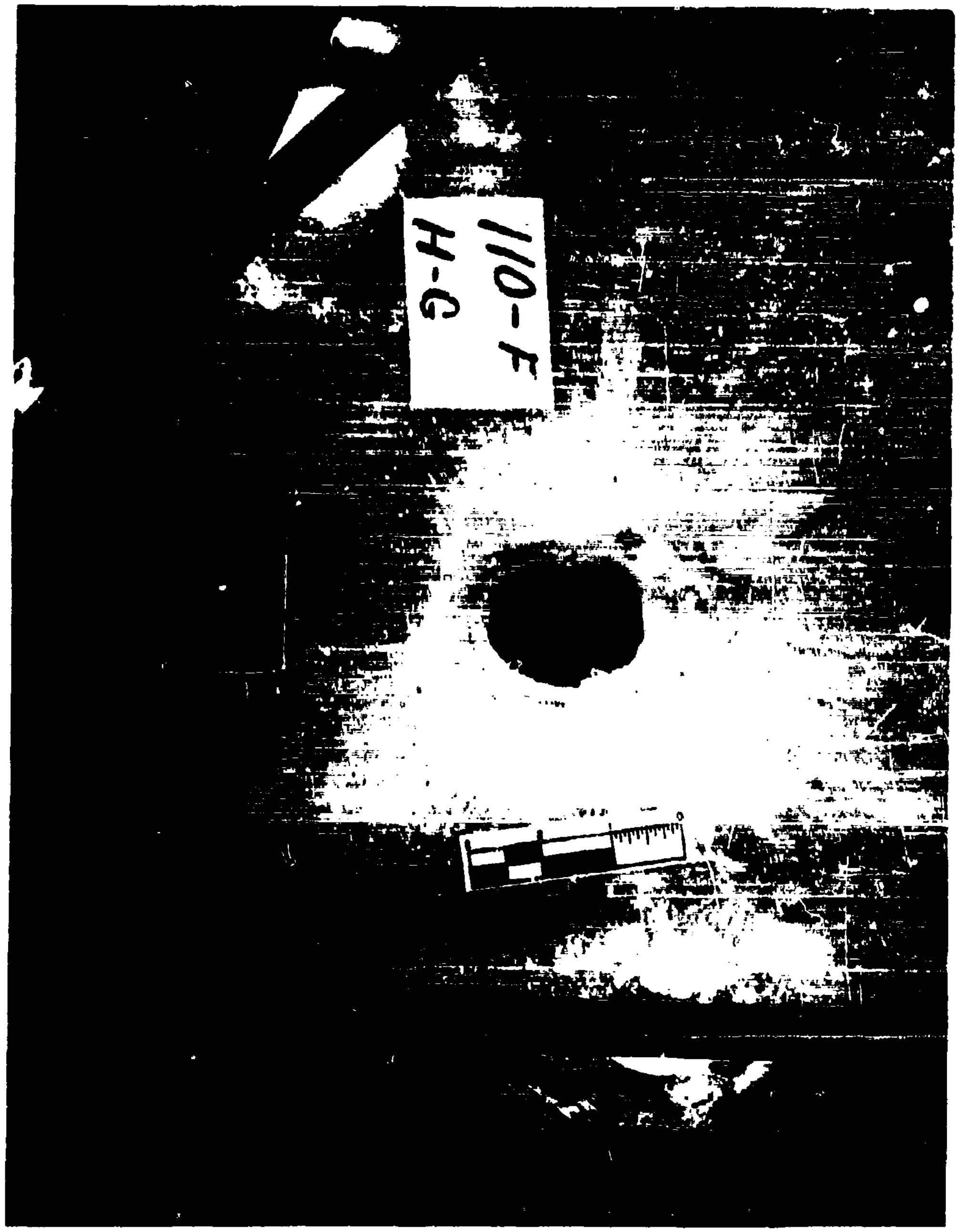

Fig. 173

Fig. 174

CONFIDENTIAL

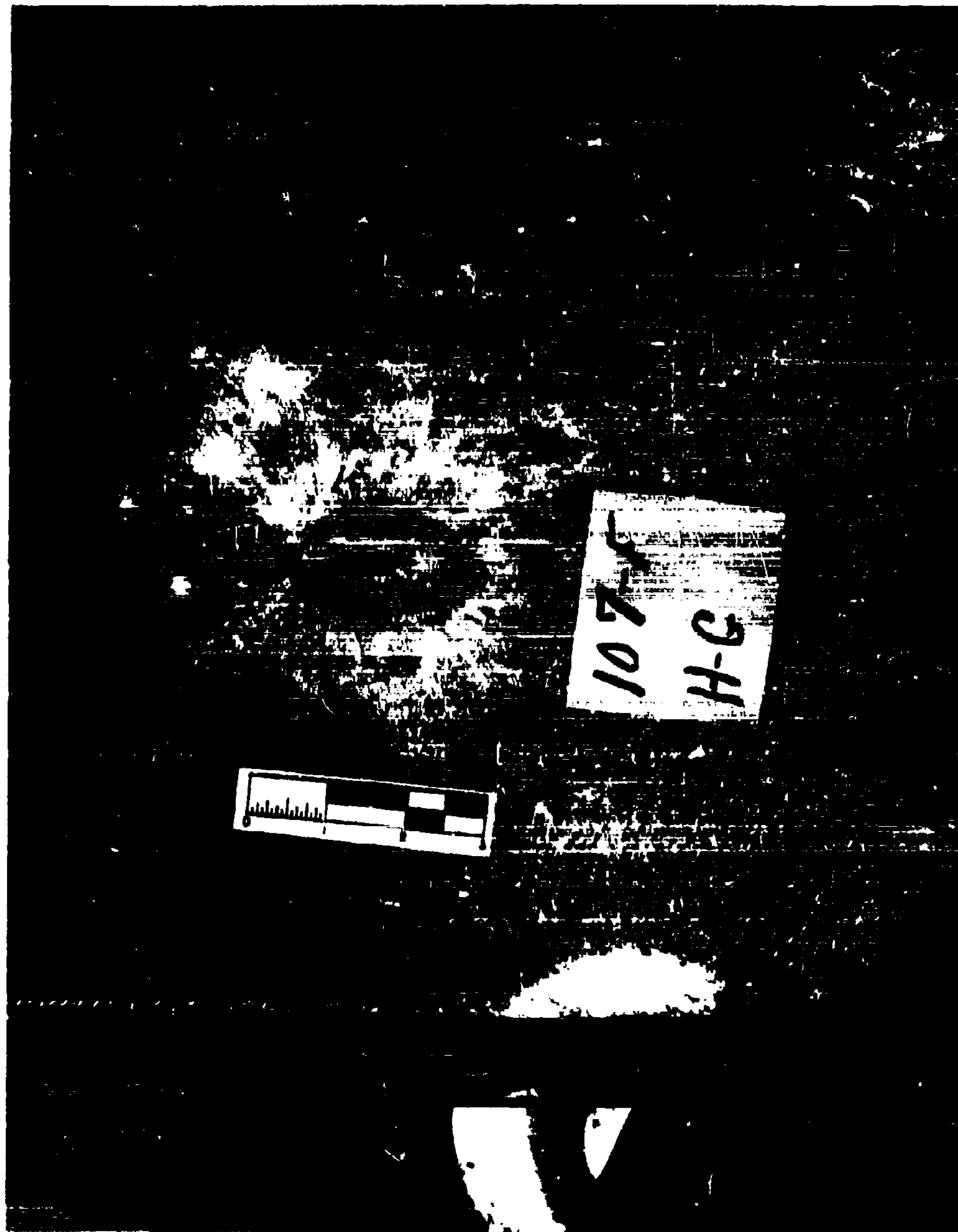

Fig. 175

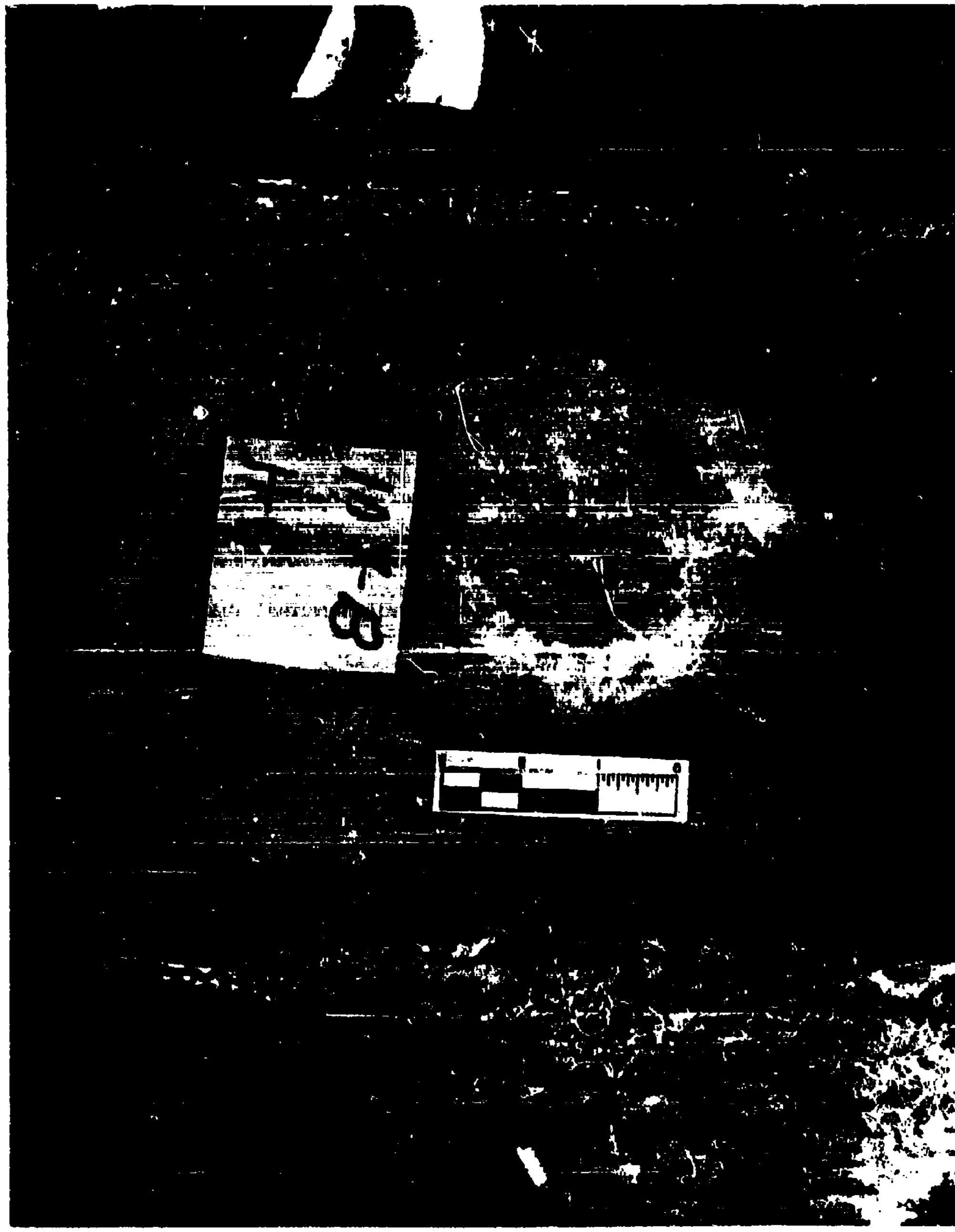

Fig. 176

Appendix I

Experimental Data; Steel Fragments

Impacting on Various Target Materials

Tables XIII-XIX

EXPERIMENTAL DATA

Table XIII : Steel Fragments Impacting on Unbonded Nylon

Datum No.	Material Thickness e(inches)	Fragment Weight m_s(grains)	Obliquity θ(degrees)	Striking Velocity V_s(fps)	Residual Velocity V_r(fps)	Residual Weight m_r(grains)	Hole Area (sq. in.)
1	.02	.85	0	325	0	-	-
2	.02	.85	0	553	428	-	-
3	.02	.85	0	682	498	-	-
4	.02	2.10	0	550	0	-	-
5	.02	2.10	0	1025	900	-	-
6	.02	2.10	0	1235	1132	-	-
7	.02	16.09	0	559	294	-	-
8	.02	16.09	0	700	485	-	-
9	.02	16.09	0	818	757	-	-
10	.02	16.09	0	917	814	-	-
11	.02	16.09	0	1002	914	-	-
12	.025	17.00	0	518	0	-	-
13	.050	.85	0	550	0	-	-
14	.050	16.09	0	690	0	-	-
15	.050	16.09	0	821	578	-	-
16	.050	16.09	0	1008	863	-	-
17	.070	.85	0	750	0	-	-
18	.070	.85	0	1027	622	-	-
19	.070	.85	0	1598	1279	-	-
20	.070	.85	0	2067	[illegible]	-	-
21	.070	.85	0	3000	2816	-	-
22	.070	.85	0	3474	3335	-	-
23	.070	2.10	0	765	0	-	-
24	.070	2.10	0	1263	816	-	-
25	.070	2.10	0	2406	2213	-	-
26	.070	2.10	0	2712	2467	-	-
27	.070	16.09	0	700	0	-	-
28	.070	16.09	0	902	628	-	-
29	.070	16.09	0	1209	1070	-	-
30	.070	16.09	0	1588	1507	-	-
31	.074	17.00	0	654	0	-	-
32	.100	.85	0	800	0	-	-
33	.100	16.09	0	800	0	-	-
34	.100	16.09	0	1003	814	-	-
35	.100	16.09	0	1207	1023	-	-
36	.100	16.09	0	1506	1381	-	-
37	.120	2.65	30	992	0	-	-
38	.120	2.65	60	1038	0	-	-
39	.120	16.00	0	800	0	-	-
40	.120	16.00	0	1145	692	-	-
41	.120	16.00	0	2111	1558	-	-
42	.120	16.09	0	838	0	-	-
43	.120	16.09	0	1013	668	-	-
44	.120	16.09	0	1246	1023	-	-
45	.120	16.09	0	1434	1233	-	-
46	.130	1.35	0	1191	0	-	-
47	.130	1.35	30	1239	0	-	-
48	.130	1.35	45	1355	0	-	-
49	.130	1.35	60	1398	0	-	-
50	.130	2.65	0	1030	0	-	-

EXPERIMENTAL DATA

Table XIII : Steel Fragments Impacting on Unbonded Nylon

Datum No.	Material Thickness e(inches)	Fragment Weight m_s(grains)	Obliquity θ(degrees)	Striking Velocity V_s(fps)	Residual Velocity V_r(fps)	Residual Weight m_r(grains)	Hole Area (sq. in.)
51	.130	2.65	45	990	0	-	-
52	.148	17.00	0	958	0	-	-
53	.150	.85	0	1050	0	-	-
54	.150	.85	0	2012	1488	-	-
55	.150	.85	0	3381	2914	-	-
56	.150	.85	0	4325	3891	-	-
57	.150	.85	0	5004	4513	-	-
58	.150	2.10	0	1065	0	-	-
59	.150	2.10	0	1298	749	-	-
60	.150	2.10	0	2321	1876	-	-
61	.150	2.10	0	2993	2603	-	-
62	.150	2.10	0	3394	2895	-	-
63	.150	16.09	0	900	0	-	-
64	.150	16.09	0	1142	831	-	-
65	.150	16.09	0	1716	1335	-	-
66	.150	16.09	0	1852	1698	-	-
67	.150	16.09	0	1955	1816	-	-
68	.200	16.09	0	950	0	-	-
69	.200	16.09	0	1158	583	-	-
70	.200	16.09	0	1425	979	-	-
71	.210	147.00	30	902	0	146.0	-
72	.218	5.85	30	1189	0	-	-
73	.218	5.85	45	1202	0	-	-
74	.218	5.83	60	1297	0	-	-
75	.218	17.00	30	1046	0	-	-
76	.218	17.00	45	1103	0	-	-
77	.218	17.00	60	1073	0	-	-
78	.218	44.00	30	993	0	-	-
79	.220	2.10	0	1400	0	-	-
80	.220	2.10	0	1812	991	-	-
81	.220	2.10	0	2792	1979	-	-
82	.220	2.10	0	3166	2561	-	-
83	.220	2.10	0	[illegible]	[illegible]		
84	.229	5.85	45	1255	0	-	-
85	.229	44.00	45	996	0	-	-
86	.229	44.00	45	1012	0	-	-
87	.248	5.00	70	5440	3574	4.9	-
88	.248	30.00	70	5965	4444	29.9	-
89	.248	30.00	70	7279	5693	17.6	-
90	.248	30.00	70	9800	7197	18.7	-
91	.249	15.00	0	9075	8128	13.0	-
92	.249	15.00	0	9727	-	12.0	-
93	.249	60.00	0	8731	7974	47.0	-
94	.250	.85	0	1960	0	-	-
95	.250	.85	0	2253	1008	-	-
96	.250	.85	0	2830	1906	-	-
97	.230	.85	0	3197	2373	-	-
98	.250	.85	0	4112	3368	-	-
99	.250	.85	0	4843	4089	-	-
100	.250	.85	0	5295	4506	-	-

EXPERIMENTAL DATA

Table XIII : Steel Fragments Impacting on Unbonded Nylon

Datum No.	Material Thickness e(inches)	Fragment Weight m_s (grains)	Obliquity (degrees)	Striking Velocity V_s (fps)	Residual Velocity V_r (fps)	Residual Weight m_r (grains)	Hole Area (sq. in.)
[illegible]	.250	[illegible]	0	1897	0	-	-
[illegible]	[illegible]	[illegible]	0	2108	1035	-	-
[illegible]	.250	2.10	0	2697	1392	-	-
104	.250	2.10	0	2936	2051	-	-
105	.250	2.10	0	3772	2532	-	-
106	.250	2.10	0	4267	2812	-	-
107	.250	2.10	0	4778	3286	-	-
108	.250	2.10	0	5307	3670	-	-
109	.266	5.85	0	1270	0	-	-
110	.266	17.00	0	1230	0	-	-
111	.266	44.00	0	1062	0	-	-
112	.266	147.00	0	950	0	146.0	-
113	.266	207 00	0	935	0	206.0	-
114	.280	2.65	0	1530	0	-	-
115	.280	2.65	45	1718	0	-	-
116	.280	2.65	60	1680	0	-	-
117	.290	2 65	30	1624	0	-	-
118	.290	5.85	30	1320	0	-	-
119	.290	5.85	45	1338	0	-	-
120	.290	5.85	60	1450	0	-	-
121	.290	7.00	30	1169	0	-	-
122	.290	17.00	45	1254	0	-	-
123	.290	17.00	60	1303	0	-	-
124	.290	44.00	30	1082	0	-	-
125	.298	30.00	0	1052	0	29.9	-
126	.298	240.00	0	900	0	239.0	-
127	.300	.85	0	1714	0	-	-
128	.300	.85	0	2074	1053	-	-
129	.300	.85	0	2573	1623	-	-
130	.300	.83	0	2993	2244	-	-
131	.300	.85	0	3529	2690	-	-
132	.300	.85	0	3867	3156	-	-
133	.300	.85	0	4238	3480	-	-
134	.300	.85	45	1691	0	-	-
135	.300	.85	45	1853	601	-	-
136	.300	.85	45	2222	1123	-	-
137	.300	.85	45	3608	2570	-	-
138	.300	.85	45	5078	4123	-	-
139	.300	.85	45	5424	4438	-	-
140	.300	.85	60	2232	0	-	-
141	.300	.85	60	2479	1027	-	-
142	.300	.85	60	2520	1054	-	-
143	.300	.85	60	2646	1418	-	-
144	.300	.85	60	2886	1299	-	-
145	.300	.85	60	3609	2334	-	-
146	.300	.85	60	3734	2306	-	-
147	.300	.85	60	4064	2679	-	-
148	.300	.85	60	4190	2508	-	-
149	.300	.85	60	4578	2814	-	-
150	.300	.83	60	4917	3229	-	-

CONFIDENTIAL

EXPERIMENTAL DATA

Table XIII : Steel Fragments Impacting on Unbonded Nylon

Datum No.	Material Thickness e(inches)	Fragment Weight m_s(grains)	Obliquity θ(degrees)	Striking Velocity V_s(fps)	Residual Velocity V_r(fps)	Residual Weight m_r(grains)	Hole Area (sq. in.)
151	.300	0.85	60	3096	3138	-	-
152	.300	1.35	0	2012	0	-	-
153	.300	1.35	30	2031	0	-	-
154	.300	1.35	45	2051	0	-	-
155	.300	1.35	60	2098	0	-	-
156	.300	2.01	0	1563	0	-	-
157	.300	2.01	0	1983	1144	-	-
158	.300	2.01	0	2231	1528	-	-
159	.300	2.01	0	3327	[illegible]	-	-
160	.300	2.01	0	3875	[illegible]	-	-
161	.300	2.01	0	4428	[illegible]	-	-
162	.300	2.01	0	5429	4752	-	-
163	.300	2.01	0	3764	3098	-	-
164	.300	2.01	0	6022	[illegible]	-	-
165	.300	2.10	0	1603	0	-	
166	.300	2.10	0	2315	1242	-	-
167	.300	2.10	0	2969	2080	-	-
168	.300	2.10	0	3834	2882	-	-
169	.300	2.10	0	4329	3597	-	-
170	.300	2.10	0	5086	1219	-	-
171	.300	16.00	0	900	0	-	-
172	.300	16.00	0	1396	679	-	-
173	.300	16.00	0	2397	1967	-	-
174	.300	16.00	0	3372	2862	-	-
175	.300	16.00	0	4898	4163	-	-
176	.300	16.09	0	1150	0	-	-
177	.300	16.09	0	[illegible]	619	-	-
178	.300	16.09	0	2543	2293	-	-
179	.300	16.09	0	4142	3796	-	-
180	.300	54.20	0	990	0	-	-
181	.300	225.00	0	550	0	-	-
182	.300	225.00	0	964	650	-	-
183	.300	225.00	0	1168	1008	-	-
184	.306	44.00	45	1113	0	-	-
185	.306	44.00	45	1128	0	-	-
186	.306	44.00	60	1137	0	-	-
187	.363	5.85	0	1435	0	-	-
188	.363	5.85	30	1482	0	-	-
189	.363	5.83	45	1482	0	-	-
190	.363	5.85	60	1654	0	-	-
191	.363	17.00	0	1340	0	-	-
192	.363	17.00	30	1322	0	-	-
193	.363	17.00	45	1399	0	-	-
194	.363	17.00	60	1413	0	-	-
195	.363	44.00	0	1152	0	-	-
196	.363	207.00	0	956	0	206.0	-
197	.382	44.00	30	1188	0	-	-
198	.382	44.00	30	1197	0	-	-
199	.382	44.00	45	1197	0	-	-
200	.382	44.00	45	1202	0	-	-

CONFIDENTIAL

[illegible]RIMEN[illegible] DATA

Table XIII [illegible]: Steel Fragments Impacting on Unbonded Nylon

Round No.	Material Thickness (inches)	Fragment Weight m_s (grains)	Obliquity θ (degrees)	Striking Velocity V_s (fps)	Residual Velocity V_r (fps)	Residual Weight m_r (grains)	Hole Area (sq. in.)
[illegible]	.342	[illegible].00	60	[illegible]	0	-	-
[illegible]	.430	4.[illegible]65	45	22[illegible]3	0	-	-
[illegible]	.460	1.[illegible]35	60	3117	[illegible]	-	-
[illegible]	.460	2.[illegible]35	0	2130	0	-	-
[illegible]	.470	2.[illegible]35	30	2049	0	-	-
[illegible]	.470	2.[illegible]35	60	2373	0	-	-
[illegible]	.480	1.[illegible]	0	2772	0	-	-
208	.480	[illegible]	30	3476	0	-	-
209	.480	3.3[illegible]	45	2174	[illegible]	-	-
[illegible]	.532	3.8[illegible]	0	1775	0	-	-
[illegible]	.532	[illegible].5[illegible]	30	1778	0	-	-
[illegible]	.532	[illegible].8[illegible]	45	[illegible]810	0	-	-
[illegible]	.532	5.8[illegible]	60	[illegible]	0	-	[illegible]
[illegible]	.532	17.[illegible]	0	[illegible]	0	-	-
[illegible]	.532	17.0[illegible]	30	[illegible]	[illegible]	[illegible]	-
216	.532	17.[illegible]	45	[illegible]	[illegible]	-	-
217	.532	1[illegible].0[illegible]	60	[illegible]	[illegible]	-	-
218	.532	44.[illegible]	0	[illegible]	[illegible]	-	-
219	.532	147.0[illegible]	0	[illegible]	[illegible]	146.0	[illegible]
220	.532	20[illegible]	0	[illegible]	[illegible]	206.0	-
221	.561	44.[illegible]0	30	[illegible]	[illegible]	-	-
222	.561	44.[illegible]0	30	[illegible]	[illegible]	-	-
223	.561	44.[illegible]	[illegible]	[illegible]	[illegible]	-	-
224	.561	[illegible].00	45	[illegible]	[illegible]	-	-
225	.561	[illegible].00	60	[illegible]	[illegible]	-	-
226	.600	[illegible].65	60	[illegible]	[illegible]	-	-
227	.620	[illegible].35	45	[illegible]	[illegible]	-	-
228	.6[illegible]	[illegible].65	45	[illegible]	[illegible]	-	[illegible]
229	[illegible]	[illegible].85	0	[illegible]	[illegible]	-	-
230	.6[illegible]	[illegible].00	0	[illegible]	[illegible]	-	-
[illegible]	[illegible]	[illegible].00	30	[illegible]	[illegible]	-	-
[illegible]	[illegible]	[illegible].00	45	[illegible]	[illegible]	-	-
[illegible]	.677	7.0[illegible]	60	[illegible]	[illegible]	-	-
[illegible]	.680	1.35	0	[illegible]	[illegible]	-	-
[illegible]	.680	1.35	30	[illegible]	[illegible]	-	-
[illegible]	.680	1.35	[illegible]	[illegible]	0	-	-
[illegible]	.700	2.[illegible]	0	[illegible]	0	-	-
[illegible]	.700	2.5[illegible]	30	[illegible]	0	-	-
[illegible]	.713	5.[illegible]	30	[illegible]	0	[illegible]	-
[illegible]	.713	5.[illegible]	30	[illegible]	0	[illegible]	-
[illegible]	.713	5.3[illegible]	45	[illegible]	0	-	-
[illegible]	[illegible]	17.00	30	[illegible]	0	-	-
[illegible]	.798	5.[illegible]	0	[illegible]	[illegible]	-	-
[illegible]	.798	17.[illegible]	0	[illegible]	[illegible]	-	-
245	.798	17.[illegible]	45	[illegible]	[illegible]	-	-
246	.798	17.[illegible]	60	[illegible]	0	[illegible]	[illegible]
247	.798	44.[illegible]	0	[illegible]	0	-	-
248	.798	[illegible].50	[illegible]	[illegible]	0	-	-
249	.820	[illegible]4.00	[illegible]	[illegible]	[illegible]	-	-
250	.840	5.[illegible]	[illegible]	[illegible]	0	[illegible]	-

EXPERIMENTAL DATA

Table XIII : Steel Fragments Impacting on Unbonded Nylon

Datum No.	Material Thickness e(inches)	Fragment Weight m_s(grains)	Obliquity θ(degrees)	Striking Velocity V_s(fps)	Residual Velocity V_r(fps)	Residual Weight m_r(grains)	Hole Area (sq. in.)
251	.840	5.85	45	2410	0	-	-
252	.840	44.00	30	1642	0	-	-
253	.840	44.00	30	1663	0	-	-
254	.84	44.00	45	1679	0	-	-
255	.944	17.00	0	2070	0	-	-
256	.944	17.00	30	2116	0	-	-
257	.944	17.00	45	2240	0	-	-
258	.944	17.00	60	2336	0	-	-
259	.944	5.85	30	2479	0	-	-
260	.944	5.85	45	2727	0	-	-
261	.944	44.00	30	[illegible]788	0	-	-
262	.944	44.00	30	1822	0	-	-
263	.944	44.00	45	1857	0	-	-
264	1.089	5.85	0	2615	0	-	-
265	1.089	17.00	0	2232	0	-	-
266	1.089	17.00	30	2229	0	-	-
267	1.089	17.00	45	2351	0	-	-
268	1.089	17.00	60	2694	0	-	-
269	1.089	44.00	0	1906	0	-	-
270	1.089	147.00	0	1532	0	[illegible]	-
271	1.089	207.00	0	[illegible]	0	[illegible]	-
272	1.145	5.85	30	2641	0	-	-
273	1.244	5.00	0	5370	3111	4.9	-
274	1.244	10.00	60	5070	770	9.9	-
275	1.244	15.00	45	10000	4733	12.0	-
276	1.244	[illegible]	60	10742	3642	8.2	-
277	1.244	15.00	70	10790	2768	12.2	-
278	1.244	30.00	60	8800	2925	18.7	-
279	1.244	30.00	70	9500	1064	14.0	-
280	1.244	60.00	60	9760	4054	48.1	-
281	1.244	60.00	70	8940	-	40.1	-
282	1.244	240.00	70	6020	2511	239.5	-
283	2.488	15.00	30	9115	2314	12.0	-
284	2.488	30.00	0	10000	3855	-	-
285	2.488	30.00	45	10850	1531	19.0	-
286	2.488	60.00	60	9500	0	-	-
287	2.488	60.00	70	11000	0	-	-
288	2.511	15.00	0	9625	3305	14.0	-
289	2.511	60.00	0	[illegible]	5106	49.0	-
290	3.781	15.00	0	7000	0	-	-
291	3.781	60.00	0	5000	0	-	-
292	3.781	240.00	0	2500	0	-	-
293	7.757	240.00	0	7500	0	-	-

EXPERIMENTAL DATA

Table XIV : Steel Fragments Impacting on Bonded Nylon

Datum No.	Material Thickness e (inches)	Fragment Weight m_s (grains)	Obliquity θ (degrees)	Striking Velocity V_s (fps)	Residual Velocity V_r (fps)	Residual Weight m_r (grains)	Hole Area (sq. in.)
1	.23	5.0	60	8900	6337	4.4	-
2	.23	5.0	70	7365	4908	3.8	-
3	.23	15.0	60	8600	7047	9.7	-
4	.23	15.0	70	9300	6190	2.9	-
5	.34	5.0	60	8000	3855	4.5	-
6	.34	5.0	70	5650	2105	4.9	-
7	.34	15.0	60	8750	5970	9.2	-
8	.34	15.0	70	8350	5255	5.6	-
9	.43	10.0	0	2831	0	9.5	-
10	.43	10.0	0	4209	3265	9.5	-
11	.43	10.0	45	4381	4975	9.5	-
12	.43	10.0	60	4946	[illegible]	9.5	
13	.43	10.0	70	5728	3383	9.5	-
14	.43	15.0	0	3990	3274	14.5	-
15	.43	15.0	45	4453	3403	14.5	-
16	.43	15.0	60	4976	3271	14.5	-
17	.43	15.0	60	10053	5868	-	-
18	.43	15.0	70	5873	3165	10.0	-
19	.43	15.0	70	8048	3425	-	-
20	.43	30.0	0	2809	2318	29.5	-
21	.43	30.0	0	9817	8000	7.6	-
22	.43	30.0	0	10202	8511	3.0	-
23	.43	30.0	45	3458	2820	29.5	-
24	.43	30.0	60	3878	2805	29.5	-
25	.43	30.0	70	5086	3226	24.0	-
26	.43	30.0	70	11032	5964	0.5	-
27	.43	60.0	0	2436	1972	59.0	-
28	.43	60.0	45	3379	2731	59.0	-
29	.43	60.0	60	4490	3449	59.0	-
30	.43	60.0	70	5046	3492	59.0	-
31	.43	60.0	70	9450	5804	15.3	-
32	.43	120.0	0	2571	2196	119.0	-
33	.43	120.0	45	2903	2333	119.0	-
34	.43	120.0	60	3537	2738	119.0	-
35	.43	120.0	70	3974	2874	119.0	-
36	.43	240.0	0	2210	2006	239.0	-
37	.43	240.0	45	2400	2163	239.0	-
38	.43	240.0	60	2876	2380	239.0	-
39	.43	240.0	70	3374	2511	239.0	-
40	.54	15.0	70	10460	-	0	-
41	.55	5.0	0	2810	2068	4.2	-
42	.55	5.0	0	6900	4188	4.7	-
43	.55	5.0	0	9004	6004	4.1	-
44	.55	30.0	70	8650	4747	15.8	-
45	.66	10.0	0	8500	6083	9.1	-
46	.66	60.0	70	8870	4740	12.1	-
47	.67	30.0	0	8650	7003	26.2	-
48	.67	30.0	60	8860	4915	22.2	-
49	.67	30.0	70	10475	4432	1.4	-
50	.773	240.0	70	9500	6152	49.2	-

EXPERIMENTAL DATA

Table XIV : Steel Fragments Impacting on Bonded Nylon

Datum No.	Material Thickness e(inches)	Fragment Weight m_s(grains)	Obliquity θ(degrees)	Striking Velocity V_s(fps)	Residual Velocity V_r(fps)	Residual Weight m_r(grains)	Hole Area (sq.in.)
51	.8	5.0	0	11799	3596	-	-
52	.8	10.0	0	5800	3756	9.5	-
53	.8	15.0	0	5471	3323	10.0	-
54	.8	15.0	0	9489	5613	2.0	-
55	.8	30.0	0	5011	3485	29.5	-
56	.8	30.0	0	10492	7582	2.0	-
57	.8	30.0	60	6057	2849	22.0	-
58	.8	30.0	70	11000	-	0	-
59	.8	60.0	0	4046	3003	59.0	-
60	.8	60.0	60	4960	2983	59.0	-
61	.8	60.0	60	9380	3594	23.3	-
62	.8	60.0	70	6171	2675	59.0	-
63	.8	60.0	70	8696	1663	10.0	-
64	.8	120.0	60	4086	2519	119.0	-
65	.8	120.0	70	5281	2522	119.0	-
66	.8	240.0	0	3025	2399	239.0	-
67	.8	240.0	60	3525	2564	239.0	-
68	.8	240.0	70	4076	2602	239.0	-
69	1.0	17.0	0	2420	0	-	-
70	1.0	17.0	30	2594	0	-	-
71	1.0	17.0	45	2736	0	-	-
72	1.0	17.0	60	3201	0	-	-
73	1.0	44.0	0	2045	0	-	-
74	1.0	44.0	30	2076	0	-	-
75	1.0	44.0	45	2177	0	-	-
76	1.0	44.0	60	2483	0	-	-
77	1.0	207.0	0	1473	0	-	-
78	1.0	207.0	30	1501	0	-	-
79	1.0	207.0	45	1632	0	-	-
80	1.0	207.0	60	1770	0	-	-
81	1.0	825.0	0	1105	0	-	-
82	1.0	825.0	30	1145	0	-	-
83	1.0	825.0	45	1265	0	-	-
84	1.0	825.0	60	1414	0	-	-
85	2.0	17.0	0	3895	0	-	-
86	2.0	17.0	30	4257	0	-	-
87	2.0	17.0	45	4876	0	-	-
88	2.0	44.0	0	3016	0	-	-
89	2.0	44.0	30	3138	0	-	-
90	2.0	44.0	45	3359	0	-	-
91	2.0	44.0	60	4206	0	-	-
92	2.0	207.0	0	2113	0	-	-
93	2.0	207.0	30	2193	0	-	-
94	2.0	207.0	45	2281	0	-	-
95	2.0	207.0	60	2676	0	-	-
96	2.0	825.0	30	1646	0	-	-
97	2.0	825.0	45	1786	0	-	-
98	2.0	825.0	60	1930	0	-	-

EXPERIMENTAL DATA

Table XV : Steel Fragments Impacting on Lexan

Datum No.	Material Thickness e(inches)	Fragment Weight m_s(grains)	Obliquity θ(degrees)	Striking Velocity V_s(fps)	Residual Velocity V_r(fps)	Residual Weight m_r(grains)	Hole Area (sq. in.)
1	.125	5.0	0	11605	9820	4.5	.35
2	.125	5.0	60	5245	4252	4.5	.02
3	.125	5.0	70	3251	2421	4.9	.01
4	.125	5.0	70	5747	4418	4.5	.04
5	.125	10.0	0	8356	-	9.5	.39
6	.125	30.0	60	830	175	29.9	-
7	.125	30.0	60	1362	902	29.9	.06
8	.125	30.0	60	4050	3425	28.5	.15
9	.125	30.0	70	2016	1367	29.9	.09
10	.125	30.0	70	5053	4104	28.5	.25
11	.125	60.0	0	2240	911	59.9	.01
12	.128	10.0	0	1684	1197	9.5	.03
13	.128	30.0	0	1309	1143	29.5	.06
14	.128	60.0	0	1402	1275	59.5	.08
15	.128	120.0	0	1279	1183	119.5	.08
16	.130	15.0	45	10635	9328	14.5	.16
17	.135	15.0	0	10198	9195	14.5	.14
18	.225	30.0	0	1314	915	29.5	.54
19	.238	120.0	0	1379	1174	119.5	.85
20	.250	5.0	60	4612	2975	4.5	.02
21	.250	5.0	70	5711	3254	-	.02
22	.250	30.0	60	4597	3398	28.5	.08
23	.250	30.0	70	5121	2570	28.5	.23
24	.258	10.0	0	1575	-	9.5	.02
25	.258	10.0	0	1740	-	9.5	.02
26	.258	10.0	0	1999	1333	9.5	.02
27	.273	60.0	0	1297	920	59.5	.07
28	.450	15.0	70	7950	3292	3.3	.20
29	.500	5.0	0	2160	1176	4.9	-
30	.500	5.0	60	3570	756	4.9	-
31	.500	5.0	60	5555	2672	4.5	.02
32	.500	30.0	0	1297	570	29.9	.05
33	.500	30.0	0	1480	1189	29.9	-
34	.500	30.0	0	1700	861	29.9	-
35	.500	30.0	0	11064	8583	18.5	.17
36	.500	30.0	60	6050	2534	28.0	.15
37	.500	30.0	70	8117	2615	7.5	.31
38	.500	60.0	60	9550	6649	5.0	.74
39	.500	60.0	70	5967	-	-	.48
40	.500	60.0	70	8730	3463	22.8	1.23
41	.500	60.0	70	8959	4412	14.0	.77
42	.500	120.0	70	4190	2349	119.0	.44
43	.500	120.0	70	9271	3388	1.0	2.04
44	.500	240.0	60	9550	7618	-	1.77
45	.500	240.0	70	5831	3726	239.0	1.53
46	.300	240.0	70	9471	6432	49.5	2.68
47	.520	15.0	0	1500E	-	-	-
48	.520	15.0	60	2800	-	-	-

E: Estimated

EXPERIMENTAL DATA

Table XV : Steel Fragments Impacting on Lexan

Datum No.	Material Thickness e(inches)	Fragment Weight m_s(grains)	Obliquity θ(degrees)	Striking Velocity V_s(fps)	Residual Velocity V_r(fps)	Residual Weight m_r(grains)	Hole Area (sq. in.)
49	.520	15.0	60	3260	1120	-	-
50	.520	30.0	0	1400	700	-	-
51	.520	30.0	60	2400	0	-	-
52	.520	30.0	60	2655	790	-	-
53	.520	30.0	70	3000	0	-	-
54	.520	30.0	70	3150	850	-	-
55	.540	120.0	0	1242	796	119.5	0.11
56	.543	30.0	0	1961	1286	29.5	0.04
57	.545	10.0	0	2728	1540	9.5	0.01
58	.534	240.0	0	1017	587	239.5	-
59	1.000	30.0	0	1800E	0	-	-
60	1.000	30.0	0	2470	1728	29.9	.01
61	1.000	30.0	0	4984	2524	28.0	.05
62	1.000	30.0	0	8847	5442	25.5	.08
63	1.000	30.0	60	4000E	0	-	-
64	1.000	30.0	60	4370	1156	-	-
65	1.000	30.0	70	8000E	0	-	-
66	1.000	60.0	45	6006	2240	56.5	.73
67	1.000	60.0	45	8859	4412	37.5	.36
68	1.000	60.0	70	8990	2385	0.1	-
69	1.000	120.0	60	6012	2783	112.2	.59
70	1.000	120.0	60	9341	4970	71.0	.91
71	1.000	240.0	0	1100E	0	239.0	-
72	1.000	240.0	0	1534	1252	239.0	0.15
73	1.000	240.0	0	1600	1056	239.0	-
74	1.000	240.0	0	9087	6859	239.0	-
75	1.000	240.0	70	8856	5918	137.0	1.11
76	2.000	30.0	0	4100E	0	-	-

E: Estimated

EXPERIMENTAL DATA

Table XVI : Steel Fragments Impacting on Cast Plexiglas

Datum No.	Material Thickness e(inches)	Fragment Weight m_s(grains)	Obliquity θ(degrees)	Striking Velocity V_s(fps)	Residual Velocity V_r(fps)	Residual Weight m_r(grains)	Hole Area (sq. in.)
1	.228	240.0	70	1939	1050	239.5	-
2	.234	240.0	70	5830	4839	-	-
3	.236	30.0	70	2056	0	29.0	-
4	.237	30.0	45	672	0	29.5	-
5	.239	30.0	45	4869	4355	29.0	-
6	.240	30.0	80	4512	0	-	-
7	.240	120.0	0	1141	974	119.5	-
8	.240	120.0	0	4853	4381	119.0	-
9	.250	5.0	70	4366	1570	4.5	0.07
10	.250	15.0	70	4931	2020	14.7	0.38
11	.250	30.0	45	1017	407	29.5	-
12	.250	30.0	45	4869	4375	-	-
13	.250	30.0	70	2556	665	29.0	-
14	.250	30.0	70	4773	2776	-	-
15	.250	120.0	70	1944	1134	119.0	-
16	.250	120.0	70	5953	4886	-	-
17	.250	240.0	0	268	0	239.5	-
18	.254	240.0	70	3770	3163	239.0	-
19	.256	120.0	70	5884	4700	-	-
20	.257	30.0	0	1695	1255	29.5	-
21	.257	240.0	0	1193	801	239.5	-
22	.257	240.0	0	5826	5685	239.0	-
23	.257	240.0	70	1115	236	239.5	-
24	.258	30.0	0	833	689	29.5	-
25	.258	30.0	0	5103	4314	-	-
26	.263	120.0	0	639	280	119.5	-
27	.486	5.0	0	5227	2740	[illegible]	0.01
28	.486	15.0	0	4373	2660	14.9	0.03
29	.486	15.0	60	4605	718	14.8	0.32
30	.486	30.0	45	4018	2310	29.3	0.11
31	.492	30.0	45	1888	474	-	-
32	.492	30.0	45	4896	3861	-	-
33	.492	240.0	45	869	193	239.5	-
34	.495	30.0	0	1064	0	29.0	-
35	.495	30.0	70	4793	1565	-	-
36	.495	60.0	0	687	309	59.0	-
37	.495	120.0	0	1198	896	119.0	-
38	.500	30.0	0	5220	4140	-	-
39	.500	30.0	70	3082	0	-	-
40	.500	30.0	70	6166	2687	-	-
41	.500	60.0	0	4911	4277	-	-
42	.500	60.0	70	2209	376	59.0	-
43	.500	60.0	70	5034	2878	-	-
44	.500	120.0	0	5785	5185	-	-
45	.500	120.0	70	5798	2524	-	-
46	.500	240.0	0	776	129	239.0	-
47	.500	240.0	0	5910	5310	-	-
48	.500	240.0	45	869	193	239.0	-
49	.500	240.0	45	5464	4553	-	-
50	.500	240.0	70	1969	483	239.0	-

EXPERIMENTAL DATA

Table XVI : Steel Fragments Impacting on Cast Plexiglas

Datum No.	Material Thickness e(inches)	Fragment Weight m_s(grains)	Obliquity θ(degrees)	Striking Velocity V_s(fps)	Residual Velocity V_r(fps)	Residual Weight m_r(grains)	Hole Area (sq. in.)
51	.500	240.0	70	5712	4189	-	-
52	.625	30.0	0	1348	570	29.0	-
53	.625	30.0	0	5483	3541	-	-
54	.625	30.0	70	3900	820	-	-
55	.625	30.0	70	5034	1425	-	-
56	.625	60.0	0	1048	410	59.0	-
57	.625	60.0	0	4450	3400	-	-
58	.625	60.0	70	3437	949	-	-
59	.625	60.0	70	5162	1601	-	-
60	.625	240.0	0	869	722	239.0	-
61	.625	240.0	0	5830	4920	-	-
62	.625	240.0	70	3892	1789	-	-
63	.625	240.0	70	5835	4140	-	-
64	.732	60.0	70	9017	3160	14.0	-
65	.735	60.0	60	3868	960	59.9	0.64
66	.744	240.0	70	3937	1507	239.5	-
67	.750	30.0	0	5800	3356	25.0E	0.07
68	.750	60.0	60	6020	2823	47.2	-
69	.750	240.0	70	6010	2166	20.3	-
70	.968	240.0	70	9346	3410	74.7	-
71	.975	30.0	0	2124	18	-	-
72	.986	240.0	0	879	0	239.0	-
73	.989	240.0	70	5387	0	-	-
74	.992	120.0	0	9187	6000	36.1	0.26
75	.995	30.0	0	3417	2993	-	-
76	.997	240.0	0	9913	7910	120.0	0.32
77	1.000	15.0	0	5550	1407	14.9	-
78	1.000	30.0	0	8200	5129	13.1	0.02
79	1.000	30.0	60	8480	4309	0.1	-
80	1.000	60.0	60	5960	-	0	2.50
81	1.000	60.0	70	9325	2072	0.1	-
82	1.000	120.0	70	5721	0	-	7.55
83	1.000	120.0	70	8620	2197	0.5	-
84	1.000	120.0	70	9374	3230	25.5	-
85	1.000	240.0	0	[illegible]	[illegible]		-
86	1.000	240.0	70	3831	883	-	-
87	1.000	240.0	70	5000	758	220.0	-
88	1.000	240.0	70	6060	650	12.3	-
89	1.000	240.0	70	6110	2335	-	-
90	1.000	475.0	70	3800	2146	474.0	-
91	1.000	475.0	70	4710	1775	457.9	-
92	1.007	60.0	45	4701	1045	54.2	1.09
93	1.010	15.0	0	5517	970	14.5	0.03
94	1.010	30.0	0	5221	1850	28.0	0.08
95	1.011	30.0	70	8992	0	0	1.93
96	1.012	240.0	0	4650	3130	209.6	2.24
97	1.025	60.0	0	8702	5610	22.5	0.05
98	1.050	60.0	70	8968	0	0	-

E: Estimated

EXPERIMENTAL DATA

Table XVII : Steel Fragments Impacting on Stretched Plexiglas

Datum No.	Material Thickness e(inches)	Fragment Weight m_s(grains)	Obliquity θ(degrees)	Striking Velocity V_s(fps)	Residual Velocity V_r(fps)	Residual Weight m_r(grains)	Hole Area (sq. in.)
1	0.05	5	70	2875	2395	4.5	0.08
2	0.05	15	45	1299	1199	14.5	0.06
3	0.05	240	70	5887	5877	239.0	1.16
4	0.05	475	70	4876	4662	474.0	1.08
5	0.14	5	0	723	357	4.5	0.01
6	0.14	5	0	881	874	4.5	0.01
7	0.14	15	0	792	632	14.5	0.03
8	0.14	15	0	8824	5900E	8.0	0.23
9	0.14	30	0	1409	1256	29.0	0.07
10	0.14	30	0	6070	5260	28.0	0.33
11	0.14	30	70	2017	1412	29.5	0.30
12	0.14	30	70	2101	1980	29.5	0.30
13	0.14	30	70	5836	4497	29.0	0.57
14	0.14	60	70	1143	680	59.0	0.55
15	0.14	60	70	5472	3969	59.0	0.95
16	0.26	5	0	1140	473	4.5	0.01
17	0.26	15	0	600E	0	14.5	-
18	0.26	15	0	1119	933	14.5	0.03
19	0.26	30	60	2078	1214	29.5	0.28
20	0.26	30	60	6394	3805	26.0	0.85
21	0.26	[illegible]	0	678	80	-	0.15
22	0.26	60	0	4726	3840	59.5	0.43
23	0.26	120	30	1188	958	119.5	0.26
24	0.26	120	30	5118	4358	116.5	0.82
25	0.26	240	0	1652	1359	239.5	0.37
26	0.26	240	0	6149	5717	234.5	1.21
27	0.33	5	70	4439	1305	4.5	-
28	0.33	5	70	5852	1423	4.5	-
29	0.33	5	70	5955	1906	4.5	-
30	0.33	15	70	5017	1603	14.5	-
31	0.33	15	70	5527	2945	14.5	-
32	0.33	15	70	5596	1800E	14.0	-
33	0.33	15	70	7755	3229	6.5	-
34	0.33	15	70	993[illegible]	3545	1.5	-
35	0.33	30	70	2949	1006	29.5	0.60
36	0.33	30	70	9690	5384	3.5	2.28
37	0.33	120	45	2742	1232	119.5	0.51
38	0.33	120	45	6239	4975	108.0	1.76
39	0.33	240	60	1107	717	239.5	0.80
40	0.33	240	70	4836	3863	238.0	1.28
41	0.351	5	70	3400	-	-	-
42	0.356	30	70	8975	4047	4.5	-
43	0.357	5	70	3700	-	-	-
44	0.357	30	70	740	-	-	-
45	0.357	30	70	2000	-	-	-
46	0.357	30	70	5670	1786	25.3	-
47	0.361	240	70	1450	741	239.0	-
48	0.40	15	70	3386	0	-	0.40
49	0.40	15	70	8858	1000E	5.5	1.92
50	0.40	30	70	5706	3090	27.5	-

E: Estimated

EXPERIMENTAL DATA

Table XVII : Steel Fragments Impacting on Stretched Plexiglas

Datum No.	Material Thickness e(inches)	Fragment Weight m_s(grains)	Obliquity θ(degrees)	Striking Velocity V_s(fps)	Residual Velocity V_r(fps)	Residual Weight m_r(grains)	Hole Area (sq. in.)
51	0.40	30	70	7328	3515	13.5	-
52	0.40	30	70	11290	-	0	-
53	0.40	60	60	2676	1507	59.5	0.73
54	0.40	60	60	8993	6600	58.0	4.10
55	0.40	120	70	2691	1242	119.5	1.45
56	0.40	120	70	6032	2677	103.0	5.34
57	0.40	240	70	2726	1838	239.0	3.98
58	0.40	240	70	6158	4115	180.0	5.28
59	0.407	30	70	5800	2687	28.1	-
60	0.409	240	70	1380	435	239.0	-
61	0.410	5	70	2650	-	-	-
62	0.410	5	70	3300	-	-	-
63	0.410	5	70	3450	-	-	-
64	0.410	5	70	3700	-	-	-
65	0.410	5	70	3835	-	-	-
66	0.414	30	70	2600	-	-	-
67	0.506	240	70	1970	849	239.0	-
68	0.507	30	70	5700	-	-	-
69	0.508	30	70	2850	-	-	-
70	0.514	5	70	4450	-	-	-
71	0.55	5	0	3352	1422	4.5	0.03
72	0.55	5	0	6844	4720	4.5	0.01
73	0.55	5	70	6405	-	-	0.36
74	0.55	5	70	8743	-	-	0.42
75	0.55	15	60	2980	804	14.5	0.16
76	0.55	15	60	3207	650	14.5	0.18
77	0.55	15	60	8161	2212	9.5	1.46
78	0.55	30	0	1989	-	29.5	0.12
79	0.55	30	0	2029	1116	29.5	0.12
80	0.55	30	70	4300	-	-	-
81	0.55	30	70	4382	-	-	0.99
82	0.55	30	70	4852	-	-	1.36
83	0.55	30	70	8000	0E	-	-
84	0.55	30	70	8319	5943	4.0	-
85	0.55	30	70	9418	-	1.0E	3.10
86	0.55	60	45	2193	1212	59.5	0.31
87	0.55	60	45	9147	6470	26.0	2.47
88	0.55	240	70	2000E	0	-	-
89	0.601	30	70	4393	-	-	-
90	0.605	5	70	5400	-	-	-
91	0.609	240	70	2825	1400	239.0	-
92	0.619	30	70	9025	2527	3.8	-
93	0.728	30	70	5900	-	-	-
94	0.728	240	70	4170	1456	233.0	-
95	0.729	30	70	8850	1802	1.5	-
96	0.730	475	70	1140	-	-	-
97	0.733	5	0	4775	1279	4.9	-
98	0.908	60	70	7950	1708	0.4	-
99	0.910	475	70	2810	1119	474.0	-

E: Estimated

EXPERIMENTAL DATA

Table XVII: Steel Fragments Impacting on Stretched Plexiglas

Datum No.	Material Thickness e(inches)	Fragment Weight m_s(grains)	Obliquity θ(degrees)	Striking Velocity V_s(fps)	Residual Velocity V_r(fps)	Residual Weight m_r(grains)	Hole Area (sq. in.)
100	0.922	240	70	6100	2172	181.0	-
101	0.930	5	0	5800	1010	4.9	-
102	0.930	5	0	6196	2094	4.9	-

EXPERIMENTAL DATA

Table XVIII : Steel Fragments Impacting on Doron

Datum No.	Material Thickness e(inches)	Fragment Weight m_s(grains)	Obliquity θ(degrees)	Striking Velocity V_s(fps)	Residual Velocity V_r(fps)	Residual Weight m_r(grains)	Hole Area (sq. in.)
1	.055	2.65	0	977	0	-	-
2	.055	2.65	30	1035	0	-	-
3	.056	2.65	45	1269	0	-	-
4	.058	2.65	60	1301	0	-	-
5	.075	15.00	0	1215	921	14.5	-
6	.075	15.00	0	1231	939	-	-
7	.075	30.00	0	1997	1801	29.5	-
8	.075	30.00	0	2018	1836	-	-
9	.075	30.00	0	3888	3592	-	-
10	.075	30.00	0	3917	3657	-	-
11	.075	30.00	60	2473	2082	29.5	-
12	.075	30.00	60	2497	2122	-	-
13	.075	30.00	60	4130	3581	-	-
14	.075	30.00	70	3968	3240	29.5	-
15	.075	60.00	70	3715	3052	-	-
16	.091	17.00	45	886	0	-	-
17	.091	44.00	60	871	0	-	-
18	.091	147.00	30	517	0	-	-
19	.092	5.85	60	1301	0	-	-
20	.092	15.00	0	2040	1635	14.5	-
21	.092	15.00	0	2063	1670	-	-
22	.092	15.00	70	3577	2631	-	-
23	.092	15.00	70	3608	2686	-	-
24	.092	17.00	30	761	0	-	-
25	.092	17.00	60	1033	0	-	-
26	.092	30.00	60	3987	3159	29.5	-
27	.092	30.00	60	4013	3214	-	-
28	.092	30.00	70	3881	3051	-	-
29	.092	30.00	70	3910	3106	-	-
30	.092	44.00	30	635	0	-	-
31	.092	44.00	45	672	0	-	-
32	.092	60.00	60	2696	2210	-	-
33	.092	60.00	60	2715	2240	-	-
34	.092	60.00	70	3538	2726	-	-
35	.092	60.00	70	3557	2761	-	-
36	.092	120.00	60	3036	2455	119.5	-
37	.092	120.00	60	3071	2482	-	-
38	.092	120.00	70	3895	3231	-	-
39	.092	120.00	70	3929	3263	-	-
40	.092	240.00	60	2164	1946	239.5	-
41	.092	240.00	60	2180	1966	-	-
42	.092	240.00	60	3176	2882	-	-
43	.092	240.00	60	3198	2907	-	-
44	.093	5.85	45	1101	0	-	-
45	.096	5.85	0	959	0	-	-
46	.096	5.85	30	1000	0	-	-
47	.096	17.00	0	930	0	-	-
48	.099	44.00	0	[illegible]	0	-	-
49	.102	0.85	0	[illegible]	0	-	-
50	.102	0.85	0	2000	750	-	-

EXPERIMENTAL DATA

TABLE XVIII : Steel Fragments Impacting on Doron

Datum No.	Material Thickness e(inches)	Fragment Weight m_s(grains)	Obliquity θ(degrees)	Striking Velocity V_s(fps)	Residual Velocity V_r(fps)	Residual Weight m_r(grains)	Hole Area (sq. in.)
51	.102	0.85	0	2500	1485	-	-
52	.102	0.85	0	2969	2039	-	-
53	.102	0.85	0	3000	2085	-	-
54	.102	0.85	0	3092	2189	-	-
55	.102	0.85	0	3500	2630	-	-
56	.102	0.85	0	4000	3140	-	-
57	.102	0.85	0	4500	3631	-	-
58	.102	0.85	0	5000	4108	-	-
59	.102	0.85	0	5190	4249	-	-
60	.102	147.00	0	606	0	-	-
61	.108	0.85	0	1920	0	-	-
62	.108	0.85	0	4063	3072	-	-
63	.108	0.85	0	5418	4361	-	-
64	.108	0.85	45	2304	0	-	-
65	.108	0.85	45	3349	2148	-	-
66	.108	0.85	45	5007	3771	-	-
67	.108	0.85	60	2701	745	-	-
68	.108	0.85	60	3130	1081	-	-
69	.108	0.85	60	3932	2566	-	-
70	.108	2.10	0	1778	0	-	-
71	.108	2.10	0	3992	2839	-	-
72	.108	2.10	0	5439	4176	-	-
73	.108	2.10	45	2361	0	-	-
74	.108	2.10	45	4014	2490	-	-
75	.108	2.10	45	5691	3534	-	-
76	.108	2.10	60	3081	0	-	-
77	.108	2.10	60	4079	1616	-	-
78	.108	2.10	60	5052	3041	-	-
79	.109	2.65	0	1490	0	-	-
80	.114	5.85	0	1259	0	-	-
81	.114	17.00	0	993	0	-	-
82	.118	2.65	60	2151	0	-	-
83	.120	5.85	30	1152	0	-	-
84	.120	17.00	30	979	0	-	-
85	.120	44.00	30	772	0	-	-
86	.122	2.65	30	1610	0	-	-
87	.122	17.00	60	1231	0	-	-
88	.123	5.85	45	1321	0	-	-
89	.124	2.65	45	1861	0	-	-
90	.124	5.85	60	1527	0	-	-
91	.124	44.00	45	797	0	-	-
92	.144	17.00	0	1079	0	-	-
93	.145	5.85	0	1409	0	-	-
94	.150	17.00	30	1152	0	-	-
95	.150	30.00	60	3201	-	28.84	-
96	.150	30.00	60	5993	-	23.30	-
97	.150	30.00	70	3827	-	28.89	-
98	.150	44.00	30	845	0	-	-
99	.151	5.85	30	1349	0	-	-
100	.151	7.20	0	737	0	-	-

EXPERIMENTAL DATA

Table XVIII : Steel Fragments Impacting on Doron

Datum No.	Material Thickness e(inches)	Fragment Weight m_s(grains)	Obliquity θ(degrees)	Striking Velocity V_s(fps)	Residual Velocity V_r(fps)	Residual Weight m_r(grains)	Hole Area (sq. in.)
101	.151	7.20	0	4439	4211	-	-
102	.151	7.20	45	757	0	-	-
103	.151	7.20	45	4450	4290	-	-
104	.151	7.20	60	887	0	-	-
105	.151	7.20	60	5063	4162	-	-
106	.152	5.85	45	1503	0	-	-
107	.152	17.00	60	1418	0	-	-
108	.152	44.00	45	918	0	-	-
109	.152	147.00	30	653	0	-	-
110	.152	207.00	0	628	0	-	-
111	.154	5.85	60	1823	0	-	-
112	.154	15.00	70	3868	-	14.0	-
113	.154	17.00	45	1270	0	-	-
114	.154	30.00	70	3405	-	29.0	-
115	.192	5.85	0	1794	0	-	-
116	.192	17.00	0	1382	0	-	-
117	.193	2.65	0	2426	0	-	-
118	.193	2.65	30	2388	0	-	-
119	.193	2.65	45	2979	0	-	-
120	.193	15.00	0	2671	1827	14.5	-
121	.193	15.00	0	2695	1870	-	-
122	.193	30.00	70	4890	2844	-	-
123	.193	30.00	70	4931	2896	-	-
124	.193	60.00	60	2795	1907	-	-
125	.193	60.00	60	2795	1882	-	-
126	.193	60.00	70	3739	1223	-	-
127	.193	60.00	70	3755	1235	-	-
128	.193	120.00	0	3148	2917	119.5	-
129	.193	120.00	0	3179	2950	-	-
130	.193	120.00	70	3979	2580	-	-
131	.193	120.00	70	4004	2610	-	-
132	.194	2.65	60	3528	0	-	-
133	.194	147.00	0	772	0	-	-
134	.195	240.00	70	3073	2359	-	-
135	.195	240.00	70	3104	2381	-	-
136	.195	240.00	70	6191	4828	-	-
137	.196	44.00	0	1062	0	-	-
138	.210	5.85	45	1936	0	-	-
139	.210	17.00	30	1355	0	-	-
140	.210	44.00	30	1114	0	-	-
141	.213	5.85	30	1741	0		-
142	.213	17.00	60	1791	0	-	-
143	.214	17.00	45	1588	0	-	-
144	.214	44.00	45	1185	0	-	-
145	.245	5.85	0	2052	0	-	-
146	.250	5.00	0	5000	3385	4.7	-
147	.250	30.00	0	3879	3121	-	-
148	.250	30.00	60	3897	2535	-	-
149	.250	30.00	60	6350	5986	2.7	-
150	.250	60.00	60	8756	5769	2.0	-

EXPERIMENTAL DATA

Table XVIII : Steel Fragments Impacting on Doron

Datum No.	Material Thickness e(inches)	Fragment Weight m_s(grains)	Obliquity θ(degrees)	Striking Velocity V_s(fps)	Residual Velocity V_r(fps)	Residual Weight m_r(grains)	Hole Area (sq. in.)
151	.250	120.0	0	3832	1682	119.5	-
152	.250	240.0	0	3959	3745	239.5	-
153	.250	240.0	45	2427	2031	239.5	-
154	.250	240.0	60	5396	4517	-	-
155	.252	207.0	0	837	0	-	-
156	.262	2.65	0	3339	0	-	-
157	.266	2.65	30	3170	0	-	-
158	.266	2.65	45	3398	0	-	-
159	.269	5.85	45	2597	0	-	-
160	.270	30.0	60	8153	-	5.69	-
161	.270	30.0	70	8137	-	0.93	-
162	.270	60.0	70	8110	-	7.56	-
163	.270	120.0	70	9034	-	109.51	-
164	.288	17.0	0	1768	0	-	-
165	.288	44.0	0	1409	0	-	-
166	.302	7.20	0	971	0	-	-
167	.302	7.20	0	4699	4230	-	-
168	.302	7.20	45	1941	0	-	-
169	.302	7.20	45	4610	4272	-	-
170	.302	7.20	60	2552	0	-	-
171	.302	7.20	60	4833	4098	-	-
172	.317	5.85	0	2624	0	-	-
173	.318	207.0	0	1004	0	-	-
174	.340	17.0	60	2651	0	-	-
175	.342	5.85	30	2448	0	-	-
176	.342	17.0	30	1886	0	-	-
177	.346	17.0	45	2254	0	-	-
178	.378	207.0	0	1066	0	-	-
179	.384	17.0	0	2273	0	-	-
180	.387	147.0	0	1229	0	-	-
181	.463	13.0	0	5421	-	8.07	-
182	.463	30.0	0	4905	-	28.61	-
183	.463	30.0	60	3900	0	-	-
184	.482	44.0	30	1937	0	-	-
185	.483	44.0	0	1952	0	-	-
186	.486	825.0	0	869	0	-	-
187	.490	17.0	0	2992	0	-	-
188	.490	17.0	30	2626	0	-	-
189	.490	17.0	45	3533	0	-	-
190	.490	17.0	60	5453	0	-	-
191	.491	44.0	45	2375	0	-	-
192	.491	400.0	0	1009	0	-	-
193	.493	44.0	60	3468	0	-	-
194	.497	207.0	45	1445	0	-	-
195	.497	600.0	0	930	0	-	-
196	.499	600.0	45	1030	0	-	-
197	.500	10.0	0	4650	2412	9.9	-
198	.500	30.0	0	4579	2698	-	-
199	.500	30.0	45	4700	2166	-	-
200	.500	30.0	45	5830	2908	13.2	-

CONFIDENTIAL

EXPERIMENTAL DATA

Table XVIII: Steel Fragments Impacting on Doron

Datum No.	Material Thickness e(inches)	Fragment Weight m_s(grains)	Obliquity θ(degrees)	Striking Velocity V_s(fps)	Residual Velocity V_r(fps)	Residual Weight m_r(grains)	Hole Area (sq. in.)
201	.500	30.0	60	7102	1475	-	-
202	.500	30.0	60	7960	-	6.65	-
203	.500	30.0	60	10578	-	0	-
204	.500	60.0	0	3198	2189	-	-
205	.500	60.0	0	5894	3744	-	-
206	.500	60.0	60	7193	3421	-	-
207	.500	60.0	60	7607	-	20.5	-
208	.500	60.0	60	7975	4597	8.4	-
209	.500	60.0	70	6195	0	-	-
210	.500	60.0	70	8184	-	2.96	-
211	.500	60.0	70	8700	-	0	-
212	.500	120.0	0	3862	-	108.52	-
213	.500	120.0	0	3881	2781	-	-
214	.500	120.0	45	3598	2251	-	-
215	.500	120.0	70	5889	0	-	-
216	.500	240.0	0	3743	2958	-	-
217	.500	240.0	45	3645	2646	-	-
218	.500	240.0	60	5366	3518	-	-
219	.500	240.0	70	4719	2145	-	-
220	.508	400.0	45	1110	0	-	-
221	.625	240.0	70	9850	6856	-	-
222	.739	400.0	45	1497	0	-	-
223	.742	400.0	60	1938	0	-	-
224	.744	207.0	0	1646	0	-	-
225	.750	30.0	0	5229	-	27.72	-
226	.750	60.0	0	6037	-	46.08	-
227	.750	120.0	45	5043	-	102.61	-
228	.750	240.0	0	3529	-	224.71	-
229	.750	240.0	60	4229	-	221.50	-
230	.750	240.0	70	5685	0	-	-
23[illegible]	.752	400.0	0	1456	0	-	-
232	.752	600.0	0	1384	0	-	-
233	.755	207.0	0	1762	0	-	-
234	.755	207.0	45	1873	0	-	-
235	.757	17.0	0	4530	0	-	-
236	.757	44.0	0	[illegible]	0	-	-
237	.763	600.0	45	1493	0	-	-
238	.963	207.0	45	2351	0	-	-
239	.966	400.0	0	1765	0	-	-
240	.966	600.0	0	1564	0	-	-
241	.998	44.0	30	4145	0	-	-
242	1.000	30.0	0	4769	0	-	-
243	1.000	30.0	0	6999	1999	-	-
244	1.000	30.0	45	7718	2013	-	-
245	1.000	30.0	60	10500E	0	-	-
246	1.000	60.0	0	5088	-	41.67	-
247	1.000	60.0	0	7376	2627	-	-
248	1.000	60.0	60	8929	4829	-	-
249	1.000	60.0	70	10000E	-	0	-
250	1.000	120.0	0	5010	-	79.74	-

E: Estimated

CONFIDENTIAL

EXPERIMENTAL DATA

Table XVIII : Steel Fragments Impacting on Doron

Datum No.	Material Thickness e(inches)	Fragment Weight m_s(grains)	Obliquity θ(degrees)	Striking Velocity V_s(fps)	Residual Velocity V_r(fps)	Residual Weight m_r(grains)	Area (sq. in.)
251	1.000	120.0	70	7500E	0	-	-
252	1.000	240.0	60	5940	2542	152.0	-
253	1.000	240.0	70	9847	-	8.50	-
254	1.000	475.0	60	5147	-	474.0	-
255	1.024	44.0	0	4175	0	-	-
256	1.400	80.0	0	8834	2950	-	-
257	1.430	30.0	0	11000E	-	0	-
258	1.448	600.0	0	2135	0	-	-
259	1.460	400.0	0	2540	0	-	-

E: Estimated

EXPERIMENTAL DATA

Table XIX Steel Fragments Impacting on Bullet Resistant Glass

Test No.	Material Thickness (inches)	Fragment Weight m_s (grains)	Obliquity (degrees)	Striking Velocity V_s (fps)	Residual Velocity V_r (fps)	Residual Weight m_r (grains)	Hole Area (sq. in.)
1	.218	30.0	0	[illegible]	127	29.5	-
2	.218	30.0	0	4811	3788	-	-
3	.218	60.0	0	5676	4428	-	-
4	.218	60.0	45	6734	5797	-	-
5	.218	60.0	70	6808	4375	-	-
6	.218	240.0	0	709	0	239.5	-
7	.218	240.0	0	9866	5188	-	-
8	.218	240.0	45	3819	4898	-	-
9	.218	240.0	70	2150	1013	239.5	-
10	.218	240.0	70	5846	3347	-	-
11	.225	15.0	70	5000 E	0	-	-
12	.225	30.0	70	3500 E	0	-	-
13	.23	5.0	45	5392	1810	3.5	.03
14	.23	10.0	60	5376	1005	7.2	.11
15	.23	30.0	0	4811	3840	27.0	.03
16	.23	30.0	0	9496	7200	1.8	.56
17	.23	30.0	45	999	845	29.5	-
18	.23	30.0	45	7106	3232	-	-
19	.23	30.0	70	7015	2956	-	-
20	.23	60.0	45	919	545	59.5	-
21	.23	240.0	0	[illegible]	0	239.0	-
22	.236	240.0	45	[illegible]	3342	-	-
23	.238	[illegible]	0	832	476	59.5	-
24	.236	60.0	45	989	361	59.5	-
25	.238	60.0	70	3508	2286	-	-
26	.265	30.0	45	5674	3009	-	-
27	.265	30.0	70	5703	3274	-	-
28	.495	30.0	0	1064	0	29.5	-
29	.500	30.0	70	3082	0	-	-
30	.500	30.0	70	8125	2941	-	.055
31	.500	60.0	70	8740	3566	1.0	.196
32	.527	30.0	45	2653	0	-	-
33	.53	30.0	0	4745	1820	27.0	.03
34	.53	30.0	70	8725	-	0	.01
35	.53	60.0	0	1096	163	59.5	-
36	.53	60.0	45	5340	2053	24.0	.10
37	.53	60.0	70	4610	-	0	-
38	.53	60.0	70	8733	-	0	.22
39	.53	60.0	70	9268	-	0	-
40	.53	120.0	0	3475	2005	116.5	.05
41	.53	120.0	70	5320	-	0	2.83
42	.53	120.0	70	6333	-	0	.29
43	.53	240.0	0	3758	2585	232.0	.14
44	.53	240.0	0	4717	3130	228.0	.11
45	.53	240.0	0	5891	4160	93.1	.25
46	.53	240.0	70	8379	3000	25.7	.91
47	.534	240.0	0	756	0	239.0	-
48	.538	120.0	0	5925	3985	-	-
49	.542	30.0	0	2480	540	29.0	-
50	.542	60.0	45	3575	1498	-	-

EXPERIMENTAL DATA

Table XIX : Steel Fragments Impacting on Bullet Resistant Glass

Datum No.	Material Thickness e(inches)	Fragment Weight m_s(grains)	Obliquity θ(degrees)	Striking Velocity V_s(fps)	Residual Velocity V_r(fps)	Residual Weight m_r(grains)	Hole Area (sq. in.)
51	1.000	30.0	0	8875	6153	20.8	.601
52	1.000	30.0	45	8777	2888	0.2	-
53	1.000	60.0	0	8850	-	-	.835
54	1.000	60.0	60	8580	2970	0.5	-
55	1.020	15.0	0	3500	0	-	-
56	1.020	30.0	0	3167	738	0	.37
57	1.020	60.0	0	3450	0	-	.29
58	1.020	120.0	0	4040	1055	118.8	-
59	1.020	120.0	45	3850	532	-	-
60	1.020	120.0	60	3560	0	-	-
61	1.020	240.0	0	5229	2290	200.0	2.41
62	1.020	240.0	60	4330	0	-	-
63	1.020	240.0	70	4560	0	-	-
64	1.56	470.0	70	6500E	0	-	-
65	1.56	475.0	0	3150	914	443.1	.59
66	1.56	473.0	60	3000E	0	-	-
67	1.56	477.0	0	1620	0	476.9	.25
68	1.58	30.0	0	9268	790	0	.33
69	1.58	60.0	45	8535	-	0	.77
70	1.58	120.0	0	4665	-	0	.71
71	1.58	120.0	0	9681	-	51.9	2.05
72	1.58	240.0	60	8322	-	1.3	3.73
73	1.58	240.0	70	8965	1950	0	2.65
74	1.60	30.0	0	8160	-	0.3	.245
75	1.60	60.0	0	8890	761	40.4	.785
76	1.6[illegible]	[illegible].0	60	9575	-	-	3.19
77	1[illegible]	[illegible].0	0	5974	248	-	-
78	1.625	[illegible]0.0	0	4811	0	-	-
79	1.625	240.0	0	3939	788	-	-
80	1.625	240.0	45	2700	324	-	-
81	1.625	240.0	45	5629	2060	-	-

E: Estimated

DISTRIBUTION LIST

No. of Copies	Organization
5	Headquarters U. S. Army Material Command Attn: AMCRD-RS-CM (L.S. Croan) AMCRD-RS-PE (Mr. Stetson) AMCPM-AI (Mr. R. Cory) Washington 25, D. C.
1	Director Advanced Res Project Agcy Attn: Mr. Franklin Department of Defense Washington 25, D. C.
16	Commanding Officer Ballistic Research Labs Attn: Mr. R. G. Bernier, WSL(1) Mr. J. J. Bailey, WSL(1) Mr. H. Peaker, WSL(1) Mr. D. C. Hardison, WSL(1) Mr. A. Hoffman, TBL(1) Mr. D. Dunn, TBL(1) Reports Dist Sec (10) Aberdeen Proving Ground, Md
6	Defense Res Member Canadian Joint Staff 2450 Massachusetts Ave, NW Washington 8, D.C. VIA: Headquarters U.S. Army Material Com Attn: AMCRD-RS-PE Mr. Stetson Washington 25, D.C.
6	Scientific Info Off Defense Res Staff British Embassy 3100 Massachusetts Ave, NW Washington 8, D.C. VIA: Headquarters U.S. Army Material Com Attn: AMCRD-RS-PE Mr. Stetson Washington 25, D.C.
1	Director Weapon Systems Evaluation Group Office, Sec of Def Washington 25, D.C.
1	Off Chief of Res and Dev Department of the Army Washington 25, D.C.
1	Commanding Officer Attn: Tech Info Branch Aberdeen Proving Ground, Md.
1	Director Dev & Proof Services Attn: Mr. W.C. Pless Aberdeen Proving Ground, Md
10	Commander Armed Services Tech Info Agcy Attn: TIPER Arlington Hall Station Arlington 12, Va
1	Commanding General U.S. Army Mobility Com 28251 Van Dyke Ave Centerline, Michigan
1	Commanding Officer U.S. Army Transp Res Com Attn: Library Fort Eustis, Virginia
3	Commanding General Redstone Scientific Info Ctr Attn: Chief, Document Sec Redstone Arsenal, Alabama
1	Commanding Officer Watertown Arsenal Attn: Watertown Arsenal Lab Armor Section ~~Redstone Arsenal, Alabama~~ Watertown 72, Mass.
1	U.S. Army Material Res Agcy Watertown 72, Massachusetts
1	Commanding General U.S. Army Weapons Com Rock Island Arsenal Rock Island Illinois
1	Commanding General U.S. Army Combat Dev Com Fort Belvoir, Virginia
1	Director NASA Marshall Space Flight Ctr Attn: Library Section Redstone Arsenal, Alabama
1	Commanding Officer U.S. Army Art & Com Dev Agcy Attn: Librarian Fort Sill, Oklahoma
3	Commanding Officer Picatinny Arsenal Feltman Res & Eng Labs Attn: Mr. F. Saxe, SMUPA-DW2 (2) PLASTEC Dover, New Jersey

DISTRIBUTION LIST (Cont.)

No. of Copies	Organization
1	Commanding Officer Frankford Arsenal Attn: Library, Br 0270, Bldg 40 Philadelphia 37, Pennsylvania
1	Commander Field Command Defense Atomic Support Agcy Attn: FCDR/4 P.O. Box 5100 Sandia Base Albuquerque, N. M.
1	Commanding General U.S. Army Com & Dev Exp Ctr Fort Ord, California
1	Commanding General USA Chemical Res & Dev Labs Attn: Biophysics Div Mr. George Stewart Edgewood Arsenal, Md.
1	Commanding Officer U.S. Army Transp Materiel Com Attn: SMOSM 12th and Spruce Streets St. Louis, Missouri
1	Commanding Officer U.S. Army Natick Labs Attn: Mr. A. Alessi Natick, Massachusetts
1	Commanding Officer Harry Diamond Labs Attn: Tech Info Office Branch 012 Washington 25, D. C.
1	Director Research Analysis Corp 6935 Arlington Road Bethesda, Maryland
1	Director Army Research Office Arlington Hall Station Arlington, Virginia
1	Commanding Officer Philadelphia Proc Dist U.S. Army Attn: CO, R & D Br 128 North Broad Street Philadelphia, Pennsylvania
1	Chief Bureau of Nav Weapons Department of the Navy Attn: DIS-33 Washington 25, D.C.
1	Commander Naval Air Dev Ctr Attn: WR-4 Johnsville, Pennsylvania
1	Commander Naval Ord Lab White Oak Silver Springs, Md.
1	Commander Naval Ord Lab Corona, California
1	Commander U.S. Naval Ord Test Sta Attn: Code 4032 China Lake, California
2	Commander U.S. Naval Weapons Lab Attn: Code T & Code WA-1 Dahlgren, Virginia
1	Commander U.S. Naval Res Lab Attn: Library Anacostia, Maryland
1	Commander U.S. Navy Nuclear Ord Eval Unit Attn: Code 40 Kirtland Air Force Base, N. M.
1	Office of Naval Res Navy Department Attn: N483 (Sc Lit Br) Washington 25, D. C.
1	Marine Experimental Sta Squadron HMX-1 Quantico, Virginia
1	Commander AF Space Weapons Ctr Kirtland Air Force Base, N. M.
1	Commander Air Proving Ground Center Attn: PGAPI Eglin Air Force Base, Fla.

DISTRIBUTION LIST (Cont.)

No. of Copies	Organization
2	Commander Foreign Tech Div Air Force Systems Com USAF Attn: Major Henderson Mr. P. Schmidt Wright-Patterson AFB, Ohio
1	Commander H.Q. Ogden Air Material Area Attn: OOOSS Hill Air Force Base, Utah
1	Rand Corporation Dept of the Air Force Attn: Library 1700 Main Street Santa Monica, California
2	Aerojet General Corp Attn: K.N. Kr[illegible]nhagen Ann B. Chase, Librarian at Downey, California [illegible], California VIA: Bureau Nav Weapons Rep
1	Aeronutronic Div of Ford Motor Co Res Lab Materials Dept Ford Road Attn: Mr. E. H. Jaffe Newport Beach, California VIA: ODU Liaison Officer (Col. R.A. Rawley)
1	Aircraft Armaments, Inc. Attn: Library Cockeysville, Maryland VIA: Philadelphia Proc Dist U.S. Army 128 North Broad Street Philadelphia 2, Pennsylvania
1	Applied Physics Laboratory The Johns Hopkins University 8621 Georgia Avenue Attn: Library Silver Springs, Maryland VIA: Bur Nav Weapons Rep
1	Armour Research Foundation 33rd and Dearborn Streets Attn: Librarian of Documents Chicago, Illinois VIA: C[illegible] Officer [illegible], Air Force [illegible] Dist [illegible] [illegible] [illegible] [illegible] Illinois
1	Arthur D. Little, Inc. 35 Acorn Park Cambridge, Massachusetts VIA: Boston Proc Dist U.S. Army Boston Army Base Boston 10, Massachusetts
1	AVCO Mfg. Corp. Res & Advanced Dev Attn: Library Wilmington, Massachusetts VIA: Commanding Officer Boston Proc Dist U.S. Army Boston Army Base Boston 10, Massachusetts
1	Bell Helicopter Corp. P. O. Box 482 Fort Worth 1, Texas VIA: Bureau Nav Weapons Rep
1	Boeing Airplane Company P.O. Box 3707 Seattle 24, Washington VIA: AF Plant Rep
1	Convair Div of Gen Dyn Corp. P.O. Box 1950 Pomona, California VIA: Res Rep Army Missile Com
1	Convair Div of Gen Dyn Corp. San Diego Div Mail Zone 6-157 Attn: Chief Librarian San Diego 12, California VIA: Bur Nav Weapon Rep
1	Cornell Aeronautical Lab Buffalo, New York VIA: Commanding Officer New York Proc Dist U.S. Army 770 Broadway New York 3, New York
1	General Electric Company Missile & Arm Dept Lakeside Avenue Burlington, Vermont VIA: Boston Proc Dist U.S. Army Boston Army Base Boston 10, Massachusetts

DISTRIBUTION LIST (Cont.)

No. of Copies	Organization
2	General Electric Company Radnor, Pennsylvania VIA: Philadelphia Proc Dist U.S. Army 128 North Broad Street Philadelphia 2, Pennsylvania
1	General Motors Corp Defense Res Lab Santa Barbara, California VIA: Los Angeles Proc Dist 55 South Grand Ave Pasadena 2, California
2	Goodyear Aircraft Corp Attn: Robert Shumaker Ed Fargo 1210 Massillon Road Akron 15, Ohio VIA: Bur Nav Weapon Rep
1	Grumman Aircraft Eng Corp Bethpage, Long Island, New York VIA: Bur Nav Weapons Rep
1	G. T. Schjeldahl Company c/o Res Management Corp Attn: Mr. Robert D. Ladd VIA: Commanding Officer Military Dist Washington Washington 25, D. C.
1	Hughes Aircraft Company Attn: Library Fullerton, California VIA: Los Angeles Proc Dist U.S. Army 55 South Grand Ave Pasadena 2, California
1	Institute for Cooperative Res The Johns Hopkins University Attn: H. R. Warfield, Dir 34th and Charles Streets Baltimore 18, Maryland
1	Lincoln Laboratory Massachusetts Inst of Tech Attn: Mr. W. Hermann Room A1-219 Cambridge, Massachusetts VIA: Boston Proc Dist U.S. Army Boston Army Base Boston 10, Massachusetts
1	Lockheed Missile and Space Div Attn: Mr. A. E. Papazoni P.O. Box 504 Sunnyvale, California VIA: Bur Nav Weapons Rep
1	Martin Company Attn: Mr. W. Porter Orlando, Florida VIA: Birmingham Proc Dist U.S. Army 2120 North Seventh Ave Birmingham, Alabama
1	McDonnell Aircraft Company Box 516 St. Louis 66, Missouri VIA: U.S. AF Plant Rep
1	North American Aviation Corp Los Angeles 45, California VIA: Bur Nav Weapon Rep
1	Nortronics 500 East Orangethorpe Ave Anaheim, California VIA: Los Angeles Proc Dist U.S. Army 55 South Grand Ave Pasadena 2, California
1	Raytheon Company Missile Systems Div Attn: Mr. Bud Hurd Spring Street Lexington 73, Massachusetts VIA: Boston Proc Dist U.S. Army Boston Army Base Boston 10, Massachusetts
1	Republic Aviation Corp Scientific Research Staff Farmingdale, New York VIA: U.S. AF Plant Rep
1	Safetee Glass Company Attn: Mr. Ernest Pescatore 4717 Stenton Ave Philadelphia 44, Pennsylvania VIA: Philadelphia Proc Dist U.S. Army 128 North Broad Street Philadelphia 2, Pa.
1	Sikorsky Aircraft Div of United Aircraft Corp Attn: Mr. E. F. Katzenberger South Avenue Bridgeport, Connecticut VIA: Bur Nav Weapon Rep
1	Space Technology Lab Inc Attn: Library Box 95001, Los Angeles 45, California VIA: Commander Ballistic Systems Div AF Unit Post Office Los Angeles 45, Calif.

DISTRIBUTION LIST (Cont.)

No. of Copies	Organization	No. of Copies	Organization
1	Stanford Research Institute Attn: Library Menlo Park, California VIA: Commanding Officer San Francisco Proc Dist U.S. Army 1615 Clay Street P.O. Box 1829 Oakland 12, California		
1	Rudlow Incorporated Attn: Mr. D.C.S. Kline 6986 Bandini Blvd Los Angeles 22, California VIA: Los Angeles Proc Dist U.S. Army 55 South Grand Ave Pasadena 2, Calif.		
1	Sylvania Electrical System Waltham 54, Massachusetts VIA: Boston Proc Dist U.S. Army Boston Army Base Boston 10, Massachusetts		
1	University Of Denver Industrial Res Inst Attn: Library Denver 10, Colorado VIA: Commanding Officer St. Louis Proc Dist U.S. Army 4300 Goodfellow Blvd. St. Louis 20, Missouri		
1	U.S. Rubber Company Res Dept Wayne, New Jersey VIA: New York Proc Dist U.S. Army 770 Broadway New York 3, N. Y.		
1	Vertol Division The Boeing Company Morton, Pennsylvania VIA: Bur of Nav Weapon Rep		
1	Hayes International Corp. Attn: Mr. J. F. Hawk Birmingham, Alabama VIA: USAF Birmingham Contr Mgmt Off P.O. Box 2583 Birmingham, Ala.		